Presentation of an energetic method for the forced response in vibroacoustics in medium-high frequency domain and its robustness analysis to modelling uncertainties

Yifu Guo

Présentation d'une méthode énergétique pour la réponse forcée en vibro-acoustique, moyennes et hautes fréquences, et analyse de sa robustesse aux incertitudes de modèle

Presentation of an energetic method for the forced response in vibroacoustics in medium-high frequency domain and its robustness analysis to modelling uncertainties

Thèse doctorale

de

YIFU GUO

UNIVERSITÉ PARIS-EST

Ecole Doctorale Sciences, Ingénierie et Environnement
UNIVERSIÉ DE PARIS-EST

SOUMIS EN JUILLET 2020

LE JURY

EXAMINATEUR	NICOLAS DAUCHEZ
RAPPORTEUR	LAURENT MAXIT
RAPPORTEUR	MOHAMED GUERICH
EXAMINATRICE	CATHERINE GUIGOU-CARTER
DIRECTEUR DE THÈSE	CHRISTOPHE DESCELIERS
INVITÉ	CORENTIN COGUENANFF

Remerciement

Au cours des trois dernières années, tout n'a pas été facile. Je suis très reconnaissant aux gens de m'avoir aidé et inspiré jusqu'à la fin de mon doctorat. En tout premier lieu je pense à mes parents qui m'ont partagé leur sagesse de la vie et m'ont donné des soutiens émotionnels. J'apprécie beaucoup la compagnie de mes amis à Paris et à Grenoble. Ils me réchauffaient chaque fois je tombais dans le creux froid. Enfin je ne remercierai jamais assez Yang pour son soutien et son amour.

Au regard de ces trois dernières années, je suis très reconnaissant envers mon directeur de thèse Christophe Desceliers pour sa patience et sa disponibilité. D'autre part, je remercie Corentin Coguenanff pour m'avoir fait confiance et pour ses formations dans la première phase de la thèse. Dans le même temps je remercie Catherine Guigou-Carter pour son suivi et son support continu. Je remercie également Patricia Planel, Béatrice Gauthier, Ghislaine Capouret, Mathilde Ernest et les autres collègues du CSTB pour leurs aides. Finalement, un grand merci à tous les doctorants et post-doctorants du CSTB et du laboratorie MSME.

J'adresse également mes remerciements à Nicolas Dauchez pour m'avoir fait l'honneur de prendre part au jury, Laurent Maxit et Mohamed Guerich pour avoir accepté d'être rapporteurs de ce mémoire et pour avoir accepté d'évaluer ce travail.

Abstract

Vibro-acoustic analysis in medium and high frequency range is always very delicate, and there are few methods that work efficiently in a broad frequency band of analysis. It is even more delicate if dissipative couplings appear between the different elements in the structure under analysis. Some recent works have proposed some extensions of the SEA (Statistical Energy Analysis) method, which is a method designed for vibration analysis in high frequency domain. These extensions make it possible to make use of SEA in the medium frequency domain. However, it seems that none of these extensions or alternatives of SEA allow the existence of non-conservative couplings. If such a restriction can be lifted, the applications of SEA method can be much easier in the engineering problems as dissipation is really important for a dynamical system. The current strategy consists in gathering together all the subsystems that are connected by dissipative couplings.

In this manuscript, a brief introduction of SEA for a coupled-oscillators system is presented with an extension to non-conservative couplings. New SEA coefficients, referred as 'Equivalent Coupling Power Proportionality' (ECPP) coefficients are introduced, which allow non-conservative couplings for $N \geq 2$ coupled-oscillators system. This formulation of the SEA with ECPP coefficients will be referred as SEA-ECPP approach. Numerical applications are presented in order to validate the proposed approach. Moreover, another outcome brought during this work concerns the construction of an *ad hoc* reduced model for vibro-acoustic systems that will be referred as 'Condensed Reduced-Order Model' (CROM) in the rest of the manuscript. CROM is based on a modal analysis in limited frequency band. A selection of modes and a re-construction including truncation and Schur complements of the global frequency response function is carried out in order to minimize the dimension of the computational model. Based on CROM, an 'Equivalent

Second-Order Model' (ESOM) is established to identify the equivalent mechanical couplings form CROM for a SEA calculation. With the conservative and non-conservative couplings identified by ESOM, the new 'Equivalent Coupling Power Proportionality' (ECPP) coefficients are proposed to solve energy relations in a system that contains non-conservative couplings, which is not allowed in classic SEA. This new approach is hereinafter named as SEA-ECPP approach.

Uncertainties related to the construction of ESOM are propagated into the SEA-ECPP approach and a probabilistic model is constructed in using the non-parametric approach. The robust analysis of the SEA-ECPP based on ESOM is carried out with respect to the modelling uncertainties in using such a non-parametric probabilistic computational model.

RÉSUMÉ

L'analyse vibro-acoustique en moyennes et hautes fréquences est toujours très délicate, et il existe peu de méthodes qui soient efficaces pour des domaines fréquentiels d'analyse. La situation est encore plus délicate en présence de couplage dissipatif entre les différents éléments de la structure étudiée. Des avancées récentes ont été publiées dans la littérature afin de proposer des extensions de la méthode SEA (Statistical Energy Analysis), laquelle a été développée spécifiquement pour l'analyse vibratoire dans le domaine des hautes fréquences, au domaine des moyennes fréquences. Cependant, il nous semble, qu'aucune méthode dérivant de la SEA n'autorise à ce jour des couplages non-conservatifs. La prise en compte des couplages non-conservatifs est importante car la dissipation et l'amortissement dans les systèmes dynamiques tiennent un rôle important, tant dans les applications en ingénierie des structures que dans la modélisation des systèmes physiques. Les stratégies présentées dans la littérature consistent à regrouper ensemble en une seul système plusieurs sous-systèmes dissipant de l'énergie au travers des couplages dissipatifs. Cette approche permet de prendre en compte l'amortissement en tant que dissipation interne d'un "macro" sous-système, ce qui est possible dans le cadre usuelle de la SEA.

Dans ce travail de thèse, nous présenterons un bref rappel de la méthode SEA appliquées aux oscillateurs avec couplages conservatifs, puis nous étendrons son cadre théorique au cas des couplages non-conservatifs. Cette extension sera faite en introduisant un nouveau coefficient, lequel sera désigné par la terminologie "Equivalent Coupling Power Proportionality" (ECPP), qui permet la formulation d'une méthode de type SEA pour des systèmes d'oscillateurs à $N \geq 2$ degrés de liberté avec couplages non-conservatifs. Des applications numériques seront présentées pour analyser les performances de l'approche proposée. Par ailleurs, un soin tout particulier sera

apporté à la construction des modèles réduits généralisés pour la vibro-acoustique. Notamment, un modèle réduit, construit par l'analyse modale, sera présenté et désigné par "Condensed Reduced-Order Model" (CROM). Ce CROM est donc issu d'une analyse modale en partitionnant la bande fréquentielle d'étude (LF, MF et HF) en bande fréquentielle plus petite, en sélectionnant les modes de vibration vibro-acoustique, dits "résonnants", qui contribuent le plus *a priori* à la représentation modale de la solution. Des compléments de Schur successifs sont effectués sur les inconnues généralisées des autres modes "non-résonants" pour réduire la dimension du modèle numérique. Un "Equivalent Second-Order Model" (ESOM) était construit pour identifier les différentes couplages dans la méthode SEA. Dans notre cas d'étude, il identifie non-seulement les couplages conservatifs mais aussi les couplages non-conservatifs qui viennent de la condensation du CROM, qui seront mis dans les coefficients ECPP sur lequel sera formulée l'extension ECPP de la méthode SEA et que nous appelerons "approche SEA-ECPP".

Les différentes sources d'incertitudes sur les paramètres et sur la modélisation des opérateurs du ESOM dues aux approximations introduites par l'approche ECPP par rapport au ESOM seront prises en compte par une approche probabiliste non paramétrique des incertitudes. L'analyse en robustesse sera menée et présentée dans un chapitre qui lui sera dédié en fin de manuscrit.

TABLE OF CONTENTS

List of Tables

Table **Page**

List of Figures

NOMENCLATURE

In this manuscript, symbols below are used to represent different variables/parameters used in scalar/vector/matrix forms.

t An instant of time

ω Angular frequency

ρ Mass density

E Young's Modulus

ν Poisson's coefficient

η Damping loss factor

Ω Three-dimensional volume domain

Γ Surface boundary

ρ_{f} Mass density of fluid medium

c_{f} Sound velocity in fluid medium

$Q(\mathbf{x};t)$ Acoustic source density at point $\mathbf{x}$ and at time t

$Q^{\mathrm{prim}}(\mathbf{x};t)$ Primitive of $Q(\mathbf{x};t)$

p Sound pressure of a linear acoustic fluid

φ Acoustic potential of a linear acoustic fluid

τ_{f} Viscosity coefficient

u Particle's displacement

v Particle's velocity

σ_{ij} Cauchy stress tensor

ε_{kh} Linear strain tensor

a_{ijkh} Elasticity tensor

b_{ijkh} Damping tensor

ρ_{s} Mass density of solid medium

ϕ_{p} Porosity of porous material

σ_{p} Resistivity of porous material

α_{p} Tortuosity of porous material

Λ_{p} Viscous characteristic length of porous material

Λ'_{p} Thermal characteristic length of porous material

k'_0 Static thermal permeability of porous material

f_{d} Phase decoupling frequency

ρ_{p} Global mass density of the porous material

$\widetilde{\rho}_{\mathrm{eq}}$ Equivalent complex mass density

$\widetilde{K}_{\mathrm{eq}}$ Equivalent complex bulk modulus

C_p Heat capacity at constant pressure

λ Eigenvalues

μ Orthogonality coefficient

$\mathbf{q}^{(i)}$ Vector of generalised coordinates of subsystem (i)

$\mathbf{f}^{(i)}$ Vector of generalised loads of subsystem (i)

$[\mathcal{M}^{(i)}]$ Generalised mass matrix of subsystem (i)

$[\mathcal{D}^{(i)}]$ Generalised damping matrix of subsystem (i)

$[\mathcal{K}^{(i)}]$ Generalised stiffness matrix of subsystem (i)

$[\mathcal{C}^{(ij)}]$ Generalised coupling matrix of subsystem (i) and (j)

$[\mathcal{A}^{(i)}(\omega)]$ Generalised dynamical stiffness matrix of subsystem (i) at angular frequency ω

$[\mathbb{M}]$ Generalised mass matrix of global system

$[\mathbb{D}]$ Generalised damping matrix of global system

$[\mathbb{K}]$ Generalised stiffness matrix of global system

$[\mathbb{C}]$ Generalised coupling matrix of global system

$\mathbb{q}$ Global vector of generalised coordinates

$\mathbb{f}$ Global vector of generalised loads

$\mathbb{B}$ Full frequency band of analysis

B A limited frequency band

$[\mathbb{Z}_B^{(i)}(\omega)]$ A complex equivalent matrix of subsystem (i) in Condensed Reduced-Order Model (CROM)

$[\mathbb{W}_B^{(ij)}(\omega)]$ A complex equivalent matrix of subsystem (i) and (j) in CROM

$[\mathbb{V}_B^{(ij)}(\omega)]$ A complex equivalent matrix of subsystem (i) and (j) in CROM

$[\mathbb{M}_B]$ Equivalent mass matrix in Equivalent Second-Order differential system Model (ESOM)

$[\mathbb{D}_B]$ Equivalent damping matrix in ESOM

$[\mathbb{G}_B]$ Equivalent gyroscopic matrix in ESOM

$[\mathbb{K}_B]$ Equivalent stiffness matrix in ESOM

$[\mathbb{R}_B]$ Equivalent "rest" matrix in ESOM

$\{\mathbf{F}(t), t \in \mathbb{R}\}$ A $\mathbb{R}^N$-valued random process modelling the external loads

$[S_{\mathbf{F}}(\omega)]$ Matrix-valued power spectral density function of $\{\mathbf{F}(t), t \in \mathbb{R}\}$

$\mathbf{Q}_B$ A vector-valued random generalised coordinates in limited frequency band B

$\langle W_{\alpha,B}^{\text{in}} \rangle$ Mean local-frequency generalised instantaneous injected power in limited frequency band B

$\langle \mathcal{E}_{\alpha,B} \rangle$ Mean local-frequency generalised instantaneous mechanical energy in limited frequency band B

$\langle W_{\alpha,B}^{\text{diss}} \rangle$ Mean local-frequency generalised instantaneous dissipated power in limited frequency band B

$\langle W_{\alpha\beta,B}^{\text{ex}} \rangle$ Mean local-frequency generalised instantaneous exchanged energy in limited frequency band B

$\mathbb{h}_{\alpha,B}$ Generalised frequency response function (a simplified writing of $\widehat{\mathbb{h}}_{\alpha,B}(\omega)$)

$z_{\alpha\beta,B}$, $x_{\alpha\beta,B}$ Equivalent Coupling Power Proportionality (ECPP) coefficients

κ Normalisation constant

δ Dispersion coefficient

$[\mathbf{M}_B]$ Random mass matrix in limited frequency band B

$[\mathbf{D}_B]$ Random damping matrix in limited frequency band B

$[\mathbf{K}_B]$ Random stiffness matrix in limited frequency band B

$[\mathbf{G}_B]$ Random gyroscopic matrix in limited frequency band B

$[\mathbf{R}_B]$ Random "rest" matrix in limited frequency band B

$\underline{\mathbf{W}}_B^{(i),\text{in}}$ Real-valued deterministic vector of mean local-frequency generalised instantaneous injected power in limited frequency band B

$\underline{\boldsymbol{\mathcal{E}}}_B^{(i)}$ Real-valued deterministic vector of mean local-frequency generalised instantaneous mechanical energy in limited frequency band B

$\boldsymbol{\mathcal{E}}_B^{(i)}$ Real-valued random vector of mean local-frequency generalised instantaneous mechanical energy in limited frequency band B

CHAPTER I

INTRODUCTION

The present research aims at defining methodologies for the robust prediction and optimisation of the acoustic performance, in medium and high frequencies, of dissipative multilayer systems used within building construction. During the last decades, there has been a strong increase of interest in lightweight buildings area, which result in an objective of 20% of wood within building construction in France by 2020 [2]. However, in short of research studies, especially in the acoustic domain, the share of lightweight construction struggles to increase [3]. With respect to acoustic comfort, from the viewpoint of designers, the main difficulties are the lack of feedback and the lack of predictive tools in the stage of designing. Consequently, several national and international research projects were initiated in Europe to push forward the scientific research about lightweight structure. Some initial approaches were introduced in [4–7] within the current set of standards [8] and extensively used for heavy constructions. Such approaches require the individual performance of the different separative systems, which are obtained from experimental measurements in laboratory. However, the lightweight systems have variations in their performances that cannot be evaluated and saved in database for each individual component. A predictive method is therefore needed to take into account not only the structural complexity of those systems but also the uncertainties lied to the diversity of lightweight systems in order to evaluate their raw acoustic performance. For a vibro-acoustic problem, the low frequency domain is defined as a domain where the coupled vibro-acoustic system has a low modal density. The high frequency domain is defined as a domain where the system's modal density is very high. The medium frequency domain is between these two domains. Numerical applications in medium frequency domain are always delicate, because of variations of modal density. Moreover, the geometry, the boundary conditions and the dissipation play big roles in medium frequency domain [9]. In low and medium frequency domain, FEM (Finite Element Method) is used universally across industries with the help of modal reductions methods [10–13].

However, these methods are no longer applicable in high frequency domain. In high frequency domain, methods like SEA (Statistical Energy Analysis) [14–16] and Ray-tracing [17, 18] are often used in vibro-acoustic problems such as room acoustic problems. In particular, SEA is an energetic method that coupled with statistical approaches, that benefits from the high modal overlap in high frequencies and can do numerical simulations with relatively low costs.

In the context of previous research project of CSTB, a solution in low frequency domain has already been presented in [19] with the use of FEM. The main objective of this thesis is to find a solution of direct transmission through lightweight heterogeneous systems in medium and high frequency range. As enlightened by many researchers over the years [14–16, 20–25], the modal approach of SEA is chosen to be used in this frequency range. Yet, the SEA method is usually limited by the restriction of its hypotheses, especially the "conservative couplings" and "light damping" [26–29]. From the industrial point of view, such hypotheses are often delicate to be satisfied when dissipative materials are used. Further and deeper studies in the fundamentals of SEA are also needed in order to extend the existing methods to the applications of absorbing materials. The heterogeneity of absorbing materials such as porous materials provokes uncertainties of mechanical properties, which may also influence the global acoustical performance of the lightweight system. Besides, there often exist uncertainties due to the wrong installations, wrong components, which make the original computational model not adapted. Hence a probabilistic study allows quantifying the propagation of all these possible uncertainties to the solution of the computational models in order to do robust prediction.

I.1 Objectives

Given the previous context, the following objectives are set in this manuscript. The first objective consists in defining a FEM-based computational framework with modal analysis, suited to medium and high frequencies and able to handle the structural complexity as well as dissipative materials. In particular, this prediction method need to be constructed at the building step in the continuity with the work already presented in [19] in low frequency range. Moreover, outputs of the computational models should be comparable to the standard evaluation indexes. The second objective consists in defining an extension of SEA, which allows the existence of non-conservative couplings (due to the previous proposed modal analysis). Then, the third objective is the validation of the proposed computational models with references. The fourth objective lies to the uncertainty quantification, which quantifies specially the uncertainties according to the construction of the proposed SEA model and constructs in a probabilistic sense, the confidence region for the quantities of interest and hence allowing robust prediction.

I.2 Strategy

With the previously formulated objectives, the following strategies are defined for this manuscript. In regard to the prediction of the acoustic performances associated with airborne sound insulation of the complex systems of interest, a computational model is constructed by the Finite Element Method with a detailed description of the structural, acoustic and poroelastic components is performed. The framework of the classical linear elastoacoustic theory [30, 31] is used with respect to the structure and internal acoustic acoustical excitation meanwhile poroelastic media are modelled by equivalent fluid models[32, 33]. Then, a deterministic ROM (Reduced Order Model) is construct based on the usual modal analysis which is valid in low frequency domain and in medium frequency domain but with a high computational cost. This ROM is optimised into Condensed ROM (CROM) within limited frequency bands with the condensations of certain selected non-resonant eigenmodes[34, 35] with a new modal analysis for a dissipative multi-layered system. Truncations and Schur complements are used for constructing this CROM. Moreover, from this CROM, an associated Equivalent Second-Order differential computational Model (ESOM) with frequency-independent matrices is deduced and is taken as a candidate for extending the usual SEA approach. New coefficients which are called Equivalent Coupling Power Proportionality (ECPP) are proposed in order to replace the classic Coupling Power Proportionality (CPP) coefficients in a system that contains non-conservative couplings, and an extended formulation of classic SEA formulation is also introduced. In the rest of this manuscript, this extended formulation of SEA is referred as SEA-ECPP in which ECPP stands for Equivalent Coupling Power Proportionality.

Due to the mathematical-mechanical modelling associated with complex systems and experimental errors into the identification of its parameters, there are many sources of uncertainties in the computational model that propagate to the solution of the problem. Among the underlying sources of uncertainties [36–43], there exists two types of uncertainties that have to be taken into account to obtain a robust prediction. Such uncertainties on the solution and the quantity of interest should be quantified in order to perform robust analysis. Note that modelling uncertainties cannot be modelled by any parametric formulation of uncertainties. In order to model and quantify statistical fluctuations among the inputs or among the system parameters as well as the model uncertainties induced by modelling errors, it is proposed to follow the generalised probabilistic approach of uncertainties introduced by Soize [44, 45]. Such an approach consists in substituting the generalised matrices of a reduced-order computational model with full random matrices, whose probabilistic models is constructed in using the MaxEnt principle and available information such as mathematical information on the output of the mechanical system.

I.3 Organisation of the manuscript

This manuscript is organised as follow:

- In Chapter II, we introduce the mechanical system of interest and the associated vibroacoustic problems to be solved. Two models, namely Model 1 and Model 2, are presented;
- A brief review of forced response problem for a linear dissipative acoustic fluid and for a linear visco-elastic solid is presented in Chapters III and IV;
- Several models for porous elastic media are presented in Chapter V;
- A Reduced-Order Model (ROM) is constructed in Chapter VI to solve the vibroacoustic problems of interest;
- A Condensed Reduced-Order Model (CROM) is then constructed, for solving in frequency domain the vibroacoustic problem in limited frequency bands that cover the complete frequency band of analysis. This computational model is constructed with a sequence of truncation and Schur complements in Chapter VII). Finally, an Equivalent Second-Order differential Model (ESOM) is developed in identifying a mass matrix, a stiffness matrix, a damping matrix, a gyroscopic matrix and a 'rest' matrix that are frequency-independent;
- An extension of the classic SEA formulations is proposed in Chapter VIII, which looses the limitation of "conservative coupling" that is fundamentally assumed in classic SEA. This extension of the SEA is referred in the manuscript as SEA-ECCP;
- In Chapter IX, a robust analysis of SEA-ECPP approach is carried out with respect to the modelling uncertainties in using a non-parametric probabilistic computational model;
- The Chapter X is dedicated to applications of ROM, ESOM and SEA-ECPP to Model 1 and Model 2 and comparisons between these different approaches are also presented. Then the robustness of the SEA-ECPP approach is tested in applications with the probabilistic model constructed in Chapter IX.

CHAPTER II

MECHANICAL SYSTEMS OF INTERESTS FOR THE VIBROACOUSTIC PROBLEM

We have specifically chosen a multi-layered system for which a computational model will be constructed and used for a numerical application and validation of the proposed methodologies developed in this manuscript. It corresponds to a mechanical system for which we can obtain numerous experimental measurements and for which there are many industrial applications. The multi-layered system under consideration is composed of 2 visco-elastic solid layers (hereinafter modelled by two visco-elastic plates) and one linear dissipative acoustic layer sandwiched between the two other layers. The noise transmission through such sandwich structures are already studied by Guerich with FEM[46]. In this manuscript, this multi-layered mechanical system is placed between two volumes made up of linear acoustic (non dissipative) fluids. For the purpose of reducing acoustical transmission, the middle layer is often an insulating layer whose material is very dissipative in dynamical vibrations. Such a multi-layered system presents the advantage of combining the dynamical properties of each layer in order to have an optimal performance to meet industrial requirements. Thanks to its design, we can obtain an improved acoustic performance in MF and HF domains with such a system with a light weight. Indeed, in theory, a double-partition system benefits up to 18 dB/octave increased Sound Transmission Loss (STL) after the mass-spring-mass resonance frequency, and still benefits an increase of 12 dB/Octave with cavity modes of the middle layer [47–49]. With regard to the dip of STL at coincidence frequencies, in practice, the decrease of STL can be efficiently reduced at the coincidence frequencies if the two visco-elastic solid plates have different mechanical properties [50]. Another important advantage is that the insulating layer can absorb a lot of mechanical energy, which means that a part of the energy is dissipated inside the layer [51, 52]. However, in real engineering systems, there can be many complex structures like

mechanical connections inside a multi-layered system [1]. In this chapter, a classic 5-subsystem multi-layered mechanical system is introduced, where a 3-subsystem multi-layered mechanical system is contained inside. In the next chapters, numerical applications and validations for the methodologies that are developed for this system in this manuscript are presented. The procedure for obtaining experimental measurements is also presented at the end of this chapter.

II.1 Mechanical systems of interest

According to some industrial needs, we are especially interested in the acoustical performances of a dissipative multi-layered panel. A designed mechanical system is presented in this section, the numerical applications will be however presented for 2 different models.

II.1.1 Model 1 (Volume-plate-volume-plate-volume)

A 5-subsystem-system shown in Fig. II.1 is considered, which is made up of an emission volume (1), a multi-layered double partition wall system (2) – (4) as shown in Fig. II.2, and a receiving volume (5). The acoustical excitation is placed in the emission volume.

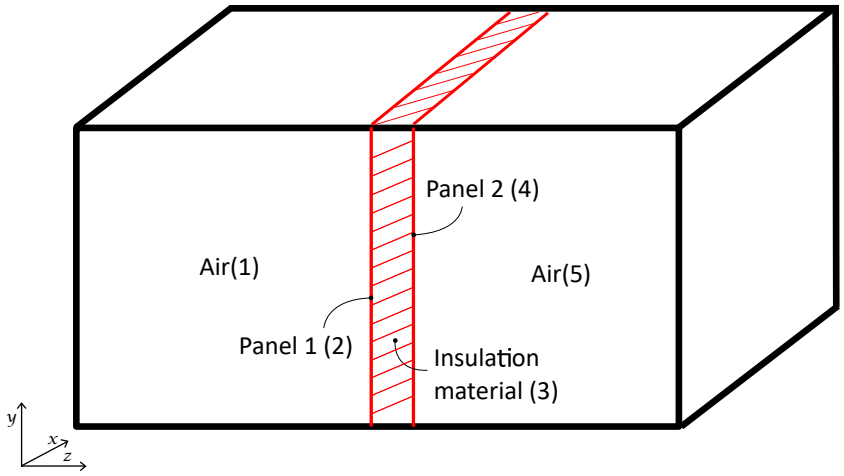

Figure II.1 – A 5-subsystem system (Model 1)

These 5 subsystems share the same rectangular section (x and y direction), and have individual depth or thickness in z direction. In this system, the two volumes (1) and (5) are assumed to be filled with air and the panels (2) and (4) are assumed to be very different in their mechanical properties (Young's Modulus, mass density, etc.). The insulation layer (3) is made up of a material with high damping ratio $\xi^{(3)}$ (or damping loss factor with $\eta^{(3)} = 2\,\xi^{(3)}$).

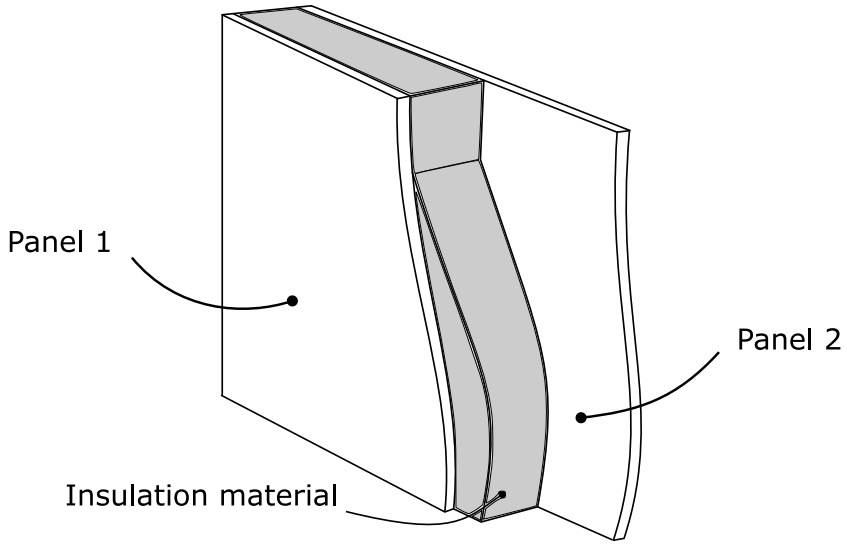

Figure II.2 – Multi-layered Panel (with insulating layer)

II.1.2 Model 2 (double-partition wall system between semi-infinite spaces)

When the dimension of such a system becomes large, the computational cost for the numerical model of large acoustic volumes becomes very high in medium and high frequency range as the modal density of acoustic volumes grows very fast with increasing frequencies. Schur complement is used to condense degrees of freedom of acoustic volumes (1) and (5) that are therefore modelled by added acoustical impedances. In the medium-high frequency domain, the influence of these added acoustical impedances become negligible and so that the 2 volumes can be considered as semi-infinite spaces. The details of this assumption will be introduced in section. VI.4.

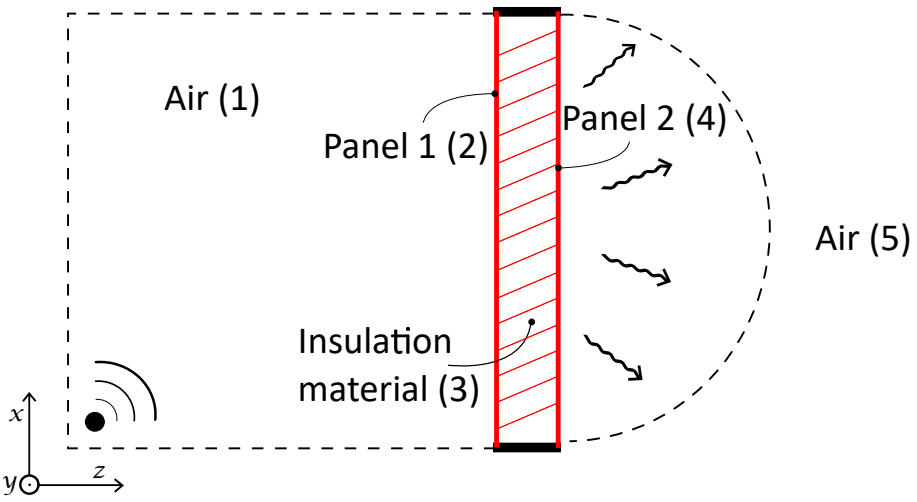

Figure II.3 – Model 2

CHAPTER III

FORCED RESPONSE PROBLEM FOR A LINEAR DISSIPATIVE ACOUSTIC FLUID

In this chapter, we present the boundary value problem and its associated weak formulation of the forced response for the problem of a linear dissipative acoustic fluid occupying a bounded domain and for which a deterministic time dependent displacement field is applied on its boundary.

III.1 Balance equations in time domain

III.1.1 Inviscid fluid

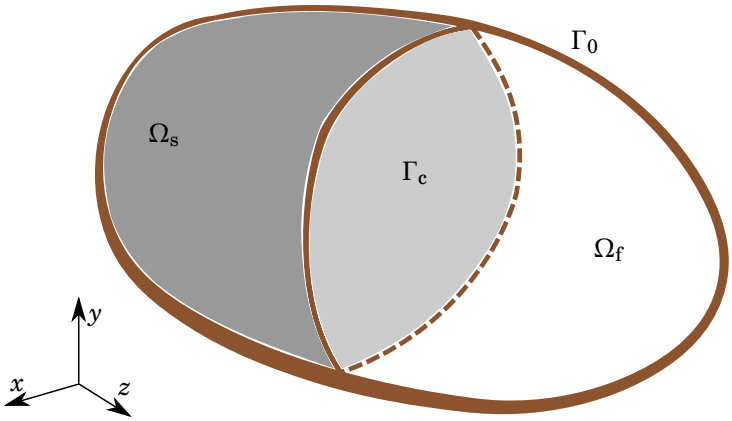

Figure III.1 – A coupled vibroacoustic system

As shown in Fig. III.1, we consider a bounded three-dimensional fluid domain Ω_f and a Cartesian

reference system (O,X,Y,Z). A point position in this domain is denoted as $\mathbf{x} = (x_1, x_2, x_3)$. The medium in Ω_f is assumed to be an inviscid acoustic fluid. Let ρ_f and c_f respectively be the mass density and the sound velocity of this acoustic fluid in a static equilibrium configuration and let $Q(\mathbf{x};t)$ be the acoustic source density at point $\mathbf{x}$ and at time t such that $t \mapsto Q(\mathbf{x};t)$ is a square integrable function on $\mathbb{R}$. In this section, we consider the equations for the forced response problem. The balance equations in time domain for the solution $t \mapsto p(\mathbf{x};t)$ of the forced response problem is written as,

$$\partial_{tt}\, p(\mathbf{x};t) - c_\mathrm{f}^2 \nabla^2 p(\mathbf{x};t) = c_\mathrm{f} \partial_t Q(\mathbf{x};t)\ , \tag{III.1}$$

where ∂_t and ∂_{tt} are the first and second partial derivatives with respect to t. Let the acoustic potential be denoted as φ (also called velocity potential) which is such that

$$p(\mathbf{x};t) = -\rho_\mathrm{f} \partial_t \varphi(\mathbf{x};t) \quad , \tag{III.2}$$

Substituting Eq. (III.2) into Eq. (III.1) and integrating with respect to t, we then obtain

$$\nabla^2 \varphi(\mathbf{x};t) - \frac{1}{c_\mathrm{f}^2}\, \partial_{tt}\, \varphi(\mathbf{x};t) = \frac{1}{\rho_\mathrm{f}} Q(\mathbf{x};t)\ . \tag{III.3}$$

III.1.2 Dissipative fluid

In this section, we consider by now the dissipation effects due to the viscosity and thermal conduction of the fluid. It introduces additional term in the balance equations (III.3). This is the model presented in [11, 53] for which an added dissipative term is introduced and is proportional to $\nabla^2 p$ with a coefficient τ_f (in practice, the dissipation due to thermal conduction is often neglected and then τ_f would depend only on viscosity of fluid). There is also an additional term at the right hand side of the balance equation. Let ζ_f be the second viscosity of the dissipative acoustic fluid. The balance equation with a dissipative term and an additional source term is then rewritten as, in the case that the dynamic viscosity η_f is small, which is the case for air,

$$-\frac{1}{c_\mathrm{f}^2} \partial_{tt} p(\mathbf{x};t) + \tau_\mathrm{f} \nabla^2 \partial p(\mathbf{x};t) + \nabla^2 p(\mathbf{x};t) = \tau_\mathrm{f} \rho_\mathrm{f} \nabla^2 Q(\mathbf{x};t) - \partial_t Q(\mathbf{x};t)\ , \tag{III.4}$$

where $\tau_\mathrm{f} \simeq \zeta_\mathrm{f}/(\rho_\mathrm{f} c_\mathrm{f}^2)$ when η_f is small. The balance equation can also be rewritten in term of φ and we then have

$$\nabla^2 \varphi(\mathbf{x};t) + \tau_\mathrm{f} \nabla^2 \partial_t \varphi(\mathbf{x};t) - \frac{1}{c_\mathrm{f}^2}\, \partial_{tt}\, \varphi(\mathbf{x};t) = \frac{1}{\rho_\mathrm{f}} \partial_t Q^{\mathrm{prim}}(\mathbf{x};t) - \frac{\tau_\mathrm{f} c_\mathrm{f}^2}{\rho_\mathrm{f}} \nabla^2 Q^{\mathrm{prim}}(\mathbf{x};t)\ , \tag{III.5}$$

where $Q^{\mathrm{prim}}(\mathbf{x};t)$ is introduced such that $Q(\mathbf{x};t) = \partial_t Q^{\mathrm{prim}}(\mathbf{x};t)$. Note that we obtain again Eq. (III.3) for an inviscid acoustical fluid with $\tau_\mathrm{f} = 0$.

III.2 Boundary conditions

Supposing that only Neumann boundary conditions are applied on the surface $\Gamma = \partial\Omega$ with $\Gamma = \Gamma_0 \cup \Gamma_c$ where Γ_0 is a rigid wall surface (fixed), and Γ_c is a boundary on which a displacement field is applied and that is written as $\mathbf{u}(\mathbf{x}\, t) = (u_1(\mathbf{x};t), u_2(\mathbf{x};t), u_3(\mathbf{x};t))$. We then have, for a dissipative acoustical fluid ($\tau_f > 0$) or a inviscid acoustical fluid ($\tau_f = 0$)

$$\nabla\Big(\varphi(\mathbf{x};t) + \tau_f \partial_t \varphi(\mathbf{x};t)\Big) \cdot \mathbf{n} = -\frac{\tau_f c_f^2}{\rho_f} \nabla Q^{\text{prim}}(\mathbf{x};t) \cdot \mathbf{n} \quad , \quad \text{on } \Gamma_0 \quad , \tag{III.6}$$

$$\nabla\Big(\varphi(\mathbf{x};t) + \tau_f \partial_t \varphi(\mathbf{x};t)\Big) \cdot \mathbf{n} = \Big(\partial_t \mathbf{u}(\mathbf{x};t) - \frac{\tau_f c_f^2}{\rho_f} \nabla Q^{\text{prim}}(\mathbf{x};t)\Big) \cdot \mathbf{n} \quad , \quad \text{on } \Gamma_c \quad . \tag{III.7}$$

In this work, it is assumed that the acoustical sources are inside the acoustic domain and are located at spatial points. Consequently $\nabla Q^{\text{prim}}(\mathbf{x};t) \cdot \mathbf{n} = 0$ on boundary $\partial\Omega_f$ and these two boundary conditions are rewritten as

$$\nabla\Big(\varphi(\mathbf{x};t) + \tau_f \partial_t \varphi(\mathbf{x};t)\Big) \cdot \mathbf{n} = 0 \quad , \quad \text{on } \Gamma_0 \quad , \tag{III.8}$$

$$\nabla\Big(\varphi(\mathbf{x};t) + \tau_f \partial_t \varphi(\mathbf{x};t)\Big) \cdot \mathbf{n} = \partial_t \mathbf{u}(\mathbf{x};t) \cdot \mathbf{n} \quad , \quad \text{on } \Gamma_c \quad . \tag{III.9}$$

Note that if an homogeneous Dirichlet condition $p(\mathbf{x};t) = 0$ was applied on one part of Γ, then it would induce that $\pi(t) = 0$ (see [11, 30]).

III.3 Boundary value problem

For an inviscid ($\tau_f = 0$) or a dissipative ($\tau_f > 0$) acoustical fluid occupying a bounded domain Ω_f, the boundary value problem for the forced response $\varphi(\mathbf{x};t)$ with a homogeneous Neumann condition applied on the part Γ_0 of $\partial\Omega_f$ and with a Neumann boundary conditions corresponding to a displacement field applied on the part Γ_c of its boundary $\partial\Omega_f$, is written as: Find $\varphi(\cdot;t)$ that is sufficiently regular such that

$$\nabla^2\varphi(\mathbf{x};t) + \tau_f \nabla^2 \partial_t \varphi(\mathbf{x};t) - \frac{1}{c_f^2} \partial_{tt} \varphi(\mathbf{x};t) = \frac{1}{\rho_f} \partial_t Q^{\text{prim}}(\mathbf{x};t) - \frac{\tau_f c_f^2}{\rho_f} \nabla^2 Q^{\text{prim}}(\mathbf{x};t) \, , \tag{III.10}$$

$$\nabla\Big(\varphi(\mathbf{x};t) + \tau_f \partial_t \varphi(\mathbf{x};t)\Big) \cdot \mathbf{n} = 0 \quad , \quad \text{on } \Gamma_0 \quad , \tag{III.11}$$

$$\nabla\Big(\varphi(\mathbf{x};t) + \tau_f \partial_t \varphi(\mathbf{x};t)\Big) \cdot \mathbf{n} = \partial_t \mathbf{u}(\mathbf{x};t) \cdot \mathbf{n} \quad , \quad \text{on } \Gamma_c \quad . \tag{III.12}$$

III.4 Weak formulation

The weak formulation for the forced response of a dissipative or inviscid acoustic fluid presented in section III.3 is deduced in using the method of the test functions. The associated weak formulation is then written as : Find φ such that, for any admissible test functions $\delta\varphi$, we have

$$\int_{\Omega_f} \nabla^2\varphi\,\overline{\delta\varphi}\,dV + \int_{\Omega_f} \tau_f \nabla^2(\partial_t\varphi)\,\overline{\delta\varphi}\,dV - \int_{\Omega_f} \frac{1}{c_f^2}\partial_{tt}\varphi\,\overline{\delta\varphi}\,dV = \int_{\Omega_f} \frac{1}{\rho_f}\partial_t Q^{\text{prim}}\,\overline{\delta\varphi}\,dV - \int_{\Omega_f} \frac{\tau_f c_f^2}{\rho_f}\nabla^2 Q^{\text{prim}}\,\overline{\delta\varphi}\,dV \quad \text{(III.13)}$$

We have

$$\int_{\Omega_f} \nabla^2\varphi\,\overline{\delta\varphi}\,dV = \int_{\Omega_f} \nabla(\nabla\varphi\,\overline{\delta\varphi})dV - \int_{\Omega_f} \nabla\varphi\cdot\nabla\overline{\delta\varphi}\,dV\ ,$$

which yields, using the Stokes theorem,

$$\begin{aligned}\int_{\Omega_f} \nabla^2\Big(\varphi+\tau_f\partial_t\varphi\Big)\overline{\delta\varphi}\,dV &= \int_{\Gamma} \nabla\Big(\varphi+\tau_f\partial_t\varphi\Big)\cdot\mathbf{n}\,\overline{\delta\varphi}\,dS - \int_{\Omega_f} \nabla\Big(\varphi+\tau_f\partial_t\varphi\Big)\varphi\cdot\nabla\overline{\delta\varphi}\,dV\ ,\\ &= \int_{\Gamma_c} \nabla\Big(\varphi+\tau_f\partial_t\varphi\Big)\cdot\mathbf{n}\,\overline{\delta\varphi}\,dS - \int_{\Omega_f} \nabla\Big(\varphi+\tau_f\partial_t\varphi\Big)\cdot\nabla\overline{\delta\varphi}\,dV\ .\end{aligned}$$

Using this equation and Eq. (III.12) into Eq. (III.13) and then multiplying the two sides by ρ_f, we then have, with $\widetilde{Q} = \partial_t Q^{\text{prim}} + \tau_f c_f^2 \nabla Q^{\text{prim}}$

$$\frac{1}{c_f^2}\int_{\Omega_f} \partial_{tt}\varphi\,\overline{\delta\varphi}\,dV + \tau_f\int_{\Omega_f} \nabla(\partial_t\varphi)\cdot\nabla\overline{\delta\varphi}\,dV + \int_{\Omega_f} \nabla\varphi\cdot\nabla\overline{\delta\varphi}\,dV - \int_{\Gamma_c} (\partial_t\mathbf{u}\cdot\mathbf{n})\overline{\delta\varphi}\,dS = -\int_{\Omega_f} \frac{1}{\rho_f}\widetilde{Q}\,\overline{\delta\varphi}\,dV\ , \quad \text{(III.14)}$$

III.5 Antilinear and sesquilinear forms associated to the weak formulation

According to the weak formulation of the problem defined by Eq. (III.14) that is multiplied by ρ_f, the classical sesquilinear and antilinear forms of the problem are introduced,

$$\begin{aligned} m_f(\varphi,\delta\varphi) &= \frac{\rho_f}{c_f^2}\int_{\Omega_f} \varphi\,\overline{\delta\varphi}\,dV \quad , \quad d_f(\varphi,\delta\varphi) = \tau_f\rho_f\int_{\Omega_f} \nabla\varphi\cdot\nabla\overline{\delta\varphi}\,dV\ ,\\ k_f(\varphi,\delta\varphi) &= \rho_f\int_{\Omega_f} \nabla\varphi\cdot\nabla\overline{\delta\varphi}\,dV \quad , \quad f(\delta\varphi) = -\int_{\Omega_f} \widetilde{Q}\,\overline{\delta\varphi}\,dV\\ c(\varphi,\delta\mathbf{u}) &= \rho_f\int_{\Gamma_c} \varphi\,\overline{\delta\mathbf{u}}\cdot\mathbf{n}\,dS \end{aligned}$$

Consequently, the weak formulation for the forced response of a dissipative or inviscid acoustical fluid is then written as : Find φ such that, for any admissible test functions $\delta\varphi$, we have

$$m_f(\partial_{tt}\varphi,\delta\varphi) + d_f(\partial_t\varphi,\delta\varphi) + k_f(\varphi,\delta\varphi) - c(\delta\varphi,\partial_t\mathbf{u}) = f(\delta\varphi)\quad , \quad \text{(III.15)}$$

CHAPTER IV

FORCED RESPONSE PROBLEM FOR A LINEAR VISCO-ELASTIC SOLID

The boundary value problem and the associated weak formulation for a linear visco-elastic solid is presented in this chapter. Same as the previous chapter, the boundary value problem and its weak formulation for the forced response problem of a visco-elastic solid excited on its boundary by a time dependent pressure field is presented[11, 30].

IV.1 Balance and constitutive equations

IV.1.1 Constitutive equations for linear elastic solid medium

Let Ω_s be a three-dimensional domain with boundary denoted by $\Gamma = \partial\Omega_s$. As defined before, $\mathbf{u}(\mathbf{x};t) = (u_1(\mathbf{x};t), u_2(\mathbf{x};t), u_3(\mathbf{x};t))$ is the displacement of a particle located at position $\mathbf{x} = (x_1, x_2, x_3)$ and at time t. In this section, we consider an homogeneous solid elastic medium and Ω_s is its reference configuration in a static equilibrium. Let σ_{ij} be the Cauchy stress tensor and let ε_{kh} be the linear strain tensor that is such that

$$\varepsilon_{kh}(\mathbf{x};t) = \frac{1}{2}\Big(\frac{\partial u_h(\mathbf{x};t)}{\partial x_k} + \frac{\partial u_k(\mathbf{x};t)}{\partial x_h}\Big)\,. \tag{IV.1}$$

The constitutive equation is then written as

$$\sigma_{ij}(\mathbf{x};t) = a_{ijkh}(\mathbf{x})\,\varepsilon_{kh}(\mathbf{x};t)\,, \tag{IV.2}$$

where a_{ijkh} are the components of the elasticity tensor.

IV.1.2 Constitutive equations for visco-elastic solid medium

For a linear visco-elastic medium and within the framework of instantaneous visco-elasticity (without time memory effects), the constitutive equations are written as

$$\sigma_{ij}(\mathbf{x};t) = \sigma_{ij}^{\text{elas}}(\mathbf{x};t) + s_{ij}^{\text{damp}}(\mathbf{x};t) \;, \tag{IV.3}$$

in which

$$\begin{aligned} \sigma_{ij}^{\text{elas}}(\mathbf{x};t) &= a_{ijkh}(\mathbf{x})\,\varepsilon_{kh}(\mathbf{x};t) \\ s_{ij}^{\text{damp}}(\mathbf{x};t) &= b_{ijkh}(\mathbf{x})\,\partial_t \varepsilon_{kh}(\mathbf{x};t) \;, \end{aligned}$$

where, in this manuscript, the elasticity tensor a_{ijkh} and the damping tensor b_{ijkh} might depend only on $\mathbf{x}$ and for which we have the usual (minor and major) symmetries and ellipticity properties.

IV.1.3 Balance equations

In case there is no external loads, the balance equations are written as, for $i = 1,\ldots,3$,

$$\rho_{\text{s}}\partial_{tt} u_i(\mathbf{x};t) - \partial_j \sigma_{ij}(\mathbf{x};t) = 0 \quad \text{in} \quad \Omega_{\text{s}} \;, \tag{IV.4}$$

where ρ_{s} is the mass density of the elastic solid medium in the reference configuration and where $\partial_j \sigma_{ij}$ is the divergence of the Cauchy stress tensor and ∂_j is the partial derivative with respect to x_j.

IV.2 Boundary conditions

We assume there is a Neumann boundary condition on part Γ_{c} of boundary $\partial\Omega_{\text{s}}$ of domain Ω_{s}, which corresponds to a pressure field $p(\mathbf{x};t)$ that is exciting the visco-elastic solid. In addition we also assume that a Dirichlet boundary condition is applied on an other part Γ_0 of boundary $\partial\Omega_{\text{s}}$. We then have, for all $i = 1,2,3$

$$\begin{aligned} \sigma_{ij}(\mathbf{x};t)\,n_j &= p\,n_i \quad \text{on} \quad \Gamma_{\text{c}} \;, \\ u_i(\mathbf{x};t) &= 0 \quad \text{on} \quad \Gamma_0 \;. \end{aligned}$$

where $\mathbf{n} = (n_1, n_2, n_3)$ is the outward unit vector of domain Ω_{s}. As described in the previous chapter, acoustic potential φ is used for modelling the equations of an acoustical fluid medium and in this case, the Neumann boundary condition is rewritten as

$$\sigma_{ij}(\mathbf{x};t)\,n_j = -\rho_{\text{f}}\partial_t \varphi(\mathbf{x};t)\,n_i \quad \text{on} \quad \Gamma_{\text{c}} \;.$$

IV.3 Boundary value problem

For a linear visco-elastic medium occupying a bounded domain Ω_s, the boundary value problem for the forced response $\mathbf{u}(\mathbf{x};t)$ with a homogeneous Dirichlet condition on the part Γ_0 of $\partial\Omega_s$ and with a Neumann boundary conditions corresponding to a pressure field applied on part Γ_c of $\partial\Omega_s$, is written as: Find $\mathbf{u}(\cdot;t)$ that is sufficiently regular such that

$$\rho_s \partial_{tt} u_i(\mathbf{x};t) - \partial_j \sigma_{ij}(\mathbf{x};t) = 0 \quad \text{in} \quad \Omega_s \ , \tag{IV.5}$$

$$\sigma_{ij}(\mathbf{x};t) = a_{ijkh}(\mathbf{x})\varepsilon_{kh}(\mathbf{x};t) + b_{ijkh}(\mathbf{x})\partial_t \varepsilon_{kh}(\mathbf{x};t) \ , \tag{IV.6}$$

$$\sigma_{ij}(\mathbf{x};t) n_j = -\rho_f \partial_t \varphi(\mathbf{x};t) n_i \quad \text{on} \quad \Gamma_c \ , \tag{IV.7}$$

$$u_i(\mathbf{x};t) = 0 \quad \text{on} \quad \Gamma_0 \ . \tag{IV.8}$$

IV.4 Weak formulation of the problem

The weak formulation for the forced response problem of a linear visco-elastic solid that is excited by a pressure field on its boundary is deduced from the boundary value problem defined by Eqs. (IV.5) to (IV.8) in using the method of the test functions. The associated weak formulation is then written as : Find u_1, u_2, u_3 such that, for any admissible test functions $\delta u_1, \delta u_2, \delta u_3$, we have

$$\int_{\Omega_s} \rho_s \partial_{tt} u_i \, \overline{\delta u_i} \, dV - \int_{\Omega_s} \partial_j \sigma_{ij} \, \overline{\delta u_i} \, dV = 0 \ , \tag{IV.9}$$

Using the Stokes' theorem on the second term of Eq. (IV.9) and the boundary conditions defined by Eqs. (IV.7) and (IV.8), we then obtain, with implicit summations over all the indexes i and j,

$$\begin{aligned} \int_{\Omega_s} (\partial_j \sigma_{ij}) \overline{\delta u_i} \, dV &= \int_{\Omega_s} \partial_j (\sigma_{ij} \overline{\delta u_i}) dV - \int_{\Omega_s} \sigma_{ij} \overline{\partial_j \delta u_i} \, dV & \text{(IV.10)} \\ &= \int_{\Gamma_c} \sigma_{ij} n_j \overline{\delta u_i} \, dS - \int_{\Omega_s} \sigma_{ij} \overline{\partial_j \delta u_i} \, dV & \text{(IV.11)} \\ &= -\int_{\Gamma_c} \rho_f \partial_t \varphi \, n_i \overline{\delta u_i} \, dS - \int_{\Omega_s} \sigma_{ij} \overline{\partial_j \delta u_i} \, dV \ , & \text{(IV.12)} \end{aligned}$$

and we then have, with an implicit summation over all indexes i, j, k, h, in using Eqs. (IV.1) and (IV.6)

$$\begin{aligned} \rho_s \int_{\Omega_s} \partial_{tt} u_i \, \overline{\delta u_i} \, dV + \int_{\Omega_s} b_{ijkh} \, \partial_h (\partial_t u_k) \overline{\partial_j \delta u_i} \, dV + \int_{\Omega_s} a_{ijkh} (\partial_h u_k) \overline{\partial_j \delta u_i} \, dV \\ + \rho_f \int_{\Gamma_c} \partial_t \varphi \, n_i \, \overline{\delta u_i} \, dS = 0 \quad . \end{aligned} \tag{IV.13}$$

IV.5 Antilinear and sesquilinear forms associated to the weak formulation of the problem

According to the weak formulation of the problem defined by Eq. (IV.13), the classical sesquilinear and antilinear forms of the problem are introduced,

$$m_{\mathrm{s}}(\mathbf{u},\delta\mathbf{u}) = \rho_{\mathrm{s}}\int_{\Omega_{\mathrm{s}}} \mathbf{u}\cdot\overline{\delta\mathbf{u}}\,dV\ , \qquad k_{\mathrm{s}}(\mathbf{u},\delta\mathbf{u}) = \int_{\Omega_{\mathrm{s}}} a_{ijkh}(\partial_h u_k)\overline{\partial_j\delta u_i}\,dV\ ,$$
$$d_{\mathrm{s}}(\mathbf{u},\delta\mathbf{u}) = \int_{\Omega_{\mathrm{s}}} b_{ijkh}(\partial_h u_k)\overline{\partial_j\delta u_i}\,dV\ , \qquad c(\varphi,\delta\mathbf{u}) = \rho_{\mathrm{f}}\int_{\Gamma_c}\varphi\,\overline{\delta\mathbf{u}}\cdot\mathbf{n}\,dS\ .$$

The weak formulation for the forced response problem of a linear visco-elastic solid that is excited by a pressure field on its boundary is then written as : Find u_1, u_2, u_3 such that, for any admissible test functions $\delta u_1, \delta u_2, \delta u_3$, we have

$$m_{\mathrm{s}}(\partial_{tt}\mathbf{u},\delta\mathbf{u}) + d_{\mathrm{s}}(\partial_t\mathbf{u},\delta\mathbf{u}) + k_{\mathrm{s}}(\mathbf{u},\delta\mathbf{u}) + c(\partial_t\varphi,\delta\mathbf{u}) = 0 \quad . \tag{IV.14}$$

CHAPTER V

MODELS FOR POROUS DISSIPATIVE MEDIUM

We present different models for porous elastic media that can be found in the literature. Porous media often offer very efficient absorbing properties for noise and vibration. There exist a large number of models that describe the kinematic of porous media [32, 33, 54–64]. Among them all, we focused on two models, the so called 'Equivalent Fluid Model' (with motionless skeleton) [32, 33, 54–60, 65] and the 'Biot Model' (with a diphasic medium) [61–64].

V.1 Fundamental parameters of porous materials

The classical fundamental parameters that allow porous materials to be modelled are listed hereinafter in this section. These parameters can all be characterised by experimental measurements. Among them all, four fundamental parameters are the usual elastic coefficients for an isotropic elastic linear solid medium: the mass density ρ, the Young's Modulus E, the Poisson's coefficient ν and the damping loss factor η. Six other acoustic parameters have to be considered for the porous material:

1. **Porosity** ϕ_{p}: The ratio of air volume over the total volume of the material.
2. **Resistivity** σ_{p}: The static air flow resistivity which quantify the resistance of the material on air flow.
3. **Tortuosity** α_{p}: The complexity of the inner skeleton of the solid micro-structure.
4. **Viscous characteristic length** Λ_{p}: The quantification of the viscous effects at medium and high acoustic frequencies.

5. **Thermal characteristic length** Λ'_{p}: Parameter involved into the thermal effects at medium and high acoustic frequencies.

6. **Static thermal permeability** k'_0: Parameter involved into the thermal effects at low frequencies.

The choice of a porous elastic model rather than another depends on the problem under consideration. Generally, a Biot model is preferably considered for a large number of applications but it is also one of the most complicated model to be implemented in computational software, compared to the 'Equivalent fluid model' and it also requires an intrusive implementation, which means that a dedicated piece of code has to be implemented in the computational software. The numerical implementation of an 'Equivalent fluid model' is easier than 'Biot model', because it is non intrusive and requires only that a linear dissipative fluid model is already implemented into the computational software. Nevertheless, it requires some hypothesis: the pressures should be applied into the acoustic fluid domain Ω and the frequency band of analysis has to be much higher than the phase decoupling frequency [66] that is denoted as f_{d} and defined as

$$f_{\mathrm{d}} = \frac{\sigma_{\mathrm{p}} \phi_{\mathrm{p}}^2}{2\pi \rho_{\mathrm{p}}} \,, \tag{V.1}$$

where ρ_{p} is the mass density of the porous material. In this case, the solid and the fluid phases of an acoustic porous material can be considered as decoupled and the material skeleton can be considered as motionless. It is the hypothesis made in this manuscript since we consider MF and HF domains.

V.2 Equivalent fluid models

In [66], the wave equation for porous media is explicitly written. It is similar to the Helmholtz equation that is used to describe the sound propagation without dissipation and it is written as

$$\nabla^2 p + \omega^2 \frac{\widetilde{\rho}_{\mathrm{eq}}}{\widetilde{K}_{\mathrm{eq}}} p = 0 \,, \tag{V.2}$$

where $\widetilde{\rho}_{\mathrm{eq}}$ and $\widetilde{K}_{\mathrm{eq}}$ are the equivalent complex mass density and the equivalent complex bulk modulus, respectively. The explicit frequency dependence of these two parameters are described for different model of porous media. More specifically, hereinafter, two of them are given as examples. (1) The empirical 'Delany-Bazley' model (see [55]) and the semi-phenomenological 'Johnson-Champoux-Allard-Lafarge' (JCAL) model (see [59]).

- **Delany-Bazley model**. This is an empirical model which is parametrised only by the resistivity σ_{p}. However, this model has many restrictions such as

    1. The porosity should be close to 1 (it is the case for most of fibrous materials).

2. Only applicable in a certain frequency domain (the valid domain is $0.01 < \frac{f}{\sigma_\mathrm{p}} < 1$).
3. It only describes correctly the straight cylindrical pores.

- **JCAL model**. It is a semi-phenomenological model that is introduced in [32, 33, 59]. This model is mostly based on the 5-parameter JCA model and the static thermal permeability k_0', introduced by Lafarge in order to describe the low frequency behaviour of thermal effects. All these 6 parameters can be predicted [67]. A complex-valued mass density and a complex-valued bulk modulus are then deduced by describing the visco-inertial dissipative effects and the thermal dissipative effects inside the porous medium. This model is adapted to micro-structures for which pore section is spatially non-uniform. We have,

$$\widetilde{\rho}_{\mathrm{eq}}(\omega) = \frac{\alpha_\mathrm{p}\rho_0}{\phi_\mathrm{p}}\Big[1 + \frac{\sigma_\mathrm{p}\phi_\mathrm{p}}{i\omega\rho_0\alpha_\mathrm{p}}\sqrt{1 + i\omega\frac{4\alpha_\mathrm{p}^2\eta\rho_0}{\sigma_\mathrm{p}^2\Lambda_\mathrm{p}^2\phi_\mathrm{p}^2}}\Big]\,, \tag{V.3}$$

$$\widetilde{K}_{\mathrm{eq}}(\omega) = \frac{\gamma P_0/\phi_\mathrm{p}}{\gamma - (\gamma-1)\Big[1 - i\frac{\phi_\mathrm{p}\kappa}{k_0' C_p \rho_0 \omega}\sqrt{1 + i\omega\frac{4{k_0'}^2 C_p\rho_0}{\kappa{\Lambda_\mathrm{p}'}^2\phi_\mathrm{p}^2}}\Big]^{-1}}\,, \tag{V.4}$$

where P_0 is the atmospheric pressure considered as a constant (101325 Pa at sea level); C_p is the heat capacity of the material at constant pressure; γ and κ are respectively the fluid specific heat ratio and thermal conduction coefficient. The limitation of this model is that values of γ and κ are uncertain in LF domain. However, in MF and HF domains, such uncertainties are small and such an equivalent fluid model is then acceptable as an approximation for porous materials.

- **Limp model**. The Limp model is derived from the poroelastic Biot model assuming that the frame has no bulk stiffness. This one-wave limp model belongs to equivalent fluid models and it takes into account the inertial effects of the solid phase, but it has fewer limitations. However, the use of the limp model depends on both the properties of porous layer but also on the boundary conditions that are applied to it. An identification process with a criterion that is called Frame Stiffness Influence (FSI) is then needed[60]. This parameter, which is based on the compressional wave numbers, shows the influence of the frame-borne wave on the fluid phase displacement.

V.3 Biot's model

Biot model (see for instance [61, 62]) proposes a theoretical formulation for modelling an isotropic porous medium saturated by a fluid. This model introduces three wave-fields: two compression wave-fields P_1 and P_2 and one shear wave-field. P_1 is the fastest compression wave and P_2 is the slowest compression wave, but only P_2 can propagate in the fluid phase. Biot model is often involved with an equivalent fluid model such as JCAL model. That is the reason why it is often

called “Biot-Allard model” or “Biot-JCAL model”. When the wavelength is much larger than the pore sizes, under an hypothesis of small strains, the properties of the fluid phase can be considered equivalent to a fixed solid phase. That is to say, only P_2 is taken into account, and $\widetilde{\rho}_{22}$ and $\widetilde{R}$ (variables in the articles[61, 62], which are not introduced in details in this manuscript) can be replaced by $\widetilde{\rho}_{\text{eq}}$ and $\widetilde{K}_{\text{eq}}$ in Eq. (V.2).

However, in this manuscript, these porous models are not used in the applications because of the simplification of interpretations. The porous model is not a core part in this work and we use a dissipative fluid in the first place in order to validate our proposed models. The advantage of using a dissipative fluid is that it does not have frequency-dependency parameters, and there is no need to verify the causality property. Limp model seems a good choice for our studying system and it can be a perspective, but it is not tested in this manuscript within the limit of time of this thesis.

CHAPTER VI

REDUCED ORDER MODELS FOR THE FORCED RESPONSE PROBLEMS OF A MULTI-COUPLED FLUID-SOLID SYSTEM

The modal analysis and the generalised eigenvalue problems constructing the functional basis used in the truncated expansion of the displacement fields and the acoustic potential solution for the forced response problems are respectively presented in chapters III and IV. We then deduce the reduced generalised matrices for the response forced problems that will be used in the next chapter dedicated to the multilayer sandwiched vibroacoustic mechanical system.

VI.1 Generalised eigenvalue problems

Two truncations of the modal expansions of the forced responses $\mathbf{u}$ and φ for the two problems presented in chapters III and IV are carried out. The following two generalised eigenvalue problems are solved and two truncated functional basis are then constructed with the eigenfunctions solutions. The two generalised eigenvalue problems are written as: Find $\{\lambda_\alpha^{\mathrm{s}}, \mathbf{u}_\alpha\}$ and $\{\lambda_\alpha^{\mathrm{f}}, \varphi_\alpha\}$ such that for any admissible test functions $\delta\mathbf{u} = (\delta u_1, \delta u_2, \delta u_3)$ and $\delta\varphi$, we have

$$k_{\mathrm{s}}(\mathbf{u}_\alpha, \delta\mathbf{u}) = \lambda_\alpha^{\mathrm{s}}\, m_{\mathrm{s}}(\mathbf{u}_\alpha, \delta\mathbf{u}) \quad , \tag{VI.1}$$

and

$$k_{\mathrm{f}}(\varphi_\alpha, \delta\varphi) = \lambda_\alpha^{\mathrm{f}}\, m_{\mathrm{f}}(\varphi_\alpha, \delta\varphi) \quad . \tag{VI.2}$$

Such generalised eigenvalue problems can be solved analytically for simple configurations of the solid and the fluid but, in general, numerical methods such as the Finite Element method are used for discretising the sesquilinear forms of mass and of stiffness. The n_{s} first eigenfunctions $\mathbf{u}_\alpha$ and the n_{f} first eigenfunctions φ_α respectively associated with eigenvalues $0 < \lambda_1^{\mathrm{s}} < \ldots < \lambda_{n_{\mathrm{s}}}^{\mathrm{s}}$

and $0 = \lambda_0^{\rm f} < \lambda_1^{\rm f} < \ldots < \lambda_{n_{\rm f}}^{\rm f}$ are respectively denoted as $\mathbf{u}_1, \ldots, \mathbf{u}_{n_{\rm s}}$ and $\varphi_1, \ldots, \varphi_{n_{\rm s}}$. In addition, we have the following orthogonality properties, with respect to the mass and stiffness sesquilinear forms $m_{\rm s}$, $k_{\rm s}$, $m_{\rm f}$, $k_{\rm f}$

$$\begin{array}{lll} m_{\rm s}(\mathbf{u}_\alpha, \mathbf{u}_\beta) = \mu_\alpha^{\rm s}\, \delta_{\alpha\beta} & , & m_{\rm f}(\varphi_\alpha, \varphi_\beta) = \mu_\alpha^{\rm f}\, \delta_{\alpha\beta} \quad , \\ k_{\rm s}(\mathbf{u}_\alpha, \mathbf{u}_\beta) = \mu_\alpha^{\rm s}\, \lambda_\alpha^{\rm s}\, \delta_{\alpha\beta} & , & k_{\rm f}(\varphi_\alpha, \varphi_\beta) = \mu_\alpha^{\rm f}\, \lambda_\alpha^{\rm f}\, \delta_{\alpha\beta} \quad . \end{array}$$

As a mathematical consequence, $\{\mathbf{u}_\alpha\}_{\alpha>0}$ and $\{\varphi_\alpha\}_{\alpha\geq 0}$ form two truncated reduced basis for a convergent expansion of the two solutions $\mathbf{u}$ and φ. We then have

$$\lim_{n_{\rm s}\to+\infty} ||\mathbf{u} - \sum_{\alpha=1}^{n_{\rm s}} q_\alpha^{\rm s}\, \mathbf{u}_\alpha\, ||_{m_{\rm s}}^2 = 0 \quad \text{with} \quad q_\alpha^{\rm s} = \left(\mu_\alpha^{\rm s}\right)^{-1} m_{\rm s}(\mathbf{u}, \mathbf{u}_\alpha) \quad ,$$

$$\lim_{n_{\rm f}\to+\infty} ||\varphi - \sum_{\alpha=0}^{n_{\rm f}} q_\alpha^{\rm f}\, \varphi_\alpha\, ||_{m_{\rm f}}^2 = 0 \quad \text{with} \quad q_\alpha^{\rm f} = \left(\mu_\alpha^{\rm f}\right)^{-1} m_{\rm f}(\varphi, \varphi_\alpha) \quad ,$$

where we defined the norms $||\mathbf{u}||_{m_{\rm s}}^2 = m_{\rm s}(\mathbf{u}, \mathbf{u})$ and $||\varphi||_{m_{\rm f}}^2 = m_{\rm f}(\varphi, \varphi)$. Note that for $\alpha = 0$ and for not incompressible acoustic fluid, it can be shown that φ_0 is a constant, *i.e* independent of position $\mathbf{x}$ and is given in [11]. In the case the fluid is compressible or if the wavelengths of the vibrations are small with respect to the size of existing holes on boundary $\partial\Omega_{\rm f}$ (for which we would have homogeneous Dirichlet conditions for the pressure field), then the additional solution $\varphi_0\, q_0^{\rm f}(t)$ does not exist and all the eigenvalues $0 < \lambda_1^{\rm f} < \ldots < \lambda_{n_{\rm f}}^{\rm f}$ are positive (there is no eigenvalue $\lambda_0^{\rm f}$). Usually, the eigenfunctions $\{\mathbf{u}_\alpha\}_{\alpha>0}$ and $\{\varphi_\alpha\}_{\alpha\geq 0}$ are not orthogonal for the damping sesquilinear forms $d_{\rm s}$ and $d_{\rm f}$. Nevertheless, we have $d_{\rm f}(\psi, \psi') = \tau_{\rm f} k_{\rm f}(\psi, \psi')$ for any admissible functions ψ and ψ'. Consequently, $\{\varphi_\alpha\}_{\alpha\geq 0}$ is a set of mutually orthogonal functions for the damping sesquilinear form $d_{\rm f}$ and we have, for any $\alpha, \beta \geq 0$

$$d_{\rm f}(\varphi_\alpha, \varphi_\beta) = 2\, \mu_\alpha^{\rm f}\, \xi_\alpha^{\rm f}\, \omega_\alpha^{\rm f}\, \delta_{\alpha\beta} \quad ,$$

where $\xi_\alpha^{\rm f} = 0.5\, \tau_{\rm f} \omega_\alpha^{\rm f}$ and $\omega_\alpha^{\rm f} = \sqrt{\lambda_\alpha^{\rm f}}$ for any $\alpha > 0$. Concerning the sesquilinear form $d_{\rm s}$ we will assume that the viscoelasticity model of components b_{ijkh} is such that, for any $\alpha, \beta > 0$

$$d_{\rm s}(\mathbf{u}_\alpha, \mathbf{u}_\beta) = 2\, \mu_\alpha^{\rm s}\, \xi_\alpha^{\rm s}\, \omega_\alpha^{\rm s}\, \delta_{\alpha\beta} \quad .$$

where $\omega_\alpha^{\rm s} = \sqrt{\lambda^{\rm s}}_\alpha$.

VI.2 Mean reduced generalised model for a coupled fluid-solid system

As explained in chapters III and IV, the approximations $\mathbf{u}_{n_{\rm s}}$ and $\varphi_{n_{\rm f}}$ of solutions $\mathbf{u}$ and φ can be constructed as the truncated expansion on $\{\mathbf{u}_\alpha\}_{\alpha>0}$ and $\{\varphi_\alpha\}_{\alpha>0}$ written as

$$\mathbf{u}_{n_{\rm s}} = \sum_{\alpha=1}^{n_{\rm s}} q_\alpha^{\rm s}\, \mathbf{u}_\alpha \quad \text{and} \quad \varphi = \sum_{\alpha=0}^{n_{\rm f}} q_\alpha^{\rm f}\, \varphi_\alpha \quad .$$

Same expansion is used for the admissible tests functions $\delta\mathbf{u}$ and $\delta\varphi$,

$$\delta\mathbf{u}_{n_s} = \sum_{\alpha=1}^{n_s} \delta q_\alpha^s \mathbf{u}_\alpha \quad \text{and} \quad \delta\varphi = \sum_{\alpha=0}^{n_f} \delta q_\alpha^f \varphi_\alpha \quad .$$

Using these expansions on the equations of the weak formulation and using the orthogonality equations yields, for all $0 \leq \alpha \leq n_f$

$$\mu_\alpha^f \partial_{tt} q_\alpha^f + 2\mu_\alpha^f \xi_\alpha^f \omega_\alpha^f \partial_t q_\alpha^f + (\omega_\alpha^f)^2 q_\alpha^f - \sum_{\beta=1}^{n_s} c(\varphi_\alpha, \mathbf{u}_\beta) \partial_t q_\beta^s = f(\varphi_\alpha) \quad , \tag{VI.3}$$

and for all $1 \leq \alpha \leq n_s$

$$\mu_\alpha^f \partial_{tt} q_\alpha^s + 2\mu_\alpha^s \xi_\alpha^s \omega_\alpha^s \partial_t q_\alpha^s + (\omega_\alpha^s)^2 q_\alpha^s + \sum_{\beta=0}^{n_f} c(\varphi_\beta, \mathbf{u}_\alpha) \partial_t q_\beta^f = 0 \quad . \tag{VI.4}$$

These two systems of equations, for the linear dissipative acoustic fluid and for the linear viscoelastic solid can be rewritten as

$$[\mathcal{M}^f]\partial_{tt}\mathbf{q}^f(t) + [\mathcal{D}^f]\partial_t\mathbf{q}^f(t) - [\mathcal{C}^{fs}]\partial_t\mathbf{q}^s(t) + [\mathcal{K}^f]\mathbf{q}^f(t) = \mathbf{f}(t) \quad , \tag{VI.5}$$

$$[\mathcal{M}^s]\partial_{tt}\mathbf{q}^s(t) + [\mathcal{D}^s]\partial_t\mathbf{q}^s(t) + [\mathcal{C}^{fs}]\partial_t\mathbf{q}^f(t) + [\mathcal{K}^s]\mathbf{q}^s(t) = 0 \quad , \tag{VI.6}$$

in which generalised mass matrices $[\mathcal{M}^f]$ and $[\mathcal{M}^s]$, generalised damping matrices $[\mathcal{D}^f]$ and $[\mathcal{D}^s]$, generalised stiffness matrices $[\mathcal{D}^f]$ and $[\mathcal{D}^s]$, the generalised coupling matrix $[\mathcal{C}^{fs}]$, the generalised vectors of coordinates $\mathbf{q}^f$ and $\mathbf{q}^s$, the generalised vector of forces $\mathbf{f}$ are,

$$\begin{aligned}
&[\mathcal{M}^f]_{\alpha\beta} = \mu_\alpha^f \delta_{\alpha_\beta} \quad , \quad [\mathcal{D}^f]_{\alpha\beta} = 2\mu_\alpha^f \xi_\alpha^f \omega_\alpha^f \delta_{\alpha_\beta} \quad , \quad [\mathcal{K}^f]_{\alpha\beta} = \mu_\alpha^f (\omega_\alpha^f)^2 \delta_{\alpha_\beta} \quad , \\
&[\mathcal{M}^s]_{\alpha\beta} = \mu_\alpha^s \delta_{\alpha_\beta} \quad , \quad [\mathcal{D}^s]_{\alpha\beta} = 2\mu_\alpha^s \xi_\alpha^s \omega_\alpha^s \delta_{\alpha_\beta} \quad , \quad [\mathcal{K}^s]_{\alpha\beta} = \mu_\alpha^s (\omega_\alpha^s)^2 \delta_{\alpha_\beta} \quad , \\
&[\mathcal{C}^{fs}]_{\alpha\beta} = c(\varphi_\alpha, \mathbf{u}_\beta) \quad , \quad \{\mathbf{q}^f\}_\alpha = q_\alpha^f \quad , \quad \{\mathbf{q}^s\}_\alpha = q_\alpha^s \quad , \quad \{\mathbf{f}\}_\alpha = f(\varphi_\alpha) \quad .
\end{aligned}$$

Consequently, if we consider a simple coupled fluid-solid system, the systems of equations (VI.3) and (VI.4) are then solved simultaneously, yielding a coupled system of equations. These systems of coupled equations can be rewritten into the form of a matrix equation,

$$\begin{bmatrix} [\mathcal{M}^f] & \\ & [\mathcal{M}^s] \end{bmatrix} \begin{Bmatrix} \partial_{tt}\mathbf{q}^f \\ \partial_{tt}\mathbf{q}^s \end{Bmatrix} + \begin{bmatrix} [\mathcal{D}^f] & \\ & [\mathcal{D}^s] \end{bmatrix} \begin{Bmatrix} \partial_t\mathbf{q}^f \\ \partial_t\mathbf{q}^s \end{Bmatrix} + \begin{bmatrix} & -[\mathcal{C}^{fs}] \\ [\mathcal{C}^{fs}]^T & \end{bmatrix} \begin{Bmatrix} \partial_t\mathbf{q}^f \\ \partial_t\mathbf{q}^s \end{Bmatrix} + \begin{bmatrix} [\mathcal{K}^f] & \\ & [\mathcal{K}^s] \end{bmatrix} \begin{Bmatrix} \mathbf{q}^f \\ \mathbf{q}^s \end{Bmatrix} = \begin{Bmatrix} \mathbf{f} \\ 0 \end{Bmatrix} \quad . \tag{VI.7}$$

Taking the Fourier transform of the two hand sides of this equations, we then obtain the mean reduced generalised model in frequency domain, that is written as

$$\begin{bmatrix} -\omega^2[\mathcal{M}^f] + i\omega[\mathcal{D}^f] + [\mathcal{K}^f] & -i\omega[\mathcal{C}^{fs}] \\ i\omega[\mathcal{C}^{fs}]^T & -\omega^2[\mathcal{M}^s] + i\omega[\mathcal{D}^s] + [\mathcal{K}^s] \end{bmatrix} \begin{Bmatrix} \mathbf{q}^f \\ \mathbf{q}^s \end{Bmatrix} = \begin{Bmatrix} \mathbf{f} \\ 0 \end{Bmatrix} \quad , \tag{VI.8}$$

where we used the same notations for the Fourier transform of $\mathbf{f}$, $\mathbf{q}^f$ and $\mathbf{q}^s$ for the sake of simplicity and because there is not ambiguity.

VI.3 Mean reduced generalised model 1

Hereinafter, the generalised matrices of the mean computational models used for simulating the mechanical system of Model 1 introduced in chapter II are presented. The equations for a multi-coupled fluid-solid mechanical system are then deduced, yielding the formulation of the usual reduced order model (ROM). For such a ROM, it is well known that the total computational cost is much smaller than the computational cost obtained with a full FEM approach. If the solid structure of a porous layer can be considered being motionless, then the porous medium can be considered as an equivalent fluid with frequency-dependent properties in frequency domain. In this manuscript, for the sake of convenience, the insulation layer (denoted as subsystem (3) in Fig II.1) is treated as a dissipative heavy fluid. In addition, it is assumed that all the mechanical properties of each subsystem (denoted as (1) to (5) in Fig II.1) are assumed to be frequency-independent. Such an assumption is an approximation of the real physics of these subsystems that allows modelling simplifications but an extension to the case of frequency-dependent coefficient is straightforward. Let us denote the displacement fields in subsystems (2) and (4) (see Fig.II.1), that are modelled as visco-elastic solid media, as $\mathbf{u}^{(2)}$ and $\mathbf{u}^{(4)}$. Furthermore, let us denote the acoustic potential fields in subsystems (1), (3) and (5) (see Fig.II.1), that are modelled as acoustic fluid media, as $\varphi^{(1)}$, $\varphi^{(3)}$ and $\varphi^{(5)}$. As explained in chapters III and IV, the approximations $\mathbf{u}^{(2)}_{n_2}$, $\mathbf{u}^{(4)}_{n_4}$, $\varphi^{(1)}_{n_1}$, $\varphi^{(3)}_{n_3}$ and $\varphi^{(5)}_{n_5}$ of solutions $\mathbf{u}^{(2)}$, $\mathbf{u}^{(4)}$, $\varphi^{(1)}$, $\varphi^{(3)}$ and $\varphi^{(5)}$, respectively, can be constructed as truncated expansion on eigenfunctions $\{\mathbf{u}^{(2)}_\alpha\}_{\alpha>0}$, $\{\mathbf{u}^{(4)}_\alpha\}_{\alpha>0}$ and $\{\varphi^{(1)}_\alpha\}_{\alpha>0}$, $\{\varphi^{(3)}_\alpha\}_{\alpha>0}$, $\{\varphi^{(5)}_\alpha\}_{\alpha>0}$, respectively solutions of the generalised eigenvalue problems for subsystems (2),(4) and (1),(3),(5), respectively. We then have

$$\mathbf{u}^{(2)}_{n_2} = \sum_{\alpha=1}^{n_2} q^{(2)}_\alpha \mathbf{u}^{(2)}_\alpha \quad , \quad \mathbf{u}^{(4)}_{n_4} = \sum_{\alpha=1}^{n_4} q^{(4)}_\alpha \mathbf{u}^{(4)}_\alpha \quad . \tag{VI.9}$$

$$\varphi^{(1)}_{n_1} = \sum_{\alpha=0}^{n_1} q^{(1)}_\alpha \varphi^{(1)}_\alpha \quad , \quad \varphi^{(3)}_{n_3} = \sum_{\alpha=0}^{n_3} q^{(3)}_\alpha \varphi^{(3)}_\alpha \quad , \quad \varphi^{(5)}_{n_5} = \sum_{\alpha=0}^{n_5} q^{(5)}_\alpha \varphi^{(5)}_\alpha \quad . \tag{VI.10}$$

These expansions yield, for each subsystem, a matrix equation that is respectively written as,

$$\begin{aligned}
[\mathcal{M}^{(1)}]\partial_{tt}\mathbf{q}^{(1)}(t) + [\mathcal{D}^{(1)}]\partial_t\mathbf{q}^{(1)}(t) + [\mathcal{K}^{(1)}]\mathbf{q}^{(1)}(t) - [\mathcal{C}^{(12)}]\partial_t\mathbf{q}^{(2)}(t) &= \mathbf{f}^{(1)}(t) \quad , \\
[\mathcal{C}^{(12)}]^T\partial_t\mathbf{q}^{(1)}(t) + [\mathcal{M}^{(2)}]\partial_{tt}\mathbf{q}^{(2)}(t) + [\mathcal{D}^{(2)}]\partial_t\mathbf{q}^{(2)}(t) + [\mathcal{K}^{(2)}]\mathbf{q}^{(2)}(t) + [\mathcal{C}^{(32)}]^T\partial_t\mathbf{q}^{(3)}(t) &= 0 \quad , \\
-[\mathcal{C}^{(32)}]\partial_t\mathbf{q}^{(2)}(t) + [\mathcal{M}^{(3)}]\partial_{tt}\mathbf{q}^{(3)}(t) + [\mathcal{D}^{(3)}]\partial_t\mathbf{q}^{(3)}(t) + [\mathcal{K}^{(3)}]\mathbf{q}^{(3)}(t) - [\mathcal{C}^{(34)}]\partial_t\mathbf{q}^{(4)}(t) &= 0 \quad , \\
[\mathcal{C}^{(34)}]^T\partial_t\mathbf{q}^{(3)}(t) + [\mathcal{M}^{(4)}]\partial_{tt}\mathbf{q}^{(4)}(t) + [\mathcal{D}^{(4)}]\partial_t\mathbf{q}^{(4)}(t) + [\mathcal{K}^{(4)}]\mathbf{q}^{(4)}(t) + [\mathcal{C}^{(54)}]^T\partial_t\mathbf{q}^{(5)}(t) &= 0 \quad , \\
-[\mathcal{C}^{(54)}]\partial_t\mathbf{q}^{(4)}(t) + [\mathcal{M}^{(5)}]\partial_{tt}\mathbf{q}^{(5)}(t) + [\mathcal{D}^{(5)}]\partial_t\mathbf{q}^{(5)}(t) + [\mathcal{K}^{(5)}]\mathbf{q}^{(5)}(t) &= 0 \quad ,
\end{aligned}$$

in which $\mathbf{q}^{(i)}$, $[\mathcal{M}^{(i)}]$, $[\mathcal{D}^{(i)}]$, $[\mathcal{K}^{(i)}]$ and $[\mathcal{C}^{(ij)}]$ respectively denote the generalised vectors of coordinates, the generalised mass matrices, generalised damping matrices, generalised stiffness matrices and the generalised coupling matrix of subsystem (i) coupled with subsystem (j). Furthermore, the generalised vector of forces in subsystem (1) is denoted as $\mathbf{f}^{(1)}$. All these generalised

matrices and vectors are defined by

$$[\mathcal{M}^{(i)}]_{\alpha\beta} = \mu_\alpha^{(i)}\delta_{\alpha_\beta} \quad , \quad [\mathcal{D}^{(i)}]_{\alpha\beta} = 2\,\mu_\alpha^{(i)}\,\xi_\alpha^{(i)}\,\omega_\alpha^{(i)}\,\delta_{\alpha_\beta} \quad , \quad [\mathcal{K}^{(i)}]_{\alpha\beta} = \mu_\alpha^{(i)}(\omega_\alpha^{(i)})^2\,\delta_{\alpha_\beta} \quad ,$$
$$[\mathcal{C}^{(ij)}]_{\alpha\beta} = c(\varphi_\alpha^{(i)}, \mathbf{u}_\beta^{(j)}) \quad , \quad \{\mathbf{q}^{(i)}\}_\alpha = q_\alpha^{(i)} \quad , \quad \{\mathbf{f}^{(1)}\}_\alpha = f(\varphi_\alpha^{(i)}) \quad ,$$

where $f(\cdot)$ is defined in chapter III and $\mu_\alpha^{(i)}$,$(\omega_\alpha^{(i)})^2$ and $\xi_\alpha^{(i)}$ are the generalised mass, the eigenvalue and the generalised damping ratio, respectively, associated with the $\alpha-$ th eigenmode of subsystem (i). The equations of the multi-coupled system are solved simultaneously and are then rewritten as

$$[\mathbb{M}]\,\partial_{tt}\mathbb{q}(t) + [\mathbb{D}]\,\partial_t\mathbb{q}(t) + [\mathbb{K}]\,\mathbb{q}(t) + [\mathbb{C}]\,\partial_t\mathbb{q}(t) = \mathbb{f}(t) \quad , \tag{VI.11}$$

where matrices $[\mathbb{M}],[\mathbb{D}],[\mathbb{K}],[\mathbb{C}]$ are defined as

$$[\mathbb{M}] = \begin{pmatrix} [\mathcal{M}^{(1)}] & & & & \\ & [\mathcal{M}^{(2)}] & & & \\ & & [\mathcal{M}^{(3)}] & & \\ & & & [\mathcal{M}^{(4)}] & \\ & & & & [\mathcal{M}^{(5)}] \end{pmatrix} \quad , \quad [\mathbb{D}] = \begin{pmatrix} [\mathcal{D}^{(1)}] & & & & \\ & [\mathcal{D}^{(2)}] & & & \\ & & [\mathcal{D}^{(3)}] & & \\ & & & [\mathcal{D}^{(4)}] & \\ & & & & [\mathcal{D}^{(5)}] \end{pmatrix} \quad ,$$

$$[\mathbb{C}] = \begin{pmatrix} & -[\mathcal{C}^{(12)}] & & & \\ [\mathcal{C}^{(12)}]^T & & [\mathcal{C}^{(32)}]^T & & \\ & -[\mathcal{C}^{(32)}] & & -[\mathcal{C}^{(34)}] & \\ & & [\mathcal{C}^{(34)}]^T & & [\mathcal{C}^{(54)}]^T \\ & & & -[\mathcal{C}^{(54)}] & \end{pmatrix} \quad , \quad [\mathbb{K}] = \begin{pmatrix} [\mathcal{K}^{(1)}] & & & & \\ & [\mathcal{K}^{(2)}] & & & \\ & & [\mathcal{K}^{(3)}] & & \\ & & & [\mathcal{K}^{(4)}] & \\ & & & & [\mathcal{K}^{(5)}] \end{pmatrix} \quad ,$$

and where $\mathbb{q}(t) = (\mathbf{q}^{(1)}(t), \mathbf{q}^{(2)}(t), \mathbf{q}^{(3)}(t), \mathbf{q}^{(4)}(t), \mathbf{q}^{(5)}(t))$ and $\mathbb{f}(t) = (\mathbf{f}^{(1)}(t), \mathbf{0}, \mathbf{0}, \mathbf{0}, \mathbf{0})$. Taking the Fourier transform of the two hand sides of Eq. (VI.11) yields the mean reduced generalised model in frequency domain, that is written as

$$\Big(-\omega^2[\mathbb{M}] + i\,\omega[\mathbb{D}] + i\,\omega[\mathbb{C}] + [\mathbb{K}]\Big)\,\mathbb{q}(\omega) = [\mathbb{A}(\omega)]\,\mathbb{q}(\omega) = \mathbb{f}(\omega) \quad , \tag{VI.12}$$

in which, we used the same notations for the Fourier transforms of $\mathbb{q}$ and $\mathbb{f}$ because there is no ambiguity when the equations are written in time or in frequency domains. The global matrix of the multi-coupled fluid-solid system is defined as $[\mathbb{A}(\omega)] = -\omega^2[\mathbb{M}] + i\,\omega[\mathbb{D}] + i\,\omega[\mathbb{C}] + [\mathbb{K}]$. Using a formulation in acoustic potential rather than in pressure for the modelling of the dissipative acoustic fluids (1), (3) and (5) yields a coupling fluid-solid matrix $[\mathbb{C}]$ that is antisymmetric and independent of ω. Note that in the next chapters, the explicit form of dynamic stiffness is used and Eq. (VI.12) is rewritten as

$$\begin{bmatrix} [\mathcal{A}^{(1)}(\omega)] & -i\omega[\mathcal{C}^{(12)}] & & & \\ i\omega[\mathcal{C}^{(12)}]^T & [\mathcal{A}^{(2)}(\omega)] & i\omega[\mathcal{C}^{(32)}]^T & & \\ & -i\omega[\mathcal{C}^{(32)}] & [\mathcal{A}^{(3)}(\omega)] & -i\omega[\mathcal{C}^{(34)}] & \\ & & i\omega[\mathcal{C}^{(34)}]^T & [\mathcal{A}^{(4)}(\omega)] & i\omega[\mathcal{C}^{(54)}]^T \\ & & & -i\omega[\mathcal{C}^{(54)}] & [\mathcal{A}^{(5)}(\omega)] \end{bmatrix} \begin{Bmatrix} \mathbf{q}^{(1)} \\ \mathbf{q}^{(2)} \\ \mathbf{q}^{(3)} \\ \mathbf{q}^{(4)} \\ \mathbf{q}^{(5)} \end{Bmatrix} = \begin{Bmatrix} \mathbf{f}^{(1)} \\ 0 \\ 0 \\ 0 \\ 0 \end{Bmatrix} , \tag{VI.13}$$

where matrix $[\mathcal{A}^{(i)}(\omega)]$ is the modal dynamical stiffness matrix of subsystem (i) that is defined as

$$[\mathcal{A}^{(i)}(\omega)] = -\omega^2[\mathcal{M}^{(i)}] + i\omega[\mathcal{D}^{(i)}] + [\mathcal{K}^{(i)}] \quad .$$

Matrix $[\mathcal{A}^{(i)}(\omega)]$ is symmetric and vibroacoustic coupling matrices $[\mathcal{C}^{(ji)}]$ between subsystems (i) and (j) is antisymmetric.

VI.4 Mean reduced generalised model 2

Hereinafter, the generalised matrices of the mean computational models used for simulating the mechanical system of Model 2 are presented in chapter II. As for Model 1, in section VI.3, the coupled system of equations for a multi-coupled fluid-solid mechanical system yielding the formulation of the usual reduced order model (ROM) are then deduced. The same assumptions are used for Model 2 too, that is to say, the porous medium is considered to be motionless and consequently it can be modelled as an equivalent fluid with frequency-dependent properties in frequency domain. As for section VI.3, medium in subsystem (3) is treated as a dissipative heavy fluid. Furthermore, we also assume again that the mechanical properties of each subsystem (denoted as (2) to (4) in Fig II.1) are frequency-independent. The full modal analysis of the multi-coupled fluid-solid system in Model 2 can be directly deduced from the multi-coupled fluid-solid system in Model 1 presented in section VI.3. Nevertheless, in Model 2, semi-infinite spaces are assumed and they are not able to be analysed with modal expansions. If the semi-infinite spaces are considered to be two large volumes, then they induce a very important computational cost for the modal analysis since a very high number of eigenmodes n_1 and n_5 are required for the modal expansions $\varphi^{(1)}_{n_1}$ and $\varphi^{(5)}_{n_5}$ in Eqs. (VI.9) when the forced response of the multi-coupled fluid-solid system is calculated in medium and high frequency range. It is proved [68] that the acoustic modes in rooms have negligible influence on the vibration of plates (that is the geometry of subsystem (2) and (4)) in medium-high frequency domain and consequently, the following strategy is used: (i) in low frequency range, the generalised vectors of coordinates $\mathbf{q}^{(1)}$ and $\mathbf{q}^{(5)}$ are condensed on other generalised vectors of coordinates $\mathbf{q}^{(2)}$, $\mathbf{q}^{(4)}$ in using a sequence of Schur complements [69]; (ii) in medium and high frequency range, the coupling between generalised vectors of coordinates, in one hand, $\mathbf{q}^{(1)}$ and $\mathbf{q}^{(2)}$, in another, $\mathbf{q}^{(4)}$ and $\mathbf{q}^{(5)}$ are negligible and equations related to $\mathbf{q}^{(1)}$ and $\mathbf{q}^{(5)}$ are removed from the system of equations to be solved. In Model 2 and in frequency domain, we then have

$$\begin{bmatrix} [\mathcal{A}^{(2)}(\omega)] - [\mathcal{A}^{(1)}_{\text{cond}}(\omega)] & i\omega[\mathcal{C}^{(23)}] & \\ -i\omega[\mathcal{C}^{(23)}]^T & [\mathcal{A}^{(3)}(\omega)] & -i\omega[\mathcal{C}^{(34)}] \\ & i\omega[\mathcal{C}^{(34)}]^T & [\mathcal{A}^{(4)}(\omega)] - [\mathcal{A}^{(5)}_{\text{cond}}(\omega)] \end{bmatrix} \begin{Bmatrix} \mathbf{q}^{(2)} \\ \mathbf{q}^{(3)} \\ \mathbf{q}^{(4)} \end{Bmatrix} = \begin{Bmatrix} \mathbf{f}^{(2)} \\ 0 \\ 0 \end{Bmatrix} , \tag{VI.14}$$

where, for $i = 1$ (respectively $i = 5$), the matrix $[\mathcal{A}^{(i)}_{\text{cond}}(\omega)]$ is an added dynamical stiffness matrix taking in account the condensation of generalised vector of coordinates $\mathbf{q}^{(1)}$ (respectively

$\mathbf{q}^{(5)}$) on generalised vector of coordinates $\mathbf{q}^{(2)}$ (respectively, $\mathbf{q}^{(4)}$). The two added dynamical stiffness matrices are defined as $[\mathcal{A}^{(i)}_{\text{cond}}(\omega)] = \omega^2[\mathcal{C}^{(ij)}]^T[\mathcal{A}^{(i)}(\omega)]^{-1}[\mathcal{C}^{(ij)}]$ in low frequency range and $[\mathcal{A}^{(i)}_{\text{cond}}(\omega)] = [0]$ in medium or high frequency range. In addition, in Eq. (VI.14), the added vector of loads $\mathbf{f}^{(2)}$ is applied on subsystem (2) and corresponds to the pressure due to the acoustic source located in emission volume (1) and is defined as

$$\mathbf{f}^{(2)} = i\omega[\mathcal{C}^{(12)}]^T[\mathcal{A}^{(1)}(\omega)]^{-1}\mathbf{f}^{(1)} \quad . \tag{VI.15}$$

The error related to the two approximations $[\mathcal{A}^{(1)}_{\text{cond}}(\omega)] = [0]$ and $[\mathcal{A}^{(5)}_{\text{cond}}(\omega)] = [0]$ in medium or high frequency is quantified by analysing the three error functions $\omega \mapsto \text{error}^{(j)}$ defined as, for $j = 2,3,4$

$$\text{error}^{(j)}(\omega) = \frac{\|\mathbf{q}^{(j)}(\omega) - \mathbf{q}^{(j),\text{ref}}(\omega)\|_2}{\|\mathbf{q}^{(j),\text{ref}}(\omega)\|_2} \ ,$$

where $\|\cdot\|_2$ is the Frobenius norm of a vector, $\omega \mapsto \mathbf{q}^{(j)}(\omega)$ is calculated with $[\mathcal{A}^{(1)}_{\text{cond}}(\omega)] = [0]$ and $[\mathcal{A}^{(5)}_{\text{cond}}(\omega)] = [0]$, and where $\omega \mapsto \mathbf{q}^{(j),\text{ref}}(\omega)$ is the reference solution calculated with $[\mathcal{A}^{(1)}_{\text{cond}}(\omega)] \neq [0]$ and $[\mathcal{A}^{(5)}_{\text{cond}}(\omega)] \neq [0]$. The graphs of $\omega \mapsto \text{error}^{(j)}(\omega)$ are presented on Figs. VI.1 to VI.3 for $j = 2,3$ and $j = 4$. The results presented on these figures show that the relative error induced by neglecting $[\mathcal{A}^{(1)}_{\text{cond}}(\omega)]$ and $[\mathcal{A}^{(5)}_{\text{cond}}(\omega)]$ is smaller than 5% for $\omega/2\pi > 500$ Hz. Consequently, the approximations $[\mathcal{A}^{(1)}_{\text{cond}}(\omega)] = [0]$ and $[\mathcal{A}^{(5)}_{\text{cond}}(\omega)] = [0]$ are acceptable only for $\omega/2\pi > 500$ Hz.

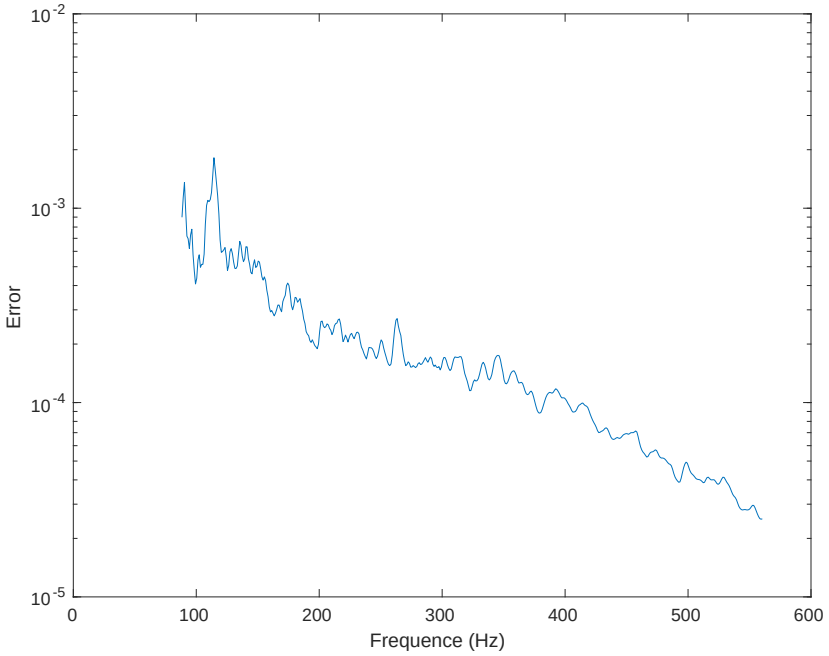

Figure VI.1 – Error related to approximations $[\mathcal{A}^{(1)}_{\text{cond}}(\omega)] = [0]$ and $[\mathcal{A}^{(5)}_{\text{cond}}(\omega)] = [0]$ on solution $\mathbf{q}^{(2)}$. Horizontal axis: frequency $\omega/2\pi$ in Hz. Vertical axis: $\text{error}^{(2)}(\omega)$.

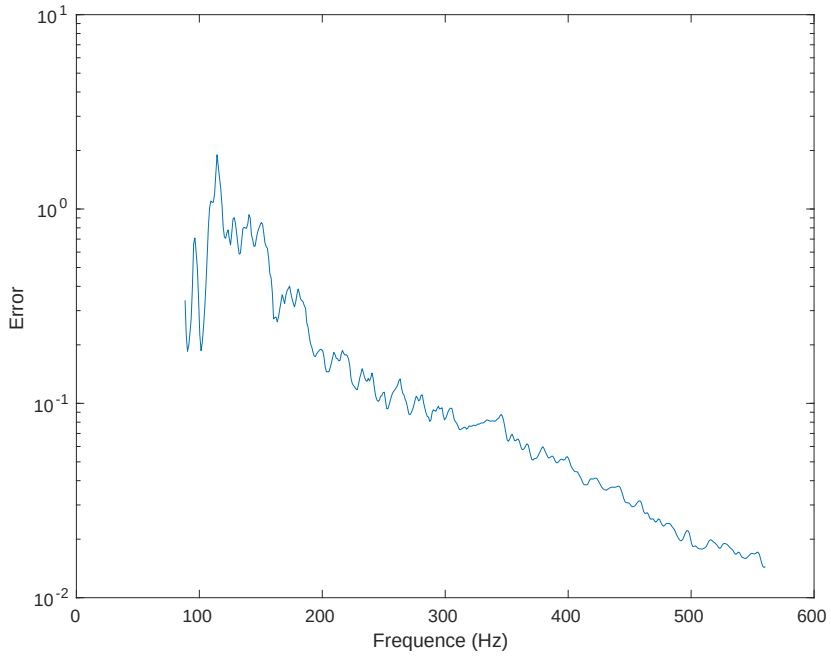

Figure VI.2 – Error related to approximations $[\mathcal{A}^{(1)}_{\text{cond}}(\omega)] = [0]$ and $[\mathcal{A}^{(5)}_{\text{cond}}(\omega)] = [0]$ on solution $\mathbf{q}^{(3)}$. Horizontal axis: frequency $\omega/2\pi$ in Hz. Vertical axis: error$^{(3)}(\omega)$.

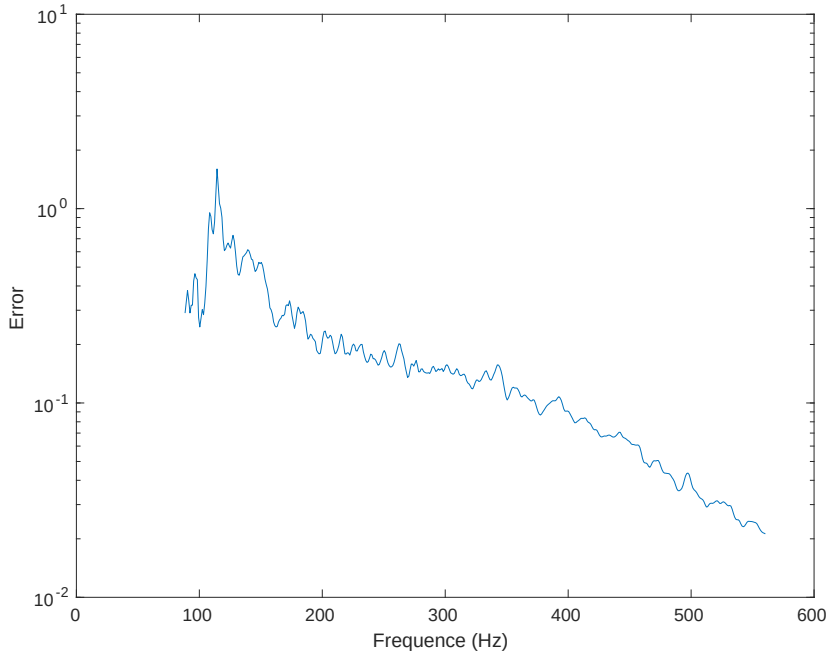

Figure VI.3 – Error related to approximations $[\mathcal{A}^{(1)}_{\text{cond}}(\omega)] = [0]$ and $[\mathcal{A}^{(5)}_{\text{cond}}(\omega)] = [0]$ on solution $\mathbf{q}^{(4)}$. Horizontal axis: frequency $\omega/2\pi$ in Hz. Vertical axis: error$^{(4)}(\omega)$.

CHAPTER VII

Modal Analysis and Condensed Reduced-Order Computational Models

The reduced-order model introduced in last chapter might still have a high computational cost that is due to the high modal density in medium and high frequency domain. In this manuscript, we decide to work in limited frequency bands, in which the number of associated eigenmodes is also limited. Nevertheless, a truncation of the generalised coordinates associated with eigenfrequencies outside the limited frequency band of analysis is not an acceptable approach in the case of multi-coupled fluid solid systems. Inspired by existing models [23, 70–74], a Condensed Reduced-Order Models (CROM) is developed for Model 1 and Model 2 (see Chapter. II). This new model is based on a modal analysis that is carried out for selecting only the generalised coordinates with non negligible contributions for the solution of the problem, especially for the case of highly dissipative system. As a result, as for [34, 35, 75–78], some non-resonant eigenmodes (for which the modal eigenfrequency does not belong to the limited frequency band of analysis) should not be ignored by truncation and must be included into the model as well as all the other resonant eigenmodes (for which the modal eigenfrequency belongs to the limited frequency band of analysis). A sequence of Schur complements [69] is used in order to reduce the dimensionality of the generalised coordinates vector for explicitly writing the equations only in terms of generalised coordinates associated with resonant eigenvectors. Consequently, non-resonant generalised coordinates, those for which the associated eigenfrequency does not belong to the limited frequency B, are either truncated or condensed. More details on how the non-resonant eigenmodes are selected are given in the following sections of this chapter. Finally, the CROM developed in this chapter will be used for constructing an energy formulation that is based on SEA principles for an ensemble of resonators, namely the generalised coordinates associated with the resonant eigenmodes in each limited frequency band.

VII.1 Methodology for constructing the Condensed Reduced Order Model (CROM)

In this section, an additional reduction is carried out on the ROM presented in chapter VI in order to be able to circumvent the dimensionality curse when the ROM is used with a high modal density. The approach consists in solving the problem of forced response for a multi-coupled fluid-solid system for a set of limited frequency bands $B_1,\ldots,B_{N_{\text{bands}}}$ that are partitions (in 1/3 octave, for instance) of the full frequency band of analysis denoted as $\mathbb{B}$. We then have $\mathbb{B} = B_1 \cup \cdots \cup B_{N_{\text{bands}}}$. For any limited frequency band B, the computational cost as well as the memory cost for performing the calculations are decreased a lot, because only the calculation between the eigenmodes with eigenfrequencies in B for each subsystem (the so called resonant eigenmodes) are carried out. Nevertheless, it is impossible to achieve such a reduction by simply doing a truncation of $\mathbf{u}^{(2)}_{n_2}$, $\mathbf{u}^{(4)}_{n_4}$, $\varphi^{(1)}_{n_1}$, $\varphi^{(3)}_{n_3}$ and $\varphi^{(5)}_{n_5}$ of solutions $\mathbf{u}^{(2)}$, $\mathbf{u}^{(4)}$, $\varphi^{(1)}$, $\varphi^{(3)}$ and $\varphi^{(5)}$, respectively, on the resonant eigenmodes only. Indeed, in many works [34, 35, 75–78], authors have pointed out there is a non-negligible contribution of the non-resonant eigenmodes (that is to say, the eigenmodes for which the eigenfrequencies do not belong to frequency band B) of panel or of heavy fluid. These non-resonant eigenmodes are in fact involved into the couplings between the generalised coordinates associated with the resonant eigenmodes of different subsystems. The frequency bands B^+ and B^- correspond to the eigenfrequencies of the non-resonant eigenmodes when the modal analysis is carried out on frequency band B, such that frequencies $\omega \in B$, $\omega^+ \in B^+$ and $\omega^- \in B^-$ are such that $\omega^- < \omega < \omega^+$. Figure VII.1 illustrates how non-resonant eigenmodes and resonant eigenmodes are coupled in a multi-coupled fluid-solid system. The thin solid black lines correspond to couplings between resonant eigenmodes of two subsystems. The blue dotted lines correspond to couplings between resonant and non-resonant modes of two different subsystems. Finally, the red dotted lines correspond to the couplings between non-resonant eigenmodes of two different subsystems. In using a similar approach than in [35], the generalised vector of coordinates $\mathbf{q}^{(i)}$ of subsystem (i) is decomposed into three parts $\mathbf{q}^{(i)} = (\mathbf{q}^{(i)}_{B^+}, \mathbf{q}^{(i)}_{B}, \mathbf{q}^{(i)}_{B^-})$ in which $\mathbf{q}^{(i)}_{B^+}$, $\mathbf{q}^{(i)}_{B}$ and $\mathbf{q}^{(i)}_{B^-}$ are the vectors of the generalised coordinates for subsystem (i) associated with eigenmodes whose eigenfrequencies belong to B^+, B and B^-, respectively. The generalised coordinates $\mathbf{q}^{(i)}_{B^+}$ and $\mathbf{q}^{(i)}_{B^-}$ are eliminated in Eq. (VI.13) by using either a truncated reduction or a sequence of Schur complements. Indeed, following the principles presented in [34, 79, 80] and applying them to the multi-coupled fluid-solid system studied in this manuscript (see Chapter II), for a heavy fluid coupled with a solid as for the medium occupying subsystem (3), eliminating $\mathbf{q}^{(3)}_{B^-}$ by using a Schur complement modifies the dynamic stiffness operator whose main altering part can be interpreted as an added stiffness for subsystems (2) and (4). In addition, eliminating $\mathbf{q}^{(3)}_{B^+}$ modifies also the dynamic stiffness operator whose main altered part can be interpreted as an added mass for subsystems (2) and (4). Nevertheless, for other acoustic fluid media, like normal air in subsystems (1) and (5), such an eliminating of the non-resonant generalised coordinates

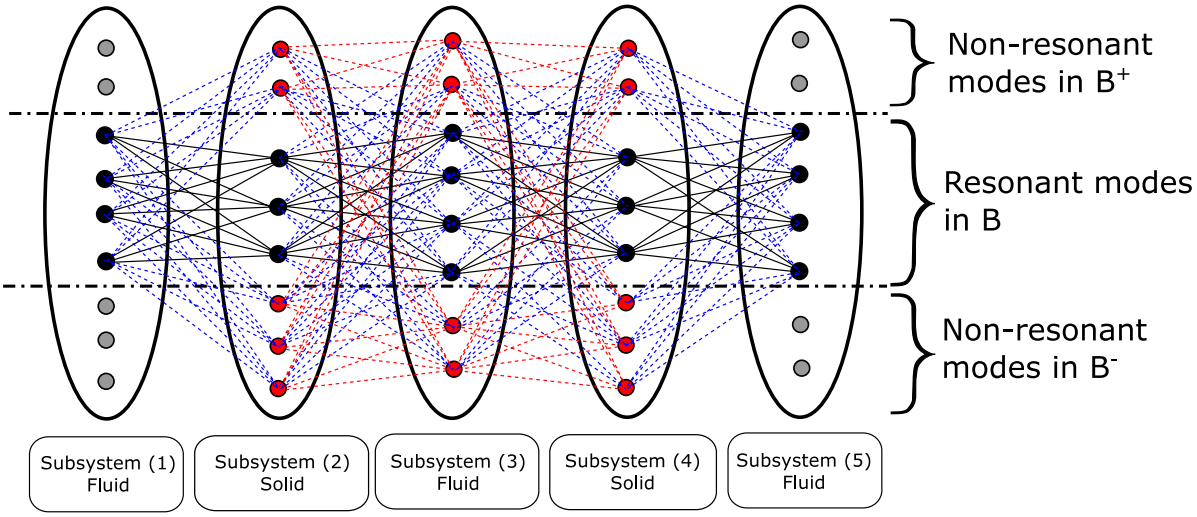

Figure VII.1 – Illustration of the non-negligible couplings between generalised coordinates for a multi-coupled fluid-solid system. In thin solid lines: couplings between resonant generalised coordinates. In blue dotted lines: Couplings between resonant and non-resonant generalised coordinates. In red dotted line: Couplings between non-resonant generalised coordinates. Plain red bullets: Non-negligible non-resonant generalised coordinates. Plain black bullets: Resonant generalised coordinates. Plain grey bullets: Negligible non-resonant generalised coordinates.

$\mathbf{q}^{(1)}_{B^+}$, $\mathbf{q}^{(1)}_{B^-}$, $\mathbf{q}^{(5)}_{B^+}$, $\mathbf{q}^{(5)}_{B^-}$ yields negligible altering of the dynamic stiffness as its mass density is very small. In this case, the reduction consists in simply eliminating the non-resonant generalised coordinates by truncating the modal expansions $\varphi^{(1)}_{n_1}$ and $\varphi^{(5)}_{n_5}$ on the resonant eigenmodes only. Concerning the two viscoelastic solid media occupying subsystems (2) and (4), many works [34, 35, 75–78] on different coupled fluid-solid systems brought interesting results. Following these results, in case subsystems (2) and (4) are panels, non-negligible contributions from $\mathbf{q}^{(2)}_{B^-}$ and $\mathbf{q}^{(4)}_{B^-}$ and negligible contributions from $\mathbf{q}^{(2)}_{B^+}$ and $\mathbf{q}^{(4)}_{B^+}$ are expected. Nevertheless, we did not observe negligible contributions from the latter and it is the reason why, for constructing the CROM, a sequence of Schur complements denoted as $[\mathcal{A}]/[\mathcal{A}^{(2)}_{B^-}]$, $[\mathcal{A}]/[\mathcal{A}^{(2)}_{B^+}]$, $[\mathcal{A}]/[\mathcal{A}^{(4)}_{B^-}]$ and $[\mathcal{A}]/[\mathcal{A}^{(4)}_{B^+}]$ of block matrices $[\mathcal{A}^{(2)}_{B^-}]$, $[\mathcal{A}^{(2)}_{B^+}]$, $[\mathcal{A}^{(4)}_{B^-}]$ and $[\mathcal{A}^{(4)}_{B^+}]$, which are associated to generalised coordinates $\mathbf{q}^{(2)}_{B^-}$, $\mathbf{q}^{(2)}_{B^-}$, $\mathbf{q}^{(2)}_{B^-}$ and $\mathbf{q}^{(4)}_{B^+}$ respectively, are carried out without combining them with any truncation of $\mathbf{q}^{(2)}_{B^+}$ and $\mathbf{q}^{(4)}_{B^+}$ in the modal expansions of $\mathbf{u}^{(2)}_{n_2}$ and $\mathbf{u}^{(4)}_{n_4}$.

VII.2 Dimensionality reduction by sequencing Schur complements

Guyan reduction [81] is a dimensionality reduction method, which requires the calculation of a Schur complement [69] and by ignoring inertial contributions. In this manuscript, we do not use the Guyan reduction but we rather use sequences of Schur complements to obtain a dimensionality reduction of the ROM. After truncating all negligible non-resonant generalised

coordinates (plain grey bullets in Fig. VII.1) in the ROM, the dimensionality of non-negligible non-resonant generalised coordinates (plain red bullets in Fig. VII.1) is still important and can be prohibitive for numerical simulations. Most of non-negligible non-resonant generalised coordinated are associated with eigenfrequencies belonging to HF domain. The main advantage of using a sequence of Schur complements consists in being able to reduce the dimension of the matrices of the problem by condensing all non-negligible non-resonant generalised coordinates without losing important information, which would be the case with a simple truncation of the modal expansion of the solution. As shown in Fig. VII.1, couplings with non-negligible non-resonant generalised coordinates create an energy path between different subsystems. Any truncation of the modal expansions would remove such energy path and it would not be correct. Using a Schur complement for reducing the dimensionality allows keeping implicitly all the energy paths, even those that are related to the eliminated generalised coordinates. The couplings related to the eliminated generalised coordinates are named “implicit couplings” in next sections of this manuscript. A simple example is presented in Appendix. A.

VII.3 Condensed Reduced Order Model for Model 1

As presented in Chapter II and in Fig. II.1, for Model 1, the generalised coordinate vectors for two air volumes (systems (1) and (5)) are included explicitly in the system of equations for the ROM in Eq. (VI.13). Hereinafter, we present the construction of the CROM for Model 1. Let B be any limited frequency bands $B_1,\dots,B_{N_{\text{bands}}}$ involved in the partition of the global frequency band $\mathbb{B} = B_1 \cup \cdots \cup B_{N_{\text{bands}}}$. According to the discussion in Section VII.1, vector of the generalised coordinates $\mathbf{q}$ is block-decomposed into vectors $\mathbf{q} = (\mathbf{q}^{(1)}, \mathbf{q}^{(2)}, \mathbf{q}^{(3)}, \mathbf{q}^{(4)}, \mathbf{q}^{(5)})$ with the additional block-decomposition $\mathbf{q}^{(i)} = (\mathbf{q}^{(i)}_{B^+}, \mathbf{q}^{(i)}_{B}, \mathbf{q}^{(i)}_{B^-})$ of resonant and non-resonant generalised coordinates for an analysis in frequency band B and for $i = 1,\dots,5$. The block-decomposition of vector $\mathbf{q}$ is then written as

$$\mathbf{q} = (\mathbf{q}^{(1)}_{B^+}, \mathbf{q}^{(1)}_{B}, \mathbf{q}^{(1)}_{B^-}, \mathbf{q}^{(2)}_{B^+}, \mathbf{q}^{(2)}_{B}, \mathbf{q}^{(2)}_{B^-}, \mathbf{q}^{(3)}_{B^+}, \mathbf{q}^{(3)}_{B}, \mathbf{q}^{(3)}_{B^-}, \mathbf{q}^{(4)}_{B^+}, \mathbf{q}^{(4)}_{B}, \mathbf{q}^{(4)}_{B^-}, \mathbf{q}^{(5)}_{B^+}, \mathbf{q}^{(5)}_{B}, \mathbf{q}^{(5)}_{B^-}) \quad .$$

The modal truncation consists in removing $\mathbf{q}^{(1)}_{B^+}$, $\mathbf{q}^{(1)}_{B^-}$, $\mathbf{q}^{(5)}_{B^+}$, $\mathbf{q}^{(5)}_{B^-}$ (see Fig.VII.1) from equations and removing the corresponding rows and columns in dynamic stiffness on the left-hand side of Eq. (VI.13). The block-decomposition of vector $\mathbf{q}$ is then rewritten as

$$\mathbf{q} = (\mathbf{q}^{(1)}_{B}, \mathbf{q}^{(2)}_{B^+}, \mathbf{q}^{(2)}_{B}, \mathbf{q}^{(2)}_{B^-}, \mathbf{q}^{(3)}_{B^+}, \mathbf{q}^{(3)}_{B}, \mathbf{q}^{(3)}_{B^-}, \mathbf{q}^{(4)}_{B^+}, \mathbf{q}^{(4)}_{B}, \mathbf{q}^{(4)}_{B^-}, \mathbf{q}^{(5)}_{B}) \quad ,$$

This truncation is validated by a numerical experiment that consists in calculating the graphs of 8 error functions $\omega \mapsto \text{error}^{(j),\text{TRUNC}}_{B}(\omega)$ with $B = B_1,\dots,B_8$ and for $j = 1,\dots,5$ for Model 1, such that

$$\text{error}^{(j),\text{TRUNC}}_{B}(\omega) = \frac{\|\mathbf{q}^{(j)}_{B}(\omega) - \mathbf{q}^{(j),\text{ref}}_{B}(\omega)\|_2}{\|\mathbf{q}^{(j),\text{ref}}_{B}(\omega)\|_2} \ ,$$

where $\|\cdot\|_2$ is the Frobenius norm of a vector, $\omega \mapsto \mathbf{q}_B^{(j)}(\omega)$ is calculated by removing the non-resonant generalised coordinates from the fluid volumes (i.e. $\mathbf{q}_{B^+}^{(1)}$, $\mathbf{q}_{B^-}^{(1)}$, $\mathbf{q}_{B^+}^{(5)}$, $\mathbf{q}_{B^-}^{(5)}$) and where $\omega \mapsto \mathbf{q}_B^{(j),\mathrm{ref}}(\omega)$ is the reference solution calculated without any such a truncation from the model. The graphs of $\omega \mapsto \mathrm{error}_B^{(j),\mathrm{TRUNC}}(\omega)$ are presented on Fig. VII.2 for $B = B_1, \ldots, B_6$ with different line colours for each bands $B = B_1, \ldots, B_6$ and for $j = 1, \ldots, 5$ (Figs. (a) to (e), respectively). The results presented on this figure show that the relative error induced by the considered truncation is low enough for $\omega/2\pi > 445$ Hz and consequently, it validates its use only after 445 Hz. Consequently, Eq. (VI.13) is rewritten as

$$
\begin{bmatrix}
[\mathcal{A}_B^{(1)}(\omega)] & -i\omega[\mathcal{C}_{BB^-}^{(12)}] & -i\omega[\mathcal{C}_B^{(12)}] & -i\omega[\mathcal{C}_{BB^+}^{(12)}] & & & & & & & & & \\
i\omega[\mathcal{C}_{B^-B}^{(21)}] & [\mathcal{A}_{B^-}^{(2)}(\omega)] & & & i\omega[\mathcal{C}_{B^-B^-}^{(23)}] & i\omega[\mathcal{C}_{B^-B}^{(23)}] & i\omega[\mathcal{C}_{B^-B^+}^{(23)}] & & & & & & \\
i\omega[\mathcal{C}_B^{(21)}] & & [\mathcal{A}_B^{(2)}(\omega)] & & i\omega[\mathcal{C}_{BB^-}^{(23)}] & i\omega[\mathcal{C}_B^{(23)}] & i\omega[\mathcal{C}_{BB^+}^{(23)}] & & & & & & \\
i\omega[\mathcal{C}_{B^+B}^{(21)}] & & & [\mathcal{A}_{B^+}^{(2)}(\omega)] & i\omega[\mathcal{C}_{B^+B^-}^{(23)}] & i\omega[\mathcal{C}_{B^+B}^{(23)}] & i\omega[\mathcal{C}_{B^+}^{(23)}] & & & & & & \\
 & -i\omega[\mathcal{C}_{B^-}^{(32)}] & -i\omega[\mathcal{C}_{B^-B}^{(32)}] & -i\omega[\mathcal{C}_{B^-B^+}^{(32)}] & [\mathcal{A}_{B^-}^{(3)}(\omega)] & & & -i\omega[\mathcal{C}_{B^-}^{(34)}] & -i\omega[\mathcal{C}_{B^-B}^{(34)}] & -i\omega[\mathcal{C}_{B^-B^+}^{(34)}] & & & \\
 & -i\omega[\mathcal{C}_{BB^-}^{(32)}] & -i\omega[\mathcal{C}_B^{(32)}] & -i\omega[\mathcal{C}_{BB^+}^{(32)}] & & [\mathcal{A}_B^{(3)}(\omega)] & & -i\omega[\mathcal{C}_{BB^-}^{(34)}] & -i\omega[\mathcal{C}_B^{(34)}] & -i\omega[\mathcal{C}_{BB^+}^{(34)}] & & & \\
 & -i\omega[\mathcal{C}_{B^+B^-}^{(32)}] & -i\omega[\mathcal{C}_{B^+B}^{(32)}] & -i\omega[\mathcal{C}_{B^+}^{(32)}] & & & [\mathcal{A}_{B^+}^{(3)}(\omega)] & -i\omega[\mathcal{C}_{B^+B^-}^{(34)}] & -i\omega[\mathcal{C}_{B^+B}^{(34)}] & -i\omega[\mathcal{C}_{B^+}^{(34)}] & & & \\
 & & & & i\omega[\mathcal{C}_{B^-}^{(43)}] & i\omega[\mathcal{C}_{B^-B}^{(43)}] & i\omega[\mathcal{C}_{B^-B^+}^{(43)}] & [\mathcal{A}_{B^-}^{(4)}(\omega)] & & & & i\omega[\mathcal{C}_{B^-B}^{(45)}] & \\
 & & & & i\omega[\mathcal{C}_{BB^-}^{(43)}] & i\omega[\mathcal{C}_B^{(43)}] & i\omega[\mathcal{C}_{BB^+}^{(43)}] & & [\mathcal{A}_B^{(4)}(\omega)] & & & i\omega[\mathcal{C}_B^{(45)}] & \\
 & & & & i\omega[\mathcal{C}_{B^+B^-}^{(43)}] & i\omega[\mathcal{C}_{B^+B}^{(43)}] & i\omega[\mathcal{C}_{B^+}^{(43)}] & & & & [\mathcal{A}_{B^+}^{(4)}(\omega)] & i\omega[\mathcal{C}_{B^+B}^{(45)}] & \\
 & & & & & & & -i\omega[\mathcal{C}_{BB^-}^{(54)}] & -i\omega[\mathcal{C}_B^{(54)}] & -i\omega[\mathcal{C}_{BB^+}^{(54)}] & [\mathcal{A}_B^{(5)}(\omega)] & &
\end{bmatrix}
\left\{
\begin{array}{l}
\mathbf{q}_B^{(1)} \\ \mathbf{q}_{B^-}^{(2)} \\ \mathbf{q}_B^{(2)} \\ \mathbf{q}_{B^+}^{(2)} \\ \mathbf{q}_{B^-}^{(3)} \\ \mathbf{q}_B^{(3)} \\ \mathbf{q}_{B^+}^{(3)} \\ \mathbf{q}_{B^-}^{(4)} \\ \mathbf{q}_B^{(4)} \\ \mathbf{q}_{B^+}^{(4)} \\ \mathbf{q}_B^{(5)}
\end{array}
\right\}
=
\left\{
\begin{array}{l}
\mathbf{f}_B^{(1)} \\ 0 \\ 0 \\ 0 \\ 0 \\ 0 \\ 0 \\ 0 \\ 0 \\ 0 \\ 0
\end{array}
\right\},
\tag{VII.1}
$$

where $\mathbf{f}_B^{(1)}$ is the vector involved into the block-decomposition of vector $\mathbf{f}^{(1)} = (\mathbf{f}_{B^+}^{(1)}, \mathbf{f}_B^{(1)}, \mathbf{f}_{B^-}^{(1)})$. Hereinafter, the matrix-valued generalised dynamical stiffness in left-hand side of Eq. (VII.1) is denoted as $[\mathcal{A}(\omega)]$. In order to eliminate $\mathbf{q}_{B^+}^{(3)}$ from equations, the Schur complement $[\mathcal{A}^{\mathrm{SC}_1}(\omega)]$ of block-matrix $[\mathcal{A}_{B^+}^{(3)}]$ in $[\mathcal{A}(\omega)]$ is calculated. Note that, at this stage, all the block-matrices are altered and affected by the Schur complement calculation. Nevertheless, for the sake of simplicity, we continue to denote the altered block-matrices in $[\mathcal{A}^{\mathrm{SC}_1}(\omega)]$ with the same notation we used for the block-decomposition of $[\mathcal{A}(\omega)]$. Then, using this notation convention, $\mathbf{q}_{B^-}^{(3)}$ is eliminated by calculating the Schur complements $[\mathcal{A}^{\mathrm{SC}_2}(\omega)]$ of block-matrix $[\mathcal{A}_{B^-}^{(3)}]$ in $[\mathcal{A}^{\mathrm{SC}_1}(\omega)]$. Note that in practice, this sequence of two Schur complements is carried out as only one Schur complement calculation. Once again, we use the same convention for denoting the block-matrices of $[\mathcal{A}^{\mathrm{SC}_2}(\omega)]$. The next two steps consist in eliminating $\mathbf{q}_{B^+}^{(2)}$ and $\mathbf{q}_{B^-}^{(2)}$ by calculating the Schur complements $[\mathcal{A}^{\mathrm{SC}_3}(\omega)]$ of block-matrices $[\mathcal{A}_{B^+}^{(2)}]$ and $[\mathcal{A}_{B^-}^{(2)}]$ in $[\mathcal{A}^{\mathrm{SC}_2}(\omega)]$. Using same convention for denoting block-matrices of $[\mathcal{A}^{\mathrm{SC}_3}(\omega)]$, the CROM is finally constructed in eliminating $\mathbf{q}_{B^+}^{(4)}$ and $\mathbf{q}_{B^-}^{(4)}$ by calculating the Schur complements $[\mathcal{A}^{\mathrm{SC}_4}(\omega)]$ of block-matrices $[\mathcal{A}_{B^-}^{(4)}]$ and $[\mathcal{A}_{B^-}^{(4)}]$ in $[\mathcal{A}^{\mathrm{SC}_3}(\omega)]$. It should be noted that the sequence order that we have used, mainly it is eliminating $\mathbf{q}_{B^+}^{(3)}$ before others, allows minimising the computational cost of the whole sequence of Schur complements because any other order would have yielded full complex-valued block-matrix $[\mathcal{A}_{B^+}^{(3)}]$ to be inverted while it is the biggest block-matrix of the problem. On the other hand, block-matrix $[\mathcal{A}_{B^+}^{(3)}]$ in $[\mathcal{A}(\omega)]$ is diagonal and, in this case, the computational cost for calculating its inverse is almost

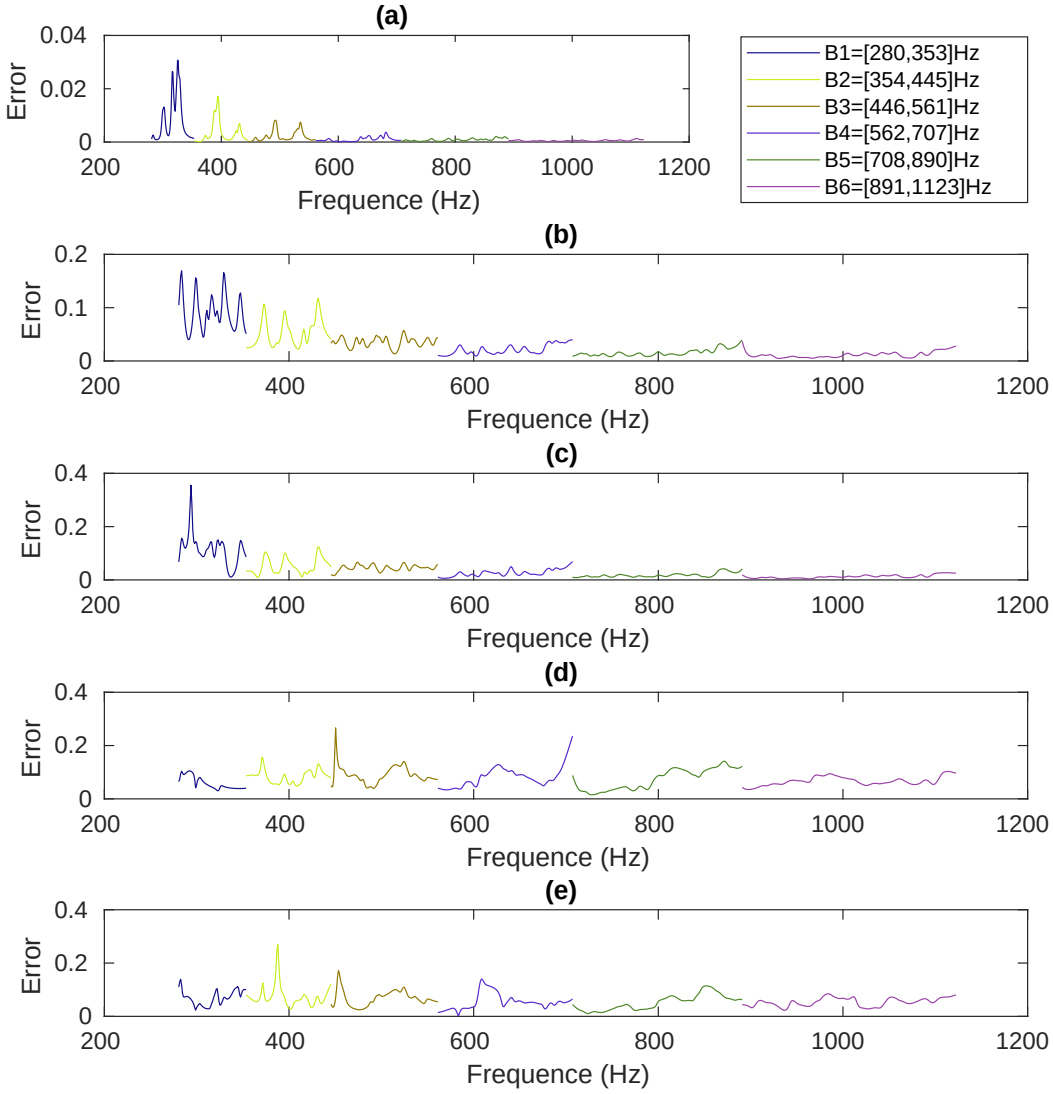

Figure VII.2 – Quantification of the error due to the truncation of the non-resonant modes from the acoustic fluid volumes. Graphs of the error functions $\omega \mapsto \text{error}_B^{(j),\text{TRUNC}}(\omega)$ with $B = B_1, \ldots, B_6$ for 6 bands in 1/3 octave and for $j = 1, \ldots, 5$ (Figs. (a) to (e), respectively).

null. Consequently, solving Eq. (VII.1) is equivalent to solve the following matrix equation

$$\begin{bmatrix} [\mathbb{Z}_B^{(1)}(\omega)] & [\mathbb{W}_B^{(12)}(\omega)] & [\mathbb{V}_B^{(13)}(\omega)] & [\mathbb{W}_B^{(14)}(\omega)] & [\mathbb{V}_B^{(15)}(\omega)] \\ [\mathbb{W}_B^{(21)}(\omega)] & [\mathbb{Z}_B^{(2)}(\omega)] & [\mathbb{W}_B^{(23)}(\omega)] & [\mathbb{V}_B^{(24)}(\omega)] & [\mathbb{W}_B^{(25)}(\omega)] \\ [\mathbb{V}_B^{(31)}(\omega)] & [\mathbb{W}_B^{(32)}(\omega)] & [\mathbb{Z}_B^{(3)}(\omega)] & [\mathbb{W}_B^{(34)}(\omega)] & [\mathbb{V}_B^{(35)}(\omega)] \\ [\mathbb{W}_B^{(41)}(\omega)] & [\mathbb{V}_B^{(42)}(\omega)] & [\mathbb{W}_B^{(43)}(\omega)] & [\mathbb{Z}_B^{(4)}(\omega)] & [\mathbb{W}_B^{(45)}(\omega)] \\ [\mathbb{V}_B^{(51)}(\omega)] & [\mathbb{W}_B^{(52)}(\omega)] & [\mathbb{V}_B^{(53)}(\omega)] & [\mathbb{W}_B^{(54)}(\omega)] & [\mathbb{Z}_B^{(5)}(\omega)] \end{bmatrix} \begin{Bmatrix} \mathbf{q}_B^{(1)} \\ \mathbf{q}_B^{(2)} \\ \mathbf{q}_B^{(3)} \\ \mathbf{q}_B^{(4)} \\ \mathbf{q}_B^{(5)} \end{Bmatrix} = \begin{Bmatrix} \mathbf{f}_B^{(1)} \\ 0 \\ 0 \\ 0 \\ 0 \end{Bmatrix}, \qquad \text{(VII.2)}$$

where the matrix in the left-hand side of Eq. (VII.2) is the block-decomposition of matrix $[\mathcal{A}^{\mathrm{SC}_4}(\omega)]$ in which complex-valued block-matrices $[\mathbb{Z}_B^{(i)}(\omega)]$, $[\mathbb{W}_B^{(ij)}(\omega)]$ and $[\mathbb{V}_B^{(ij)}(\omega)]$ for $i,j=1,\ldots,5$ are full matrices and are given in details in Appendix. B. The coupling matrices are either symmetric or antisymmetric, their properties are listed below,

$$
\begin{aligned}
&[\mathbb{W}_B^{(21)}(\omega)] = -[\mathbb{W}_B^{(12)}(\omega)]^T \quad , \quad [\mathbb{W}_B^{(41)}(\omega)] = -[\mathbb{W}_B^{(14)}(\omega)]^T \quad , \quad [\mathbb{W}_B^{(32)}(\omega)] = -[\mathbb{W}_B^{(23)}(\omega)]^T \quad ,\\
&[\mathbb{W}_B^{(52)}(\omega)] = -[\mathbb{W}_B^{(25)}(\omega)]^T \quad , \quad [\mathbb{W}_B^{(43)}(\omega)] = -[\mathbb{W}_B^{(34)}(\omega)]^T \quad , \quad [\mathbb{W}_B^{(54)}(\omega)] = -[\mathbb{W}_B^{(45)}(\omega)]^T \quad ,\\
&[\mathbb{V}_B^{(31)}(\omega)] = [\mathbb{V}_B^{(13)}(\omega)]^T \quad , \quad [\mathbb{V}_B^{(51)}(\omega)] = [\mathbb{V}_B^{(15)}(\omega)]^T \quad , \quad [\mathbb{V}_B^{(42)}(\omega)] = [\mathbb{V}_B^{(24)}(\omega)]^T \quad ,\\
&[\mathbb{V}_B^{(53)}(\omega)] = [\mathbb{V}_B^{(35)}(\omega)]^T \quad .
\end{aligned}
$$

The validity of the CROM for Model 1 is quantified by calculating the error functions $\mathrm{error}_B^{(j),\mathrm{CROM}}(\omega)$ with $B=B_1,\ldots,B_6$ and $j=1,\ldots,5$ such that

$$
\mathrm{error}_B^{(j),\mathrm{CROM}}(\omega) = \frac{\|\mathbf{q}_B^{(j)}(\omega)-\mathbf{q}_B^{(j),\mathrm{ref}}(\omega)\|_2}{\|\mathbf{q}_B^{(j),\mathrm{ref}}(\omega)\|_2} \quad ,
$$

where $\omega \mapsto \mathbf{q}_B^{(j)}(\omega)$ is solution of the CROM and where $\omega \mapsto \mathbf{q}_B^{(j),\mathrm{ref}}(\omega)$ is the reference solution of the ROM. The graphs of $\omega \mapsto \mathrm{error}_B^{(j),\mathrm{CROM}}(\omega)$ are presented on Fig. VII.3 for $B=B_1,\ldots,B_6$ with different line colours for each bands $B=B_1,\ldots,B_6$ and for $j=1,\ldots,5$ (Figs. (a) to (e) respectively). The results presented on this figure show that the relative error in using the CROM is low enough and consequently, it validates the CROM for Model 1.

VII.4 Condensed Reduced Order Model for Model 2

As presented in Chapter II and in Fig. II.2, in Model 2 approximation, the generalised coordinates vectors of air volumes (subsystems (1) and (5)) are removed from the equations of the ROM in using a Schur complement. We then obtained Eq. (VI.14). Hereinafter, we present the construction of the CROM for Model 2. In this case, the block-decomposition of vector $\mathbf{q}$ in Eq. (VI.14) is written as

$$
\mathbf{q} = (\mathbf{q}_{B^+}^{(2)}, \mathbf{q}_B^{(2)}, \mathbf{q}_{B^-}^{(2)}, \mathbf{q}_{B^+}^{(3)}, \mathbf{q}_B^{(3)}, \mathbf{q}_{B^-}^{(3)}, \mathbf{q}_{B^+}^{(4)}, \mathbf{q}_B^{(4)}, \mathbf{q}_{B^-}^{(4)}) \quad .
$$

and Eq. (VI.14) is rewritten as

$$
\begin{bmatrix}
[\mathcal{A}_{B^-}^{(2)}(\omega)] & & & i\omega[\mathcal{C}_{B^-B^-}^{(23)}] & i\omega[\mathcal{C}_{B^-B}^{(23)}] & i\omega[\mathcal{C}_{B^-B^+}^{(23)}] & & & & & & \\
& [\mathcal{A}_B^{(2)}(\omega)] & & i\omega[\mathcal{C}_{BB^-}^{(23)}] & i\omega[\mathcal{C}_B^{(23)}] & i\omega[\mathcal{C}_{BB^+}^{(23)}] & & & & & & \\
& & [\mathcal{A}_{B^+}^{(2)}(\omega)] & i\omega[\mathcal{C}_{B^+B^-}^{(23)}] & i\omega[\mathcal{C}_{B^+B}^{(23)}] & i\omega[\mathcal{C}_{B^+}^{(23)}] & & & & & & \\
-i\omega[\mathcal{C}_{B^-}^{(32)}] & -i\omega[\mathcal{C}_{B^-B}^{(32)}] & -i\omega[\mathcal{C}_{B^-B^+}^{(32)}] & [\mathcal{A}_{B^-}^{(3)}(\omega)] & & & -i\omega[\mathcal{C}_{B^-}^{(34)}] & -i\omega[\mathcal{C}_{B^-B}^{(34)}] & -i\omega[\mathcal{C}_{B^-B^+}^{(34)}] & & & \\
-i\omega[\mathcal{C}_{BB^-}^{(32)}] & -i\omega[\mathcal{C}_B^{(32)}] & -i\omega[\mathcal{C}_{BB^+}^{(32)}] & & [\mathcal{A}_B^{(3)}(\omega)] & & -i\omega[\mathcal{C}_{BB^-}^{(34)}] & -i\omega[\mathcal{C}_B^{(34)}] & -i\omega[\mathcal{C}_{BB^+}^{(34)}] & & & \\
-i\omega[\mathcal{C}_{B^+B^-}^{(32)}] & -i\omega[\mathcal{C}_{B^+B}^{(32)}] & -i\omega[\mathcal{C}_{B^+}^{(32)}] & & & [\mathcal{A}_{B^+}^{(3)}(\omega)] & -i\omega[\mathcal{C}_{B^+B^-}^{(34)}] & -i\omega[\mathcal{C}_{B^+B}^{(34)}] & -i\omega[\mathcal{C}_{B^+}^{(34)}] & & & \\
& & & i\omega[\mathcal{C}_{B^-}^{(43)}] & i\omega[\mathcal{C}_{B^-B}^{(43)}] & i\omega[\mathcal{C}_{B^-B^+}^{(43)}] & [\mathcal{A}_{B^-}^{(4)}(\omega)] & & & & & \\
& & & i\omega[\mathcal{C}_{BB^-}^{(43)}] & i\omega[\mathcal{C}_B^{(43)}] & i\omega[\mathcal{C}_{BB^+}^{(43)}] & & [\mathcal{A}_B^{(4)}(\omega)] & & & & \\
& & & i\omega[\mathcal{C}_{B^+B^-}^{(43)}] & i\omega[\mathcal{C}_{B^+B}^{(43)}] & i\omega[\mathcal{C}_{B^+}^{(43)}] & & & & [\mathcal{A}_{B^+}^{(4)}(\omega)] & & \\
\end{bmatrix}
\begin{Bmatrix}
\mathbf{q}_{B^-}^{(2)} \\ \mathbf{q}_B^{(2)} \\ \mathbf{q}_{B^+}^{(2)} \\ \mathbf{q}_{B^-}^{(3)} \\ \mathbf{q}_B^{(3)} \\ \mathbf{q}_{B^+}^{(3)} \\ \mathbf{q}_{B^-}^{(4)} \\ \mathbf{q}_B^{(4)} \\ \mathbf{q}_{B^+}^{(4)}
\end{Bmatrix}
=
\begin{Bmatrix}
\mathbf{f}_{B^-}^{(2)} \\ \mathbf{f}_B^{(2)} \\ \mathbf{f}_{B^+}^{(2)} \\ 0 \\ 0 \\ 0 \\ 0 \\ 0 \\ 0
\end{Bmatrix} ,
\tag{VII.3}
$$

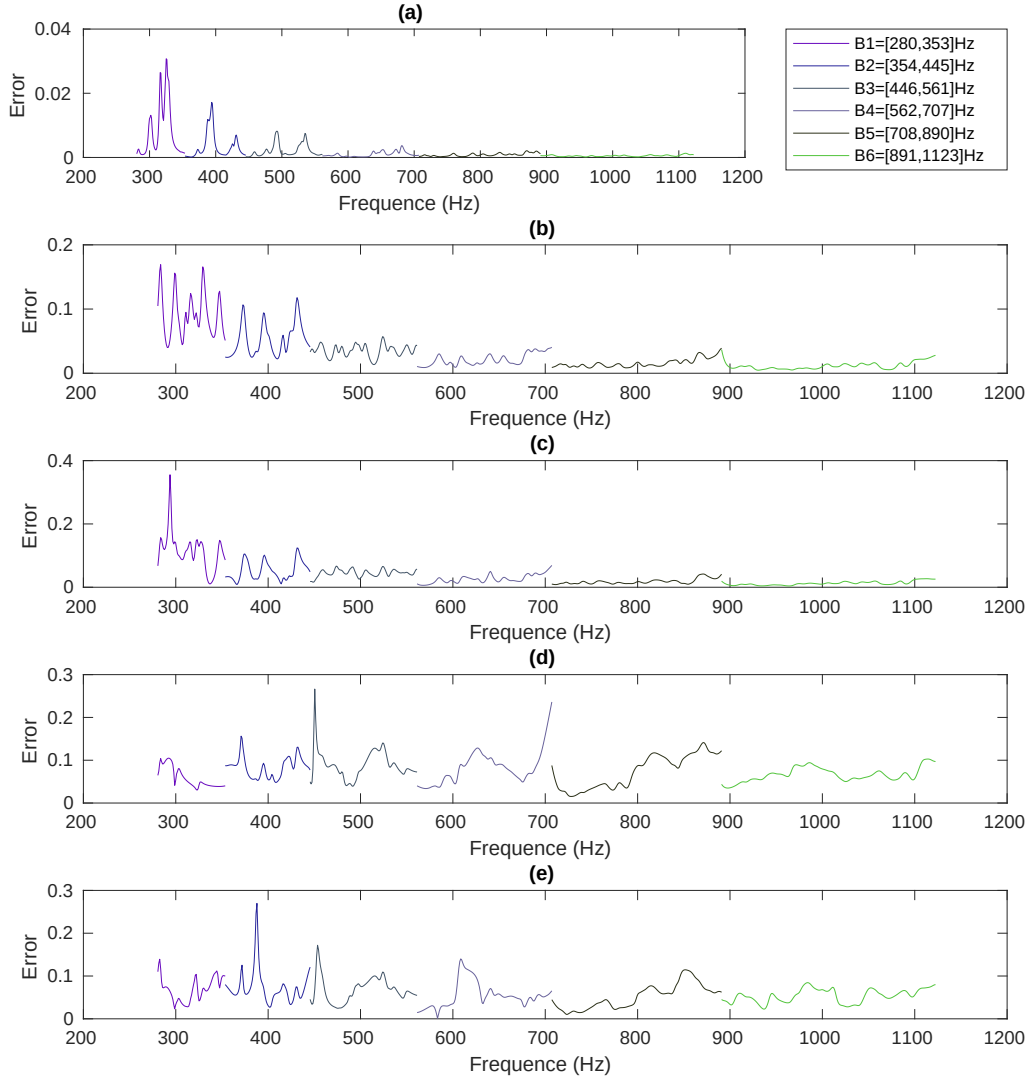

Figure VII.3 – Quantification of the error due to the Schur complements to construct the CROM for Model 1. Graphs of the error functions $\omega \mapsto \text{error}_B^{(j),\text{CROM}}(\omega)$ with $B = B_1, \ldots, B_6$ for 6 bands in 1/3 octave and for $j = 1, \ldots, 5$ (Figs. (a) to (e) respectively).

where $\mathbf{f}_{B^-}^{(2)}$, $\mathbf{f}_B^{(2)}$ and $\mathbf{f}_{B^+}^{(2)}$ are the vectors involved into the block-decomposition of vector $\mathbf{f}^{(2)} = (\mathbf{f}_{B^-}^{(2)}, \mathbf{f}_B^{(2)}, \mathbf{f}_{B^+}^{(2)})$ and $\mathbf{f}^{(2)}$ is defined in Eq. (VI.15). Hereinafter, the matrix-valued generalised dynamical stiffness in left-hand side of Eq. (VII.3) is again, as for Model 1, denoted as $[\mathcal{A}_B(\omega)]$. In order to eliminate $\mathbf{q}_{B^+}^{(3)}$ from equations, the Schur complement $[\mathcal{A}_B^{\text{SC}_1}(\omega)]$ of block-matrix $[\mathcal{A}_{B^+}^{(3)}]$

in $[\mathcal{A}_B(\omega)]$ is calculated. Again, we use the same convention as in section VII.3 for denoting the block-matrices. Then, $\mathbf{q}_{B^-}^{(3)}$ is eliminated by calculating the Schur complements $[\mathcal{A}_B^{\mathrm{SC}_2}(\omega)]$ of block-matrix $[\mathcal{A}_{B^-}^{(3)}]$ in $[\mathcal{A}_B^{\mathrm{SC}_1}(\omega)]$. Note that again, as for Model 1, in practice, this sequence of two Schur complements is carried out as only one Schur complement calculation. Once again, we use the same convention for denoting the block-matrices of $[\mathcal{A}_B^{\mathrm{SC}_2}(\omega)]$. The next two next steps consist in eliminating $\mathbf{q}_{B^+}^{(2)}$ and $\mathbf{q}_{B^-}^{(2)}$ by calculating the Schur complements $[\mathcal{A}^{\mathrm{SC}_3}(\omega)]$ of block-matrices $[\mathcal{A}_{B^+}^{(2)}]$ and $[\mathcal{A}_{B^-}^{(2)}]$ in $[\mathcal{A}^{\mathrm{SC}_2}(\omega)]$. Using same convention for denoting block-matrices of $[\mathcal{A}^{\mathrm{SC}_3}(\omega)]$, the CROM is finally constructed in eliminating $\mathbf{q}_{B^+}^{(4)}$ and $\mathbf{q}_{B^-}^{(4)}$ by calculating the Schur complements $[\mathcal{A}^{\mathrm{SC}_4}(\omega)]$ of block-matrices $[\mathcal{A}_{B^-}^{(4)}]$ and $[\mathcal{A}_{B^-}^{(4)}]$ in $[\mathcal{A}^{\mathrm{SC}_3}(\omega)]$. As for Model 1, the sequence order for the Schur complements allows minimising computational costs. Consequently, solving Eq. (VII.3) is equivalent to solve the following matrix equation

$$\begin{bmatrix} [\mathbb{Z}_B^{(2)}(\omega)] & [\mathbb{W}_B^{(23)}(\omega)] & [\mathbb{V}_B^{(24)}(\omega)] \\ [\mathbb{W}_B^{(32)}(\omega)] & [\mathbb{Z}_B^{(3)}(\omega)] & [\mathbb{W}_B^{(34)}(\omega)] \\ [\mathbb{V}_B^{(42)}(\omega)] & [\mathbb{W}_B^{(43)}(\omega)] & [\mathbb{Z}_B^{(4)}(\omega)] \end{bmatrix} \begin{Bmatrix} \mathbf{q}_B^{(2)} \\ \mathbf{q}_B^{(3)} \\ \mathbf{q}_B^{(4)} \end{Bmatrix} = \begin{Bmatrix} \mathbb{f}_B^{(2)}(\omega) \\ \mathbb{f}_B^{(3)}(\omega) \\ \mathbb{f}_B^{(4)}(\omega) \end{Bmatrix} , \tag{VII.4}$$

where the matrix in the left-hand side of Eq. (VII.4) is the block-decomposition of matrix $[\mathcal{A}_B^{\mathrm{SC}_4}(\omega)]$ in which complex-valued block-matrices $[\mathbb{Z}_B^{(i)}]$, $[\mathbb{W}_B^{(ij)}(\omega)]$ and $[\mathbb{V}_B^{(ij)}(\omega)]$, and complex-valued vectors $\mathbb{F}_B^{(i)}(\omega)$ for $i,j=2,3,4$ are full matrices and vectors that are given in details in Appendix. C. Note that these matrices are not the same as the corresponding matrices in section VII.3 despite the same notation is used for the sake of simplicity. The coupling matrices are either symmetric or antisymmetric and their properties are listed below,

$$[\mathbb{W}_B^{(32)}(\omega)] = -[\mathbb{W}_B^{(23)}(\omega)]^T \quad , \quad [\mathbb{W}_B^{(43)}(\omega)] = -[\mathbb{W}_B^{(34)}(\omega)]^T \quad , \quad [\mathbb{V}_B^{(42)}(\omega)] = [\mathbb{V}_B^{(24)}(\omega)]^T \quad .$$

The validity of the CROM for Model 2 is quantified by calculating the error functions $\mathrm{error}_B^{(j),\mathrm{CROM}}(\omega)$ with $B = B_1,\ldots,B_8$ and $j=2,3,4$ such that

$$\mathrm{error}_B^{(j),\mathrm{CROM}}(\omega) = \frac{\|\mathbf{q}_B^{(j)}(\omega) - \mathbf{q}_B^{(j),\mathrm{ref}}(\omega)\|_2}{\|\mathbf{q}_B^{(j),\mathrm{ref}}(\omega)\|_2} ,$$

where $\omega \mapsto \mathbf{q}_B^{(j)}(\omega)$ is solution of the CROM and where $\omega \mapsto \mathbf{q}_B^{(j),\mathrm{ref}}(\omega)$ is the reference solution of the ROM. The graphs of $\omega \mapsto \mathrm{error}_B^{(j),\mathrm{CROM}}(\omega)$ are presented on Fig. VII.4 for $B = B_1,\ldots,B_8$ with different line colours for each bands $B = B_1,\ldots,B_8$ and for $j=2$ (Fig. (a)), $j=3$ (Fig. (b)) and $j=4$ (Fig. (c)). The results presented on this figure show that the relative error in using the CROM is low enough and consequently, it validates the CROM for Model 2.

VII.5 Equivalent second-order differential system of equations

In the following we introduce matrices for rewriting the matrix equations of the CROM (for Model 1 and Model 2) into an approximated form of a second-order differential system of equations.

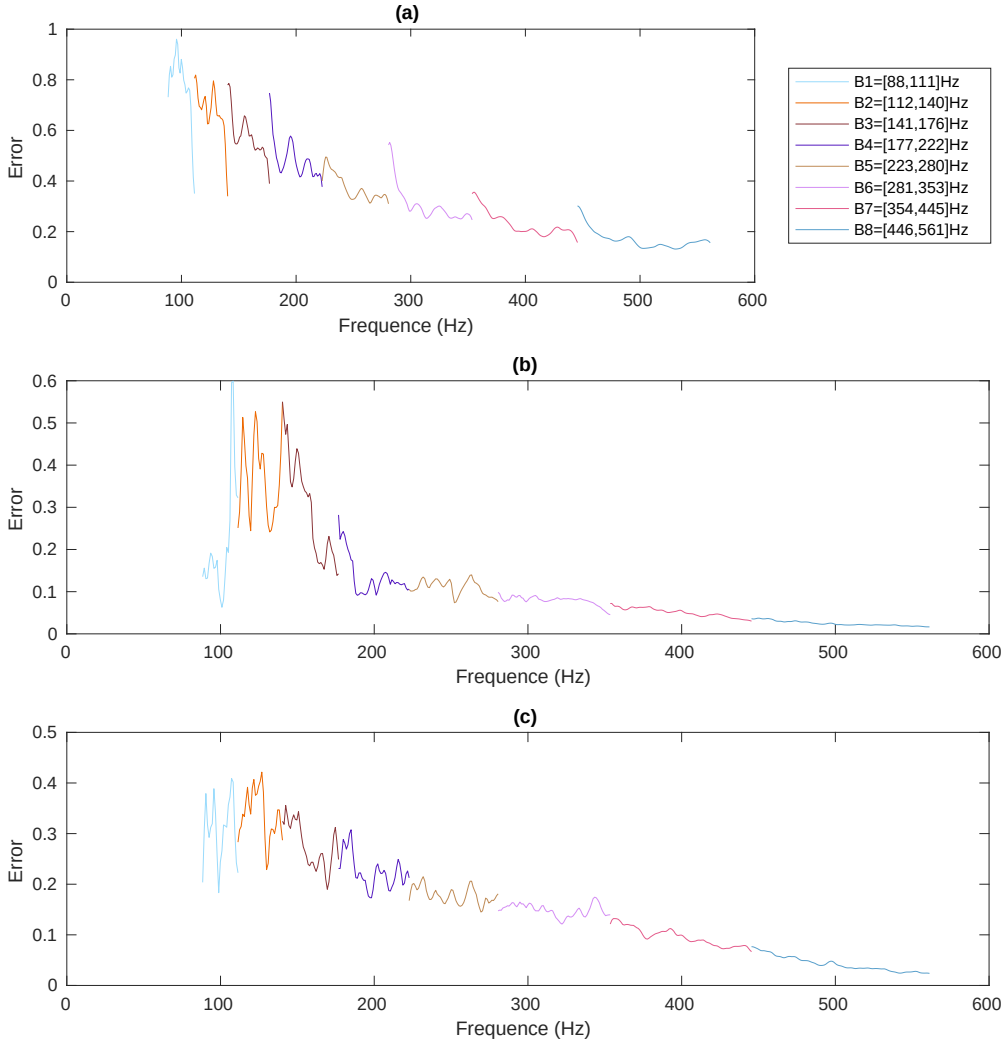

Figure VII.4 – Quantification of the error due to the Schur complements to construct the CROM for Model 2. Graphs of the error functions $\omega \mapsto \text{error}_B^{(j),\text{CROM}}(\omega)$ with $B = B_1, \ldots, B_8$ for 8 bands in 1/3 octave and for $j = 2$ (Fig. (a)), $j = 3$ (Fig. (b)) and $j = 4$ (Fig. (c)).

The block-matrices $[\mathbb{Z}_B^{(i)}(\omega)]$ in Eqs. (VII.2) or (VII.4), for any subsystem (i), can be written as a second-order differential operator, with an additional non-local off-diagonal symmetric matrix $[\mathbb{O}_B]$ written as follow

$$[\mathbb{Z}_B^{(i)}(\omega)] \simeq -\omega^2 [\mathbb{M}_B^{(i)}] + i\,\omega\,[\mathbb{D}_B^{(i)}] + [\mathbb{K}_{0,B}^{(i)}] + [\mathbb{O}_B^{(i)}(\omega)] \quad .$$

Identification of matrices $[\mathbb{M}_B^{(i)}]$, $[\mathbb{D}_B^{(i)}]$ and $[\mathbb{K}_{0,B}^{(i)}]$ might not be unique but we present, hereinafter, the approximations that have been made in this work for lowering the computational cost of their

identification. We then introduce the full matrix-valued equivalent damping $[\mathbb{D}_B^{(i)}]$ defined as

$$[\mathbb{D}_B^{(i)}]_{\alpha\beta} = \frac{1}{\omega_c}\mathrm{Im}\Big\{[\mathbb{Z}_B^{(i)}(\omega_c)]_{\alpha\beta}\Big\} \,. \tag{VII.5}$$

Let $[\mathbb{M}_B^{(i)}]$ and $[\mathbb{K}_{0,B}^{(i)}]$ be the full matrix-valued equivalent mass and stiffness defined as

$$[\mathbb{M}_B^{(i)}]_{\alpha\beta} = X_{\alpha\beta} \quad , \quad [\mathbb{K}_{0,B}^{(i)}]_{\alpha\beta} = Y_{\alpha\beta} \quad ,$$

where $X_{\alpha\beta}$ and $Y_{\alpha\beta}$ are the two real-valued solutions of the following system of equations

$$-\omega_a^2 X_{\alpha\beta} + Y_{\alpha\beta} = \mathrm{Re}\Big\{[\mathbb{Z}_B^{(i)}(\omega_a)]_{\alpha\beta}\Big\} \tag{VII.6}$$

$$-\omega_b^2 X_{\alpha\beta} + Y_{\alpha\beta} = \mathrm{Re}\Big\{[\mathbb{Z}_B^{(i)}(\omega_b)]_{\alpha\beta}\Big\} \,. \tag{VII.7}$$

Let ω_c be the centre angular frequency of the limited band B, and we have $\omega_a = \omega_c\, 2^{-1/12}$ and $\omega_b = \omega_c\, 2^{1/12}$ as two angular frequencies belonging to limited frequency band B. In addition, since every limited frequency band B are assumed to be narrow enough, it is assumed that the variations of real symmetric matrix $[\mathbb{O}_B^{(i)}(\omega)]$ are small in B and hence the approximation $[\mathbb{O}_B^{(i)}] \approx [\mathbb{O}_B^{(i)}(\omega_c)]$ is acceptable. Consequently, a frequency-independent stiffness matrix $[\mathbb{K}_B^{(i)}]$ is introduced and defined as

$$[\mathbb{K}_B^{(i)}] = [\mathbb{K}_{0,B}^{(i)}] + [\mathbb{O}_B^{(i)}] \,.$$

The block-matrices $[\mathbb{V}_B^{(ij)}(\omega)]$ in Eqs. (VII.2) or (VII.4), for (i,j) in $\{(1,3), (3,1), (2,4),(4,2), (1,5), (5,1), (3,5), (5,3)\}$ for Model 1 and (i,j) in $\{(2,4),(4,2)\}$ for Model 2, can be written as a second-order operator, with an additional non-local matrix $[\mathbb{P}_B^{(ij)}(\omega)]$ rewritten as follow

$$[\mathbb{V}_B^{(ij)}(\omega)] = -\omega^2 [\mathbb{M}_B^{(ij)}] + i\,\omega [\mathbb{D}_B^{(ij)}] + [\mathbb{K}_{0,B}^{(ij)}] + [\mathbb{P}_B^{(ij)}(\omega)] \quad .$$

Identification of matrices $[\mathbb{M}_B^{(ij)}]$, $[\mathbb{D}_B^{(ij)}]$ and $[\mathbb{K}_{0,B}^{(ij)}]$ might not be unique but we present, hereinafter, the approximations that have been made in this work. The full matrix-valued equivalent dissipative coupling $[\mathbb{D}_B^{(ij)}]$ is defined as

$$[\mathbb{D}_B^{(ij)}]_{\alpha\beta} = \frac{1}{\omega_c}\mathrm{Im}\Big\{[\mathbb{V}_B^{(ij)}(\omega_c)]_{\alpha\beta}\Big\} \,. \tag{VII.8}$$

Let $[\mathbb{M}_B^{(ij)}]$ and $[\mathbb{K}_{0,B}^{(ij)}]$ be the full matrix-valued equivalent inertial coupling and elastic coupling defined as

$$[\mathbb{M}_B^{(ij)}]_{\alpha\beta} = X_{\alpha\beta} \quad , \quad [\mathbb{K}_{0,B}^{(ij)}]_{\alpha\beta} = Y_{\alpha\beta} \quad ,$$

where $X_{\alpha\beta}$ and $Y_{\alpha\beta}$ are the two real-valued solutions of the following system of equations

$$-\omega_a^2 X_{\alpha\beta} + Y_{\alpha\beta} = \mathrm{Re}\Big\{[\mathbb{V}_B^{(ij)}(\omega_a)]_{\alpha\beta}\Big\} \tag{VII.9}$$

$$-\omega_b^2 X_{\alpha\beta} + Y_{\alpha\beta} = \mathrm{Re}\Big\{[\mathbb{V}_B^{(ij)}(\omega_b)]_{\alpha\beta}\Big\} \,. \tag{VII.10}$$

In addition, since every limited frequency band B are assumed to be narrow enough, it is assumed that the variations of $[\mathbb{P}_B^{(ij)}(\omega)]$ are small in B and hence the approximation $[\mathbb{P}_B^{(ij)}] \approx [\mathbb{P}_B^{(ij)}(\omega_c)]$ is acceptable. Consequently, a frequency-independent stiffness matrix $[\mathbb{K}_B^{(ij)}]$ is introduced and defined as

$$[\mathbb{K}_B^{(ij)}] = [\mathbb{K}_{0,B}^{(ij)}] + [\mathbb{P}_B^{(ij)}] \, .$$

The block-matrices $[\mathbb{W}_B^{(ij)}(\omega)]$ in Eqs. (VII.2) or (VII.4), for (i,j) in $\{(1,2), (2,1), (1,4), (4,1), (2,3), (3,2), (2,5), (5,2), (3,4), (4,3), (4,5), (5,4)\}$ for Model 1 and (i,j) in $\{(2,3),(3,2),(3,4),(4,3)\}$ for Model 2, can be written as a second-order differential operator, with an additional non-local antisymmetric matrix $[\mathbb{R}_B^{(ij)}(\omega)]$, as follow

$$[\mathbb{W}_B^{(ij)}(\omega)] = i\,\omega\,[\mathbb{G}_B^{(ij)}] + [\mathbb{R}_B^{(ij)}] \quad .$$

Identification of matrices $[\mathbb{G}_B^{(ij)}]$ and $[\mathbb{R}_B^{(ij)}]$ might not be unique but we present, hereinafter, the approximations that have been made in this work. The full matrix-valued equivalent gyroscopic coupling $[\mathbb{G}_B^{(ij)}]$ is defined as

$$[\mathbb{G}_B^{(ij)}]_{\alpha\beta} = \frac{1}{\omega_c} \mathrm{Im}\Big\{ [\mathbb{W}_B^{(ij)}(\omega_c)]_{\alpha\beta} \Big\} \, , \tag{VII.11}$$

$$[\mathbb{R}_B^{(ij)}]_{\alpha\beta} = \mathrm{Re}\Big\{ [\mathbb{W}_B^{(ij)}(\omega_c)]_{\alpha\beta} \Big\} \, , \tag{VII.12}$$

where we assumed small variations of $\mathrm{Re}\{[\mathbb{W}_B^{(ij)}(\omega)]_{\alpha\beta}\}$ in frequency band B. An approximated form of equivalent second-order differential system for Model 1 and Model 2 is then written as, for all $\omega \in B$

$$\Big(-\omega^2 [\mathbb{M}_B] + i\,\omega [\mathbb{D}_B] + i\,\omega [\mathbb{G}_B] + [\mathbb{K}_B] + [\mathbb{R}_B] \Big) \mathbb{q}_B(\omega) = [\mathbb{A}_B] \mathbb{q}_B(\omega) = \mathbb{f}_B(\omega) \quad , \tag{VII.13}$$

where $[\mathbb{A}_B] = -\omega^2 [\mathbb{M}_B] + i\,\omega [\mathbb{D}_B] + i\,\omega [\mathbb{G}_B] + [\mathbb{K}_B] + [\mathbb{R}_B]$ and $[\mathbb{M}_B]$, $[\mathbb{D}_B]$, $[\mathbb{G}_B]$, $[\mathbb{K}_B]$ and $[\mathbb{R}_B]$ are defined as, for Model 1

$$[\mathbb{M}_B] = \begin{bmatrix} [\mathbb{M}_B^{(1)}] & [\mathbb{M}_B^{(13)}] & [\mathbb{M}_B^{(15)}] & & \\ [\mathbb{M}_B^{(31)}] & [\mathbb{M}_B^{(3)}] & [\mathbb{M}_B^{(35)}] & & \\ [\mathbb{M}_B^{(51)}] & [\mathbb{M}_B^{(53)}] & [\mathbb{M}_B^{(5)}] & & \\ & & & [\mathbb{M}_B^{(2)}] & [\mathbb{M}_B^{(24)}] \\ & & & [\mathbb{M}_B^{(42)}] & [\mathbb{M}_B^{(4)}] \end{bmatrix} \quad , \quad [\mathbb{G}_B] = \begin{bmatrix} & & & [\mathbb{G}_B^{(12)}] & [\mathbb{G}_B^{(14)}] \\ & & & [\mathbb{G}_B^{(32)}] & [\mathbb{G}_B^{(34)}] \\ & & & [\mathbb{G}_B^{(52)}] & [\mathbb{G}_B^{(54)}] \\ [\mathbb{G}_B^{(21)}] & [\mathbb{G}_B^{(23)}] & [\mathbb{G}_B^{(25)}] & & \\ [\mathbb{G}_B^{(41)}] & [\mathbb{G}_B^{(43)}] & [\mathbb{G}_B^{(45)}] & & \end{bmatrix} \quad ,$$

$$[\mathbb{D}_B] = \begin{bmatrix} [\mathbb{D}_B^{(1)}] & [\mathbb{D}_B^{(13)}] & [\mathbb{D}_B^{(15)}] & & \\ [\mathbb{D}_B^{(31)}] & [\mathbb{D}_B^{(3)}] & [\mathbb{D}_B^{(35)}] & & \\ [\mathbb{D}_B^{(51)}] & [\mathbb{D}_B^{(53)}] & [\mathbb{D}_B^{(5)}] & & \\ & & & [\mathbb{D}_B^{(2)}] & [\mathbb{D}_B^{(24)}] \\ & & & [\mathbb{D}_B^{(42)}] & [\mathbb{D}_B^{(4)}] \end{bmatrix} \quad , \quad [\mathbb{R}_B] = \begin{bmatrix} & & & [\mathbb{R}_B^{(12)}] & [\mathbb{R}_B^{(14)}] \\ & & & [\mathbb{R}_B^{(32)}] & [\mathbb{R}_B^{(34)}] \\ & & & [\mathbb{R}_B^{(52)}] & [\mathbb{R}_B^{(54)}] \\ [\mathbb{R}_B^{(21)}] & [\mathbb{R}_B^{(23)}] & [\mathbb{R}_B^{(25)}] & & \\ [\mathbb{R}_B^{(41)}] & [\mathbb{R}_B^{(43)}] & [\mathbb{R}_B^{(45)}] & & \end{bmatrix} \quad ,$$

$$[\mathbb{K}_B] = \begin{bmatrix} [\mathbb{K}_B^{(1)}] & [\mathbb{K}_B^{(13)}] & [\mathbb{K}_B^{(15)}] & & \\ [\mathbb{K}_B^{(31)}] & [\mathbb{K}_B^{(3)}] & [\mathbb{K}_B^{(35)}] & & \\ [\mathbb{K}_B^{(51)}] & [\mathbb{K}_B^{(53)}] & [\mathbb{K}_B^{(5)}] & & \\ & & & [\mathbb{K}_B^{(2)}] & [\mathbb{K}_B^{(24)}] \\ & & & [\mathbb{K}_B^{(42)}] & [\mathbb{K}_B^{(4)}] \end{bmatrix} \quad , \quad \mathbb{q}_B(\omega) = \begin{Bmatrix} \mathbf{q}_B^{(1)} \\ \mathbf{q}_B^{(3)} \\ \mathbf{q}_B^{(5)} \\ \mathbf{q}_B^{(2)} \\ \mathbf{q}_B^{(4)} \end{Bmatrix} \quad , \quad \mathbb{f}_B(\omega) = \begin{Bmatrix} \mathbf{f}_B^{(1)} \\ 0 \\ 0 \\ 0 \\ 0 \end{Bmatrix} \quad ,$$

and where $[\mathbb{M}_B]$, $[\mathbb{D}_B]$, $[\mathbb{G}_B]$, $[\mathbb{K}_B]$ and $[\mathbb{R}_B]$ are defined as, for Model 2

$$[\mathbb{M}_B] = \begin{bmatrix} [\mathbb{M}_B^{(3)}] & & \\ & [\mathbb{M}_B^{(2)}] & [\mathbb{M}_B^{(24)}] \\ & [\mathbb{M}_B^{(42)}] & [\mathbb{M}_B^{(4)}] \end{bmatrix} , \qquad [\mathbb{G}_B] = \begin{bmatrix} & [\mathbb{G}_B^{(32)}] & [\mathbb{G}_B^{(34)}] \\ [\mathbb{G}_B^{(23)}] & & \\ [\mathbb{G}_B^{(43)}] & & \end{bmatrix} ,$$

$$[\mathbb{D}_B] = \begin{bmatrix} [\mathbb{D}_B^{(3)}] & & \\ & [\mathbb{D}_B^{(2)}] & [\mathbb{D}_B^{(24)}] \\ & [\mathbb{D}_B^{(42)}] & [\mathbb{D}_B^{(4)}] \end{bmatrix} , \qquad [\mathbb{R}_B] = \begin{bmatrix} & [\mathbb{R}_B^{(32)}] & [\mathbb{R}_B^{(34)}] \\ [\mathbb{R}_B^{(23)}] & & \\ [\mathbb{R}_B^{(43)}] & & \end{bmatrix} ,$$

$$[\mathbb{K}_B] = \begin{bmatrix} [\mathbb{K}_B^{(3)}] & & \\ & [\mathbb{K}_B^{(2)}] & [\mathbb{K}_B^{(24)}] \\ & [\mathbb{K}_B^{(42)}] & [\mathbb{K}_B^{(4)}] \end{bmatrix} , \qquad \mathbb{q}_B(\omega) = \begin{Bmatrix} \mathbf{q}_B^{(3)} \\ \mathbf{q}_B^{(2)} \\ \mathbf{q}_B^{(4)} \end{Bmatrix} , \quad \mathbb{f}_B(\omega) = \begin{Bmatrix} \mathbb{f}_B^{(3)}(\omega) \\ \mathbb{f}_B^{(2)}(\omega) \\ \mathbb{f}_B^{(4)}(\omega) \end{Bmatrix} .$$

VII.6 Analysis of the algebraic properties of the Equivalent second-order differential system matrices

In the previous section, an Equivalent second-order differential system is introduced. Nevertheless, for such a system being physically acceptable, the frequency independent matrices must satisfy some mathematical properties. Hence, matrices $[\mathbb{M}_B]$, $[\mathbb{D}_B]$ and $[\mathbb{K}_B]$ should be symmetric and definite-positive. While it is obvious that they are symmetric, they are *a priori* not definite-positive because this property has not been enforced by the proposed methodology for their constructions. There are no mathematical evidences for the definite-positiveness of matrices $[\mathbb{M}_B]$, $[\mathbb{D}_B]$ and $[\mathbb{K}_B]$. Nevertheless, it is possible to numerically check their definite-positiveness for Model 1 and for Model 2 in studying the graphs of the functions $\omega \mapsto \kappa_B(\omega;[A])$ with $[A] = [\mathbb{M}_B]$, $[\mathbb{D}_B]$ and $[\mathbb{K}_B]$ for each limited frequency band B, defined as

$$\kappa(\omega;[A]) = \frac{\lambda_{\min}([A])}{\lambda_{\max}([A])} , \tag{VII.14}$$

where $\lambda_{\min}([A])$ and $\lambda_{\max}([A])$ are respectively the minimal and the maximal eigenvalues (by algebraic values) of a given symmetric matrix $[A]$. The graphs of $\omega \mapsto \kappa_B(\omega;[A])$ with $[A] = [\mathbb{M}_B]$, $[\mathbb{D}_B]$ and $[\mathbb{K}_B]$ and for $B = B_1,\ldots,B_6$ are shown in Figs. VII.5 to VII.6 for Model 1 and for $B = B_1,\ldots,B_8$ in Figs. VII.7 to VII.8 for Model 2. It can be deduced that matrices $[\mathbb{M}_B]$, $[\mathbb{D}_B]$, $[\mathbb{K}_B]$ are definite-positive on each frequency band B and for the two Model 1 and Model 2.

VII.7 Error analysis of the Equivalent second-order differential system

Comparison of the Equivalent second-order differential system with the CROM is carried out by calculating the error functions $\omega \mapsto \text{error}_B^{(j),\text{EQU}}(\omega)$ with $j = 1,\ldots,5$ for Model 1 and with $j = 2,3,4$ Model 2 such that,

$$\text{error}_B^{(j),\text{EQU}}(\omega) = \frac{\|\mathbf{q}_B^{(j)}(\omega) - \mathbf{q}_B^{(j),\text{ref}}(\omega)\|_2}{\|\mathbf{q}_B^{(j),\text{ref}}(\omega)\|_2} ,$$

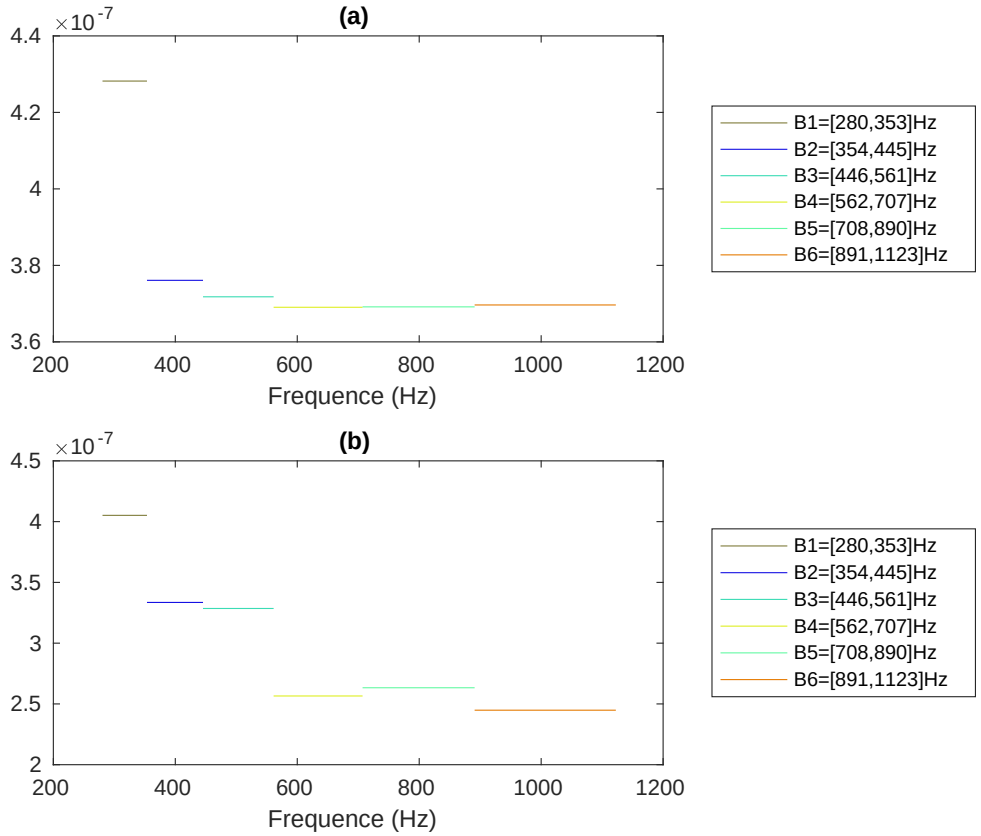

Figure VII.5 – Analysis of the definite-positiveness of $[\mathbb{M}_B]$ and $[\mathbb{K}_B]$ for Model 1. Graphs of $\omega \mapsto \kappa_B(\omega;[\mathbb{M}_B])$ (fig. a) and $\omega \mapsto \kappa_B(\omega;[\mathbb{M}_B])$ (fig. b) for 6 bands $B = B_1,\ldots,B_6$ in 1/3 octave.

where $\omega \mapsto \mathbf{q}_B^{(j)}(\omega)$ is the solution of the equivalent second-order differential system and where $\omega \mapsto \mathbf{q}_B^{(j),\mathrm{ref}}(\omega)$ is the solution of the CROM. The graphs of $\omega \mapsto \mathrm{error}_B^{(j),\mathrm{EQU}}(\omega)$ are presented in Fig. VII.9 for Model 1 with $j = 1,\ldots,5$ in Figs (a) to (e) respectively, and in Fig. VII.10 for Model 2 with $j = 2,3,4$ in Figs. (a), (b) and (c) respectively. The results presented on these figures show that the relative error between the equivalent second-order system and the ROM does not uniformly decreases with the frequency $\omega/2\pi$ for most of the subsystems (1) to (5) for Model 1 and for Model 2. It is due to the approximations used for the identification of the second-order system of matrices. The optimal values of matrices $[\mathbb{M}_B]$, $[\mathbb{D}_B]$, $[\mathbb{G}_B]$, $[\mathbb{K}_B]$ and $[\mathbb{R}_B]$ are not determined and consequently can be considered as uncertain. It is why a probabilistic modelling of the modelling uncertainties should be carried out in order to quantify the confidence level of the equivalent second-order differential system. Such a probabilistic modelling is presented in Chapter IX. Applying the inverse Fourier transform of the two hand sides of Eq. (VII.13) yields the equivalent second-order system in time domain, that is written as

$$[\mathbb{M}_B]\partial_{tt}\mathbb{q}_B(t) + [\mathbb{D}_B]\partial_t\mathbb{q}_B(t) + [\mathbb{G}_B]\partial_t\mathbb{q}_B(t) + [\mathbb{K}_B]\mathbb{q}_B(t) + [\mathbb{R}_B]\mathbb{q}_B(t) = \mathbb{f}_B(t) \quad . \tag{VII.15}$$

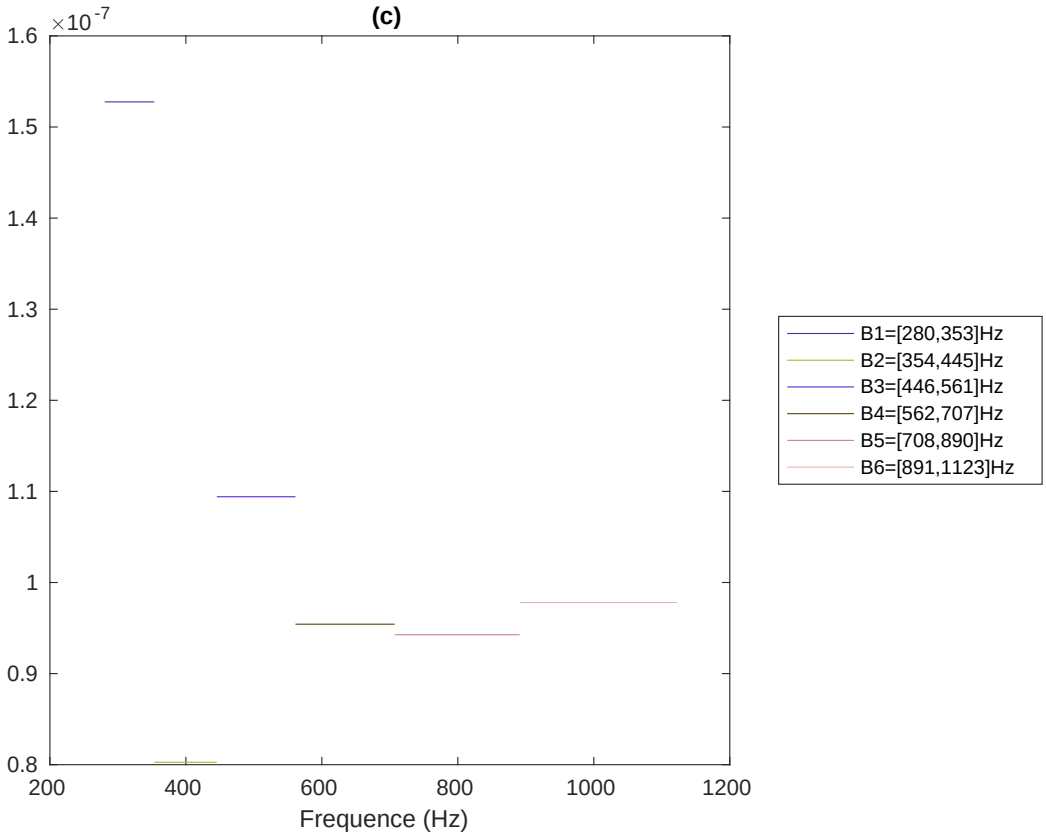

Figure VII.6 – Analysis of the definite-positiveness of $[\mathbb{D}_B]$ for Model 1. Graphs of $\omega \mapsto \kappa_B(\omega; [\mathbb{D}_B])$ for 6 bands $B = B_1, \ldots, B_6$ in 1/3 octave.

in which, we used the same notations for the Fourier transforms of equivalent matrices, $\mathbb{q}_B$ and $\mathbb{f}_B$ because there is no ambiguity when the equations are written in time or in frequency domains.

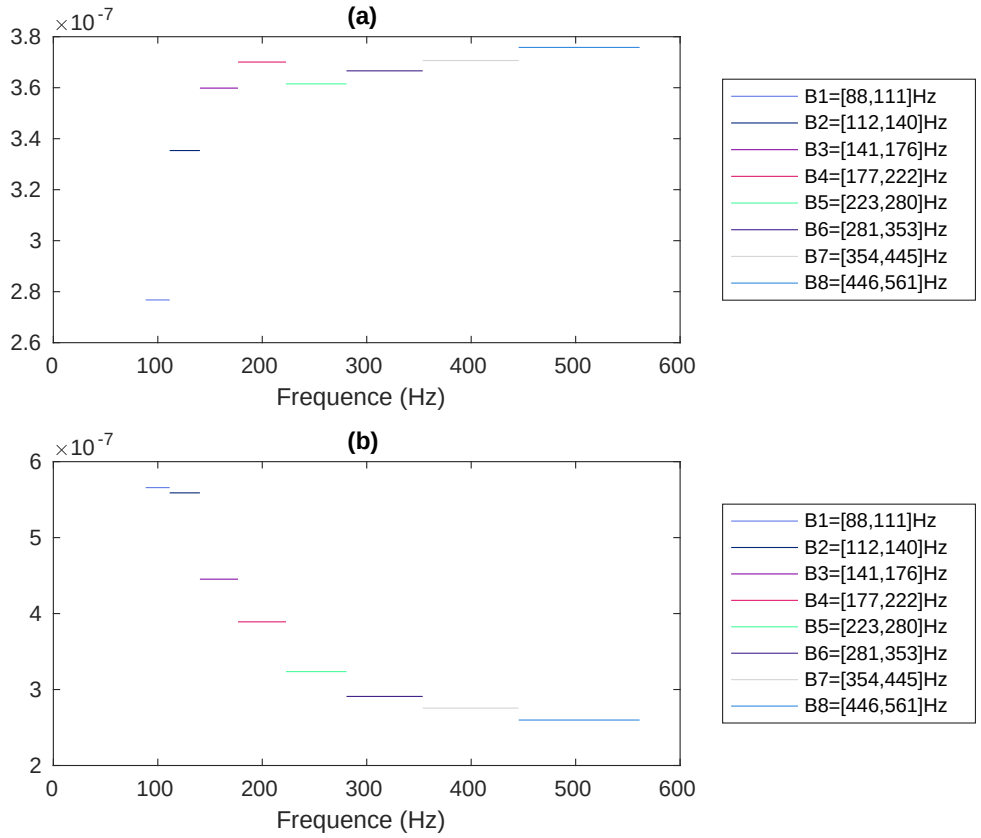

Figure VII.7 – Analysis of the definite-positiveness of $[\mathbb{M}_B]$ and $[\mathbb{K}_B]$ for Model 2. Graphs of $\omega \mapsto \kappa_B(\omega;[\mathbb{M}_B])$ (fig. a) and $\omega \mapsto \kappa_B(\omega;[\mathbb{M}_B])$ (fig. b) for 8 bands $B = B_1,\ldots,B_8$ in 1/3 octave.

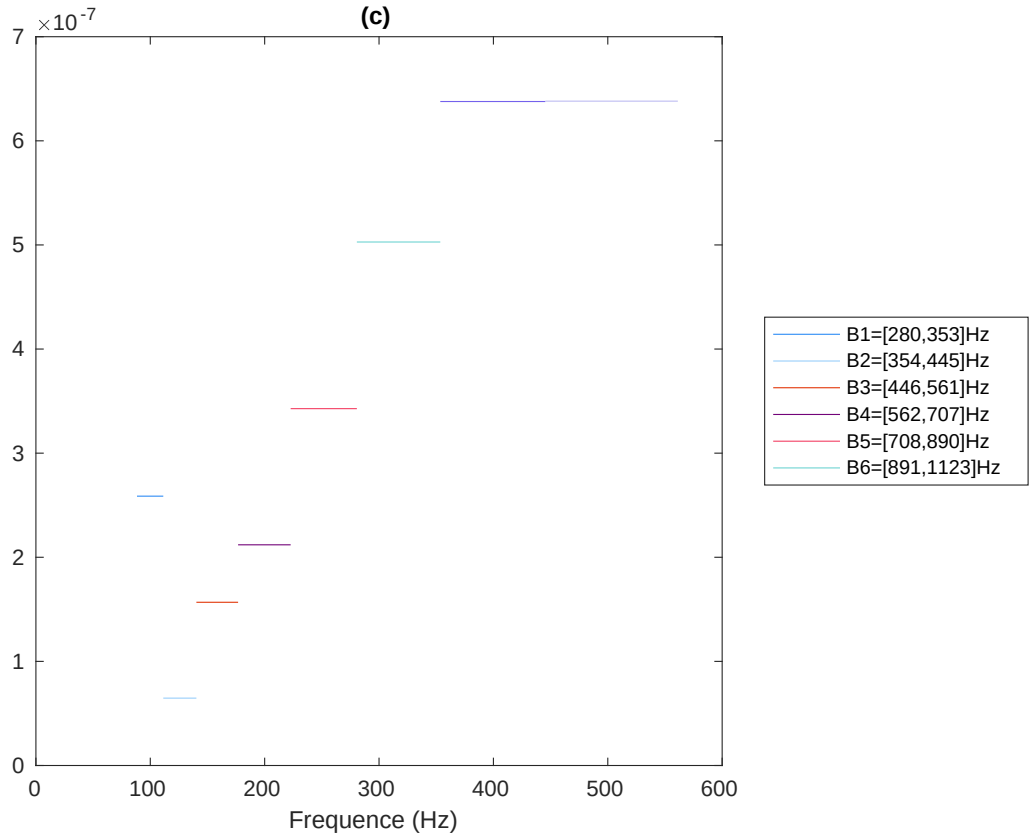

Figure VII.8 – Analysis of the definite-positiveness of $[\mathbb{D}_B]$ for Model 2. Graphs of $\omega \mapsto \kappa_B(\omega; [\mathbb{D}_B])$ for 8 bands $B = B_1, \ldots, B_8$ in 1/3 octave.

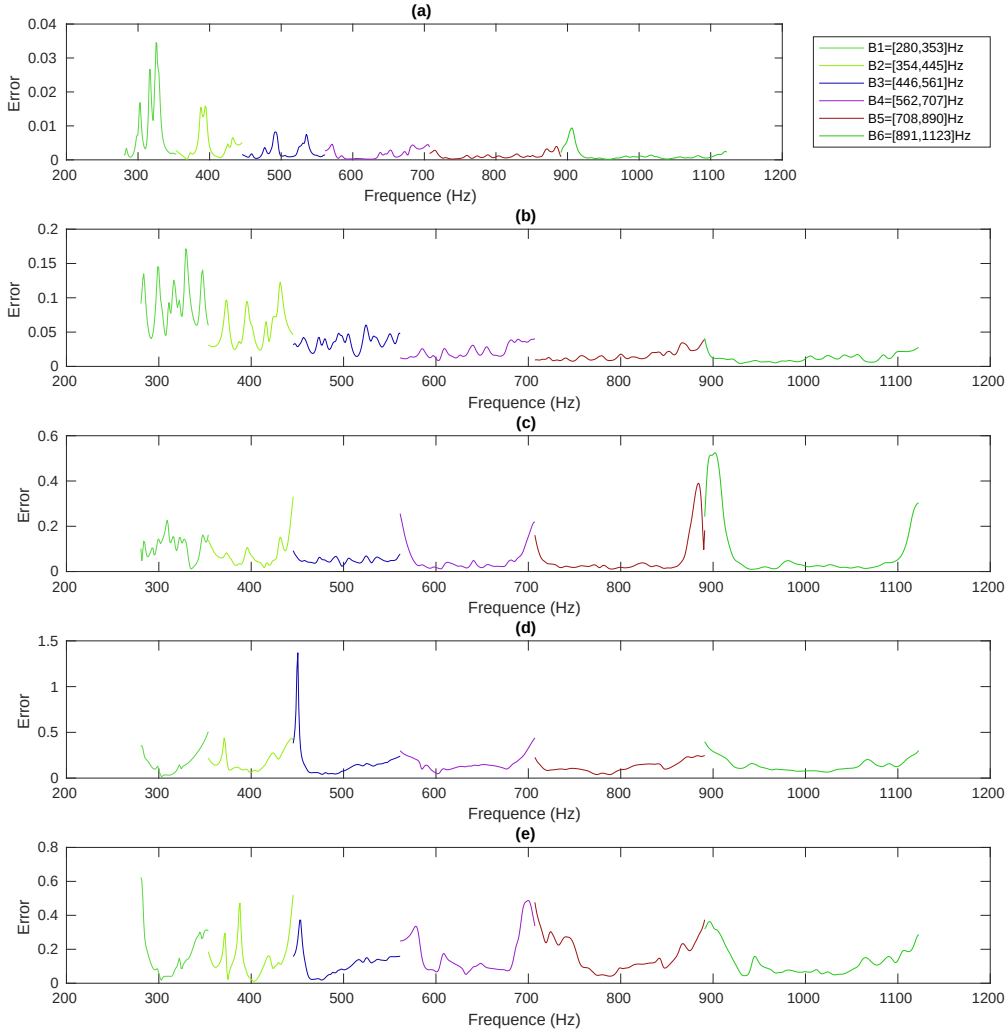

Figure VII.9 – Comparison of the Equivalent second-order differential system with CROM. Graphs of error functions $\omega \mapsto \text{error}_B^{(j),\text{EQU}}(\omega)$ for Model 1 with $B = B_1, \ldots, B_6$ for 6 bands in 1/3 octave and with $j = 1, \ldots, 5$ in Figs (a) to (e) respectively.

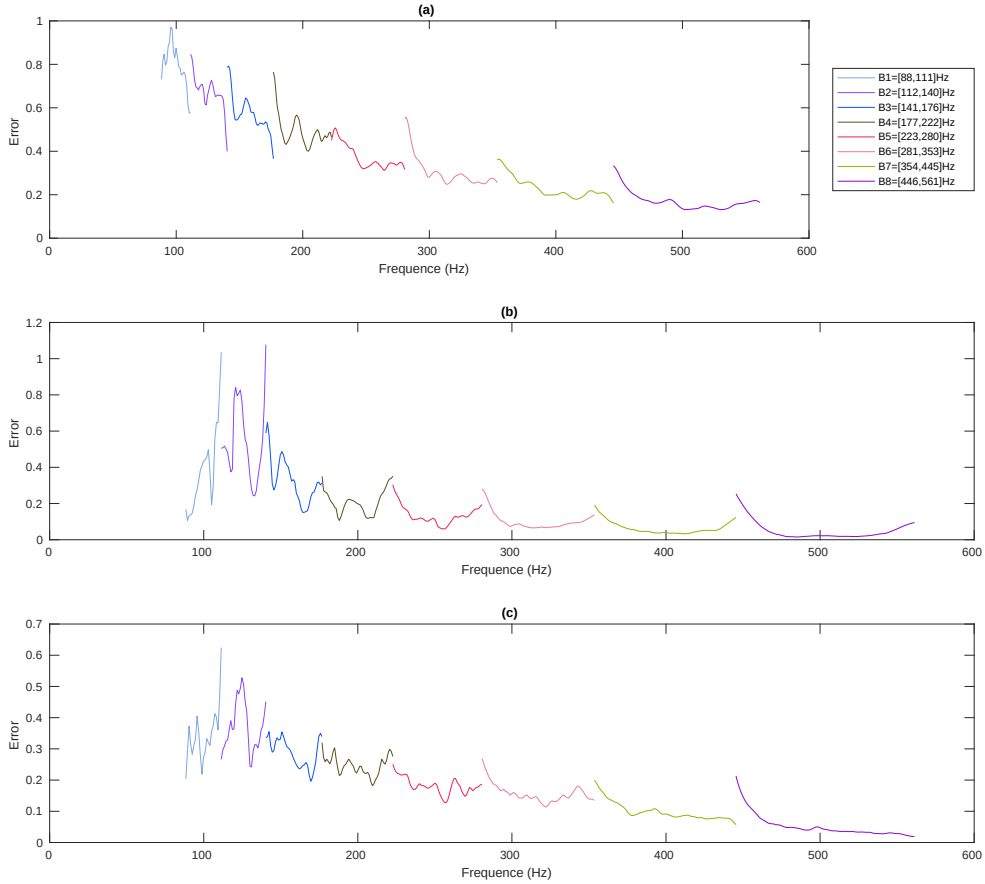

Figure VII.10 – Comparison of the Equivalent second-order differential system with CROM. Graphs of $\omega \mapsto \text{error}_B^{(j),\text{EQU}}(\omega)$ for Model 2 with $B = B_1, \ldots, B_8$ for 8 bands in 1/3 octave with $j = 2, 3, 4$ in Figs. (a), (b) and (c) respectively.

CHAPTER VIII

STATISTICAL ENERGY ANALYSIS AND THE PROPOSED ECPP APPROACH

The Statistical Energy Analysis (SEA) is a method that was introduced by Lyon and other authors [14–16] in the 1960s. This method allows estimating the energy of different subsystems of a complex structure in the high-frequency range by a statistical analysis. In the literature, many works have been devoted to SEA. On our behalf, there are 2 main approaches: wave approach and modal approach. The wave approach is based on the evaluation of the reflection and transmission coefficients at a junction [82–84], which results in the coupling loss factors in SEA. The modal approach is based on basic equations of oscillators [12, 14, 15, 20, 48, 85–100]. It is demonstrated [101] that the two procedures give essentially the same results for some particular systems.

One difficulty of using SEA in engineering problems is that its formulation requires a set of hypotheses. Many studies have been carried out around the hypotheses of SEA [26–28, 102–110]. In this chapter, the usual hypotheses of the classic modal approach SEA formulations is firstly presented. A SEA-based energy method which is called SEA-ECPP is then proposed to solve the vibroacoustic problem under consideration in this manuscript. Some of the usual hypotheses in SEA are then altered in order to take non-conservative couplings into account.

VIII.1 Hypotheses of classic SEA

The study of Statistical Energy Analysis is based on the forced response of mechanical oscillators. Any mechanical system in linear vibroacoustic can be modelled as a set of coupled one-degree-of-freedom oscillators, where each of them represents the generalised coordinates related to the elastic eigenmodes of vibration. The method of SEA is developed under a set of hypotheses that are presented in this section. Under these hypotheses, the key coefficient, namely the Coupling Power Proportionality (CPP), is introduced, which allows writing balance equations between the mean local mechanical energies of each coupled oscillator.

Hypothesis 1 : Couplings are conservative

The first hypothesis concerns the couplings between the single oscillators which are assumed to be conservative. A conservative coupling does not involve any dissipation or energy loss, such as linear elastic coupling, gyroscopic coupling, and inertial coupling. Concerning the elastic and inertial couplings, they both involve symmetric matrices while the gyroscopic couplings involve antisymmetric matrices. However, the dissipative couplings (that is to say a coupling that is not a conservative coupling) are excluded from the framework of the classic SEA. Consequently, in the framework of SEA formulation for a system of oscillators, dissipation of energy is not prohibited but it is limited to internal dissipation in each oscillator. For instance, let $[M]$, $[D]$, $[G]$ and $[K]$ be the $(N \times N)$ matrices of mass, damping, gyroscopic coupling and stiffness, respectively, of a linear system of N coupled oscillators, then such a hypothesis implies that $[D]$ is a diagonal matrix.

Hypothesis 2 : External loads are uncorrelated white noises

The second hypothesis concerns the external loads that are assumed to be uncertain and modelled as uncorrelated white noises. Consequently, if $\{\mathbf{F}(t), t \in \mathbb{R}\}$ is a $\mathbb{R}^N$-valued random process modelling the external loads, it can be characterised by its matrix-valued power spectral density function $\omega \mapsto [S_{\mathbf{F}}(\omega)]$ that is such that for all $\alpha, \beta \in 1, \ldots, N$ and for all $\omega \in \mathbb{R}$, we have $[S_{\mathbf{F}}(\omega)]_{\alpha\beta} = S_\alpha \, \delta_{\alpha\beta}$ where S_α is a constant.

Hypothesis 3 : Couplings are weak

The last hypothesis assumes that every couplings are weak. For instance, let $[M]$, $[D]$, $[G]$ and $[K]$ be the $(N \times N)$ matrices of mass, damping, gyroscopic coupling and stiffness, respectively, of a linear system of N coupled oscillators, then such a hypothesis implies that, for $\beta \neq \alpha$, we have $[M]_{\alpha\beta} \ll [M]_{\alpha\alpha}$, $[G]_{\alpha\beta} \ll [D]_{\alpha\alpha}$, $[K]_{\alpha\beta} \ll [K]_{\alpha\alpha}$.

VIII.2 ECPP Approach

Such hypotheses in classic SEA prevent the use of the ESOM presented in chapter VII as a candidate for the SEA. Indeed, the ESOM exhibits non conservative couplings that are not negligible and does not fulfil hypothesis 1 in the previous section. Indeed, the damping in subsystem (3) is not small because the main role of subsystem (3) consists in decaying the vibration energy that is transmitted to subsystem (5) in order to increase vibroacoustic insulation of the two air volumes (subsystems (1) and (5)). The Schur complements used for constructing the CROM then spreads such non-negligible damping contributions on most of the block-matrices of the CROM, as well as the equivalent identified damping matrices in ESOM. In order to circumvent such limitations, we use a similar approach presented in [27] for the case of a 2-degrees-of-freedom coupled oscillators that we extend to the case of a n-degrees-of-freedom coupled oscillator. In addition, another issue is related to the formulation of the ESOM in limited frequency bands $B \in \{B_1, \ldots, B_{N_{\text{bands}}}\}$. When rewritten in time domain, the external loads $\mathbb{f}_B$ (see Eqs. (VII.13) and (VII.15)) is modelled as a vector-valued random process denoted as $\mathbf{F}_B$ that is indexed by time t in $\mathbb{R}$. Nevertheless, it cannot be modelled as a white noise for which the support of the power spectral density function is $\mathbb{R}$. Indeed, by construction, the support of the matrix-valued power spectral density function $[S_{\mathbf{F}_B}]$ of $\mathbf{F}_B$ should be B. As a result, a new energetic coefficient is introduced which can be considered as an extension of the usual CPP coefficient in classical SEA formulations.

Altered Hypotheses

Among the hypotheses presented in previous section, we actually need to relax hypotheses 1 and 2. The assumption of uncorrelated white noises for the external loads is then changed in assuming that the external loads are modelled as uncorrelated second-order, mean-square stationary processes $F_{B,1}, \ldots, F_{B,N}$ with coloured power spectral density functions for which the value is constant over limited frequency band $B \in \{B_1, \ldots, B_{N_{\text{bands}}}\}$. In addition, we no longer assume that couplings are necessarily conservatives. Nevertheless, hypothesis 3 is maintained and we then assume that, in the framework of the ESOM presented in chapter VII, for all α and all $\beta \neq \alpha$

$$
\begin{aligned}
&[\mathbb{M}_B]_{\alpha\beta} \ll [\mathbb{M}_B]_{\alpha\alpha} \quad , \quad [\mathbb{D}_B]_{\alpha\beta} \ll [\mathbb{D}_B]_{\alpha\alpha} \quad , \quad [\mathbb{K}_B]_{\alpha\beta} \ll [\mathbb{K}_B]_{\alpha\alpha} \quad , \\
&[\mathbb{G}_B]_{\alpha\beta} \ll [\mathbb{D}_B]_{\alpha\alpha} \quad , \quad [\mathbb{R}_B]_{\alpha\beta} \ll [\mathbb{K}_B]_{\alpha\alpha} \quad .
\end{aligned}
$$

Since the external loads $\mathbb{f}_B$ is uncertain and modelled as a second-order, centred, stationary in mean square, vector-valued random process denoted as $\mathbf{F}_B$, then the solution $\mathbb{q}_B$ of (VII.15) is also uncertain and modelled as a vector-valued random process $\mathbf{Q}_B$ indexed by time $t \in \mathbb{R}$. We

then have

$$\sum_{\beta=1}[\mathbb{M}_B]_{\alpha\beta}\ddot{Q}_{\beta,B}+\sum_{\beta=1}[\mathbb{D}_B]_{\alpha\beta}\dot{Q}_{\beta,B}+\sum_{\beta\neq\alpha}[\mathbb{G}_B]_{\alpha\beta}\dot{Q}_{\beta,B}+\sum_{\beta=1}[\mathbb{K}_B]_{\alpha\beta}Q_{\beta,B}+\sum_{\beta\neq\alpha}[\mathbb{R}_B]Q_{\beta,B}=F_{\alpha,B}\ , \tag{VIII.1}$$

where $Q_{\alpha,B}(t)=\{\mathbf{Q}_B(t)\}_\alpha$ and $F_{\alpha,B}(t)=\{\mathbf{F}_B(t)\}_\alpha$. Eq. (VIII.1) can be rewritten as

$$\begin{aligned}&[\mathbb{M}_B]_{\alpha\alpha}\ddot{Q}_{\alpha,B}+[\mathbb{D}_B]_{\alpha\alpha}\dot{Q}_{\alpha,B}+[\mathbb{K}_B]_{\alpha\alpha}Q_{\alpha,B}\\&+\sum_{\beta\neq\alpha}\Big([\mathbb{M}_B]_{\alpha\beta}\ddot{Q}_{\beta,B}+[\mathbb{D}_B]_{\alpha\beta}\dot{Q}_{\beta,B}+[\mathbb{G}_B]_{\alpha\beta}\dot{Q}_{\beta,B}+[\mathbb{K}_B]_{\alpha\beta}Q_{\beta,B}+[\mathbb{R}_B]_{\alpha\beta}Q_{\beta,B}\Big)=F_{\alpha,B}\ .\end{aligned} \tag{VIII.2}$$

VIII.2.1 Mean generalised instantaneous power balance equation

A frequency-local power balance equation for the random generalised coordinates $Q_{\alpha,B}$ is obtained by multiplying each side of Eq. VIII.2 by $\dot{Q}_{\alpha,B}$. We then have

$$\begin{aligned}&[\mathbb{M}_B]_{\alpha\alpha}\ddot{Q}_{\alpha,B}\dot{Q}_{\alpha,B}+[\mathbb{D}_B]_{\alpha\alpha}\dot{Q}^2_{\alpha,B}+[\mathbb{K}_B]_{\alpha\alpha}Q_{\alpha,B}\dot{Q}_{\alpha,B}+\sum_{\beta\neq\alpha}\Big([\mathbb{M}_B]_{\alpha\beta}\ddot{Q}_{\beta,B}\dot{Q}_{\alpha,B}+[\mathbb{D}_B]_{\alpha\beta}\dot{Q}_{\beta,B}\dot{Q}_{\alpha,B}\\&+[\mathbb{G}_B]_{\alpha\beta}\dot{Q}_{\beta,B}\dot{Q}_{\alpha,B}+[\mathbb{K}_B]_{\alpha\beta}Q_{\beta,B}\dot{Q}_{\alpha,B}+[\mathbb{R}_B]_{\alpha\beta}Q_{\beta,B}\dot{Q}_{\alpha,B}\Big)=F_{\alpha,B}\dot{Q}_{\alpha,B}\ .\end{aligned} \tag{VIII.3}$$

Applying expectation operator $\langle\cdot\rangle$ on the two sides of the previous equation yields the mean local-frequency generalised instantaneous power balance equation that is then written as follows,

$$\langle\dot{\mathcal{E}}_{\alpha,B}\rangle+\langle W^{\text{diss}}_{\alpha,B}\rangle+\sum_{\beta\neq\alpha}\langle W^{\text{ex}}_{\alpha\beta,B}\rangle=\langle W^{\text{in}}_{\alpha,B}\rangle\ , \tag{VIII.4}$$

where $\langle W^{\text{in}}_{\alpha,B}\rangle=\langle F_{\alpha,B}\dot{Q}_{\alpha,B}\rangle$ is the mean local-frequency generalised instantaneous injected power and where we defined the mean local-frequency generalised instantaneous mechanical energy $\langle\mathcal{E}_{\alpha,B}\rangle$, the mean local-frequency generalised instantaneous dissipated power $\langle W^{\text{diss}}_{\alpha,B}\rangle$, the mean local-frequency generalised instantaneous exchanged power $\langle W^{\text{ex}}_{\alpha\beta,B}\rangle$ that all are defined as

$$\langle\mathcal{E}_{\alpha,B}\rangle\ =\frac{1}{2}\Big([\mathbb{M}_B]_{\alpha\alpha}\langle\dot{Q}^2_{\alpha,B}\rangle+[\mathbb{K}_B]_{\alpha\alpha}\langle Q^2_{\alpha,B}\rangle\Big)\ , \tag{VIII.5}$$

$$\langle W^{\text{diss}}_{\alpha,B}\ \rangle=[\mathbb{D}_B]_{\alpha\alpha}\langle\dot{Q}^2_{\alpha,B}\rangle\ , \tag{VIII.6}$$

$$\begin{aligned}\langle W^{\text{ex}}_{\alpha\beta,B}\rangle=&[\mathbb{M}_B]_{\alpha\beta}\langle\ddot{Q}_{\beta,B}\dot{Q}_{\alpha,B}\rangle+[\mathbb{D}_B]_{\alpha\beta}\langle\dot{Q}_{\beta,B}\dot{Q}_{\alpha,B}\rangle+[\mathbb{G}_B]_{\alpha\beta}\langle\dot{Q}_{\beta,B}\dot{Q}_{\alpha,B}\rangle+[\mathbb{K}_B]_{\alpha\beta}\langle Q_{\beta,B}\dot{Q}_{\alpha,B}\rangle\\&+[\mathbb{R}_B]_{\alpha\beta}\langle Q_{\beta,B}\dot{Q}_{\alpha,B}\rangle\ .\end{aligned} \tag{VIII.7}$$

Due to the altered hypothesis 2, power spectral density functions of random processes $F_{1,B},\ldots,F_{N,B}$ can be respectively written as $S_{F_{1,B}}(\omega)=(\mathbb{1}_B(\omega)+\mathbb{1}_B(-\omega))S_{1,B}$, …, $S_{F_{N,B}}(\omega)=(\mathbb{1}_B(\omega)+\mathbb{1}_B(-\omega))S_{N,B}$ where $S_{1,B},\ldots,S_{N,B}$ are positive real-valued constants and $\omega\mapsto\mathbb{1}_B(\omega)$ is the indicator function of

B. We then have $\langle \dot{Q}_{\alpha,B} Q_{\alpha,B} \rangle = \langle Q_{\alpha,B} \dot{Q}_{\alpha,B} \rangle = 0$ and $\langle \ddot{Q}_{\alpha,B} \dot{Q}_{\alpha,B} \rangle = \langle \dot{Q}_{\alpha,B} \ddot{Q}_{\alpha,B} \rangle = 0$. Consequently, it can be deduced that

$$\langle \dot{\mathcal{E}}_{\alpha,B} \rangle = 0 , \tag{VIII.8}$$

and Eq. (VIII.4) is rewritten as

$$\langle W^{\text{diss}}_{\alpha,B} \rangle + \sum_{\beta \neq \alpha} \langle W^{\text{ex}}_{\alpha\beta,B} \rangle = \langle W^{\text{in}}_{\alpha,B} \rangle , \tag{VIII.9}$$

Since the random generalised external loads $F_{1,B}, \ldots, F_{N,B}$ are mutually uncorrelated, centred, mean-square stationary random processes then, at any time t, we have $\langle \ddot{Q}_{\beta,B} \dot{Q}_{\alpha,B} \rangle = -\langle \dot{Q}_{\beta,B} \ddot{Q}_{\alpha,B} \rangle$, $\langle \dot{Q}_{\beta,B} Q_{\alpha,B} \rangle = -\langle Q_{\beta,B} \dot{Q}_{\alpha,B} \rangle$. Hence, we have

$$\begin{aligned}
\langle W^{\text{ex}}_{\alpha\beta,B} \rangle &= [\mathbb{M}_B]_{\alpha\beta} \langle \ddot{Q}_{\beta,B} \dot{Q}_{\alpha,B} \rangle + [\mathbb{D}_B]_{\alpha\beta} \langle \dot{Q}_{\beta,B} \dot{Q}_{\alpha,B} \rangle + [\mathbb{G}_B]_{\alpha\beta} \langle \dot{Q}_{\beta,B} \dot{Q}_{\alpha,B} \rangle \\
&\quad + [\mathbb{K}_B]_{\alpha\beta} \langle Q_{\beta,B} \dot{Q}_{\alpha,B} \rangle + [\mathbb{R}_B]_{\alpha\beta} \langle Q_{\beta,B} \dot{Q}_{\alpha,B} \rangle \\
&= [\mathbb{M}_B]_{\alpha\beta} \langle \ddot{Q}_{\beta,B} \dot{Q}_{\alpha,B} \rangle + [\mathbb{D}_B]_{\alpha\beta} \langle \dot{Q}_{\beta,B} \dot{Q}_{\alpha,B} \rangle + [\mathbb{G}_B]_{\alpha\beta} \langle \dot{Q}_{\beta,B} \dot{Q}_{\alpha,B} \rangle \\
&\quad - [\mathbb{K}_B]_{\alpha\beta} \langle \dot{Q}_{\beta,B} Q_{\alpha,B} \rangle - [\mathbb{R}_B]_{\alpha\beta} \langle \dot{Q}_{\beta,B} Q_{\alpha,B} \rangle .
\end{aligned} \tag{VIII.10}$$

VIII.2.2 Weak couplings

A perturbation technique is used in order to formalise the altered hypothesis on weak couplings because it includes dissipative weak couplings that is not included in the classic SEA. We then rewrite matrices $[\mathbb{M}_B]$, $[\mathbb{D}_B]$, $[\mathbb{G}_B]$, $[\mathbb{K}_B]$ and $[\mathbb{R}_B]$, for $\alpha \neq \beta$,

$$[\mathbb{M}_B]_{\alpha\beta} = \epsilon [\mathrm{m}_B]_{\alpha\beta} \quad , \quad [\mathbb{D}_B]_{\alpha\beta} = \epsilon [\mathrm{d}_B]_{\alpha\beta} \quad , \quad [\mathbb{G}_B]_{\alpha\beta} = \epsilon [\mathrm{g}_B]_{\alpha\beta} \quad , \quad [\mathbb{K}_B]_{\alpha\beta} = \epsilon [\mathrm{k}_B]_{\alpha\beta} \quad ,$$
$$[\mathbb{R}_B]_{\alpha\beta} = \epsilon [\mathrm{r}_B]_{\alpha\beta} .$$

The solution $Q_{\alpha,B}$ is then rewritten as

$$Q_{\alpha,B} = Q_{\alpha,B0} + \epsilon Q_{\alpha,B1} + \epsilon^2 Q_{\alpha,B2} + o(\epsilon^2) . \tag{VIII.11}$$

The development in Eq. (VIII.11) is used in Eq. (VIII.2) and then, gathering together terms that exhibit same power of ϵ yields a system of equations at ϵ^0, ϵ^1 and ϵ^2, respectively. These equations are written as

$$[\mathbb{M}_B]_{\alpha\alpha} \ddot{Q}_{\alpha,B0} + [\mathbb{D}_B]_{\alpha\alpha} \dot{Q}_{\alpha,B0} + [\mathbb{K}_B]_{\alpha\alpha} Q_{\alpha,B0} = F_{\alpha,B} \quad , \tag{VIII.12}$$

$$\begin{aligned}
[\mathbb{M}_B]_{\alpha\alpha} \ddot{Q}_{\alpha,B1} + [\mathbb{D}_B]_{\alpha\alpha} \dot{Q}_{\alpha,B1} + [\mathbb{K}_B]_{\alpha\alpha} Q_{\alpha,B1} = &- \sum_{\beta \neq \alpha} [\mathbb{M}_B]_{\alpha\beta} \ddot{Q}_{\beta,B0} - \sum_{\beta \neq \alpha} [\mathbb{D}_B]_{\alpha\beta} \dot{Q}_{\beta,B0} \\
&- \sum_{\beta \neq \alpha} [\mathbb{G}_B]_{\alpha\beta} \dot{Q}_{\beta,B0} - \sum_{\beta \neq \alpha} [\mathbb{K}_B]_{\alpha\beta} Q_{\beta,B0} - \sum_{\beta \neq \alpha} [\mathbb{R}_B]_{\alpha\beta} Q_{\beta,B0} \quad ,
\end{aligned} \tag{VIII.13}$$

$$[\mathbb{M}_B]_{\alpha\alpha}\ddot{Q}_{\alpha,B2} + [\mathbb{D}_B]_{\alpha\alpha}\dot{Q}_{\alpha,B2} + [\mathbb{K}_B]_{\alpha\alpha}Q_{\alpha,B2} = -\sum_{\beta\neq\alpha}[\mathbb{M}_B]_{\alpha\beta}\ddot{Q}_{\beta,B1} - \sum_{\beta\neq\alpha}[\mathbb{D}_B]_{\alpha\beta}\dot{Q}_{\beta,B1} - \sum_{\beta\neq\alpha}[\mathbb{G}_B]_{\alpha\beta}\dot{Q}_{\beta,B1} - \sum_{\beta\neq\alpha}[\mathbb{K}_B]_{\alpha\beta}Q_{\beta,B1} - \sum_{\beta\neq\alpha}[\mathbb{R}_B]_{\alpha\beta}Q_{\beta,B1} \quad . \tag{VIII.14}$$

The random solutions $Q_{\alpha,B0}$, $Q_{\alpha,B1}$ and $Q_{\alpha,B2}$ of Eqs. (VIII.12) to (VIII.14) in time domain are defined as the outputs of a convolution product with the impulse response function $\mathbb{h}_{\alpha,B}$ that is the inverse Fourier transform of the frequency response function $\widehat{\mathbb{h}}_{\alpha,B}(\omega) = (-\omega^2[\mathbb{M}_B]_{\alpha\alpha} + i\omega[\mathbb{D}_B]_{\alpha\alpha} + [\mathbb{K}_B]_{\alpha\alpha})^{-1}$. We then have

$$\begin{aligned}
Q_{\alpha,B0} &= \mathbb{h}_{\alpha,B} * F_{\alpha,B}\\
Q_{\alpha,B1} &= \mathbb{h}_{\alpha,B} * \sum_{\beta\neq\alpha}\Big(-[\mathbb{M}_B]_{\alpha\beta}\ddot{Q}_{\beta,B0} - [\mathbb{D}_B]_{\alpha\beta}\dot{Q}_{\beta,B0} - [\mathbb{G}_B]_{\alpha\beta}\dot{Q}_{\beta,B0} - [\mathbb{K}_B]_{\alpha\beta}Q_{\beta,B0} - [\mathbb{R}_B]_{\alpha\beta}Q_{\beta,B0}\Big)\\
Q_{\alpha,B2} &= \mathbb{h}_{\alpha,B} * \sum_{\beta\neq\alpha}\Big(-[\mathbb{M}_B]_{\alpha\beta}\ddot{Q}_{\beta,B1} - [\mathbb{D}_B]_{\alpha\beta}\dot{Q}_{\beta,B1} - [\mathbb{G}_B]_{\alpha\beta}\dot{Q}_{\beta,B1} - [\mathbb{K}_B]_{\alpha\beta}Q_{\beta,B1} - [\mathbb{R}_B]_{\alpha\beta}Q_{\beta,B1}\Big)
\end{aligned}$$

Consequently, for $\alpha \neq \beta$, $Q_{\alpha,B0}$ and $Q_{\beta,B0}$ (as well as $\dot{Q}_{\alpha,B0}$ and $\ddot{Q}_{\beta,B0}$) are centred, mean square stationary and mutually uncorrelated random processes since $F_{\alpha,B}$ and $F_{\beta,B}$ are assumed to be centred, mean square stationary and mutually uncorrelated random processes. Note that, in the following, the frequency response function $\widehat{\mathbb{h}}_\alpha$ is rewritten as $\mathbb{h}_\alpha$ for the sake of simplicity and when there is no ambiguity. The second order development of $\langle W^{\text{ex}}_{\alpha\beta,B}\rangle$ in ϵ is written as

$$\begin{aligned}
\langle W^{\text{ex}}_{\alpha\beta,B}\rangle &= [\mathbb{M}_B]_{\alpha\beta}\langle\ddot{Q}_{\beta,B}\dot{Q}_{\alpha,B}\rangle + [\mathbb{D}_B]_{\alpha\beta}\langle\dot{Q}_{\beta,B}\dot{Q}_{\alpha,B}\rangle + [\mathbb{G}_B]_{\alpha\beta}\langle\dot{Q}_{\beta,B}\dot{Q}_{\alpha,B}\rangle - [\mathbb{K}_B]_{\alpha\beta}\langle\dot{Q}_{\beta,B}Q_{\alpha,B}\rangle - [\mathbb{R}_B]_{\alpha\beta}\langle\dot{Q}_{\beta,B}Q_{\alpha,B}\rangle\\
&= \epsilon\Big([\mathbb{m}_B]_{\alpha\beta}\langle\ddot{Q}_{\beta,B0}\dot{Q}_{\alpha,B0}\rangle + [\mathbb{d}_B]_{\alpha\beta}\langle\dot{Q}_{\beta,B0}\dot{Q}_{\alpha,B0}\rangle + [\mathbb{g}_B]_{\alpha\beta}\langle\dot{Q}_{\beta,B0}\dot{Q}_{\alpha,B0}\rangle - [\mathbb{k}_B]_{\alpha\beta}\langle\dot{Q}_{\beta,B0}Q_{\alpha,B0}\rangle\\
&\quad - [\mathbb{r}_B]_{\alpha\beta}\langle\dot{Q}_{\beta,B0}Q_{\alpha,B0}\rangle\Big) + \epsilon^2\Big([\mathbb{m}_B]_{\alpha\beta}(\langle\ddot{Q}_{\beta,B1}\dot{Q}_{\alpha,B0}\rangle + \langle\ddot{Q}_{\beta,B0}\dot{Q}_{\alpha,B1}\rangle) + [\mathbb{d}_B]_{\alpha\beta}(\langle\dot{Q}_{\beta,B1}\dot{Q}_{\alpha,B0}\rangle + \langle\dot{Q}_{\beta,B0}\dot{Q}_{\alpha,B1}\rangle)\\
&\quad + [\mathbb{g}_B]_{\alpha\beta}(\langle\dot{Q}_{\beta,B1}\dot{Q}_{\alpha,B0}\rangle + \langle\dot{Q}_{\beta,B0}\dot{Q}_{\alpha,B1}\rangle)\\
&\quad - [\mathbb{k}_B]_{\alpha\beta}(\langle\dot{Q}_{\beta,B1}Q_{\alpha,B0}\rangle + \langle\dot{Q}_{\beta,B0}Q_{\alpha,B1}\rangle) - [\mathbb{r}_B]_{\alpha\beta}(\langle\dot{Q}_{\beta,B1}Q_{\alpha,B0}\rangle + \langle\dot{Q}_{\beta,B0}Q_{\alpha,B1}\rangle)\Big) + o(\epsilon^2)\,.
\end{aligned} \tag{VIII.15}$$

Since $\dot{Q}_{\alpha,B0}$ and $\ddot{Q}_{\beta,B0}$ are centred, mean square stationary and uncorrelated random processes then all the first order terms in ϵ in Eq. (VIII.15) are zeros. The second order terms in ϵ^2 in Eq. (VIII.15) are not zeros and are calculated as follows.

$$\begin{aligned}
\epsilon\langle Q_{\alpha,B0}\dot{Q}_{\beta,B1}\rangle &= \int_{-\infty}^{+\infty} -i\omega\Big(\omega^2[\mathbb{M}_B]_{\beta\alpha} + i\omega[\mathbb{G}_B]_{\beta\alpha} - [\mathbb{K}_B]_{\beta\alpha} + i\omega[\mathbb{D}_B]_{\beta\alpha} - [\mathbb{R}_B]_{\beta\alpha}\Big)\left|\mathbb{h}_{\alpha,B}\right|^2\overline{\mathbb{h}_{\beta,B}}\,S_{F_{\alpha,B}}\,d\omega\\
\epsilon\langle Q_{\alpha,B1}\dot{Q}_{\beta,B0}\rangle &= \int_{-\infty}^{+\infty} -i\omega\Big(\omega^2[\mathbb{M}_B]_{\alpha\beta} - i\omega[\mathbb{G}_B]_{\alpha\beta} - [\mathbb{K}_B]_{\alpha\beta} - i\omega[\mathbb{D}_B]_{\beta\alpha} - [\mathbb{R}_B]_{\beta\alpha}\Big)\mathbb{h}_{\alpha,B}\left|\mathbb{h}_{\beta,B}\right|^2 S_{F_{\beta,B}}\,d\omega\\
\epsilon\langle\dot{Q}_{\alpha,B0}\dot{Q}_{\beta,B1}\rangle &= \int_{-\infty}^{+\infty} \omega^2\Big(\omega^2[\mathbb{M}_B]_{\beta\alpha} + i\omega[\mathbb{G}_B]_{\beta\alpha} - [\mathbb{K}_B]_{\beta\alpha} + i\omega[\mathbb{D}_B]_{\beta\alpha} - [\mathbb{R}_B]_{\beta\alpha}\Big)\left|\mathbb{h}_{\alpha,B}\right|^2\overline{\mathbb{h}_{\beta,B}}\,S_{F_{\alpha,B}}\,d\omega\\
\epsilon\langle\dot{Q}_{\alpha,B1}\dot{Q}_{\beta,B0}\rangle &= \int_{-\infty}^{+\infty} \omega^2\Big(\omega^2[\mathbb{M}_B]_{\alpha\beta} - i\omega[\mathbb{G}_B]_{\alpha\beta} - [\mathbb{K}_B]_{\alpha\beta} - i\omega[\mathbb{D}_B]_{\beta\alpha} - [\mathbb{R}_B]_{\beta\alpha}\Big)\mathbb{h}_{\alpha,B}\left|\mathbb{h}_{\beta,B}\right|^2 S_{F_{\beta,B}}\,d\omega\\
\epsilon\langle\dot{Q}_{\alpha,B0}\ddot{Q}_{\beta,B1}\rangle &= \int_{-\infty}^{+\infty} -i\omega^3\Big(\omega^2[\mathbb{M}_B]_{\beta\alpha} + i\omega[\mathbb{G}_B]_{\beta\alpha} - [\mathbb{K}_B]_{\beta\alpha} + i\omega[\mathbb{D}_B]_{\beta\alpha} - [\mathbb{R}_B]_{\beta\alpha}\Big)\left|\mathbb{h}_{\alpha,B}\right|^2\overline{\mathbb{h}_{\beta,B}}\,S_{F_{\alpha,B}}\,d\omega\\
\epsilon\langle\dot{Q}_{\alpha,B1}\ddot{Q}_{\beta,B0}\rangle &= \int_{-\infty}^{+\infty} -i\omega^3\Big(\omega^2[\mathbb{M}_B]_{\alpha\beta} - i\omega[\mathbb{G}_B]_{\alpha\beta} - [\mathbb{K}_B]_{\alpha\beta} - i\omega[\mathbb{D}_B]_{\beta\alpha} - [\mathbb{R}_B]_{\beta\alpha}\Big)\mathbb{h}_{\alpha,B}\left|\mathbb{h}_{\beta,B}\right|^2 S_{F_{\beta,B}}\,d\omega\,.
\end{aligned}$$

Mean local-frequency generalised instantaneous exchanged power

Using these expressions in Eq. (VIII.15) yields the following expression of the mean local-frequency generalised instantaneous exchanged power $\langle W^{\text{ex}}_{\alpha\beta,B}\rangle$,

$$\begin{aligned}\langle W^{\text{ex}}_{\alpha\beta,B}\rangle = &\int_{-\infty}^{+\infty} -i\omega\Big((\omega^2[\mathbb{M}_B]_{\alpha\beta}-[\mathbb{K}_B]_{\alpha\beta})^2+\omega^2[\mathbb{G}_B]^2_{\alpha\beta}-\omega^2[\mathbb{D}_B]^2_{\alpha\beta}-[\mathbb{R}_B]^2_{\alpha\beta}\Big)\left|\mathbb{h}_{\alpha,B}\right|^2\overline{\mathbb{h}_{\beta,B}}S_{F_{\alpha,B}}\,d\omega\\
&+\int_{-\infty}^{+\infty} 2\omega^2\Big((\omega^2[\mathbb{M}_B]_{\alpha\beta}-[\mathbb{K}_B]_{\alpha\beta})[\mathbb{D}_B]_{\alpha\beta}+[\mathbb{G}_B]_{\alpha\beta}[\mathbb{R}_B]_{\alpha\beta}\Big)\left|\mathbb{h}_{\alpha,B}\right|^2\overline{\mathbb{h}_{\beta,B}}S_{F_{\alpha,B}}\,d\omega\\
&+\int_{-\infty}^{+\infty} -i\omega\Big((\omega^2[\mathbb{M}_B]_{\alpha\beta}-[\mathbb{K}_B]_{\alpha\beta})^2+\omega^2([\mathbb{G}_B]_{\alpha\beta}+[\mathbb{D}_B]_{\alpha\beta})^2+[\mathbb{R}_B]^2_{\alpha\beta}\Big)\mathbb{h}_{\alpha,B}\left|\mathbb{h}_{\beta,B}\right|^2 S_{F_{\beta,B}}\,d\omega\\
&+\int_{-\infty}^{+\infty} 2i\omega(\omega^2[\mathbb{M}_B]_{\alpha\beta}-[\mathbb{K}_B]_{\alpha\beta})[\mathbb{R}_B]_{\alpha\beta}\mathbb{h}_{\alpha,B}\left|\mathbb{h}_{\beta,B}\right|^2 S_{F_{\beta,B}}\,d\omega+o(\epsilon^2)\,. \qquad \text{(VIII.16)}\end{aligned}$$

Moreover, support of power spectral density $S_{F_{\alpha,B}}(\omega)=(\mathbb{1}_B(\omega)+\mathbb{1}_B(-\omega))S_{\alpha,B}$ is the limited frequency band $\mathbb{B}=-B\cup B$ and considering the parity of the integrands in ω, which allows the dropping of the complex conjugate, we then obtain

$$\begin{aligned}\langle W^{\text{ex}}_{\alpha\beta,B}\rangle =&S_{\alpha,B}\int_{\mathbb{B}} i\omega\Big((\omega^2[\mathbb{M}_B]_{\alpha\beta}-[\mathbb{K}_B]_{\alpha\beta})^2+\omega^2[\mathbb{G}_B]^2_{\alpha\beta}-\omega^2[\mathbb{D}_B]^2_{\alpha\beta}-[\mathbb{R}_B]^2_{\alpha\beta}\Big)\left|\mathbb{h}_{\alpha,B}\right|^2\mathbb{h}_{\beta,B}\,d\omega\\
&+S_{\alpha,B}\int_{\mathbb{B}} 2\omega^2\left((\omega^2[\mathbb{M}_B]_{\alpha\beta}-[\mathbb{K}_B]_{\alpha\beta})[\mathbb{D}_B]_{\alpha\beta}+[\mathbb{G}_B]_{\alpha\beta}[\mathbb{R}_B]_{\alpha\beta}\right)\left|\mathbb{h}_{\alpha,B}\right|^2\mathbb{h}_{\beta,B}\,d\omega\\
&-S_{\beta,B}\int_{\mathbb{B}} i\omega\Big((\omega^2[\mathbb{M}_B]_{\alpha\beta}-[\mathbb{K}_B]_{\alpha\beta})^2+\omega^2([\mathbb{G}_B]_{\alpha\beta}+[\mathbb{D}_B]_{\alpha\beta})^2+[\mathbb{R}_B]^2_{\alpha\beta}\Big)\mathbb{h}_{\alpha,B}\left|\mathbb{h}_{\beta,B}\right|^2 d\omega\\
&+S_{\beta,B}\int_{\mathbb{B}} 2i\omega(\omega^2[\mathbb{M}_B]_{\alpha\beta}-[\mathbb{K}_B]_{\alpha\beta})[\mathbb{R}_B]_{\alpha\beta}\mathbb{h}_{\alpha,B}\left|\mathbb{h}_{\beta,B}\right|^2 d\omega+o(\epsilon^2)\,. \qquad \text{(VIII.17)}\end{aligned}$$

Mean local-frequency generalised instantaneous mechanical energy

Similarly, the development in ϵ of the mean local-frequency generalised instantaneous mechanical energy can be obtained and we then have, at the zero order in ϵ^0

$$\begin{aligned}\langle\mathcal{E}_{\alpha,B}\rangle &= \frac{1}{2}\Big([\mathbb{M}_B]_{\alpha\alpha}\langle\dot{Q}^2_{\alpha,B}\rangle+[\mathbb{K}_B]_{\alpha\alpha}\langle Q^2_{\alpha,B}\rangle\Big)\\
&= [\mathbb{M}_B]_{\alpha\alpha}\langle\dot{Q}^2_{\alpha,B0}\rangle+o(1)\\
&= S_{\alpha,B}\int_{\mathbb{B}}\omega^2[\mathbb{M}_B]_{\alpha\alpha}\left|\mathbb{h}_{\alpha,B}\right|^2 d\omega+o(1)\,. \qquad \text{(VIII.18)}\end{aligned}$$

Mean local-frequency generalised instantaneous dissipated energy

Using a Neumann expansion of the inverse matrix $([\mathbb{A}_B(\omega)]+[\Delta\mathbb{A}_B(\omega)])^{-1}$ which can be rewritten as $([I_B]+[\mathbb{H}_B(\omega)][\Delta\mathbb{A}_B(\omega)])^{-1}[\mathbb{H}_B]$ where

$$[\mathbb{H}_B(\omega)]=\Big(-\omega^2[\mathbb{M}_B]+i\omega[\mathbb{D}_B]+i\,\omega[\mathbb{G}_B]+[\mathbb{K}_B]+[\mathbb{R}_B]\Big)^{-1},$$

$$[\mathbb{A}_B(\omega)]_{\alpha\beta} = \delta_{\alpha\beta}\Big(-\omega^2[\mathbb{M}_B]_{\alpha\beta} + i\omega[\mathbb{D}_B]_{\alpha\beta} + i\,\omega[\mathbb{G}_B]_{\alpha\beta} + [\mathbb{K}_B]_{\alpha\beta} + [\mathbb{R}_B]_{\alpha\beta}\Big),$$

$$[\Delta\mathbb{A}_B(\omega)] = -\omega^2[\mathbb{M}_B] + i\omega[\mathbb{D}_B] + i\,\omega[\mathbb{G}_B] + [\mathbb{K}_B] + [\mathbb{R}_B] - [\mathbb{A}_B(\omega)],$$

we then have, at the second order in ϵ

$$\langle \dot{Q}^2_{\alpha,B}\rangle = S_{\alpha,B}\left(\int_{\mathbb{R}} \omega^2 \left|\mathbb{h}_{\alpha,B}(\omega)\right| d\omega + \int_{\mathbb{R}} 2\,\omega^2\, \mathcal{R}_{\text{eal}}\Big\{ \mathbb{h}_{\alpha,B}(\omega) \sum_{\beta\neq\alpha} [\Delta\mathbb{A}_B(\omega)]_{\alpha\beta}[\Delta\mathbb{A}_B(\omega)]_{\beta\alpha} \Big\}\, d\omega \right) + \sum_{\beta\neq\alpha} S_{\beta,B} \int_R \omega^2 \left|\mathbb{h}_{\alpha,B}(\omega)\right|^2 \left|[\Delta\mathbb{A}_B(\omega)]_{\alpha\beta}\right|^2 d\omega + o(\epsilon^2). \quad \text{(VIII.19)}$$

Furthermore, from Eq. (VIII.6), in any limited frequency band B, it is deduced that mean local-frequency generalised dissipated power $\langle W^{\text{diss}}_{\alpha,B}\rangle$ can be rewritten as, at second order in ϵ,

$$\begin{aligned}\langle W^{\text{diss}}_{\alpha,B}\rangle &= [\mathbb{D}_B]_{\alpha\alpha}\langle \dot{Q}^2_{\alpha,B}\rangle \\ &= S_{\alpha,B}\,[\mathbb{D}_B]_{\alpha\alpha}\left(\int_{\mathbb{R}} \omega^2 \left|\mathbb{h}_{\alpha,B}(\omega)\right| d\omega + \int_{\mathbb{R}} 2\,\omega^2\, \mathcal{R}_{\text{eal}}\Big\{ \mathbb{h}_{\alpha,B}(\omega) \sum_{\beta\neq\alpha} [\Delta\mathbb{A}_B(\omega)]_{\alpha\beta}[\Delta\mathbb{A}_B(\omega)]_{\beta\alpha} \Big\}\, d\omega \right) \\ &+ \sum_{\beta\neq\alpha} S_{\beta,B}\,[\mathbb{D}_B]_{\alpha\alpha} \int_R \omega^2 \left|\mathbb{h}_{\alpha,B}(\omega)\right|^2 \left|[\Delta\mathbb{A}_B(\omega)]_{\alpha\beta}\right|^2 d\omega + o(\epsilon^2). \end{aligned} \quad \text{(VIII.20)}$$

This equation is valid in any case up to second-order in ϵ. Nevertheless, as for numerous authors, the same equation can be rewritten at first order in ϵ as

$$\langle W^{\text{diss}}_{\alpha,B}\rangle = S_{\alpha,B}\,[\mathbb{D}_B]_{\alpha\alpha} \int_{\mathbb{R}} \omega^2 \left|\mathbb{h}_{\alpha,B}(\omega)\right| d\omega + o(\epsilon). \quad \text{(VIII.21)}$$

which does not mean that mean local-frequency generalised dissipated power $\langle W^{\text{diss}}_{\alpha,B}\rangle$ is proportional to mean local-frequency generalised instantaneous mechanical energy $\langle \mathcal{E}_{\alpha,B}\rangle$ since Eq. (VIII.18) is valid at order 1 only.

VIII.2.3 Equivalent Coupling Power Proportionality (ECPP) coefficients

Using Eq. (VIII.18) into Eq. (VIII.17), we then obtain, for $\beta \neq \alpha$,

$$\langle W^{\text{ex}}_{\alpha\beta,B}\rangle = z_{\alpha\beta,B}\,\langle \mathcal{E}_{\alpha,B}\rangle - x_{\alpha\beta,B}\,\langle \mathcal{E}_{\beta,B}\rangle + o(\epsilon^2)\,, \quad \text{(VIII.22)}$$

where the Equivalent Coupling Power Proportionality coefficients are defined as

$$\begin{aligned} z_{\alpha\beta,B} &= \frac{\int_{\mathbb{B}} i\omega \Big((\omega^2[\mathbb{M}_B]_{\alpha\beta} - [\mathbb{K}_B]_{\alpha\beta})^2 + \omega^2[\mathbb{G}_B]^2_{\alpha\beta} - \omega^2[\mathbb{D}_B]^2_{\alpha\beta} - [\mathbb{R}_B]^2_{\alpha\beta} \Big) |\mathbb{h}_\alpha|^2\, \mathbb{h}_\beta\, d\omega}{\int_{\mathbb{B}} \omega^2[\mathbb{M}_B]_{\alpha\alpha}\,|\mathbb{h}_\alpha|^2\, d\omega} \\ &+ \frac{2\int_{\mathbb{B}} \omega^2 \left((\omega^2[\mathbb{M}_B]_{\alpha\beta} - [\mathbb{K}_B]_{\alpha\beta})[\mathbb{D}_B]_{\alpha\beta} + [\mathbb{G}_B]_{\alpha\beta}[\mathbb{R}_B]_{\alpha\beta} \right) |\mathbb{h}_\alpha|^2\, \mathbb{h}_\beta\, d\omega}{\int_{\mathbb{B}} \omega^2[\mathbb{M}_B]_{\alpha\alpha}\,|\mathbb{h}_\alpha|^2\, d\omega} \\ x_{\alpha\beta,B} &= \frac{\int_{\mathbb{B}} i\omega \Big((\omega^2[\mathbb{M}_B]_{\alpha\beta} - [\mathbb{K}_B]_{\alpha\beta})^2 + \omega^2([\mathbb{G}_B]_{\alpha\beta} + [\mathbb{D}_B]_{\alpha\beta})^2 + [\mathbb{R}_B]^2_{\alpha\beta} \Big)\, \mathbb{h}_\alpha\, |\mathbb{h}_\beta|^2\, d\omega}{\int_{\mathbb{B}} \omega^2[\mathbb{M}_B]_{\beta\beta}\,|\mathbb{h}_\beta|^2\, d\omega} \end{aligned}$$

$$- \frac{2\int_{\mathbb{B}} i\omega(\omega^2[\mathbb{M}_B]_{\alpha\beta} - [\mathbb{K}_B]_{\alpha\beta})[\mathbb{R}_B]_{\alpha\beta}\, \mathbb{h}_\alpha \left|\mathbb{h}_\beta\right|^2 d\omega}{\int_{\mathbb{B}} \omega^2 [\mathbb{M}_B]_{\beta\beta} \left|\mathbb{h}_\beta\right|^2 d\omega} \,. \tag{VIII.23}$$

It should be noted that the ECPP coefficients introduced in this section do not have the same reciprocity properties as CPP coefficients in classic SEA. It can be observed that, compared to the original CPP expression (see for instance [110]), the only added terms are those in $[\mathbb{D}_B]_{\alpha\beta}$ and $[\mathbb{R}_B]_{\alpha\beta}$ that exist only in a reduced model like CROM or ESOM and its associated equivalent second-order model for highly dissipative system. Without any high dissipative materials, the expressions of ECPP coefficients can be simplified into the original CPP coefficients. These equations are rewritten in using the previous convention for the block-matrices with subscripts (ij) when a block-matrix corresponds to couplings between subsystems (i) and (j). We then have, for $\beta \neq \alpha$,

$$\begin{aligned}
z^{(ij)}_{\alpha\beta,B} &= \frac{\int_{\mathbb{B}} i\omega \left((\omega^2[\mathbb{M}^{(ij)}_B]_{\alpha\beta} - [\mathbb{K}^{(ij)}_B]_{\alpha\beta})^2 + \omega^2[\mathbb{G}^{(ij)}_B]^2_{\alpha\beta} - \omega^2[\mathbb{D}^{(ij)}_B]^2_{\alpha\beta} - [\mathbb{R}^{(ij)}_B]^2_{\alpha\beta}\right) \left|\mathbb{h}^{(i)}_{\alpha,B}\right|^2 \mathbb{h}^{(j)}_{\beta,B}\, d\omega}{\int_{\mathbb{B}} \omega^2 [\mathbb{M}^{(i)}_B]_{\alpha\alpha} \left|\mathbb{h}^{(i)}_{\alpha,B}\right|^2 d\omega} \\
&\quad + \frac{2\int_{\mathbb{B}} \omega^2 \left((\omega^2[\mathbb{M}^{(ij)}_B]_{\alpha\beta} - [\mathbb{K}^{(ij)}_B]_{\alpha\beta})[\mathbb{D}^{(ij)}_B]_{\alpha\beta} + [\mathbb{G}^{(ij)}_B]_{\alpha\beta}[\mathbb{R}^{(ij)}_B]_{\alpha\beta}\right) \left|\mathbb{h}^{(i)}_{\alpha,B}\right|^2 \mathbb{h}^{(j)}_{\beta,B}\, d\omega}{\int_{\mathbb{B}} \omega^2 [\mathbb{M}^{(i)}_B]_{\alpha\alpha} \left|\mathbb{h}^{(i)}_{\alpha,B}\right|^2 d\omega} \\
x^{(ij)}_{\alpha\beta,B} &= \frac{\int_{\mathbb{B}} i\omega \left((\omega^2[\mathbb{M}^{(ij)}_B]_{\alpha\beta} - [\mathbb{K}^{(ij)}_B]_{\alpha\beta})^2 + \omega^2([\mathbb{G}^{(ij)}_B]_{\alpha\beta} + [\mathbb{D}^{(ij)}_B]_{\alpha\beta})^2 + [\mathbb{R}^{(ij)}_B]^2_{\alpha\beta}\right) \mathbb{h}^{(i)}_{\alpha,B} \left|\mathbb{h}^{(j)}_{\beta,B}\right|^2 d\omega}{\int_{\mathbb{B}} \omega^2 [\mathbb{M}^{(j)}_B]_{\beta\beta} \left|\mathbb{h}^{(j)}_{\beta,B}\right|^2 d\omega} \\
&\quad - \frac{2\int_{\mathbb{B}} i\omega \left(\omega^2[\mathbb{M}^{(ij)}_B]_{\alpha\beta}[\mathbb{R}^{(ij)}_B]_{\alpha\beta} - [\mathbb{K}^{(ij)}_B]_{\alpha\beta}[\mathbb{R}^{(ij)}_B]_{\alpha\beta}\right) \mathbb{h}^{(i)}_{\alpha,B} \left|\mathbb{h}^{(j)}_{\beta,B}\right|^2 d\omega}{\int_{\mathbb{B}} \omega^2 [\mathbb{M}^{(j)}_B]_{\beta\beta} \left|\mathbb{h}^{(j)}_{\beta,B}\right|^2 d\omega} \,,
\end{aligned} \tag{VIII.24}$$

with $\omega \mapsto \mathbb{h}^{(i)}_{\alpha,B}(\omega)$, the α-th equivalent generalised FRF of subsystem (i) that is defined as, for all $\omega \in B$

$$\mathbb{h}^{(i)}_{\alpha,B}(\omega) = \left(-\omega^2 [\mathbb{M}^{(i)}_B]_{\alpha\alpha} + i\omega [\mathbb{D}^{(i)}_B]_{\alpha\alpha} + [\mathbb{K}^{(i)}_B]_{\alpha\alpha} \right)^{-1} .$$

Finally, Eqs. (VIII.9) and (VIII.22) are rewritten as, with the same block-matrix notation,

$$\langle W^{(i),\mathrm{diss}}_{\alpha,B} \rangle + \sum_{j \neq i} \langle W^{(ij),\mathrm{ex}}_{\alpha\beta,B} \rangle = \langle W^{(i),\mathrm{in}}_{\alpha,B} \rangle \,, \tag{VIII.25}$$

$$\langle W^{(i),\mathrm{ex}}_{\alpha\beta,B} \rangle = z^{(ij)}_{\alpha\beta,B} \langle \mathcal{E}^{(i)}_{\alpha,B} \rangle - x^{(ij)}_{\alpha\beta,B} \langle \mathcal{E}^{(j)}_{\beta,B} \rangle + o(\epsilon^2) \,. \tag{VIII.26}$$

An analytical calculation of the ECPP coefficients $z^{(ij)}_{\alpha\beta,B}$ and $x^{(ij)}_{\alpha\beta,B}$ is given in Appendix. D. Furthermore, from Eq. (VIII.6) and (VIII.18), in any limited frequency band B, for any subsystem (i), it is deduced that mean local-frequency generalised dissipated power $\langle W^{(i),\mathrm{diss}}_{\alpha,B} \rangle$ can be rewritten as, using again the block-matrix notation,

$$\langle W^{(i),\mathrm{diss}}_{\alpha,B} \rangle = [\mathbb{D}^{(i)}_B]_{\alpha\alpha} \langle \dot{Q}^{(i)\,2}_{\alpha,B} \rangle = \frac{[\mathbb{D}^{(i)}_B]_{\alpha\alpha}}{[\mathbb{M}^{(i)}_B]_{\alpha\alpha}} \langle \mathcal{E}^{(i)}_{\alpha,B} \rangle + o(\epsilon) \,. \tag{VIII.27}$$

which means that mean local-frequency generalised dissipated power $\langle W_{\alpha,B}^{(i),\mathrm{diss}} \rangle$ is proportional to mean local-frequency generalised instantaneous mechanical energy $\langle \mathcal{E}_{\alpha,B}^{(i)} \rangle$. This equation is true at order one but is false at greater orders in ϵ.

VIII.2.4 SEA-ECPP approach

Finally, the matrix equation of Eq. (VIII.9) in a limited frequency band B of SEA-ECPP approach based on the ESOM of the CROM for the Model 1 can be written as,

$$\begin{bmatrix} [Z_B^{(1)}]-[X_B^{(11)}] & -[X_B^{(12)}] & -[X_B^{(13)}] & -[X_B^{(14)}] & -[X_B^{(15)}] \\ -[X_B^{(21)}] & [Z_B^{(2)}]-[X_B^{(22)}] & -[X_B^{(23)}] & -[X_B^{(24)}] & -[X_B^{(25)}] \\ -[X_B^{(31)}] & -[X_B^{(32)}] & [Z_B^{(3)}]-[X_B^{(33)}] & -[X_B^{(34)}] & -[X_B^{(35)}] \\ -[X_B^{(41)}] & -[X_B^{(42)}] & -[X_B^{(43)}] & [Z_B^{(4)}]-[X_B^{(44)}] & -[X_B^{(45)}] \\ -[X_B^{(51)}] & -[X_B^{(52)}] & -[X_B^{(53)}] & -[X_B^{(54)}] & [Z_B^{(5)}]-[X_B^{(55)}] \end{bmatrix} \begin{Bmatrix} \underline{\boldsymbol{\mathcal{E}}}_B^{(1)} \\ \underline{\boldsymbol{\mathcal{E}}}_B^{(2)} \\ \underline{\boldsymbol{\mathcal{E}}}_B^{(3)} \\ \underline{\boldsymbol{\mathcal{E}}}_B^{(4)} \\ \underline{\boldsymbol{\mathcal{E}}}_B^{(5)} \end{Bmatrix} = \begin{Bmatrix} \underline{\mathbf{W}}_B^{(1),\mathrm{in}} \\ 0 \\ 0 \\ 0 \\ 0 \end{Bmatrix}, \tag{VIII.28}$$

and for the Model 2,

$$\begin{bmatrix} [Z_B^{(2)}]-[X_B^{(22)}] & -[X_B^{(23)}] & -[X_B^{(24)}] \\ -[X_B^{(32)}] & [Z_B^{(3)}]-[X_B^{(33)}] & -[X_B^{(34)}] \\ -[X_B^{(42)}] & -[X_B^{(43)}] & [Z_B^{(4)}]-[X_B^{(44)}] \end{bmatrix} \begin{Bmatrix} \underline{\boldsymbol{\mathcal{E}}}_B^{(2)} \\ \underline{\boldsymbol{\mathcal{E}}}_B^{(3)} \\ \underline{\boldsymbol{\mathcal{E}}}_B^{(4)} \end{Bmatrix} = \begin{Bmatrix} \underline{\mathbf{W}}_B^{(2),\mathrm{in}} \\ \underline{\mathbf{W}}_B^{(3),\mathrm{in}} \\ \underline{\mathbf{W}}_B^{(4),\mathrm{in}} \end{Bmatrix}, \tag{VIII.29}$$

where, for all subsystems (i) and (j), the entries (α,β) of matrices $[X_B^{(ij)}]$ are equal to $x_{\alpha\beta,B}^{(ij)}$; where the $\alpha-$th component of vector $\underline{\mathbf{W}}_B^{(i),\mathrm{in}}$ is equal to $\langle W_{\alpha,B}^{(i),\mathrm{in}} \rangle$; where the $\alpha-$th component of vector $\underline{\boldsymbol{\mathcal{E}}}_B^{(i)}$ is equal to $\langle \mathcal{E}_{\alpha,B}^{(i)} \rangle$ and where matrix $[Z_B^{(i)}]$ is defined as, for all $\alpha \neq \beta$,

$$[Z_B^{(i)}]_{\alpha\alpha} = \frac{[\mathbb{D}_B^{(i)}]_{\alpha\alpha}}{[\mathbb{M}_B^{(i)}]_{\alpha\alpha}} + \sum_j \sum_\gamma z_{\alpha\gamma,B}^{(ij)} \quad \text{and} \quad [Z_B^{(i)}]_{\alpha\beta} = -x_{\alpha\beta,B}^{(ii)} \quad .$$

Numerical applications of SEA-ECPP approach will be shown in Chapter. X.

CHAPTER IX

UNCERTAINTY QUANTIFICATION

The different sources of uncertainties in computational mechanics are mainly related to the parameters of the computational model and related to the hypotheses and approximations used in the modelling process. These sources of uncertainties propagate on the solutions of the computational model. There exist different methodologies for taking into account the level of uncertainties on the solution of the computational model with uncertain parameters or with uncertain modelling. Among the numerous methodologies proposed in the literature, those that are based on the theory of probability are very much well-tested and much experienced and with the strongest mathematical background. In the framework of those probabilistic approaches of the uncertainties in computational mechanics, the uncertain parameters of the computational model are modelled as random variables for which a probabilistic model has to be constructed. The use of the MaxEnt principle and the theory of information can be used for constructing the *prior* probabilistic model of the uncertain parameters. Such an approach for modelling the uncertainties is referred as *parametric probabilistic approach* (see for instance, [111–119]). In addition, in linear dynamics, the values of the generalised matrices of the computational model are modelled as random matrices in order to account the uncertainties related to the modelling process (see for instance, [44, 120–122] and [123–131]. Such a probabilistic approach is referred as *non parametric probabilistic approach*. In the previous chapter, an Equivalent second-order computational model has been deduced from the CROM and some hypotheses. This process required the identifications of a set of frequency independent matrices. Not only, such a frequency independence is a very strong approximation but also, this identification is not unique. Actually, the error is minimal at the centre frequency of each band B where error is minimal as the error analysis presented in the same chapter showed it. Another approximation would have decreased at other frequencies or more globally. Consequently, the values of the matrices of the Equivalent second-order model are uncertain. For taking into account such uncertainties,

the values of those uncertain matrices are modelled by a set of matrix-valued random variable. Such a probabilistic approach corresponds to the *non parametric probabilistic approach* for the modelling uncertainties. In the next sections of this chapter, we will briefly recall some results on the theory of random matrices and then the probabilistic model for uncertain Equivalent second-order model will be presented.

IX.1 Random Matrix Ensemble SG_0^+

A random matrix $[\mathbf{H}_0]$ in SG_0^+ with values in $\mathbb{M}_n^+(\mathbb{R})$ is defined and such that

$$E\{[\mathbf{H}_0]\} = [I_n] \quad , \quad E\{\log(\det([\mathbf{H}_0]))\} = \nu_{\mathbf{H}_0} \quad , \quad |\nu_{\mathbf{H}_0}| < +\infty. \tag{IX.1}$$

Condition $E\{\log(\det([\mathbf{H}_0]))\} = \nu_{\mathbf{H}_0}$ allows the invertibility and the integration of random inverse matrix $[\mathbf{H}_0]^{-1}$ to be satisfied. The probability density function of random matrix $[\mathbf{H}_0]$ defined on $\mathbb{S}_n = \mathbb{M}_n^+(\mathbb{R})$ is then written as

$$p_{[\mathbf{H}_0]}([H]) = \mathbb{1}_{\mathbb{S}_n}([H])\, \kappa\, (det[H])^{(n+1)\frac{1-\delta^2}{2\delta^2}}\; e^{-\frac{n+1}{2\delta^2}\mathrm{tr}[H]}\,. \tag{IX.2}$$

The normalisation constant κ is defined as

$$\kappa = (2\pi)^{-n(n-1)/4}\Big(\frac{n+1}{2\delta^2}\Big)^{\frac{n(n+1)}{2\delta^2}}\Big(\prod_{j=1}^{n}\Gamma(\frac{n+1}{2\delta^2}+\frac{1-j}{2})\Big)^{-1} \tag{IX.3}$$

where, for all $z>0$, $\Gamma(z) = \int_0^{+\infty} t^{z-1}e^{-t}dt$. Hence, $[\mathbf{H}_0]$ is defined by an unique parameter δ that control the statistical dispersion and with values in $[\,0\,,\sqrt{\frac{n+1}{n+5}}\,]$. This dispersion coefficient is defined as

$$\delta = \Big\{\frac{E\{||[\mathbf{H}_0]-E\{[\mathbf{H}_0]\}||_F^2\}}{||E\{[\mathbf{H}_0]\}||_F^2}\Big\}^{\frac{1}{2}}\,. \tag{IX.4}$$

Since random matrix $[\mathbf{H}_0]$ is almost surely positive definite, then there exists an unique random upper triangular matrix denoted as $[\mathbf{L}]$ that is such that the Cholesky factorisation of random matrix $[\mathbf{H}_0]$ is written as

$$[\mathbf{H}_0] = [\mathbf{L}]^T[\mathbf{L}]\,,\ \text{almost surely}\,. \tag{IX.5}$$

It is then possible to show that random entries $[\mathbf{L}]_{jj'}$ random upper triangular matrix $[\mathbf{L}]$ are such that

$$[\mathbf{L}]_{j'j} = \xi V_{j'j} \quad , \quad \text{for} \quad j' < j \le n\,, \tag{IX.6}$$

$$[\mathbf{L}]_{jj} = \xi\sqrt{2h(\eta_j, V_{jj})} \quad \text{for} \quad j \le n\,, \tag{IX.7}$$

where $\{V_{j'j}, 1 \le j' \le j \le n\}$ is a set of normalised Gaussian real-valued random variables that are mutually statistically independent. The real-valued parameters ξ and η_j are such that $\xi = \delta(n+1)^{-\frac{1}{2}}$ and $\eta_j = \frac{n+1}{2\delta^2} + \frac{1-j}{2}$. The function h is written as $h(\eta, V) = F_{\Gamma_\eta}^{-1}(F_V(v))$ where F_V is the cumulative function of a normalised Gaussian real-valued random variable V and F_{Γ_η} is

the cumulative function of a Gamma real-valued random variable Γ_η of parameter η. Statistically random realisations $[H_0(\theta_1)],\ldots,[H_0(\theta_{n_R})]$ of random matrix $[\mathbf{H}_0]$ are constructed in using Eqs. (IX.5), (IX.6) and (IX.7) and statistically independent realisations $v_{j'j}(\theta_1),\ldots,v_{j'j}(\theta_{n_R})$ of random variable $V_{j'j}$. Consequently, for all $1 \leq r \leq n_R$ and for all $j' < j \leq n$, we have

$$[G_0(\theta_r)] = [L(\theta_r)]^T [L(\theta_r)] \quad , \quad [L(\theta_r)]_{j'j} = \xi v_{j'j}(\theta_r) \quad , \quad [L(\theta_r)]_{jj} = \xi \sqrt{2h(\eta_j, v_{jj}(\theta_r))} \, . \tag{IX.8}$$

IX.2 Ensemble SE^{rect}

Let SE^{rect} be the set of the $\mathbb{M}_{mn}(\mathbb{R})$-valued second-order random matrix $[\mathbf{A}^{\rm rect}]$. Let $[A^{\rm rect}] = E\{[\mathbf{A}^{\rm rect}]\}$ be the mean value of random matrix $[\mathbf{A}^{\rm rect}]$ for which the kernel is assumed to be only the null vector of $\mathbb{R}^n$. We then have

$$[A^{\rm rect}] = [U][A] \tag{IX.9}$$

where $[A] \in \mathbb{M}_n^+(\mathbb{R})$ and $[U] \in \mathbb{M}_{mn}(\mathbb{R})$ such that $[U]^T[U] = [I_n]$. Such a factorisation can be directly deduced from a singular value decomposition (SVD) of matrix $[A^{\rm rect}]$. Indeed, the SVD of $[A^{\rm rect}]$ is written as $[A^{\rm rect}] = [\tilde{U}][S][\tilde{V}]^T$. We then have

$$[U] = [\tilde{U}][\tilde{V}]^T \tag{IX.10}$$

and

$$[A] = [\tilde{V}][S][\tilde{V}]^T \, . \tag{IX.11}$$

Ensemble SE^{rect} is then constructed as the set of the random matrices $[\mathbf{A}^{\rm rect}]$ that are written as

$$[\mathbf{A}^{\rm rect}] = [U][\mathbf{A}] \, , \tag{IX.12}$$

where $[\mathbf{A}]$ is written as $[\mathbf{A}] = [L_A]^T [\mathbf{H}_0][L_A]$ where the deterministic upper triangular matrix $[L_A]$ is such that $[L_A]^T[L_A] = [A]$ and where $[\mathbf{H}_0]$ is a random matrix in ensemble SE$_0^+$ for which the dispersion coefficient is δ_A. Statistically random realisations $[A^{\rm rect}(\theta_1)]$, ..., $[A^{\rm rect}(\theta_{n_R})]$ of random matrix $[\mathbf{A}^{\rm rect}]$ are constructed in using statistically independent realisations $[H_0(\theta_1)]$, ..., $[H_0(\theta_{n_R})]$ of random matrix $[\mathbf{H}_0] \in \mathrm{SG}_0^+$ in using Eq. (IX.12),

$$[A^{\rm rect}(\theta_r)] = [U][L_A]^T [G_0(\theta_r)][L_A] \, . \tag{IX.13}$$

However, it is possible that in certain cases the matrix $[A]$ are not always positive definite, and the Cholesky factorization can therefore not be used. In this case, the solution chosen in this work is doing Cholesky factorization on matrix $[S]$, which is guaranteed to be positive definite (at least for its economical size). We then have $[\mathbf{A}] = [\tilde{V}][\mathbf{S}][\tilde{V}]^T = [\tilde{V}][L_S]^T [\mathbf{H}_0][L_S][\tilde{V}]^T$. And the expression of random rectangular matrix $[\mathbf{A}^{\rm rect}]$ is always $[\mathbf{A}^{\rm rect}] = [U][\mathbf{A}]$.

IX.3 Random Equivalent Second-Order model

As explained in the introduction of this chapter, the methodology used in order to construct the Equivalent second-order model introduces some uncertainties that all are related to the values of matrices $[\mathbb{M}_B]$, $[\mathbb{D}_B]$, $[\mathbb{G}_B]$, $[\mathbb{K}_B]$ and $[\mathbb{R}_B]$. Consequently, the solution of the Equivalent second-order model is also uncertain because the uncertainties on $[\mathbb{M}_B]$, $[\mathbb{D}_B]$, $[\mathbb{G}_B]$, $[\mathbb{K}_B]$ and $[\mathbb{R}_B]$ propagates to $q_B(\omega)$. Consequently, the matrices with uncertain values are modelled as random matrices $[\mathbf{M}_B]$, $[\mathbf{D}_B]$, $[\mathbf{G}_B]$, $[\mathbf{K}_B]$, $[\mathbf{R}_B]$ and the uncertain solution is then modelled as a random vector $\mathbf{Q}_B(\omega)$ for all $\omega \in B$. Let n_f and n_s be the number of generalised coordinates that correspond to the acoustic volumes and the visco-elastic solids respectively. Hence, for Model 1, n_f is equal to the dimension of vector $(\mathbf{q}_B^{(1)}, \mathbf{q}_B^{(3)}, \mathbf{q}_B^{(5)})$ and n_s is equal to the dimension of vector $(\mathbf{q}_B^{(2)}, \mathbf{q}_B^{(4)})$. For Model 2, n_f is equal to the dimension of vector $\mathbf{q}_B^{(3)}$ and n_s is also equal to the dimension of vector $(\mathbf{q}_B^{(2)}, \mathbf{q}_B^{(4)})$. The Cholesky factorisation of matrices $[\mathbb{M}_B]$, $[\mathbb{D}_B]$, $[\mathbb{G}_B]$ are rewritten as

$$[\mathbb{M}_B] = [L_{M_B}]^T [L_{M_B}] \quad , \quad [\mathbb{D}_B] = [L_{D_B}]^T [L_{D_B}] \quad , \quad [\mathbb{K}_B] = [L_{K_B}]^T [L_{K_B}] \, . \tag{IX.14}$$

The probabilistic models of random matrices $[\mathbf{M}_B]$, $[\mathbf{D}_B]$ and $[\mathbf{K}_B]$ are then defined as

$$[\mathbf{M}_B] = [L_{M_B}]^T [\mathbf{H}_{M_B}][L_{M_B}] \quad , \quad [\mathbf{D}_B] = [L_{D_B}]^T [\mathbf{H}_{D_B}][L_{D_B}] \quad , \quad [\mathbf{K}_B] = [L_{K_B}]^T [\mathbf{H}_{K_B}][L_{K_B}] \, , \tag{IX.15}$$

where the block decompositions of random matrices $[\mathbf{H}_{M_B}]$, $[\mathbf{H}_{D_B}]$ and $[\mathbf{H}_{K_B}]$ are written as

$$[\mathbf{H}_{M_B}] = \begin{bmatrix} [\mathbf{H}^\mathrm{f}_{M_B}] & \\ & [\mathbf{H}^\mathrm{s}_{M_B}] \end{bmatrix} \quad , \quad [\mathbf{H}_{D_B}] = \begin{bmatrix} [\mathbf{H}^\mathrm{f}_{D_B}] & \\ & [\mathbf{H}^\mathrm{s}_{D_B}] \end{bmatrix} \quad , \quad [\mathbf{H}_{K_B}] = \begin{bmatrix} [\mathbf{H}^\mathrm{f}_{K_B}] & \\ & [\mathbf{H}^\mathrm{s}_{K_B}] \end{bmatrix} \quad ,$$

in which random matrices $[\mathbf{H}^\mathrm{f}_{M_B}]$, $[\mathbf{H}^\mathrm{s}_{M_B}]$, $[\mathbf{H}^\mathrm{f}_{D_B}]$, $[\mathbf{H}^\mathrm{s}_{D_B}]$, $[\mathbf{H}^\mathrm{f}_{K_B}]$ and $[\mathbf{H}^\mathrm{s}_{K_B}]$ belong to ensemble SG_0^+, with dimensions $(n_\mathrm{f} \times n_\mathrm{f})$ for random matrices with superscript 'f' and dimensions $(n_\mathrm{s} \times n_\mathrm{s})$ for random matrices with superscript 's'. Similar to the case in the previous section, when the matrices $[\mathbb{M}_B]$, $[\mathbb{K}_B]$ or $[\mathbb{D}_B]$ are not guaranteed to be always positive definite, the random germ matrix $[\mathbf{H}_0]$ should be created based on the $[S]$ matrix after a SVD decomposition. Let us take matrix $[\mathbb{M}_B]$ as an example. The probabilistic models written in Eq. (IX.14) and Eq. (IX.15) can be rewritten as,

$$[\mathbb{M}_B] = [\tilde{V}_{M_B}][S_{M_B}][\tilde{V}_{M_B}]^T \quad , \quad [\mathbf{M}_B] = [\tilde{V}_{M_B}][\mathbf{H}_{S_{M_B}}][\tilde{V}_{M_B}]^T \tag{IX.16}$$

Random matrices $[\mathbf{M}_B^{(i)}]$, $[\mathbf{M}_B^{(ij)}]$, $[\mathbf{D}_B^{(i)}]$, $[\mathbf{D}_B^{(ij)}]$, $[\mathbf{K}_B^{(i)}]$ and $[\mathbf{K}_B^{(ij)}]$ are extracted from the block decompositions of random matrices $[\mathbf{M}_B]$, $[\mathbf{D}_B]$ and $[\mathbf{K}_B]$ that is such that, for Model 1,

$$[\mathbf{M}_B] = \begin{bmatrix} [\mathbf{M}_B^{(1)}] & [\mathbf{M}_B^{(13)}] & [\mathbf{M}_B^{(15)}] & & \\ [\mathbf{M}_B^{(31)}] & [\mathbf{M}_B^{(3)}] & [\mathbf{M}_B^{(35)}] & & \\ [\mathbf{M}_B^{(51)}] & [\mathbf{M}_B^{(53)}] & [\mathbf{M}_B^{(5)}] & & \\ & & & [\mathbf{M}_B^{(2)}] & [\mathbf{M}_B^{(24)}] \\ & & & [\mathbf{M}_B^{(42)}] & [\mathbf{M}_B^{(4)}] \end{bmatrix} \quad , \quad [\mathbf{D}_B] = \begin{bmatrix} [\mathbf{D}_B^{(1)}] & [\mathbf{D}_B^{(13)}] & [\mathbf{D}_B^{(15)}] & & \\ [\mathbf{D}_B^{(31)}] & [\mathbf{D}_B^{(3)}] & [\mathbf{D}_B^{(35)}] & & \\ [\mathbf{D}_B^{(51)}] & [\mathbf{D}_B^{(53)}] & [\mathbf{D}_B^{(5)}] & & \\ & & & [\mathbf{D}_B^{(2)}] & [\mathbf{D}_B^{(24)}] \\ & & & [\mathbf{D}_B^{(42)}] & [\mathbf{D}_B^{(4)}] \end{bmatrix} \quad ,$$

$$[\mathbf{K}_B] = \begin{bmatrix} [\mathbf{K}_B^{(1)}] & [\mathbf{K}_B^{(13)}] & [\mathbf{K}_B^{(15)}] & & \\ [\mathbf{K}_B^{(31)}] & [\mathbf{K}_B^{(3)}] & [\mathbf{K}_B^{(35)}] & & \\ [\mathbf{K}_B^{(51)}] & [\mathbf{K}_B^{(53)}] & [\mathbf{K}_B^{(5)}] & & \\ & & & [\mathbf{K}_B^{(2)}] & [\mathbf{K}_B^{(24)}] \\ & & & [\mathbf{K}_B^{(42)}] & [\mathbf{K}_B^{(4)}] \end{bmatrix} ,$$

and such that, for Model 2,

$$[\mathbf{M}_B] = \begin{bmatrix} [\mathbf{M}_B^{(3)}] & & \\ & [\mathbf{M}_B^{(2)}] & [\mathbf{M}_B^{(24)}] \\ & [\mathbf{M}_B^{(42)}] & [\mathbf{M}_B^{(4)}] \end{bmatrix} , \quad [\mathbf{D}_B] = \begin{bmatrix} [\mathbf{D}_B^{(3)}] & & \\ & [\mathbf{D}_B^{(2)}] & [\mathbf{D}_B^{(24)}] \\ & [\mathbf{D}_B^{(42)}] & [\mathbf{D}_B^{(4)}] \end{bmatrix} , \quad [\mathbf{K}_B] = \begin{bmatrix} [\mathbf{K}_B^{(3)}] & & \\ & [\mathbf{K}_B^{(2)}] & [\mathbf{K}_B^{(24)}] \\ & [\mathbf{K}_B^{(42)}] & [\mathbf{K}_B^{(4)}] \end{bmatrix} ,$$

where the dimensions of the random block matrices $[\mathbf{M}_B^{(i)}]$, $[\mathbf{M}_B^{(ij)}]$, $[\mathbf{D}_B^{(i)}]$, $[\mathbf{D}_B^{(ij)}]$, $[\mathbf{K}_B^{(i)}]$ and $[\mathbf{K}_B^{(ij)}]$ are compliant with the block decomposition of vector $\mathbb{q}_B = (\mathbf{q}_B^{(1)}, \mathbf{q}_B^{(3)}, \mathbf{q}_B^{(5)}, \mathbf{q}_B^{(2)}, \mathbf{q}_B^{(4)})$ for Model 1 and $\mathbb{q}_B = (\mathbf{q}_B^{(3)}, \mathbf{q}_B^{(2)}, \mathbf{q}_B^{(4)})$ for Model 2. Concerning random skew symmetric matrices $[\mathbf{G}_B]$ and $[\mathbf{R}_B]$, their probabilistic model is defined as

$$[\mathbf{G}_B] = \begin{bmatrix} & [\mathbf{G}_B^{\rm sf}] \\ -[\mathbf{G}_B^{\rm sf}]^T & \end{bmatrix} , \quad [\mathbf{R}_B] = \begin{bmatrix} & [\mathbf{R}_B^{\rm sf}] \\ -[\mathbf{R}_B^{\rm sf}]^T & \end{bmatrix} ,$$

in which the random $(n_{\rm f} \times n_{\rm s})$ matrices $[\mathbf{G}_B^{\rm sf}]$ and $[\mathbf{R}_B^{\rm sf}]$ belong to ensemble SE^{rect} with dispersion coefficients δ_{G_B} and δ_{R_B}, respectively and with mean value $[\mathbb{G}_B^{\rm sf}]$ and $[\mathbb{R}_B^{\rm sf}]$ respectively defined as, for Model 1,

$$[\mathbb{G}_B^{\rm sf}] = \begin{bmatrix} [\mathbb{G}_B^{(12)}] & [\mathbb{G}_B^{(14)}] \\ [\mathbb{G}_B^{(32)}] & [\mathbb{G}_B^{(34)}] \\ [\mathbb{G}_B^{(52)}] & [\mathbb{G}_B^{(54)}] \end{bmatrix} , \quad [\mathbb{R}_B^{\rm sf}] = \begin{bmatrix} [\mathbb{R}_B^{(12)}] & [\mathbb{R}_B^{(14)}] \\ [\mathbb{R}_B^{(32)}] & [\mathbb{R}_B^{(34)}] \\ [\mathbb{R}_B^{(52)}] & [\mathbb{R}_B^{(54)}] \end{bmatrix} ,$$

and such that, for Model 2,

$$[\mathbb{G}_B^{\rm sf}] = \begin{bmatrix} [\mathbb{G}_B^{(32)}] & [\mathbb{G}_B^{(34)}] \end{bmatrix} , \quad [\mathbb{R}_B^{\rm sf}] = \begin{bmatrix} [\mathbb{R}_B^{(32)}] & [\mathbb{R}_B^{(34)}] \end{bmatrix} ,$$

Random matrices $[\mathbf{G}_B^{(i)}]$, $[\mathbf{G}_B^{(ij)}]$, $[\mathbf{R}_B^{(i)}]$ and $[\mathbf{R}_B^{(ij)}]$ are extracted from the block decompositions of random matrices $[\mathbf{G}_B]$ and $[\mathbf{R}_B]$ such that, for Model 1

$$[\mathbf{G}_B] = \begin{bmatrix} & & & [\mathbf{G}_B^{(12)}] & [\mathbf{G}_B^{(14)}] \\ & & & [\mathbf{G}_B^{(32)}] & [\mathbf{G}_B^{(34)}] \\ & & & [\mathbf{G}_B^{(52)}] & [\mathbf{G}_B^{(54)}] \\ [\mathbf{G}_B^{(21)}] & [\mathbf{G}_B^{(23)}] & [\mathbf{G}_B^{(25)}] & & \\ [\mathbf{G}_B^{(41)}] & [\mathbf{G}_B^{(43)}] & [\mathbf{G}_B^{(45)}] & & \end{bmatrix} , \quad [\mathbf{R}_B] = \begin{bmatrix} & & & [\mathbf{R}_B^{(12)}] & [\mathbf{R}_B^{(14)}] \\ & & & [\mathbf{R}_B^{(32)}] & [\mathbf{R}_B^{(34)}] \\ & & & [\mathbf{R}_B^{(52)}] & [\mathbf{R}_B^{(54)}] \\ [\mathbf{R}_B^{(21)}] & [\mathbf{R}_B^{(23)}] & [\mathbf{R}_B^{(25)}] & & \\ [\mathbf{R}_B^{(41)}] & [\mathbf{R}_B^{(43)}] & [\mathbf{R}_B^{(45)}] & & \end{bmatrix} ,$$

and for Model 2,

$$[\mathbb{G}_B] = \begin{bmatrix} & [\mathbf{G}_B^{(32)}] & [\mathbf{G}_B^{(34)}] \\ [\mathbf{G}_B^{(23)}] & & \\ [\mathbf{G}_B^{(43)}] & & \end{bmatrix} , \quad [\mathbf{R}_B] = \begin{bmatrix} & [\mathbf{G}_B^{(32)}] & [\mathbf{G}_B^{(34)}] \\ [\mathbf{G}_B^{(23)}] & & \\ [\mathbf{G}_B^{(43)}] & & \end{bmatrix} ,$$

where the dimensions of the random block matrices are compliant with the block decomposition of vector $\mathbb{q}_B = (\mathbf{q}_B^{(1)}, \mathbf{q}_B^{(3)}, \mathbf{q}_B^{(5)}, \mathbf{q}_B^{(2)}, \mathbf{q}_B^{(4)})$ for Model 1 and $\mathbb{q}_B = (\mathbf{q}_B^{(3)}, \mathbf{q}_B^{(2)}, \mathbf{q}_B^{(4)})$ for Model 2.

IX.4 Random ECPP-SEA approach

Since the values of the block matrices $[\mathbb{M}_B^{(ij)}]$, $[\mathbb{D}_B^{(ij)}]$ and $[\mathbb{K}_B^{(ij)}]$ are modelled as random matrices $[\mathbf{M}_B^{(ij)}]$, $[\mathbf{D}_B^{(ij)}]$ and $[\mathbf{K}_B^{(ij)}]$ respectively, then the ECCP coefficients are also modelled as real-valued random variables $Z_{\alpha\beta,B}^{(ij)}$ and $X_{\alpha\beta,B}^{(ij)}$ that are almost surely defined as, for $\beta \neq \alpha$,

$$Z_{\alpha\beta,B}^{(ij)} = \frac{\int_{\mathbb{B}} i\omega \left((\omega^2 [\mathbf{M}_B^{(ij)}]_{\alpha\beta} - [\mathbf{K}_B^{(ij)}]_{\alpha\beta})^2 + \omega^2 [\mathbf{G}_B^{(ij)}]_{\alpha\beta}^2 - \omega^2 [\mathbf{D}_B^{(ij)}]_{\alpha\beta}^2 - [\mathbf{R}_B^{(ij)}]_{\alpha\beta}^2 \right) \left| \mathbf{H}_{\alpha,B}^{(i)} \right|^2 \mathbf{H}_{\beta,B}^{(j)} \, d\omega}{\int_{\mathbb{B}} \omega^2 [\mathbf{M}_B^{(i)}]_{\alpha\alpha} \left| \mathbf{H}_{\alpha,B}^{(i)} \right|^2 d\omega}$$
$$+ \frac{2 \int_{\mathbb{B}} \omega^2 \left((\omega^2 [\mathbf{M}_B^{(ij)}]_{\alpha\beta} - [\mathbf{K}_B^{(ij)}]_{\alpha\beta}) [\mathbf{D}_B^{(ij)}]_{\alpha\beta} + [\mathbf{G}_B^{(ij)}]_{\alpha\beta} [\mathbf{R}_B^{(ij)}]_{\alpha\beta} \right) \left| \mathbf{H}_{\alpha,B}^{(i)} \right|^2 \mathbf{H}_{\beta,B}^{(j)} \, d\omega}{\int_{\mathbb{B}} \omega^2 [\mathbf{M}_B^{(i)}]_{\alpha\alpha} \left| \mathbf{H}_{\alpha,B}^{(i)} \right|^2 d\omega}$$

$$X_{\alpha\beta,B}^{(ij)} = \frac{\int_{\mathbb{B}} i\omega \left((\omega^2 [\mathbf{M}_B^{(ij)}]_{\alpha\beta} - [\mathbf{K}_B^{(ij)}]_{\alpha\beta})^2 + \omega^2 ([\mathbf{G}_B^{(ij)}]_{\alpha\beta} + [\mathbf{D}_B^{(ij)}]_{\alpha\beta})^2 + [\mathbf{R}_B^{(ij)}]_{\alpha\beta}^2 \right) \mathbf{H}_{\alpha,B}^{(i)} \left| \mathbf{H}_{\beta,B}^{(j)} \right|^2 d\omega}{\int_{\mathbb{B}} \omega^2 [\mathbf{M}_B^{(j)}]_{\beta\beta} \left| \mathbf{H}_{\beta,B}^{(j)} \right|^2 d\omega}$$
$$- \frac{2 \int_{\mathbb{B}} i\omega \left(\omega^2 [\mathbf{M}_B^{(ij)}]_{\alpha\beta} [\mathbf{R}_B^{(ij)}]_{\alpha\beta} - [\mathbf{K}_B^{(ij)}]_{\alpha\beta} [\mathbf{R}_B^{(ij)}]_{\alpha\beta} \right) \mathbf{H}_{\alpha,B}^{(i)} \left| \mathbf{H}_{\beta,B}^{(j)} \right|^2 d\omega}{\int_{\mathbb{B}} \omega^2 [\mathbf{M}_B^{(j)}]_{\beta\beta} \left| \mathbf{H}_{\beta,B}^{(j)} \right|^2 d\omega} , \tag{IX.17}$$

with $\omega \mapsto \mathbb{H}_{\alpha,B}^{(i)}(\omega)$, the α-th real-valued random equivalent generalised FRF of subsystem (i) that is defined as, for all $\omega \in B$

$$\mathbf{H}_{\alpha,B}^{(i)}(\omega) = \left(-\omega^2 [\mathbf{M}_B^{(i)}]_{\alpha\alpha} + i\omega [\mathbf{D}_B^{(i)}]_{\alpha\alpha} + [\mathbf{K}_B^{(i)}]_{\alpha\alpha} \right)^{-1} .$$

Finally, in a limited frequency band B, the random SEA-ECPP formulation consists in solving the random system of equations written as follows, for the Model 1,

$$\begin{bmatrix} [\mathbf{Z}_B^{(1)}] & -[\mathbf{X}_B^{(12)}] & -[\mathbf{X}_B^{(13)}] & -[\mathbf{X}_B^{(14)}] & -[\mathbf{X}_B^{(15)}] \\ -[\mathbf{X}_B^{(21)}] & [\mathbf{Z}_B^{(2)}] & -[\mathbf{X}_B^{(23)}] & -[\mathbf{X}_B^{(24)}] & -[\mathbf{X}_B^{(25)}] \\ -[\mathbf{X}_B^{(31)}] & -[\mathbf{X}_B^{(32)}] & [\mathbf{Z}_B^{(3)}] & -[\mathbf{X}_B^{(34)}] & -[\mathbf{X}_B^{(35)}] \\ -[\mathbf{X}_B^{(41)}] & -[\mathbf{X}_B^{(42)}] & -[\mathbf{X}_B^{(43)}] & [\mathbf{Z}_B^{(4)}] & -[\mathbf{X}_B^{(45)}] \\ -[\mathbf{X}_B^{(51)}] & -[\mathbf{X}_B^{(52)}] & -[\mathbf{X}_B^{(53)}] & -[\mathbf{X}_B^{(54)}] & [\mathbf{Z}_B^{(5)}] \end{bmatrix} \begin{Bmatrix} \mathcal{E}_B^{(1)} \\ \mathcal{E}_B^{(2)} \\ \mathcal{E}_B^{(3)} \\ \mathcal{E}_B^{(4)} \\ \mathcal{E}_B^{(5)} \end{Bmatrix} = \begin{Bmatrix} \underline{\mathbf{W}}_B^{(1),\mathrm{in}} \\ 0 \\ 0 \\ 0 \\ 0 \end{Bmatrix} , \tag{IX.18}$$

and for the Model 2,

$$\begin{bmatrix} [\mathbf{Z}_B^{(2)}] & -[\mathbf{X}_B^{(23)}] & -[\mathbf{X}_B^{(24)}] \\ -[\mathbf{X}_B^{(32)}] & [\mathbf{Z}_B^{(3)}] & -[\mathbf{X}_B^{(34)}] \\ -[\mathbf{X}_B^{(42)}] & -[\mathbf{X}_B^{(43)}] & [\mathbf{Z}_B^{(4)}] \end{bmatrix} \begin{Bmatrix} \mathcal{E}_B^{(2)} \\ \mathcal{E}_B^{(3)} \\ \mathcal{E}_B^{(4)} \end{Bmatrix} = \begin{Bmatrix} \underline{\mathbf{W}}_B^{(2),\mathrm{in}} \\ \underline{\mathbf{W}}_B^{(3),\mathrm{in}} \\ \underline{\mathbf{W}}_B^{(4),\mathrm{in}} \end{Bmatrix} , \tag{IX.19}$$

where, for all subsystems (i) and (j), the real-valued random entries (α, β) of matrices $[\mathbf{X}_B^{(ij)}]$ are equal to $X_{\alpha\beta,B}^{(ij)}$; where the $\alpha-$th real-valued deterministic component of vector $\underline{\mathbf{W}}_B^{(i),\mathrm{in}}$ is still equal

to $\langle W_{\alpha,B}^{(i),\mathrm{in}} \rangle$ but where the $\alpha-$th real-valued random component of random vector $\boldsymbol{\mathcal{E}}_B^{(i)}$ is no longer equal to real-valued random variable $\mathcal{E}_{\alpha,B}^{(i)}$ and where random matrix $[\mathbf{Z}_B^{(i)}]$ is defined as, for all $\alpha \neq \beta$,

$$[\mathbf{Z}_B^{(i)}]_{\alpha\alpha} = \frac{[\mathbf{D}_B^{(i)}]_{\alpha\alpha}}{[\mathbf{M}_B^{(i)}]_{\alpha\alpha}} + \sum_j \sum_\gamma Z_{\alpha\gamma,B}^{(ij)} \quad , \quad \text{and} \quad , \quad [\mathbf{Z}_B^{(i)}]_{\alpha\beta} = -X_{\alpha\beta,B}^{(ii)} \quad .$$

Numerical applications of this probabilistic model will be shown in Chapter. X.

CHAPTER X

NUMERICAL APPLICATIONS OF ESOM AND SEA-ECPP APPROACH

Several applications are shown for Model 1 and 2 in this chapter. The calculations of Energy Reduction (ER) for Model 1 and of Sound Transmission Loss (STL) for Model 2 will be respectively carried out with ROM (truncated), Equivalent second-order model (ESOM) and SEA-ECPP and will be compared in this chapter.

Moreover, an application of the probabilistic model on the SEA-ECPP approach will be applied in order to test the robustness of SEA-ECPP approach.

X.1 Numerical application on Model 1

In this section, a numerical example is presented on the ER calculation of the Model 1. The ER represents the difference of energies in two subsystems on unity of dB. In this manuscript, the ER is defined as,

$$\mathrm{ER} = 10\log\frac{\langle\mathcal{E}_B^{(1)}\rangle}{\langle\mathcal{E}_B^{(5)}\rangle}\,, \tag{X.1}$$

where $\langle\mathcal{E}_B^{(i)}\rangle$ is the mean local-frequency global instantaneous mechanical energy that are defined for each approach, respectively: $\langle\mathcal{E}_B^{(i),\mathrm{ROM}}\rangle$, $\langle\mathcal{E}_B^{(i),\mathrm{ESOM}}\rangle$ and $\langle\mathcal{E}_B^{(i),\mathrm{SEA\text{-}ECPP}}\rangle$.

$$\begin{aligned}\langle\mathcal{E}_B^{(i),\mathrm{ROM}}\rangle &\approx \sum_{\alpha}\langle\mathcal{E}_{\alpha,B}^{(i),\mathrm{ROM}}\rangle \\ &= \sum_{j,\alpha,\gamma}\frac{1}{2}\left([\mathcal{M}^{(i)}]_{\alpha\alpha}\int_{\mathbb{B}}\omega^2\left|h_{\alpha\gamma}^{(ij)}\right|^2 S_\gamma^{(j)}\,d\omega + [\mathcal{K}^{(i)}]_{\alpha\alpha}\int_{\mathbb{B}}\left|h_{\alpha\gamma}^{(ij)}\right|^2 S_\gamma^{(j)}\,d\omega\right)\,.\end{aligned}$$

where $S_\gamma^{(j)}$ is constant and $h_{\alpha\gamma}^{(ij)}$ is the value of $\alpha-$th line and $\gamma-$th column of a bloc-matrix $[\mathbb{H}^{(ij)}(\omega)]$ of the matrix $[\mathbb{H}(\omega)]$ that is defined as $[\mathbb{H}(\omega)] = [\mathbb{A}(\omega)]^{-1}$ with definitions given in Eq. (VI.12). It

should be noted that, in this section, the truncated ROM (Eq. (VII.1)) is used as a reference, because in one hand the error$_B^{(j),\mathrm{TRUNC}}(\omega)$ is quite small that can be neglected in medium-high frequencies; in another hand, the computational cost of a full ROM is too high to be used in medium-high frequencies.

$$\begin{aligned}\langle \mathcal{E}_B^{(i),\mathrm{ESOM}} \rangle &\approx \sum_\beta \langle \mathcal{E}_{\beta,B}^{(i),\mathrm{ESOM}} \rangle \\ &= \sum_{j,\beta,\gamma} \frac{1}{2} \left([\mathbb{M}_B^{(i)}]_{\beta\beta} \int_{\mathbb{B}} \omega^2 \left| \mathbb{h}_{\beta\gamma,B}^{(ij)} \right|^2 S_{\gamma,B}^{(j)} \, d\omega + [\mathbb{K}_B^{(i)}]_{\beta\beta} \int_{\mathbb{B}} \left| \mathbb{h}_{\beta\gamma,B}^{(ij)} \right|^2 S_{\gamma,B}^{(j)} \, d\omega \right) .\end{aligned}$$

where $\mathbb{h}_{\beta\gamma,B}^{(ij)}$ is the value of $\beta-$th line and $\gamma-$th column of a bloc-matrix $[\mathbb{H}_B^{(ij)}(\omega)]$ of the matrix $[\mathbb{H}(\omega)_B]$ that is defined as $[\mathbb{H}_B(\omega)] = [\mathbb{A}_B(\omega)]^{-1}$ with definitions given in Eq. (VII.13). It should be noted that, we have to compare the mean local-frequency global instantaneous mechanical energies, which represent the sum of the mean local-frequency generalised instantaneous mechanical energies that correspond to the same generalised coordinates. However, ROM and ESOM do not have the same dimensions. This is the reason that we use another subscript β for ESOM.

$$\langle \mathcal{E}_B^{(j),\mathrm{SEA\text{-}ECPP}} \rangle = \sum_\beta (\underline{\boldsymbol{\mathcal{E}}}_B^{(1)})_\beta \, .$$

For SEA-ECPP, the mean local-frequency global instantaneous mechanical energy for each subsystem is the solution of Eq. (IX.18) with a vector of injected power $\underline{\mathbf{W}}_B^{(i),\mathrm{in}}$ as the input. In order to have the same input for these 3 approaches, the injected power $\underline{\mathbf{W}}_B^{(i),\mathrm{in}}$ can be calculated with ROM with the same input of PSD,

$$\begin{aligned}(\underline{\mathbf{W}}_B^{(i),\mathrm{in}})_\beta &= \langle W_\alpha^{(i),\mathrm{in}} \rangle \quad \text{(generalised coordinates of ROM)} \\ &= \langle F_\alpha^{(i)} \dot{Q}_\alpha^{(i)} \rangle \\ &= \mathrm{Re} \left\{ \int_{\mathbb{B}} i\omega \, h_{\alpha\alpha}^{(ii)} S_\alpha^i \, d\omega \right\} .\end{aligned}$$

Again, here the $\alpha-$th generalised coordinate of injected power in SEA-ECPP corresponds to the $\alpha-$th generalised coordinate of truncated ROM.

Mechanical properties of each subsystem of Model 1 in this numerical example is listed in Table. X.1. It can be seen that, the emission volume (1) and the receiving volume (5) are filled with normal air. The materials of the two panels ((2) and (4)) are chosen to be very different (panel (2) is a steel plate and panel (4) is a plasterboard). For the sake of convenience, the insulating layer (3) is considered to be a very dissipative heavy fluid, whose properties are frequency-independent. In the demonstration of formulations in previous chapters, we have used a fluid model for subsystem (3) to avoid complex writing and excessive assumptions. One acoustic source is placed at a corner that is far from the panel (2) of the volume (1) in order to ensure that it excite all the modes of the emission volume. It is assumed that this application

Subsystems	L_x (m)	L_y (m)	L_z (m)	ρ (kg/m^3)	C (m/s)	ξ/η
(1)	0.8	0.6	0.8	1.29	340	0.005 / 0.01
(3)	0.8	0.6	0.045	3	200	0.5 / 1
(5)	0.8	0.6	0.7	1.29	340	0.005 / 0.01

Subsystems	L_x (m)	L_y (m)	L_z (m)	ρ (kg/m^3)	E (Pa)	ν	ξ/η
(2)	0.8	0.6	0.001	7800	2×10^{11}	0.3	0.005 / 0.01
(4)	0.8	0.6	0.0125	736	2.7×10^{9}	0.1	0.015 / 0.03

Table X.1 – Mechanical properties of each subsystem for the Model 1

is carried out for N times and each time this source generates uncorrelated white noises whose PSD has values only for the 1/3 octave frequency band B_n that $n = 1, ..., n, ..., N$. Calculations are performed for the frequency range between [300, 3000] Hz in one-third octave bands which allow the validation of the SEA-ECPP to be asserted. The reason of choosing this frequency interval is that the reference (truncated ROM) can hardly exceed 3000 Hz for such a system because of its high cost.

In Fig. X.1, the ER is calculated between subsystem (1) and (5). It can be seen that the ER

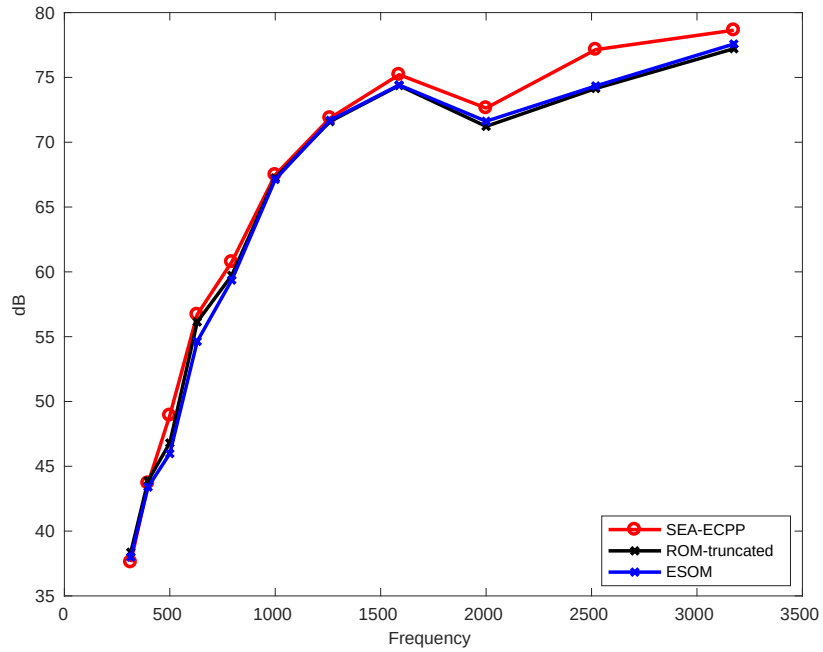

Figure X.1 – Validation. Black curve: reference, ER calculated with truncated ROM. Blue curve: ER calculated with ESOM. Red curve: ER calculated with SEA-ECPP.

result calculated with ESOM (blue curve) is nearly the same with the reference (black curve),

which proves that the ESOM can be used to correctly estimate the mean local-frequency global instantaneous mechanical energy for each subsystem and for each limited frequency band some approximations are applied. The ER result of SEA-ECPP approach (red curve) is also very close to these 2 results, but some differences can still be observed. These differences come from the model uncertainties (defects of SEA-ECPP model) induced by the weak coupling assumption and by the approximations introduced in Eq. (VIII.18),(VIII.21), and that is why a probabilistic application is needed to take all these model uncertainties into account. However, it should be noted that the computational time of SEA-ECPP approach (about 60 seconds) is much smaller than that of the ESOM (about 30 mins) or that of the truncated ROM (about 2 days) with the same computational facilities (30 cores 2.4Ghz CPU).

The comparisons of mean local-frequency global instantaneous mechanical energies in limited frequency band B are also presented for each subsystem. In Fig. X.2, we firstly validate the SEA-ECPP approach for both emission volume and receiving volume. In Fig. X.3, the same comparisons

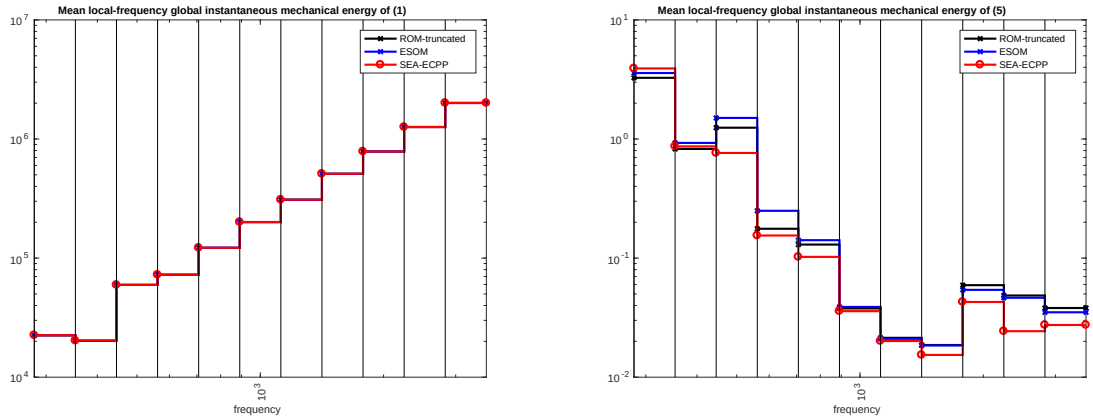

(a) Mean local-frequency global instantaneous mechanical energy of subsystem (1).

(b) Mean local-frequency global instantaneous mechanical energy of subsystem (5).

Figure X.2 – Validations of mean local-frequency global instantaneous mechanical energy in subsystems (1) and (5). Black curve: reference, calculated with truncated ROM. Blue curve: calculated with ESOM. Red curve: calculated with SEA-ECPP.

have been carried out for the subsystems (2), (3) and (4). The results for all subsystems are so close that SEA-ECPP can be proved to correctly predict the mean local-frequency global instantaneous mechanical energy in limited frequency bands.

A comparison between SEA-ECPP and SEA with classic CPP coefficients is also carried out to show that the ECPP coefficients have advantages when non-conservative couplings appear, which extends the usage of SEA methods. Firstly, let us recall that non-conservative couplings are not allowed in classic SEA, so that there is no such couplings in the formulation of CPP coefficient (it

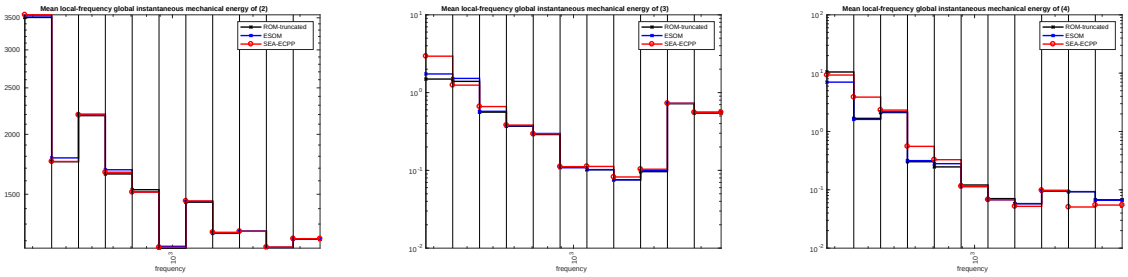

(a) Mean local-frequency global instantaneous mechanical energy of subsystem (2).

(b) Mean local-frequency global instantaneous mechanical energy of subsystem (3).

(c) Mean local-frequency global instantaneous mechanical energy of subsystem (4).

Figure X.3 – Validations of mean local-frequency global instantaneous mechanical energy in subsystems (2)-(4). Black curve: reference, calculated with truncated ROM. Blue curve: calculated with ESOM. Red curve: calculated with SEA-ECPP.

is expressed as $\gamma^{(ij)}_{\alpha\beta,B}$ with the same identification of ESOM),

$$\gamma^{(ij)}_{\alpha\beta,B} = \frac{\int_{\mathbb{B}} i\omega \left((\omega^2 [\mathbb{M}^{(ij)}_B]_{\alpha\beta} - [\mathbb{K}^{(ij)}_B]_{\alpha\beta})^2 + \omega^2 [\mathbb{G}^{(ij)}_B]^2_{\alpha\beta} \right) \left| \mathbb{h}^{(i)}_{\alpha,B} \right|^2 \mathbb{h}^{(j)}_{\beta,B} \, d\omega}{\int_{\mathbb{B}} \omega^2 [\mathbb{M}^{(i)}_B]_{\alpha\alpha} \left| \mathbb{h}^{(i)}_{\alpha,B} \right|^2 d\omega} \, .$$

It should be noted that, this expressions can be different from the classic expression because this equation is under the identification of ESOM. The CPP allows that

$$\langle W^{(i),\mathrm{ex}}_{\alpha\beta,B} \rangle = \gamma^{(ij)}_{\alpha\beta,B} (\langle \mathcal{E}^{(i)}_{\alpha,B} \rangle - \langle \mathcal{E}^{(j)}_{\beta,B} \rangle) + o(\epsilon^2) \, .$$

With CPP coefficients, the same numerical application is also carried out, and the comparison is shown below in Fig. X.2. It is observed that the CPP coefficients do not work well in this case, because in a condensed model, non-conservative couplings may appear. It means that when there are non-negligible non-conservative couplings, the SEA-ECPP approach should be used instead.

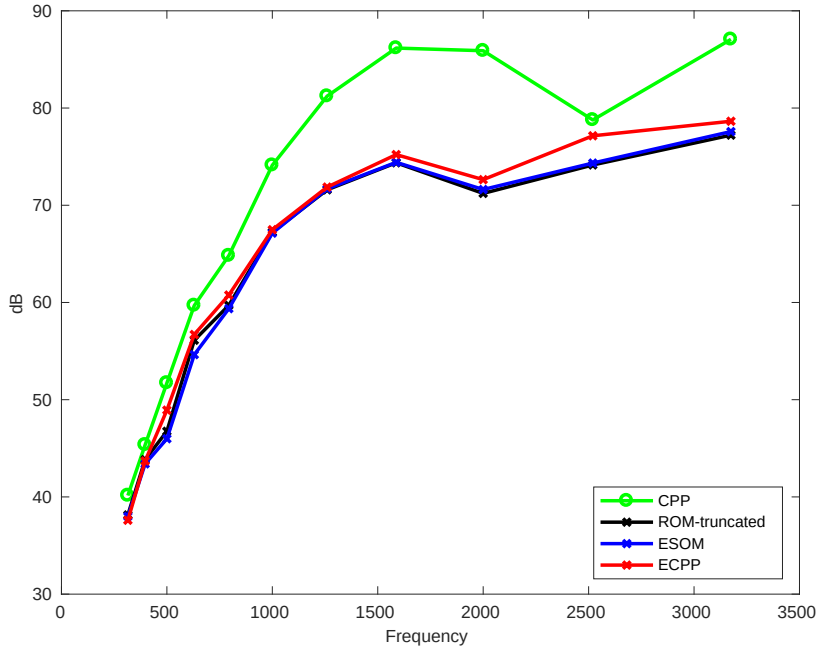

Figure X.4 – Validation. Black curve: reference, ER calculated with truncated ROM. Blue curve: ER calculated with ESOM. Red curve: ER calculated with SEA-ECPP. Green curve: ER calculated with CPP coefficients

X.2 Numerical application on Model 2

A numerical application of Sound Transmission Loss (STL) calculation is carried out on Model 2 for a bloc of a double leaf wall (0.6m's large and 2.5m's high, which respectively correspond to the horizontal distance between studs and the vertical distance between rails). These dimensions are chosen, because we have made an hypothesis that the partition-wall is totally separated with studs and each bloc (0.6m x 2.5m) is assumed to be an individual system. The two plates of this individual system are assumed to be simply-supported, which makes it possible to solve the sound radiation of plate in a theoretical way. The parameters are shown in Table. X.2 below. The

Subsystems	L_x (m)	L_y (m)	L_z (m)	ρ (kg/m^3)	C (m/s)	ξ/η
(1)	0.6	2.5	∞	1.29	340	
(3)	0.6	2.5	0.045	3	200	0.05 / 0.1
(5)	0.6	2.5	∞	1.29	340	

Subsystems	L_x (m)	L_y (m)	L_z (m)	ρ (kg/m^3)	E (Pa)	ν	ξ/η
(2)	0.6	2.5	0.0125	736	2.7×10^9	0.1	0.015 / 0.03
(4)	0.6	2.5	0.0125	736	2.7×10^9	0.1	0.015 / 0.03

Table X.2 – Properties of each layer for Model 2

semi-infinite fluid volumes ((1) and (5)) are supposed to be filled with normal air, and subsystem (3) is a dissipative fluid. The two panels are made of plasterboards that have the same properties. It is assumed that the multi-layer system is a bloc (0.6m x 2.5m) of a real double leaf wall like in Fig. X.5. the boundaries of each multi-layered partition are fixed on studs, and the boundary condition is assumed to be simply supported in this manuscript.

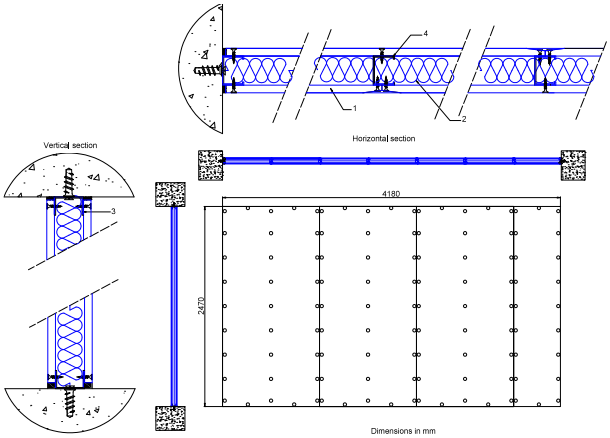

Figure X.5 – a double leaf wall system [1]

Different from the numerical example of Model 1, for semi-infinite acoustic volumes, it is impossible to calculate their mean mechanical energy. Instead, we calculate the mean incident power $\langle W^{(2),\mathrm{in}}\rangle$ on the first plate and the mean radiated power $\langle W^{(4),\mathrm{rad}}\rangle$ of the second plate in order to directly find the STL. The mean incident power $\langle W^{(2),\mathrm{in}}\rangle$ is defined as the product of mean incident intensity and the surface of section: $\langle W^{(2),\mathrm{in}}\rangle = \langle I^{\mathrm{in}}\rangle S$. In a fluid volume, the mean intensity is defined as

$$\langle I^{\mathrm{in}}\rangle = \frac{\langle \overline{p^2}\rangle}{\rho_{\mathrm{f}} c_{\mathrm{f}}} \,.$$

The boundary condition makes that the mean-square sound pressure $\langle \overline{p^2}\rangle$ equals to the loads applied on the panel (2). An hypothesis is proposed that the loads meet the condition that they are uncorrelated white noises, whose power spectral density $S_{F^{(2)}}$ is already known. For each frequency band B, the external loads will excite the resonant modes in the band B and the non-resonant modes in lower frequency bands B^- of the panel (2). We do not excite the non-resonant modes in HF, because we cannot do that for our references like the truncated ROM or ESOM for a reason of computing cost. We excite the same modes for these 3 methods and we can compare them in a same figure. By using SEA-ECPP approach, with given PSD of external loads $S_{F^{(2)}}$, we can then calculate the mean local-frequency global instantaneous mechanical energies to find the mean square value of the resonant generalised coordinates $\langle(\mathbf{q}_B^{(i)})^2\rangle$ with $i = 2,3,4$ for limited frequency band B. However, the mean radiated power $\langle W^{(4),\mathrm{rad}}\rangle$ is calculated not only with the resonant generalised coordinates $\langle(\mathbf{q}_B^{(4)})^2\rangle$ but also the non-resonant generalised coordinates

$\langle(\mathbf{q}^{(4)}_{B^{\mathrm{NR}}})^2\rangle$ (in both LF and HF). As the panel (4) is assumed as a simply supported thin plate, the mean radiated power $\langle W^{(4),\mathrm{rad}}\rangle$ radiated is calculated from the surface integral over a hemisphere encompassing the plate. To calculate the mean radiated power at any far point, the far-field

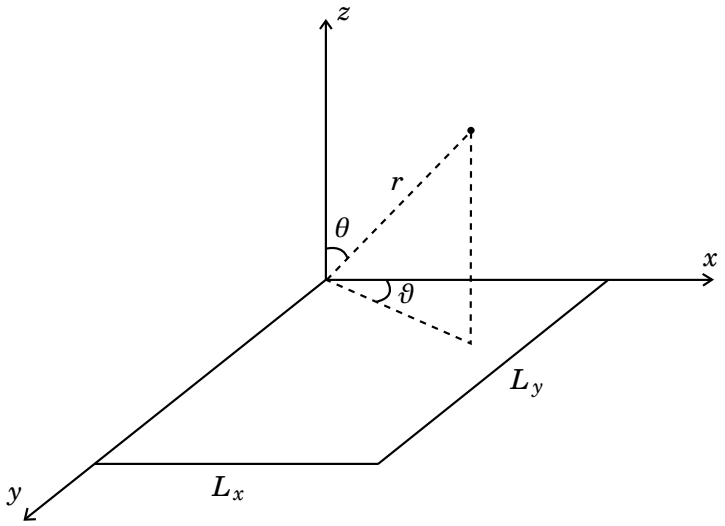

Figure X.6 – Radiation of thin plates

condition (Wallace 1972, Fahy 1985) is applied with all variables defined in Fig. X.6. The mean radiated power $\langle W^{(4),\mathrm{rad}}\rangle$ over the limited frequency band B is then calculated as,

$$\langle W^{(4),\mathrm{rad}}\rangle = \sum_{\beta}\int_B \omega^2 [S_{\mathbf{q}^{(4)}}]_{\beta\beta}\int_0^{2\pi}\int_0^{\frac{\pi}{2}} 2\rho_{\mathrm{f}}^{(5)} c_{\mathrm{f}}^{(5)}\left(\frac{L_x L_y}{c_{\mathrm{f}}^{(5)}\pi^3}\right)^2 \tau_\beta(\theta,\vartheta;\omega)\, d\theta\, d\vartheta\, d\omega\ , \tag{X.2}$$

with $\tau_\beta(\theta,\vartheta;\omega)$ a coefficient related to eigenmode β, angles θ,ϑ, and angular frequency ω for any r. $[S_{\mathbf{q}^{(4)}}]$ is composed with $[S_{\mathbf{q}^{(4)}_{B^{\mathrm{NR}}}}(\omega)]$ and $[S_{\mathbf{q}^{(4)}_B}(\omega)]$ that can be deduced from $\underline{\underline{\mathcal{E}}}^{(4)}_B$, which is the solution of SEA-ECPP. The Sound Transmission Loss (STL) of such a system is then calculated as,

$$\mathrm{STL} = 10\lg\frac{\langle W^{(2),\mathrm{in}}\rangle}{\langle W^{(4),\mathrm{rad}}\rangle}\ . \tag{X.3}$$

$[S_{\mathbf{q}^{(4)}_B}]$ can be directly calculated with $\underline{\underline{\mathcal{E}}}^{(4)}_B$ and the equivalent mass matrix $[\mathbb{M}^{(4)}_B]$. However, $[S_{\mathbf{q}^{(4)}_{B^{\mathrm{NR}}}}]$ should be calculated with an inverted method of the Schur complement in Appendix. C. Imaging that when we do the condensation of $\mathbf{q}^{(4)}_{B^{\mathrm{NR}}}$, we might have the relations like,

$$\mathbf{q}^{(4)}_{B^{\mathrm{NR}}} = [\mathcal{W}^1_B]F^{(2)}_{B^{\mathrm{NR}}} + [\mathcal{W}^2_B]\mathbf{q}^{(2)}_B + [\mathcal{W}^3_B]\mathbf{q}^{(3)}_B + [\mathcal{W}^4_B]\mathbf{q}^{(4)}_B\ ,$$

with $[\mathcal{W}^i]$ some matrices associated to subsystem (i) (i = 2,3,4) in limited frequency band B and their expressions are not listed in details. The PSD of the non-resonant generalised coordinates

for subsystem (4) is,

$$[S_{\mathbf{q}_{B^{\mathrm{NR}}}^{(4)}}] = [\mathcal{W}_{\mathrm{all,B}}] \begin{bmatrix} [S_{F_{B^{\mathrm{NR}}}^{(2)}}] & & & \\ & [S_{\mathbf{q}_B^{(2)}}] & & \\ & & [S_{\mathbf{q}_B^{(3)}}] & \\ & & & [S_{\mathbf{q}_B^{(4)}})] \end{bmatrix} [\mathcal{W}_{\mathrm{all,B}}]^* , \tag{X.4}$$

where $[\mathcal{W}_{\mathrm{all,B}}] = [\mathcal{W}_B^1\ \mathcal{W}_B^2\ \mathcal{W}_B^3\ \mathcal{W}_B^4]$. It should be noted that, in the ESOM or SEA-ECPP approach, these matrices are approximated with the central angular frequency ω_c of the limited frequency band B.

Under these dimensions, the computing cost of truncated ROM is very high, and that is why we stop at 2000 Hz for this approach. However, as we have proved that ESOM works well in the numerical application of Model 1, this lower-costly approach will be used as a reference to validate the SEA-ECPP in medium-high frequency range. The numerical results of ESOM and SEA-ECPP are compared in Fig. X.7. The black curve (ends at 2000 Hz), blue curve and the red curve are respectively the result of truncated ROM, ESOM and SEA-ECPP approach. It

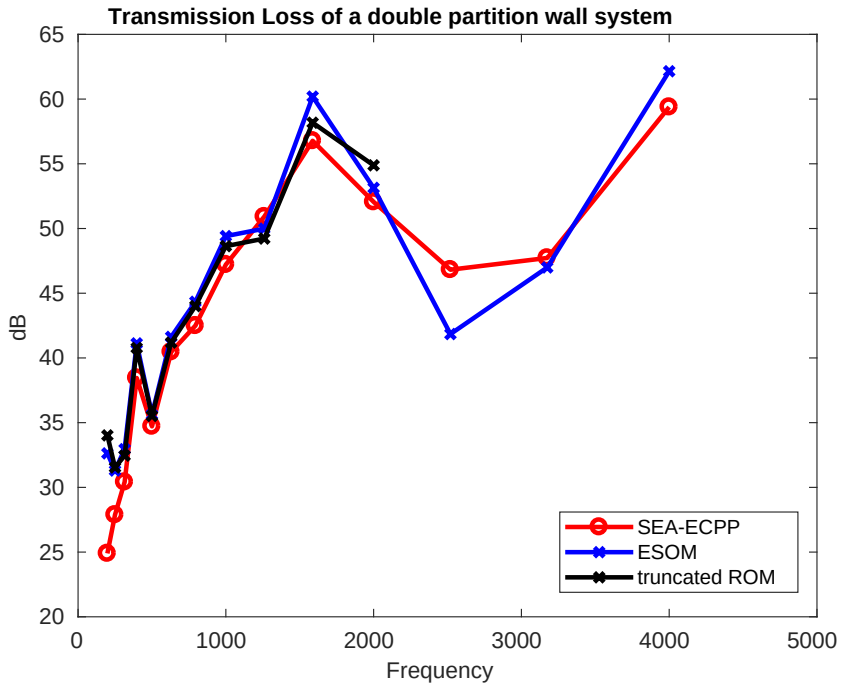

Figure X.7 – STL simulation for Model 2. Black curve: result calculated with truncated ROM. Blue curve: result calculated with ESOM. Red curve: result calculated with SEA-ECPP.

can be seen that the red curve is very close to the black and blue curves, which means that the

SEA-ECPP approach works well for a system like Model 2. Also it has a faster computing speed and a lower computing cost compared to classic modal formulations.

X.3 Random SEA-ECPP approach

The non-parametric probabilistic approach is tested on both the Model 1 and the Model 2. Firstly, the probabilistic models are tested with a very small dispersion coefficient $\delta = 1e-7$ to verify that we can find the same curve in a case that very close to the deterministic model. The Figures X.8a and X.8b are respectively the simulation results of 100 realisations on Model 1 and Model 2.

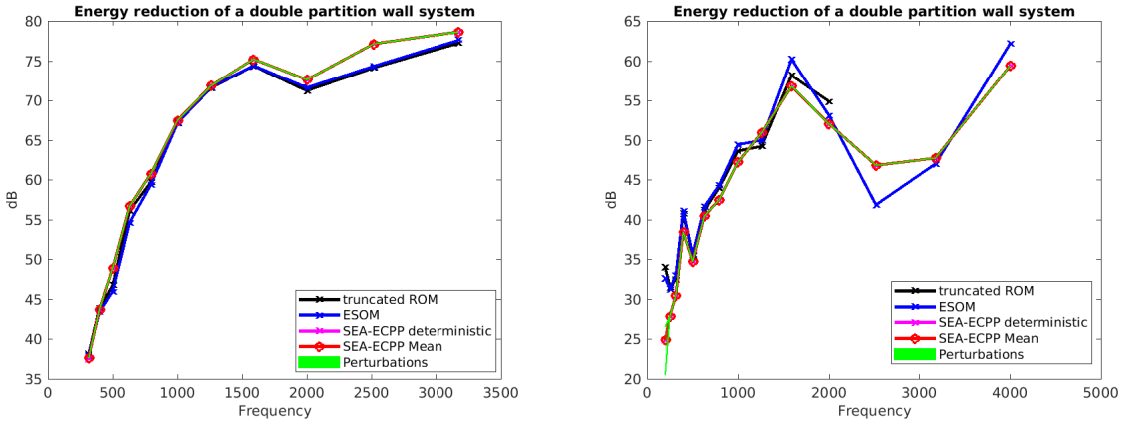

(a) 100 realisations of probabilistic Model 1 with δ=1e-7.

(b) 100 realisations of probabilistic Model 2 with δ=1e-7.

Figure X.8 – Validations of probabilistic models with a very small dispersion coefficient. Black curve: calculated with truncated ROM. Blue curve: calculated with ESOM. Magenta curve: calculated with SEA-ECPP. Red curve: mean values of 100 realisations with probabilistic models

Different from the previous figures, the deterministic SEA-ECPP curve is shown in magenta colour and the mean-valued curve of these 100 realisations is shown in red colour. A green zone shows the confident zone of the probabilistic model.

We have then tested with a dispersion coefficient $\delta = 0.1$, which roughly means an uncertainty of 10%. However, the results are not satisfying at all. As shown in Figures X.9a and X.9b, the ER and the STL calculated by the probabilistic model are far below the references and the deterministic curves, which means that much more energy are transferred in our probabilistic model.

The reason of this performance is that when the global matrices are random, the new random matrices are related to the dispersion coefficient, which gives a global fuzzy effect and they become much bigger than what they were before. The coupling matrices in SEA-ECPP are all condensed matrices which are calculated accurately with modal relationships, and nearly all the couplings (non-diagonal values) are very small compared to the diagonal values, which makes

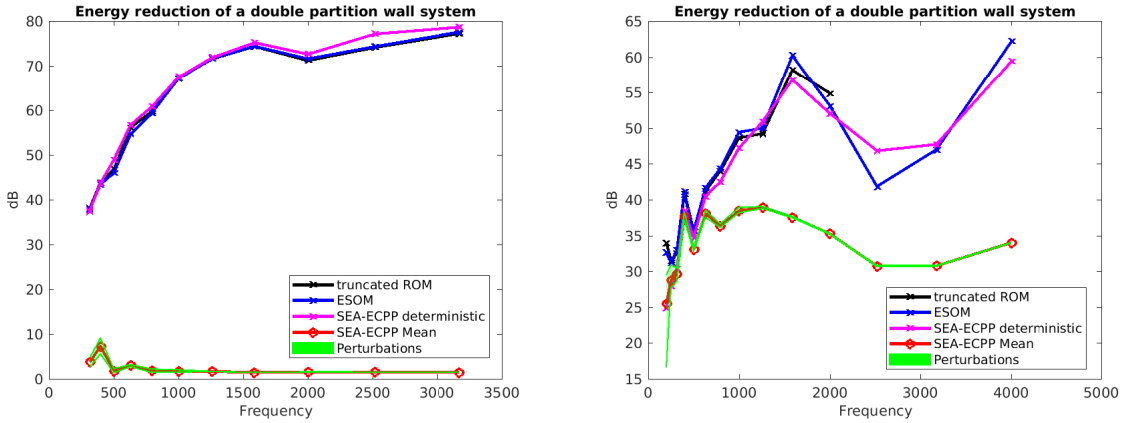

(a) 100 realisations of probabilistic Model 1 with δ=0.1.

(b) 100 realisations of probabilistic Model 2 with δ=0.1.

Figure X.9 – Validations of probabilistic models with a dispersion coefficient δ=0.1. Black curve: calculated with truncated ROM. Blue curve: calculated with ESOM. Magenta curve: calculated with SEA-ECPP. Red curve: mean values of 100 realisations with probabilistic models

this approach not robust at all. It can be noticed that the non-robustness of Model 1 is more significant than that of the Model 2. That is because in Model 1, certain equivalent coupling matrices in Model 1 such as $[\mathbb{M}_B^{(15)}]$ are very small and not robust. When a probabilistic model is applied, $[\mathbf{M}_B^{(15)}]$ may be 100000 times bigger than $[\mathbb{M}_B^{(15)}]$, and that will possibly result in a 100000 times bigger transmission of energy directly from subsystem (1) to subsystem (5).
It is concluded above that SEA-ECPP is not robust, and we assumed that it is because of the way that it construct its coupling matrices. To confirm this, a test is then proposed that the coupling matrices are kept deterministic and only the values in diagonal positions in matrices are random. That is to say, the expression of the Eq. (IX.17) is changed as below,

$$
\begin{aligned}
Z_{\alpha\beta,B}^{(ij)} = & \frac{\int_{\mathbb{B}} i\omega \left((\omega^2 [\mathbb{M}_B^{(ij)}]_{\alpha\beta} - [\mathbb{K}_B^{(ij)}]_{\alpha\beta})^2 + \omega^2 [\mathbb{G}_B^{(ij)}]_{\alpha\beta}^2 - \omega^2 [\mathbb{D}_B^{(ij)}]_{\alpha\beta}^2 - [\mathbb{R}_B^{(ij)}]_{\alpha\beta}^2 \right) \left| \mathbf{H}_{\alpha,B}^{(i)} \right|^2 \mathbf{H}_{\beta,B}^{(j)} \, d\omega}{\int_{\mathbb{B}} \omega^2 [\mathbf{M}_B^{(i)}]_{\alpha\alpha} \left| \mathbf{H}_{\alpha,B}^{(i)} \right|^2 d\omega} \\
& + \frac{2 \int_{\mathbb{B}} \omega^2 \left((\omega^2 [\mathbb{M}_B^{(ij)}]_{\alpha\beta} - [\mathbb{K}_B^{(ij)}]_{\alpha\beta}) [\mathbb{D}_B^{(ij)}]_{\alpha\beta} + [\mathbb{G}_B^{(ij)}]_{\alpha\beta} [\mathbb{R}_B^{(ij)}]_{\alpha\beta} \right) \left| \mathbf{H}_{\alpha,B}^{(i)} \right|^2 \mathbf{H}_{\beta,B}^{(j)} \, d\omega}{\int_{\mathbb{B}} \omega^2 [\mathbf{M}_B^{(i)}]_{\alpha\alpha} \left| \mathbf{H}_{\alpha,B}^{(i)} \right|^2 d\omega} \\
X_{\alpha\beta,B}^{(ij)} = & \frac{\int_{\mathbb{B}} i\omega \left((\omega^2 [\mathbb{M}_B^{(ij)}]_{\alpha\beta} - [\mathbb{K}_B^{(ij)}]_{\alpha\beta})^2 + \omega^2 ([\mathbb{G}_B^{(ij)}]_{\alpha\beta} + [\mathbb{D}_B^{(ij)}]_{\alpha\beta})^2 + [\mathbb{R}_B^{(ij)}]_{\alpha\beta}^2 \right) \mathbf{H}_{\alpha,B}^{(i)} \left| \mathbf{H}_{\beta,B}^{(j)} \right|^2 d\omega}{\int_{\mathbb{B}} \omega^2 [\mathbf{M}_B^{(j)}]_{\beta\beta} \left| \mathbf{H}_{\beta,B}^{(j)} \right|^2 d\omega} \\
& - \frac{2 \int_{\mathbb{B}} i\omega \left(\omega^2 [\mathbb{M}_B^{(ij)}]_{\alpha\beta} [\mathbb{R}_B^{(ij)}]_{\alpha\beta} - [\mathbb{K}_B^{(ij)}]_{\alpha\beta} [\mathbb{R}_B^{(ij)}]_{\alpha\beta} \right) \mathbf{H}_{\alpha,B}^{(i)} \left| \mathbf{H}_{\beta,B}^{(j)} \right|^2 d\omega}{\int_{\mathbb{B}} \omega^2 [\mathbf{M}_B^{(j)}]_{\beta\beta} \left| \mathbf{H}_{\beta,B}^{(j)} \right|^2 d\omega} ,
\end{aligned}
\tag{X.5}
$$

with $\omega \mapsto \mathbf{H}_{\alpha,B}^{(i)}(\omega)$, the α-th real-valued random equivalent generalised FRF of subsystem (i) that

is defined as, for all $\omega \in B$

$$\mathbf{H}^{(i)}_{\alpha,B}(\omega) = \left(-\omega^2 [\mathbf{M}^{(i)}_B]_{\alpha\alpha} + i\omega [\mathbf{D}^{(i)}_B]_{\alpha\alpha} + [\mathbf{K}^{(i)}_B]_{\alpha\alpha} \right)^{-1} .$$

With these changes, it can be observed that mean-valued curve of probabilistic model is now close to the deterministic curve in Figures X.10a and X.10b, which proves our assumption.

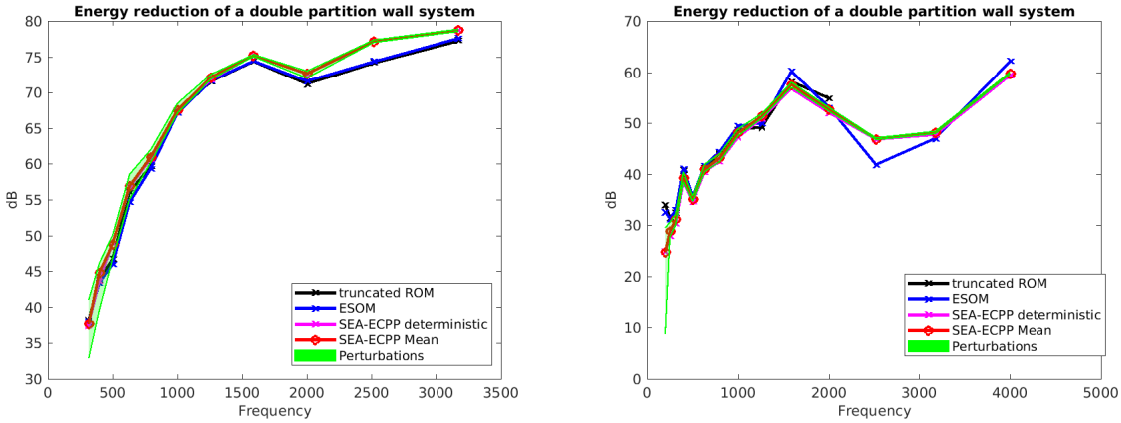

(a) 100 realisations of probabilistic Model 1 with deterministic couplings and δ=0.1.

(b) 100 realisations of probabilistic Model 2 with deterministic couplings and δ=0.1.

Figure X.10 – Test with deterministic coupling matrices. Black curve: calculated with truncated ROM. Blue curve: calculated with ESOM. Magenta curve: calculated with SEA-ECPP. Red curve: mean values of 100 realisations with probabilistic models and deterministic couplings

CHAPTER XI

CONCLUSION

In this chapter, some conclusions and perspectives are introduced and discussed. The main results of this manuscript are the newly proposed models CROM, ESOM for multi-layered systems. An energetic approach SEA-ECPP, which is based on ESOM, is proposed in order to find the Transmission Loss or the Energy Reduction of a multi-layered system in medium and high frequency range. This newly proposed approach uses new coefficients that are named as ECPP coefficients, whose formulas are very close to the classic CPP coefficients in SEA. The main differences between ECPP coefficients and CPP coefficient is that ECPP coefficients take non-conservative couplings into account, which makes it possible for SEA-ECPP approach to deal with highly dissipative mechanical systems. However, the proposed models and coefficients are not robust in the model construction because the new created equivalent matrices in these models are too sensitive to modelling uncertainties. Then, building a robust SEA-ECPP approach might be an interesting perspective, which is not realized within the limit of time during this thesis.

XI.1 Summary of present work

To answer the problematic introduced in the Chapter. I, a solution of Condensed Reduced-Order Model (CROM) with smaller computing cost is proposed in order to replace the classic Reduced-Order Model (ROM) in this manuscript. Particular modal analyses in limited frequency bands for the multi-layered dissipative systems in examples (Model 1 and Model 2) are carried out, which results in equivalent condensed models for each limited frequency band that gives equivalent information as ROM in the same limited frequency band. With this modal analysis, the eigenmodes are classified into resonant modes and non-resonant modes according to each studying limited frequency band. The advantage of CROM is that the generalised coordinates of

all non-resonant modes are able to be condensed into added terms on the equations of resonant modes with the theory of Schur complement. When only resonant generalised coordinates are important in our studies, this technique reduces a lot the computing cost as they calculate only resonant generalised coordinates. Moreover, the condensed non-resonant generalised coordinates can be re-found by inverting the condensation. This CROM is proved to be an equivalent writing to the original ROM model, but with smaller computing cost.

In medium and high frequency range, SEA is often used because this method has certain advantages such as low computing cost. However, this method requires that all couplings should be identified as conservative couplings, which mean internal, gyroscopic and elastic couplings, and no non-conservative coupling is allowed in SEA. Based on CROM, an Equivalent Second-Order Model (ESOM) is again proposed to obtain these equivalent couplings in order to use SEA. Apart from the conservative couplings introduced above, two non-negligible non-conservatives couplings are also identified for the highly-dissipative systems in examples. These non-conservatives couplings do not come from the highly-dissipative systems themselves, but come from the condensations done in CROM. They are non-negligible because these couplings are condensed from some highly-dissipative materials. If the studying system is lowly-dissipative, these non-conservative couplings can be totally negligible and classic SEA can be used on it. As non-conservative couplings can not be accounted for the calculation of Coupling Power Proportionality (CPP) coefficients in classic SEA, new Equivalent Coupling Power Proportionality (ECPP) coefficients are then developed. With these new coefficients, a modified SEA approach can be used to deal with systems that contain non-conservative couplings, and this approach is named SEA-ECPP approach.

The identification of ESOM proposed in this manuscript is very fast but it is however at the cost of accuracy. The identified frequency-independent matrices might not be the optimized matrices, where uncertainties of modelling are propagated into the SEA-ECPP approach. Probabilistic models on the SEA-ECPP approach are constructed with non-parametric approach. However, after some tests, it can be concluded that the SEA-ECPP approach is not robust because of the way it construct its coupling matrices.

XI.2 Perspectives

The main perspectives related to this work are the development of the robustness on the SEA-ECPP approach. The reasons of the non-robustness are already analysed during the applications. It will be interesting to find a more accurate and more efficient way to identify the equivalent couplings in ESOM, which allows the uncertainties to be propagated. Moreover, a better method of applying non-parametric probabilistic model is also an interesting perspective.

APPENDIX A

APPENDIX A

A.1 Schur complements in Condensed Reduced Order Model (CROM)

In the following, we present an example of the application of Schur complement. Let us consider a subsystem (j), which is coupled with subsystem (i) and subsystem (k),

$$\begin{bmatrix} [\mathcal{A}^{(i)}(\omega)] & -i\omega[\mathcal{C}^{(ij)}] & \\ i\omega[\mathcal{C}^{(ji)}] & [\mathcal{A}^{(j)}(\omega)] & i\omega[\mathcal{C}^{(jk)}] \\ & -i\omega[\mathcal{C}^{(kj)}] & [\mathcal{A}^{(k)}(\omega)] \end{bmatrix} \begin{Bmatrix} \mathbf{q}^{(i)} \\ \mathbf{q}^{(j)} \\ \mathbf{q}^{(k)} \end{Bmatrix} = \begin{Bmatrix} \mathbf{f}^{(i)} \\ 0 \\ 0 \end{Bmatrix}, \tag{A.1}$$

It is assumed that the generalised dynamical stiffness matrix of subsystem (j) is a full matrix and its resonant and non-resonant generalised coordinates are coupled with all generalised coordinates of subsystems (i) and (k). When reducing the non-resonant generalised coordinates of the subsystem (j), the generalised dynamical stiffness matrix $[\mathcal{A}^{(j)}(\omega)]$ and the associated coupling matrices such as $[\mathcal{C}^{(ij)}]$ in the total frequency band $\mathbb{B} = B^- \cup B \cup B^+$ are divided as below,

$$[\mathcal{A}^{(j)}(\omega)] = \begin{bmatrix} [\mathcal{A}^{(j)}_{B^-}(\omega)] & [\mathcal{A}^{(j)}_{B^-B}(\omega)] & [\mathcal{A}^{(j)}_{B^-B^+}(\omega)] \\ [\mathcal{A}^{(j)}_{BB^-}(\omega)] & [\mathcal{A}^{(j)}_{B}(\omega)] & [\mathcal{A}^{(j)}_{BB^+}(\omega)] \\ [\mathcal{A}^{(j)}_{B^+B^-}(\omega)] & [\mathcal{A}^{(j)}_{B^+B}(\omega)] & [\mathcal{A}^{(j)}_{B^+}(\omega)] \end{bmatrix}, \quad [\mathcal{C}^{(ij)}] = \left[[\mathcal{C}^{(ij)}_{\mathbb{B}B^-}] \, [\mathcal{C}^{(ij)}_{\mathbb{B}B}] \, [\mathcal{C}^{(ij)}_{\mathbb{B}B^+}] \right]. \tag{A.2}$$

The double subscripts like $\mathbb{B}B^-$ represents the individual frequency domain of line and column indexes, respectively. It should be noted that, the generalised dynamical stiffness matrix $[\mathcal{A}^{(j)}(\omega)]$ should verify the property of symmetry.

After the decomposition, the global matrix Eq. (A.2) is then rewritten

$$\begin{bmatrix} [\mathcal{A}^{(i)}(\omega)] & i\omega[\mathcal{C}^{(ij)}_{\mathbb{B}B^-}] & i\omega[\mathcal{C}^{(ij)}_{\mathbb{B}B}] & i\omega[\mathcal{C}^{(ij)}_{\mathbb{B}B^+}] & \\ -i\omega[\mathcal{C}^{(ji)}_{B^-\mathbb{B}}] & [\mathcal{A}^{(j)}_{B^-}(\omega)] & [\mathcal{A}^{(j)}_{B^-B}(\omega)] & [\mathcal{A}^{(j)}_{B^-B^+}(\omega)] & -i\omega[\mathcal{C}^{(jk)}_{B^-\mathbb{B}}] \\ -i\omega[\mathcal{C}^{(ji)}_{B\mathbb{B}}] & [\mathcal{A}^{(j)}_{BB^-}(\omega)] & [\mathcal{A}^{(j)}_{B}(\omega)] & [\mathcal{A}^{(j)}_{BB^+}(\omega)] & -i\omega[\mathcal{C}^{(jk)}_{B\mathbb{B}}] \\ -i\omega[\mathcal{C}^{(ji)}_{B^+\mathbb{B}}] & [\mathcal{A}^{(j)}_{B^+B^-}(\omega)] & [\mathcal{A}^{(j)}_{B^+B}(\omega)] & [\mathcal{A}^{(j)}_{B^+}(\omega)] & -i\omega[\mathcal{C}^{(jk)}_{B^+\mathbb{B}}] \\ & i\omega[\mathcal{C}^{(kj)}_{\mathbb{B}B^-}] & i\omega[\mathcal{C}^{(kj)}_{\mathbb{B}B}] & i\omega[\mathcal{C}^{(kj)}_{\mathbb{B}B^+}] & [\mathcal{A}^{(k)}(\omega)] \end{bmatrix} \begin{Bmatrix} \mathbf{q}^{(i)} \\ \mathbf{q}^{(j)}_{B^-} \\ \mathbf{q}^{(j)}_{B} \\ \mathbf{q}^{(j)}_{B^+} \\ \mathbf{q}^{(k)} \end{Bmatrix} = \begin{Bmatrix} \mathbf{f}^{(i)} \\ 0 \\ 0 \\ 0 \\ 0 \end{Bmatrix}, \tag{A.3}$$

where the global matrix at the left-hand side of Eq. (A.3) is denoted as $[\mathcal{A}(\omega)]$. The objective is to get rid of the non-resonant generalised coordinates of subsystem (j) (lines and columns that are double-strike-through) in order to reduce the dimension of matrix. As in this example, the matrices $[\mathcal{A}^{(j)}_{B^-}(\omega)]$ and $[\mathcal{A}^{(j)}_{B^+}(\omega)]$ are full matrices, we would gain nothing of computational cost from the order of computation. It is suggested that we move the condensed terms together and consider them do only once calculation of Schur complement for the equation below,

$$\begin{bmatrix} [\mathcal{A}^{(i)}(\omega)] & i\omega[\mathcal{C}^{(ij)}_{\mathbb{B}B}] & & i\omega[\mathcal{C}^{(ij)}_{\mathbb{B}B^-}] & i\omega[\mathcal{C}^{(ij)}_{\mathbb{B}B^+}] \\ -i\omega[\mathcal{C}^{(ji)}_{B\mathbb{B}}] & [\mathcal{A}^{(j)}_{B}(\omega)] & -i\omega[\mathcal{C}^{(jk)}_{B\mathbb{B}}] & [\mathcal{A}^{(j)}_{BB^-}(\omega)] & [\mathcal{A}^{(j)}_{BB^+}(\omega)] \\ & i\omega[\mathcal{C}^{(kj)}_{\mathbb{B}B}] & [\mathcal{A}^{(k)}(\omega)] & i\omega[\mathcal{C}^{(kj)}_{\mathbb{B}B^-}] & i\omega[\mathcal{C}^{(kj)}_{\mathbb{B}B^+}] \\ -i\omega[\mathcal{C}^{(ji)}_{B^-\mathbb{B}}] & [\mathcal{A}^{(j)}_{B^-B}(\omega)] & -i\omega[\mathcal{C}^{(jk)}_{B^-\mathbb{B}}] & [\mathcal{A}^{(j)}_{B^-}(\omega)] & [\mathcal{A}^{(j)}_{B^-B^+}(\omega)] \\ -i\omega[\mathcal{C}^{(ji)}_{B^+\mathbb{B}}] & [\mathcal{A}^{(j)}_{B^+B}(\omega)] & -i\omega[\mathcal{C}^{(jk)}_{B^+\mathbb{B}}] & [\mathcal{A}^{(j)}_{B^+B^-}(\omega)] & [\mathcal{A}^{(j)}_{B^+}(\omega)] \end{bmatrix} \begin{Bmatrix} \mathbf{q}^{(i)} \\ \mathbf{q}^{(j)}_{B} \\ \mathbf{q}^{(k)} \\ \mathbf{q}^{(j)}_{B^-} \\ \mathbf{q}^{(j)}_{B^+} \end{Bmatrix} = \begin{Bmatrix} \mathbf{f}^{(i)} \\ 0 \\ 0 \\ 0 \\ 0 \end{Bmatrix}. \tag{A.4}$$

We can then regroup the block-matrices together as below,

$$[\mathbb{A}(\omega)] = \begin{bmatrix} [\mathcal{A}^{(i)}(\omega)] & i\omega[\mathcal{C}^{(ij)}_{\mathbb{B}B}] & \\ -i\omega[\mathcal{C}^{(ji)}_{B\mathbb{B}}] & [\mathcal{A}^{(j)}_{B}(\omega)] & -i\omega[\mathcal{C}^{(jk)}_{B\mathbb{B}}] \\ & i\omega[\mathcal{C}^{(kj)}_{\mathbb{B}B}] & [\mathcal{A}^{(k)}(\omega)] \end{bmatrix}, \quad [\mathbb{A}_{\mathrm{NR}}(\omega)] = \begin{bmatrix} [\mathcal{A}^{(j)}_{B^-}(\omega)] & [\mathcal{A}^{(j)}_{B^-B^+}(\omega)] \\ [\mathcal{A}^{(j)}_{B^+B^-}(\omega)] & [\mathcal{A}^{(j)}_{B^+}(\omega)] \end{bmatrix},$$

$$[\mathbb{W}_{B^-B^+}(\omega)] = \begin{bmatrix} i\omega[\mathcal{C}^{(ij)}_{\mathbb{B}B^-}] & i\omega[\mathcal{C}^{(ij)}_{\mathbb{B}B^+}] \\ [\mathcal{A}^{(j)}_{BB^-}(\omega)] & [\mathcal{A}^{(j)}_{BB^+}(\omega)] \\ i\omega[\mathcal{C}^{(kj)}_{\mathbb{B}B^-}] & i\omega[\mathcal{C}^{(kj)}_{\mathbb{B}B^+}] \end{bmatrix}, \quad [\mathbb{W}_{B^+B^-}(\omega)] = \begin{bmatrix} -i\omega[\mathcal{C}^{(ji)}_{B^-\mathbb{B}}] & [\mathcal{A}^{(j)}_{B^-B}(\omega)] & -i\omega[\mathcal{C}^{(jk)}_{B^-\mathbb{B}}] \\ -i\omega[\mathcal{C}^{(ji)}_{B^+\mathbb{B}}] & [\mathcal{A}^{(j)}_{B^+B}(\omega)] & -i\omega[\mathcal{C}^{(jk)}_{B^+\mathbb{B}}] \end{bmatrix}.$$

The Schur complement $[\mathcal{A}^{\mathrm{SC}}(\omega)]$ is therefore deduced as,

$$[\mathcal{A}(\omega)]/[\mathbb{A}_{\mathrm{NR}}(\omega)] = [\mathbb{A}(\omega)] - [\mathbb{W}_{B^-B^+}(\omega)][\mathbb{A}_{\mathrm{NR}}(\omega)]^-1[\mathbb{W}_{B^+B^-}(\omega)] .$$

The generalised coordinates solution of Eq. (A.1) in limited frequency band B can now simply be calculated with the equation below,

$$[\mathcal{A}^{\mathrm{SC}}(\omega)] \begin{Bmatrix} \mathbf{q}^{(i)} \\ \mathbf{q}^{(j)}_{B} \\ \mathbf{q}^{(k)} \end{Bmatrix} = \begin{Bmatrix} \mathbf{f}^{(i)} \\ 0 \\ 0 \end{Bmatrix}.$$

APPENDIX B

APPENDIX B

B.1 CROM of the Model 1

We start from the Eq. (VII.1), and the objective is to reduce the lines and columns that associated to the non-resonant generalised coordinates, which are double-strike-through as below,

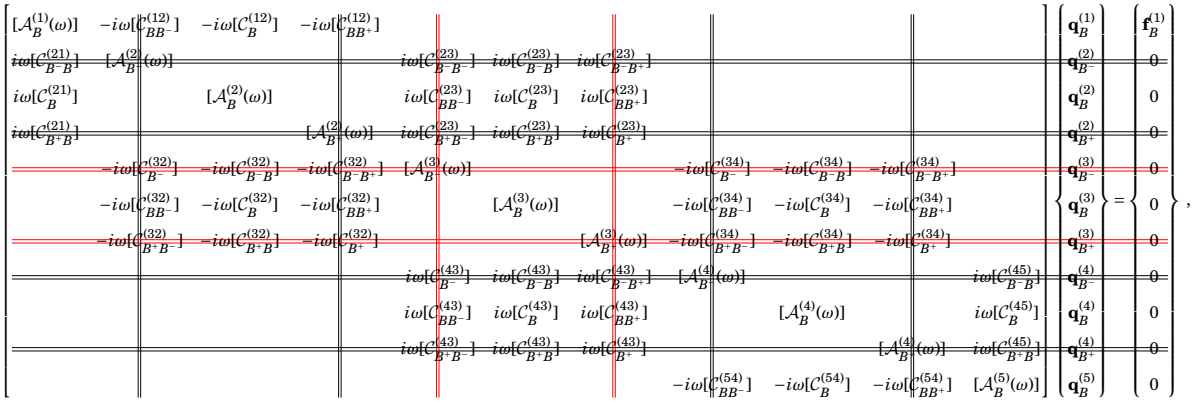

(B.1)

As mentioned in section. VII.2, a good order of doing Schur complements can optimise the computational cost for the Model 1. In order to avoid inverting large size full matrices, we start the reduction with the lines and columns that are double-strike-through with red lines in Eq. (B.1). According to the Schur complement of matrices $[\mathcal{A}^{(3)}_{B^-}(\omega)]$ and $[\mathcal{A}^{(3)}_{B^+}(\omega)]$, matrices $[\mathcal{A}^{(2)}(\omega)]$ and $[\mathcal{A}^{(4)}(\omega)]$ are modified and two new matrices $[\mathcal{W}^{(24)}(\omega)]$ and $[\mathcal{W}^{(42)}(\omega)]$ are created.

$$[A^{(2)}(\omega)] = [\mathcal{A}^{(2)}(\omega)] - \omega^2[\mathcal{C}^{(23)}_{\mathbb{B}B^-}][\mathcal{A}^{(3)}_{B^-}(\omega)]^{-1}[\mathcal{C}^{(32)}_{B^-\mathbb{B}}] - \omega^2[\mathcal{C}^{(23)}_{\mathbb{B}B^+}][\mathcal{A}^{(3)}_{B^+}(\omega)]^{-1}[\mathcal{C}^{(32)}_{B^+\mathbb{B}}]$$
$$[A^{(4)}(\omega)] = [\mathcal{A}^{(4)}(\omega)] - \omega^2[\mathcal{C}^{(43)}_{\mathbb{B}B^-}][\mathcal{A}^{(3)}_{B^-}(\omega)]^{-1}[\mathcal{C}^{(34)}_{B^-\mathbb{B}}] - \omega^2[\mathcal{C}^{(43)}_{\mathbb{B}B^+}][\mathcal{A}^{(3)}_{B^+}(\omega)]^{-1}[\mathcal{C}^{(34)}_{B^+\mathbb{B}}]$$
$$[\mathcal{W}^{(24)}(\omega)] = -\omega^2[\mathcal{C}^{(23)}_{\mathbb{B}B^-}][\mathcal{A}^{(3)}_{B^-}(\omega)]^{-1}[\mathcal{C}^{(34)}_{B^-\mathbb{B}}] - \omega^2[\mathcal{C}^{(23)}_{\mathbb{B}B^+}][\mathcal{A}^{(3)}_{B^+}(\omega)]^{-1}[\mathcal{C}^{(34)}_{B^+\mathbb{B}}]$$

$$[\mathcal{W}^{(42)}(\omega)] = [\mathcal{W}^{(24)}_{\mathbb{B}}(\omega)]^T \ , \tag{B.2}$$

with

$$[\mathcal{A}^{(2)}(\omega)] = \begin{bmatrix} [\mathcal{A}^{(2)}_{B^-}(\omega)] & [\mathcal{A}^{(2)}_{B^-B}(\omega)] & [\mathcal{A}^{(2)}_{B^-B^+}(\omega)] \\ [\mathcal{A}^{(2)}_{BB^-}(\omega)] & [\mathcal{A}^{(2)}_{B}(\omega)] & [\mathcal{A}^{(2)}_{BB^+}(\omega)] \\ [\mathcal{A}^{(2)}_{B^+B^-}(\omega)] & [\mathcal{A}^{(2)}_{B^+B}(\omega)] & [\mathcal{A}^{(2)}_{B^+}(\omega)] \end{bmatrix} \quad , \quad [\mathcal{C}^{(23)}_{\mathbb{B}B^-}] = \begin{bmatrix} [\mathcal{C}^{(23)}_{B^-B^-}] \\ [\mathcal{C}^{(23)}_{BB^-}] \\ [\mathcal{C}^{(23)}_{B^+B^-}] \end{bmatrix} \ ,$$

$$[\mathcal{A}^{(4)}(\omega)] = \begin{bmatrix} [\mathcal{A}^{(4)}_{B^-}(\omega)] & [\mathcal{A}^{(4)}_{B^-B}(\omega)] & [\mathcal{A}^{(4)}_{B^-B^+}(\omega)] \\ [\mathcal{A}^{(4)}_{BB^-}(\omega)] & [\mathcal{A}^{(4)}_{B}(\omega)] & [\mathcal{A}^{(4)}_{BB^+}(\omega)] \\ [\mathcal{A}^{(4)}_{B^+B^-}(\omega)] & [\mathcal{A}^{(4)}_{B^+B}(\omega)] & [\mathcal{A}^{(4)}_{B^+}(\omega)] \end{bmatrix} \quad , \quad [\mathcal{C}^{(23)}_{\mathbb{B}B^+}] = \begin{bmatrix} [\mathcal{C}^{(23)}_{B^-B^+}] \\ [\mathcal{C}^{(23)}_{BB^+}] \\ [\mathcal{C}^{(23)}_{B^+}] \end{bmatrix} \ ,$$

$$[\mathcal{C}^{(34)}_{B^-\mathbb{B}}] = \begin{bmatrix} [\mathcal{C}^{(34)}_{B^-}] & [\mathcal{C}^{(34)}_{B^-B}] & [\mathcal{C}^{(34)}_{B^-B^+}] \end{bmatrix} \ , \qquad [\mathcal{C}^{(34)}_{B^+\mathbb{B}}] = \begin{bmatrix} [\mathcal{C}^{(34)}_{B^+B^-}] & [\mathcal{C}^{(34)}_{B^+B}] & [\mathcal{C}^{(34)}_{B^+}] \end{bmatrix} \ .$$

that are defined with a pre-truncated reduction before this step. The new created matrix can also be divided into several parts,

$$[A^{(2)}(\omega)] = \begin{bmatrix} [A^{(2)}_{B^-}(\omega)] & [A^{(2)}_{B^-B}(\omega)] & [A^{(2)}_{B^-B^+}(\omega)] \\ [A^{(2)}_{BB^-}(\omega)] & [A^{(2)}_{B}(\omega)] & [A^{(2)}_{BB^+}(\omega)] \\ [A^{(2)}_{B^+B^-}(\omega)] & [A^{(2)}_{B^+B}(\omega)] & [A^{(2)}_{B^+}(\omega)] \end{bmatrix} \ ,$$

$$[A^{(4)}(\omega)] = \begin{bmatrix} [A^{(4)}_{B^-}(\omega)] & [A^{(4)}_{B^-B}(\omega)] & [A^{(4)}_{B^-B^+}(\omega)] \\ [A^{(4)}_{BB^-}(\omega)] & [A^{(4)}_{B}(\omega)] & [A^{(4)}_{BB^+}(\omega)] \\ [A^{(4)}_{B^+B^-}(\omega)] & [A^{(4)}_{B^+B}(\omega)] & [A^{(4)}_{B^+}(\omega)] \end{bmatrix} \ ,$$

$$[\mathcal{W}^{(24)}(\omega)] = \begin{bmatrix} [\mathcal{W}^{(24)}_{B^-}(\omega)] & [\mathcal{W}^{(24)}_{B^-B}(\omega)] & [\mathcal{W}^{(24)}_{B^-B^+}(\omega)] \\ [\mathcal{W}^{(24)}_{BB^-}(\omega)] & [\mathcal{W}^{(24)}_{B}(\omega)] & [\mathcal{W}^{(24)}_{BB^+}(\omega)] \\ [\mathcal{W}^{(24)}_{B^+B^-}(\omega)] & [\mathcal{W}^{(24)}_{B^+B}(\omega)] & [\mathcal{W}^{(24)}_{B^+}(\omega)] \end{bmatrix} \ ,$$

$$[\mathcal{W}^{(42)}(\omega)] = \begin{bmatrix} [\mathcal{W}^{(42)}_{B^-}(\omega)] & [\mathcal{W}^{(42)}_{B^-B}(\omega)] & [\mathcal{W}^{(42)}_{B^-B^+}(\omega)] \\ [\mathcal{W}^{(42)}_{BB^-}(\omega)] & [\mathcal{W}^{(42)}_{B}(\omega)] & [\mathcal{W}^{(42)}_{BB^+}(\omega)] \\ [\mathcal{W}^{(42)}_{B^+B^-}(\omega)] & [\mathcal{W}^{(42)}_{B^+B}(\omega)] & [\mathcal{W}^{(42)}_{B^+}(\omega)] \end{bmatrix} \ ,$$

After the first reduction with Schur complement and with the definitions given in Eq. (B.2), we obtain a reduced equation of Eq. (B.1) as below and the next step is to reduce the rest lines and columns that are associated to $\mathbf{q}^{(2)}_{B^-}$, $\mathbf{q}^{(2)}_{B^+}$, $\mathbf{q}^{(4)}_{B^-}$ and $\mathbf{q}^{(4)}_{B^+}$.

$$\left[\begin{array}{ccccccccc}
[\mathcal{A}^{(1)}_B(\omega)] & -i\omega[\mathcal{C}^{(12)}_{BB^-}] & -i\omega[\mathcal{C}^{(12)}_{B}] & -i\omega[\mathcal{C}^{(12)}_{BB^+}] & & & & & \\
\cancel{i\omega[\mathcal{C}^{(21)}_{B^-B}]} & [A^{(2)}_{B^-B}(\omega)] & [A^{(2)}_{B^-B}(\omega)] & [A^{(2)}_{B^-B^+}(\omega)] & i\omega[\mathcal{C}^{(23)}_{B^-B}] & [\mathcal{W}^{(24)}_{B^-}(\omega)] & [\mathcal{W}^{(24)}_{B^-B}(\omega)] & [\mathcal{W}^{(24)}_{B^-B^+}(\omega)] & \\
i\omega[\mathcal{C}^{(21)}_{B}] & [A^{(2)}_{BB^-}(\omega)] & [A^{(2)}_{B}(\omega)] & [A^{(2)}_{BB^+}(\omega)] & i\omega[\mathcal{C}^{(23)}_{B}] & [\mathcal{W}^{(24)}_{BB^-}(\omega)] & [\mathcal{W}^{(24)}_{B}(\omega)] & [\mathcal{W}^{(24)}_{BB^+}(\omega)] & \\
\cancel{i\omega[\mathcal{C}^{(21)}_{B^+B}]} & \cancel{[A^{(2)}_{B^+B^-}(\omega)]} & \cancel{[A^{(2)}_{B^+B}(\omega)]} & \cancel{[A^{(2)}_{B^+}(\omega)]} & \cancel{i\omega[\mathcal{C}^{(23)}_{B^+B}]} & \cancel{[\mathcal{W}^{(24)}_{B^+B^-}(\omega)]} & \cancel{[\mathcal{W}^{(24)}_{B^+B}(\omega)]} & \cancel{[\mathcal{W}^{(24)}_{B^+}(\omega)]} & \\
 & -i\omega[\mathcal{C}^{(32)}_{BB^-}] & -i\omega[\mathcal{C}^{(32)}_{B}] & -i\omega[\mathcal{C}^{(32)}_{BB^+}] & [\mathcal{A}^{(3)}_B(\omega)] & -i\omega[\mathcal{C}^{(34)}_{BB^-}] & -i\omega[\mathcal{C}^{(34)}_{B}] & -i\omega[\mathcal{C}^{(34)}_{BB^+}] & \\
\cancel{[\mathcal{W}^{(42)}_{B^-}(\omega)]} & \cancel{[\mathcal{W}^{(42)}_{B^-B}(\omega)]} & \cancel{[\mathcal{W}^{(42)}_{B^-B^+}(\omega)]} & \cancel{i\omega[\mathcal{C}^{(43)}_{B^-B}]} & \cancel{[A^{(4)}_{B^-}(\omega)]} & \cancel{[A^{(4)}_{B^-B}(\omega)]} & \cancel{[A^{(4)}_{B^-B^+}(\omega)]} & \cancel{i\omega[\mathcal{C}^{(45)}_{B^-B}]} & \\
[\mathcal{W}^{(42)}_{BB^-}(\omega)] & [\mathcal{W}^{(42)}_{B}(\omega)] & [\mathcal{W}^{(42)}_{BB^+}(\omega)] & i\omega[\mathcal{C}^{(43)}_{B}] & [A^{(4)}_{BB^-}(\omega)] & [A^{(4)}_{B}(\omega)] & [A^{(4)}_{BB^+}(\omega)] & i\omega[\mathcal{C}^{(45)}_{B}] & \\
\cancel{[\mathcal{W}^{(42)}_{B^+B^-}(\omega)]} & \cancel{[\mathcal{W}^{(42)}_{B^+B}(\omega)]} & \cancel{[\mathcal{W}^{(42)}_{B^+}(\omega)]} & \cancel{i\omega[\mathcal{C}^{(43)}_{B^+B}]} & \cancel{[A^{(4)}_{B^+B^-}(\omega)]} & \cancel{[A^{(4)}_{B^+B}(\omega)]} & \cancel{[A^{(4)}_{B^+}(\omega)]} & \cancel{i\omega[\mathcal{C}^{(45)}_{B^+B}]} & \\
 & & & & -i\omega[\mathcal{C}^{(54)}_{BB^-}] & -i\omega[\mathcal{C}^{(54)}_{B}] & -i\omega[\mathcal{C}^{(54)}_{BB^+}] & [\mathcal{A}^{(5)}_B(\omega)] &
\end{array}\right]
\left\{\begin{array}{c}
\mathbf{q}^{(1)}_B \\ \cancel{\mathbf{q}^{(2)}_{B^-}} \\ \mathbf{q}^{(2)}_B \\ \cancel{\mathbf{q}^{(2)}_{B^+}} \\ \mathbf{q}^{(3)}_B \\ \cancel{\mathbf{q}^{(4)}_{B^-}} \\ \mathbf{q}^{(4)}_B \\ \cancel{\mathbf{q}^{(4)}_{B^+}} \\ \mathbf{q}^{(5)}_B
\end{array}\right\} =
\left\{\begin{array}{c}
\mathbf{f}^{(1)}_B \\ \cancel{0} \\ 0 \\ \cancel{0} \\ 0 \\ \cancel{0} \\ 0 \\ \cancel{0} \\ 0
\end{array}\right\} \ , \tag{B.3}$$

$\mathbf{q}^{(2)}_{B^-}$, $\mathbf{q}^{(2)}_{B^+}$, $\mathbf{q}^{(4)}_{B^-}$ and $\mathbf{q}^{(4)}_{B^+}$ can be reduced at the same time as introduced in Appendix. A, or can be reduced one by one. In Eq. (B.3), as $[A^{(2)}_{B^-}(\omega)]$, $[A^{(2)}_{B^+}(\omega)]$, $[A^{(4)}_{B^-}(\omega)]$ and $[A^{(4)}_{B^+}(\omega)]$ are all full matrices, so there is no interest to doing the reduction one by one like for the subsystem (3).

$$
\left[\begin{array}{ccccccccccc}
[\mathcal{A}^{(1)}_B(\omega)] & -i\omega[\mathcal{C}^{(12)}_B] & & & & -i\omega[\mathcal{C}^{(12)}_{BB^-}] & -i\omega[\mathcal{C}^{(12)}_{BB^+}] & & & & \\
i\omega[\mathcal{C}^{(21)}_B] & [A^{(2)}_B(\omega)] & i\omega[\mathcal{C}^{(23)}_B] & [\mathcal{W}^{(24)}_B(\omega)] & & [A^{(2)}_{BB^-}(\omega)] & [A^{(2)}_{BB^+}(\omega)] & [\mathcal{W}^{(24)}_{BB^-}(\omega)] & [\mathcal{W}^{(24)}_{BB^+}(\omega)] & & \\
 & -i\omega[\mathcal{C}^{(32)}_B] & [\mathcal{A}^{(3)}_B(\omega)] & -i\omega[\mathcal{C}^{(34)}_B] & & -i\omega[\mathcal{C}^{(32)}_{BB^-}] & -i\omega[\mathcal{C}^{(32)}_{BB^+}] & -i\omega[\mathcal{C}^{(34)}_{BB^-}] & -i\omega[\mathcal{C}^{(34)}_{BB^+}] & & \\
 & [\mathcal{W}^{(42)}_B(\omega)] & i\omega[\mathcal{C}^{(43)}_B] & [A^{(4)}_B(\omega)] & i\omega[\mathcal{C}^{(45)}_B] & [\mathcal{W}^{(42)}_{BB^-}(\omega)] & [\mathcal{W}^{(42)}_{BB^+}(\omega)] & [A^{(4)}_{BB^-}(\omega)] & [A^{(4)}_{BB^+}(\omega)] & & \\
 & & & -i\omega[\mathcal{C}^{(54)}_B] & [\mathcal{A}^{(5)}_B(\omega)] & & & -i\omega[\mathcal{C}^{(54)}_{BB^-}] & -i\omega[\mathcal{C}^{(54)}_{BB^+}] & & \\
\cancel{i\omega[\mathcal{C}^{(21)}_{B^-B}]} & \cancel{[A^{(2)}_{B^-B}(\omega)]} & \cancel{i\omega[\mathcal{C}^{(23)}_{B^-B}]} & \cancel{[\mathcal{W}^{(24)}_{B^-B}(\omega)]} & & \cancel{[A^{(2)}_{B^-}(\omega)]} & \cancel{[A^{(2)}_{B^-B^+}(\omega)]} & \cancel{[\mathcal{W}^{(24)}_{B^-}(\omega)]} & \cancel{[\mathcal{W}^{(24)}_{B^-B^+}(\omega)]} & \cancel{\mathbf{q}^{(2)}_{B^-}} & \cancel{0} \\
\cancel{i\omega[\mathcal{C}^{(21)}_{B^+B}]} & \cancel{[A^{(2)}_{B^+B}(\omega)]} & \cancel{i\omega[\mathcal{C}^{(23)}_{B^+B}]} & \cancel{[\mathcal{W}^{(24)}_{B^+B}(\omega)]} & & \cancel{[A^{(2)}_{B^+B^-}(\omega)]} & \cancel{[A^{(2)}_{B^+}(\omega)]} & \cancel{[\mathcal{W}^{(24)}_{B^+B}(\omega)]} & \cancel{[\mathcal{W}^{(24)}_{B^+}(\omega)]} & \cancel{\mathbf{q}^{(2)}_{B^+}} & \cancel{0} \\
 & \cancel{[\mathcal{W}^{(42)}_{B^-B}(\omega)]} & \cancel{i\omega[\mathcal{C}^{(43)}_{B^-B}]} & \cancel{[A^{(4)}_{B^-B}(\omega)]} & \cancel{i\omega[\mathcal{C}^{(45)}_{B^-B}]} & \cancel{[\mathcal{W}^{(42)}_{B^-}(\omega)]} & \cancel{[\mathcal{W}^{(42)}_{B^-B^+}(\omega)]} & \cancel{[A^{(4)}_{B^-}(\omega)]} & \cancel{[A^{(4)}_{B^-B^+}(\omega)]} & \cancel{\mathbf{q}^{(4)}_{B^-}} & \cancel{0} \\
 & \cancel{[\mathcal{W}^{(42)}_{B^+B}(\omega)]} & \cancel{i\omega[\mathcal{C}^{(43)}_{B^+B}]} & \cancel{[A^{(4)}_{B^+B}(\omega)]} & \cancel{i\omega[\mathcal{C}^{(45)}_{B^+B}]} & \cancel{[\mathcal{W}^{(42)}_{B^+B^-}(\omega)]} & \cancel{[\mathcal{W}^{(42)}_{B^+}(\omega)]} & \cancel{[A^{(4)}_{B^+B}(\omega)]} & \cancel{[A^{(4)}_{B^+}(\omega)]} & \cancel{\mathbf{q}^{(4)}_{B^+}} & \cancel{0}
\end{array}\right]
\left\{\begin{array}{c}
\mathbf{q}^{(1)}_B \\ \mathbf{q}^{(2)}_B \\ \mathbf{q}^{(3)}_B \\ \mathbf{q}^{(4)}_B \\ \mathbf{q}^{(5)}_B \\ \cancel{\mathbf{q}^{(2)}_{B^-}} \\ \cancel{\mathbf{q}^{(2)}_{B^+}} \\ \cancel{\mathbf{q}^{(4)}_{B^-}} \\ \cancel{\mathbf{q}^{(4)}_{B^+}}
\end{array}\right\}
=
\left\{\begin{array}{c}
\mathbf{f}^{(1)}_B \\ 0 \\ 0 \\ 0 \\ 0 \\ \cancel{0} \\ \cancel{0} \\ \cancel{0} \\ \cancel{0}
\end{array}\right\},
\tag{B.4}
$$

By regrouping these block-matrices into 4 matrices,

$$
[\mathbb{A}] = \begin{bmatrix}
[\mathcal{A}^{(1)}_B(\omega)] & -i\omega[\mathcal{C}^{(12)}_B] & & & \\
i\omega[\mathcal{C}^{(21)}_B] & [A^{(2)}_B(\omega)] & i\omega[\mathcal{C}^{(23)}_B] & [\mathcal{W}^{(24)}_B(\omega)] & \\
 & -i\omega[\mathcal{C}^{(32)}_B] & [\mathcal{A}^{(3)}_B(\omega)] & -i\omega[\mathcal{C}^{(34)}_B] & \\
 & [\mathcal{W}^{(42)}_B(\omega)] & i\omega[\mathcal{C}^{(43)}_B] & [A^{(4)}_B(\omega)] & i\omega[\mathcal{C}^{(45)}_B] \\
 & & & -i\omega[\mathcal{C}^{(54)}_B] & [\mathcal{A}^{(5)}_B(\omega)]
\end{bmatrix},
$$

$$
[\mathbb{W}_{\mathrm{UR}}] = \begin{bmatrix}
-i\omega[\mathcal{C}^{(12)}_{BB^-}] & -i\omega[\mathcal{C}^{(12)}_{BB^+}] & & \\
[A^{(2)}_{BB^-}(\omega)] & [A^{(2)}_{BB^+}(\omega)] & [\mathcal{W}^{(24)}_{BB^-}(\omega)] & [\mathcal{W}^{(24)}_{BB^+}(\omega)] \\
-i\omega[\mathcal{C}^{(32)}_{BB^-}] & -i\omega[\mathcal{C}^{(32)}_{BB^+}] & -i\omega[\mathcal{C}^{(34)}_{BB^-}] & -i\omega[\mathcal{C}^{(34)}_{BB^+}] \\
[\mathcal{W}^{(42)}_{BB^-}(\omega)] & [\mathcal{W}^{(42)}_{BB^+}(\omega)] & [A^{(4)}_{BB^-}(\omega)] & [A^{(4)}_{BB^+}(\omega)] \\
 & & -i\omega[\mathcal{C}^{(54)}_{BB^-}] & -i\omega[\mathcal{C}^{(54)}_{BB^+}]
\end{bmatrix},
$$

$$
[\mathbb{W}_{\mathrm{DL}}] = \begin{bmatrix}
i\omega[\mathcal{C}^{(21)}_{B^-B}] & [A^{(2)}_{B^-B}(\omega)] & i\omega[\mathcal{C}^{(23)}_{B^-B}] & [\mathcal{W}^{(24)}_{B^-B}(\omega)] & \\
i\omega[\mathcal{C}^{(21)}_{B^+B}] & [A^{(2)}_{B^+B}(\omega)] & i\omega[\mathcal{C}^{(23)}_{B^+B}] & [\mathcal{W}^{(24)}_{B^+B}(\omega)] & \\
 & [\mathcal{W}^{(42)}_{B^-B}(\omega)] & i\omega[\mathcal{C}^{(43)}_{B^-B}] & [A^{(4)}_{B^-B}(\omega)] & i\omega[\mathcal{C}^{(45)}_{B^-B}] \\
 & [\mathcal{W}^{(42)}_{B^+B}(\omega)] & i\omega[\mathcal{C}^{(43)}_{B^+B}] & [A^{(4)}_{B^+B}(\omega)] & i\omega[\mathcal{C}^{(45)}_{B^+B}]
\end{bmatrix},
$$

$$[\mathbb{A}_{\mathrm{NR}}] = \begin{bmatrix} [A^{(2)}_{B^-}(\omega)] & [A^{(2)}_{B^-B^+}(\omega)] & [\mathcal{W}^{(24)}_{B^-}(\omega)] & [\mathcal{W}^{(24)}_{B^-B^+}(\omega)] \\ [A^{(2)}_{B^+B^-}(\omega)] & [A^{(2)}_{B^+}(\omega)] & [\mathcal{W}^{(24)}_{B^+B^-}(\omega)] & [\mathcal{W}^{(24)}_{B^+}(\omega)] \\ [\mathcal{W}^{(42)}_{B^-}(\omega)] & [\mathcal{W}^{(42)}_{B^-B^+}(\omega)] & [A^{(4)}_{B^-}(\omega)] & [A^{(4)}_{B^-B^+}(\omega)] \\ [\mathcal{W}^{(42)}_{B^+B^-}(\omega)] & [\mathcal{W}^{(42)}_{B^+}(\omega)] & [A^{(4)}_{B^+B^-}(\omega)] & [A^{(4)}_{B^+}(\omega)] \end{bmatrix} .$$

If we define the global matrix at the left-hand side of Eq. (B.4) as matrix $[\mathbb{A}]$, then its Schur complement $[\mathbb{A}^{\mathrm{SC}}]$ is therefore deduced as,

$$[\mathbb{A}^{\mathrm{SC}}] = [\mathbb{A}]/[\mathbb{A}_{\mathrm{NR}}] = [\mathbb{A}] - [\mathbb{W}_{\mathrm{DL}}][\mathbb{A}_{\mathrm{NR}}]^{-1}[\mathbb{W}_{\mathrm{UR}}] ,$$

and

$$[\mathbb{A}^{\mathrm{SC}}] = \begin{bmatrix} [\mathbb{Z}^{(1)}_B(\omega)] & [\mathbb{W}^{(12)}_B(\omega)] & [\mathbb{V}^{(13)}_B(\omega)] & [\mathbb{W}^{(14)}_B(\omega)] & [\mathbb{V}^{(15)}_B(\omega)] \\ [\mathbb{W}^{(21)}_B(\omega)] & [\mathbb{Z}^{(2)}_B(\omega)] & [\mathbb{W}^{(23)}_B(\omega)] & [\mathbb{V}^{(24)}_B(\omega)] & [\mathbb{W}^{(25)}_B(\omega)] \\ [\mathbb{V}^{(31)}_B(\omega)] & [\mathbb{W}^{(32)}_B(\omega)] & [\mathbb{Z}^{(3)}_B(\omega)] & [\mathbb{W}^{(34)}_B(\omega)] & [\mathbb{V}^{(35)}_B(\omega)] \\ [\mathbb{W}^{(41)}_B(\omega)] & [\mathbb{V}^{(42)}_B(\omega)] & [\mathbb{W}^{(43)}_B(\omega)] & [\mathbb{Z}^{(4)}_B(\omega)] & [\mathbb{W}^{(45)}_B(\omega)] \\ [\mathbb{V}^{(51)}_B(\omega)] & [\mathbb{W}^{(52)}_B(\omega)] & [\mathbb{V}^{(53)}_B(\omega)] & [\mathbb{W}^{(54)}_B(\omega)] & [\mathbb{Z}^{(5)}_B(\omega)] \end{bmatrix}$$

APPENDIX C

APPENDIX C

C.1 CROM of the Model 2

Similar to the Model 1, in order to avoid inverting large size full matrices, we start the reduction with the lines and columns that are associated to the non-resonant generalised coordinates $\mathbf{q}^{(3)}_{B^-}$ and $\mathbf{q}^{(3)}_{B^+}$ in Eq. (VII.3). The Schur complement of matrices $[\mathcal{A}^{(3)}_{B^-}(\omega)]$ and $[\mathcal{A}^{(3)}_{B^+}(\omega)]$ will create some added matrices,

$$
\begin{aligned}
[A^{(2)}(\omega)] &= [\mathcal{A}^{(2)}(\omega)] - [\mathcal{A}^{(1)}_{\text{cond}}(\omega)] - \omega^2[\mathcal{C}^{(23)}_{\mathbb{B}B^-}][\mathcal{A}^{(3)}_{B^-}(\omega)]^{-1}[\mathcal{C}^{(32)}_{B^-\mathbb{B}}] - \omega^2[\mathcal{C}^{(23)}_{\mathbb{B}B^+}][\mathcal{A}^{(3)}_{B^+}(\omega)]^{-1}[\mathcal{C}^{(32)}_{B^+\mathbb{B}}] \\
[A^{(4)}(\omega)] &= [\mathcal{A}^{(4)}(\omega)] - [\mathcal{A}^{(5)}_{\text{cond}}(\omega)] - \omega^2[\mathcal{C}^{(43)}_{\mathbb{B}B^-}][\mathcal{A}^{(3)}_{B^-}(\omega)]^{-1}[\mathcal{C}^{(34)}_{B^-\mathbb{B}}] - \omega^2[\mathcal{C}^{(43)}_{\mathbb{B}B^+}][\mathcal{A}^{(3)}_{B^+}(\omega)]^{-1}[\mathcal{C}^{(34)}_{B^+\mathbb{B}}] \\
[\mathcal{W}^{(24)}(\omega)] &= -\omega^2[\mathcal{C}^{(23)}_{\mathbb{B}B^-}][\mathcal{A}^{(3)}_{B^-}(\omega)]^{-1}[\mathcal{C}^{(34)}_{B^-\mathbb{B}}] - \omega^2[\mathcal{C}^{(23)}_{\mathbb{B}B^+}][\mathcal{A}^{(3)}_{B^+}(\omega)]^{-1}[\mathcal{C}^{(34)}_{B^+\mathbb{B}}] \\
[\mathcal{W}^{(42)}(\omega)] &= [\mathcal{W}^{(24)}_{\mathbb{B}}(\omega)]^T \ ,
\end{aligned}
\tag{C.1}
$$

As mentioned in section. VI.4, the acoustic impedance matrices $[\mathcal{A}^{(1)}_{\text{cond}}(\omega)]$ and $[\mathcal{A}^{(5)}_{\text{cond}}(\omega)]$ are possible to be neglected if the actual studying frequency band B is in medium and high frequency domain. Like the Model 1 in Appendix. B, we then do the reductions for the non-resonant

generalised coordinates $\mathbf{q}^{(2)}_{B^-}$, $\mathbf{q}^{(2)}_{B^+}$, $\mathbf{q}^{(4)}_{B^-}$ and $\mathbf{q}^{(4)}_{B^+}$.

$$\left[\begin{array}{ccc|ccc} [A^{(2)}_{B}(\omega)] & [A^{(2)}_{B^-B}(\omega)] & [A^{(2)}_{B^-B^+}(\omega)] & i\omega[\mathcal{C}^{(23)}_{B^-B}] & [\mathcal{W}^{(24)}_{B}(\omega)] & [\mathcal{W}^{(24)}_{B^-B}(\omega)] & [\mathcal{W}^{(24)}_{B^-B^+}(\omega)] \\ [A^{(2)}_{BB^-}(\omega)] & [A^{(2)}_{B}(\omega)] & [A^{(2)}_{BB^+}(\omega)] & i\omega[\mathcal{C}^{(23)}_{B}] & [\mathcal{W}^{(24)}_{BB^-}(\omega)] & [\mathcal{W}^{(24)}_{B}(\omega)] & [\mathcal{W}^{(24)}_{BB^+}(\omega)] \\ [A^{(2)}_{B^+B^-}(\omega)] & [A^{(2)}_{B^+B}(\omega)] & [A^{(2)}_{B^+}(\omega)] & i\omega[\mathcal{C}^{(23)}_{B^+B}] & [\mathcal{W}^{(24)}_{B^+B^-}(\omega)] & [\mathcal{W}^{(24)}_{B^+B}(\omega)] & [\mathcal{W}^{(24)}_{B^+}(\omega)] \\ -i\omega[\mathcal{C}^{(32)}_{BB^-}] & -i\omega[\mathcal{C}^{(32)}_{B}] & -i\omega[\mathcal{C}^{(32)}_{BB^+}] & [\mathcal{A}^{(3)}_{B}(\omega)] & -i\omega[\mathcal{C}^{(34)}_{BB^-}] & -i\omega[\mathcal{C}^{(34)}_{B}] & -i\omega[\mathcal{C}^{(34)}_{BB^+}] \\ [\mathcal{W}^{(42)}_{B}(\omega)] & [\mathcal{W}^{(42)}_{B^-B}(\omega)] & [\mathcal{W}^{(42)}_{B^-B^+}(\omega)] & i\omega[\mathcal{C}^{(43)}_{B^-B}] & [A^{(4)}_{B}(\omega)] & [A^{(4)}_{B^-B}(\omega)] & [A^{(4)}_{B^-B^+}(\omega)] \\ [\mathcal{W}^{(42)}_{BB^-}(\omega)] & [\mathcal{W}^{(42)}_{B}(\omega)] & [\mathcal{W}^{(42)}_{BB^+}(\omega)] & i\omega[\mathcal{C}^{(43)}_{B}] & [A^{(4)}_{BB^-}(\omega)] & [A^{(4)}_{B}(\omega)] & [A^{(4)}_{BB^+}(\omega)] \\ [\mathcal{W}^{(42)}_{B^+B^-}(\omega)] & [\mathcal{W}^{(42)}_{B^+B}(\omega)] & [\mathcal{W}^{(42)}_{B^+}(\omega)] & i\omega[\mathcal{C}^{(43)}_{B^+B}] & [A^{(4)}_{B^+B^-}(\omega)] & [A^{(4)}_{B^+B}(\omega)] & [A^{(4)}_{B^+}(\omega)] \end{array}\right] \left\{\begin{array}{c} \mathbf{q}^{(2)}_{B^-} \\ \mathbf{q}^{(2)}_{B} \\ \mathbf{q}^{(2)}_{B^+} \\ \mathbf{q}^{(3)}_{B} \\ \mathbf{q}^{(4)}_{B^-} \\ \mathbf{q}^{(4)}_{B} \\ \mathbf{q}^{(4)}_{B^+} \end{array}\right\} = \left\{\begin{array}{c} \mathbf{f}^{(2)}_{B^-} \\ \mathbf{f}^{(2)}_{B} \\ \mathbf{f}^{(2)}_{B^+} \\ 0 \\ 0 \\ 0 \\ 0 \end{array}\right\}, \tag{C.2}$$

In this example, as the reduced generalised coordinates $\mathbf{q}^{(2)}_{B^-}$, $\mathbf{q}^{(2)}_{B^+}$ are associated to external generalised forces and $\mathbf{q}^{(4)}_{B^-}$, $\mathbf{q}^{(4)}_{B^+}$ are not, its solution is not a similar case to the Schur complement proposed in Appendix. B. A reduction of the non-resonant generalised coordinates $\mathbf{q}^{(2)}_{B^-}$ and $\mathbf{q}^{(2)}_{B^+}$ will not only result in some added complement matrices, but also the added equivalent external generalised forces. The non-resonant generalised coordinates for subsystem (2) and (4) can be grouped as well as the external generalised forces, which means

$$\left\{\mathbf{q}^{(2)}_{B^{\mathrm{NR}}}\right\} = \left\{\begin{array}{c} \mathbf{q}^{(2)}_{B^-} \\ \mathbf{q}^{(2)}_{B^+} \end{array}\right\} \quad , \quad \left\{\mathbf{q}^{(4)}_{B^{\mathrm{NR}}}\right\} = \left\{\begin{array}{c} \mathbf{q}^{(4)}_{B^-} \\ \mathbf{q}^{(4)}_{B^+} \end{array}\right\} \quad , \quad \left\{\mathbf{f}^{(2)}_{B^{\mathrm{NR}}}\right\} = \left\{\begin{array}{c} \mathbf{f}^{(2)}_{B^-} \\ \mathbf{f}^{(2)}_{B^+} \end{array}\right\} \quad .$$

Eq. (C.2) can be rewritten as,

$$\left[\begin{array}{ccc|ccc} [A^{(2)}_{B}(\omega)] & [A^{(2)}_{B^-B^+}(\omega)] & [A^{(2)}_{B^-B}(\omega)] & i\omega[\mathcal{C}^{(23)}_{B^-B}] & [\mathcal{W}^{(24)}_{B}(\omega)] & [\mathcal{W}^{(24)}_{B^-B^+}(\omega)] & [\mathcal{W}^{(24)}_{B^-B}(\omega)] \\ [A^{(2)}_{B^+B^-}(\omega)] & [A^{(2)}_{B^+}(\omega)] & [A^{(2)}_{B^+B}(\omega)] & i\omega[\mathcal{C}^{(23)}_{B^+B}] & [\mathcal{W}^{(24)}_{B^+B^-}(\omega)] & [\mathcal{W}^{(24)}_{B^+}(\omega)] & [\mathcal{W}^{(24)}_{B^+B}(\omega)] \\ [A^{(2)}_{BB^-}(\omega)] & [A^{(2)}_{BB^+}(\omega)] & [A^{(2)}_{B}(\omega)] & i\omega[\mathcal{C}^{(23)}_{B}] & [\mathcal{W}^{(24)}_{BB^-}(\omega)] & [\mathcal{W}^{(24)}_{BB^+}(\omega)] & [\mathcal{W}^{(24)}_{B}(\omega)] \\ -i\omega[\mathcal{C}^{(32)}_{BB^-}] & -i\omega[\mathcal{C}^{(32)}_{BB^+}] & -i\omega[\mathcal{C}^{(32)}_{B}] & [\mathcal{A}^{(3)}_{B}(\omega)] & -i\omega[\mathcal{C}^{(34)}_{BB^-}] & -i\omega[\mathcal{C}^{(34)}_{BB^+}] & -i\omega[\mathcal{C}^{(34)}_{B}] \\ [\mathcal{W}^{(42)}_{B}(\omega)] & [\mathcal{W}^{(42)}_{B^-B^+}(\omega)] & [\mathcal{W}^{(42)}_{B^-B}(\omega)] & i\omega[\mathcal{C}^{(43)}_{B^-B}] & [A^{(4)}_{B}(\omega)] & [A^{(4)}_{B^-B^+}(\omega)] & [A^{(4)}_{B^-B}(\omega)] \\ [\mathcal{W}^{(42)}_{B^+B^-}(\omega)] & [\mathcal{W}^{(42)}_{B^+}(\omega)] & [\mathcal{W}^{(42)}_{B^+B}(\omega)] & i\omega[\mathcal{C}^{(43)}_{B^+B}] & [A^{(4)}_{B^+B^-}(\omega)] & [A^{(4)}_{B^+}(\omega)] & [A^{(4)}_{B^+B}(\omega)] \\ [\mathcal{W}^{(42)}_{BB^-}(\omega)] & [\mathcal{W}^{(42)}_{BB^+}(\omega)] & [\mathcal{W}^{(42)}_{B}(\omega)] & i\omega[\mathcal{C}^{(43)}_{B}] & [A^{(4)}_{BB^-}(\omega)] & [A^{(4)}_{BB^+}(\omega)] & [A^{(4)}_{B}(\omega)] \end{array}\right] \left\{\begin{array}{c} \mathbf{q}^{(2)}_{B^-} \\ \mathbf{q}^{(2)}_{B^+} \\ \mathbf{q}^{(2)}_{B} \\ \mathbf{q}^{(3)}_{B} \\ \mathbf{q}^{(4)}_{B^-} \\ \mathbf{q}^{(4)}_{B^+} \\ \mathbf{q}^{(4)}_{B} \end{array}\right\} = \left\{\begin{array}{c} \mathbf{f}^{(2)}_{B^-} \\ \mathbf{f}^{(2)}_{B^+} \\ \mathbf{f}^{(2)}_{B} \\ 0 \\ 0 \\ 0 \\ 0 \end{array}\right\}, \tag{C.3}$$

then

$$\begin{bmatrix} [A^{(2)}_{B^{\mathrm{NR}}}(\omega)] & [A^{(2)}_{B^{\mathrm{NR}}B}(\omega)] & i\omega[C^{(23)}_{B^{\mathrm{NR}}B}] & [\mathcal{W}^{(24)}_{B^{\mathrm{NR}}}(\omega)] & [\mathcal{W}^{(24)}_{B^{\mathrm{NR}}B}(\omega)] \\ [A^{(2)}_{BB^{\mathrm{NR}}}(\omega)] & [A^{(2)}_{B}(\omega)] & i\omega[C^{(23)}_{B}] & [\mathcal{W}^{(24)}_{BB^{\mathrm{NR}}}(\omega)] & [\mathcal{W}^{(24)}_{B}(\omega)] \\ -i\omega[C^{(32)}_{BB^{\mathrm{NR}}}] & -i\omega[C^{(32)}_{B}] & [\mathcal{A}^{(3)}_{B}(\omega)] & -i\omega[C^{(34)}_{BB^{\mathrm{NR}}}] & -i\omega[C^{(34)}_{B}] \\ [\mathcal{W}^{(42)}_{B^{\mathrm{NR}}}(\omega)] & [\mathcal{W}^{(42)}_{B^{\mathrm{NR}}B}(\omega)] & i\omega[C^{(43)}_{B^{\mathrm{NR}}B}] & [A^{(4)}_{B^{\mathrm{NR}}}(\omega)] & [A^{(4)}_{B^{\mathrm{NR}}B}(\omega)] \\ [\mathcal{W}^{(42)}_{BB^{\mathrm{NR}}}(\omega)] & [\mathcal{W}^{(42)}_{B}(\omega)] & i\omega[C^{(43)}_{B}] & [A^{(4)}_{BB^{\mathrm{NR}}}(\omega)] & [A^{(4)}_{B}(\omega)] \end{bmatrix} \begin{Bmatrix} \mathbf{q}^{(2)}_{B^{\mathrm{NR}}} \\ \mathbf{q}^{(2)}_{B} \\ \mathbf{q}^{(3)}_{B} \\ \mathbf{q}^{(4)}_{B^{\mathrm{NR}}} \\ \mathbf{q}^{(4)}_{B} \end{Bmatrix} = \begin{Bmatrix} \mathbf{f}^{(2)}_{B^{\mathrm{NR}}} \\ \mathbf{f}^{(2)}_{B} \\ 0 \\ 0 \\ 0 \end{Bmatrix}, \tag{C.4}$$

with

$$[A^{(2)}_{B^{\mathrm{NR}}}(\omega)] = \begin{bmatrix} [A^{(2)}_{B^-}(\omega)] & [A^{(2)}_{B^-B^+}(\omega)] \\ [A^{(2)}_{B^+B^-}(\omega)] & [A^{(2)}_{B^+}(\omega)] \end{bmatrix} \quad , \quad [A^{(4)}_{B^{\mathrm{NR}}}(\omega)] = \begin{bmatrix} [A^{(4)}_{B^-}(\omega)] & [A^{(4)}_{B^-B^+}(\omega)] \\ [A^{(4)}_{B^+B^-}(\omega)] & [A^{(4)}_{B^+}(\omega)] \end{bmatrix} ,$$
$$[\mathcal{W}^{(24)}_{B^{\mathrm{NR}}}(\omega)] = \begin{bmatrix} [\mathcal{W}^{(24)}_{B^-}(\omega)] & [\mathcal{W}^{(24)}_{B^-B^+}(\omega)] \\ [\mathcal{W}^{(24)}_{B^+B^-}(\omega)] & [\mathcal{W}^{(24)}_{B^+}(\omega)] \end{bmatrix} \quad , \quad [\mathcal{W}^{(42)}_{B^{\mathrm{NR}}}(\omega)] = \begin{bmatrix} [\mathcal{W}^{(42)}_{B^+B^-}(\omega)] & [\mathcal{W}^{(42)}_{B^+}(\omega)] \\ [\mathcal{W}^{(42)}_{BB^-}(\omega)] & [\mathcal{W}^{(42)}_{BB^+}(\omega)] \end{bmatrix} ,$$

$$[A^{(2)}_{B^{\mathrm{NR}}B}(\omega)] = \begin{bmatrix} [A^{(2)}_{B^-B}(\omega)] \\ [A^{(2)}_{B^+B}(\omega)] \end{bmatrix} \quad , \quad [C^{(23)}_{B^{\mathrm{NR}}B}] = \begin{bmatrix} [C^{(23)}_{B^-B}] \\ [C^{(23)}_{B^+B}] \end{bmatrix} \quad , \quad [\mathcal{W}^{(24)}_{B^{\mathrm{NR}}B}(\omega)] = \begin{bmatrix} [\mathcal{W}^{(24)}_{B^-B}(\omega)] \\ [\mathcal{W}^{(24)}_{B^+B}(\omega)] \end{bmatrix} ,$$
$$[\mathcal{W}^{(42)}_{B^{\mathrm{NR}}B}(\omega)] = \begin{bmatrix} [\mathcal{W}^{(42)}_{B^-B}(\omega)] \\ [\mathcal{W}^{(42)}_{B^+B}(\omega)] \end{bmatrix} \quad , \quad [C^{(43)}_{B^{\mathrm{NR}}B}] = \begin{bmatrix} [C^{(43)}_{B^-B}] \\ [C^{(43)}_{B^+B}] \end{bmatrix} \quad , \quad [A^{(4)}_{B^{\mathrm{NR}}B}(\omega)] = \begin{bmatrix} [A^{(4)}_{B^-B}(\omega)] \\ [A^{(4)}_{B^+B}(\omega)] \end{bmatrix} .$$

$$[A^{(2)}_{BB^{\mathrm{NR}}}(\omega)] = \begin{bmatrix} [A^{(2)}_{BB^-}(\omega)] & [A^{(2)}_{BB^+}(\omega)] \end{bmatrix} \quad , \quad [\mathcal{W}^{(24)}_{BB^{\mathrm{NR}}}(\omega)] = \begin{bmatrix} [\mathcal{W}^{(24)}_{BB^-}(\omega)] & [\mathcal{W}^{(24)}_{BB^+}(\omega)] \end{bmatrix} ,$$
$$[C^{(32)}_{BB^{\mathrm{NR}}}] = \begin{bmatrix} [C^{(32)}_{BB^-}] & [C^{(32)}_{BB^+}] \end{bmatrix} \quad , \quad [C^{(34)}_{BB^{\mathrm{NR}}}] = \begin{bmatrix} [C^{(34)}_{BB^-}] & [C^{(34)}_{BB^+}] \end{bmatrix} ,$$
$$[\mathcal{W}^{(42)}_{BB^{\mathrm{NR}}}(\omega)] = \begin{bmatrix} [\mathcal{W}^{(42)}_{BB^-}(\omega)] & [\mathcal{W}^{(42)}_{BB^+}(\omega)] \end{bmatrix} \quad , \quad [A^{(4)}_{BB^{\mathrm{NR}}}(\omega)] = \begin{bmatrix} [A^{(4)}_{BB^-}(\omega)] & [A^{(4)}_{BB^+}(\omega)] \end{bmatrix} .$$

Reductions will be carried out firstly with $\mathbf{q}^{(4)}_{B^{\mathrm{NR}}}$ as no external loads are associated to it.

$$\mathbf{q}^{(4)}_{B^{\mathrm{NR}}} = [A^{(4)}_{B^{\mathrm{NR}}}(\omega)]^{-1}\Big(-[\mathcal{W}^{(42)}_{B^{\mathrm{NR}}}(\omega)]\mathbf{q}^{(2)}_{B^{\mathrm{NR}}} - [\mathcal{W}^{(42)}_{B^{\mathrm{NR}}B}(\omega)]\mathbf{q}^{(2)}_{B} - i\omega[C^{(43)}_{B^{\mathrm{NR}}B}]\mathbf{q}^{(3)}_{B} - [A^{(4)}_{B^{\mathrm{NR}}B}(\omega)]\mathbf{q}^{(4)}_{B}\Big) . \tag{C.5}$$

Putting Eq. (C.5) into the first line of Eq. (C.2), and we can have some new matrices that can facilitate the expressions of other matrices,

$$\begin{aligned}
[\tilde{A}^{(2)}_{B^{\mathrm{NR}}}(\omega)] &= [A^{(2)}_{B^{\mathrm{NR}}}(\omega)] - [\mathcal{W}^{(24)}_{B^{\mathrm{NR}}}(\omega)][A^{(4)}_{B^{\mathrm{NR}}}(\omega)]^{-1}[\mathcal{W}^{(42)}_{B^{\mathrm{NR}}}(\omega)] \\
[\tilde{A}^{(2)}_{B^{\mathrm{NR}}B}(\omega)] &= [A^{(2)}_{B^{\mathrm{NR}}B}(\omega)] - [\mathcal{W}^{(24)}_{B^{\mathrm{NR}}}(\omega)][A^{(4)}_{B^{\mathrm{NR}}}(\omega)]^{-1}[\mathcal{W}^{(42)}_{B^{\mathrm{NR}}B}(\omega)] \\
[\mathcal{W}^{(23)}_{B^{\mathrm{NR}}B}(\omega)] &= i\omega[C^{(23)}_{B^{\mathrm{NR}}B}] - i\omega[\mathcal{W}^{(24)}_{B}(\omega)][A^{(4)}_{B^-}(\omega)]^{-1}[C^{(43)}_{B^{\mathrm{NR}}B}] \\
[\tilde{\mathcal{W}}^{(24)}_{B^{\mathrm{NR}}B}(\omega)] &= [\mathcal{W}^{(24)}_{B^{\mathrm{NR}}B}(\omega)] - [\mathcal{W}^{(24)}_{B^{\mathrm{NR}}}(\omega)][A^{(4)}_{B^{\mathrm{NR}}}(\omega)]^{-1}[A^{(4)}_{B^{\mathrm{NR}}B}(\omega)] .
\end{aligned}$$

Here we give the expression of each element in Eq. (VII.4),

$$[\mathbb{Z}_B^{(2)}(\omega)] = [A_B^{(2)}(\omega)] - [\mathcal{W}_{BB^{\rm NR}}^{(24)}(\omega)][A_{B^{\rm NR}}^{(4)}(\omega)]^{-1}[\mathcal{W}_{B^{\rm NR}B}^{(42)}(\omega)] - [A_{BB^{\rm NR}}^{(2)}(\omega)][\tilde{A}_{B^{\rm NR}}^{(2)}(\omega)]^{-1}[\tilde{A}_{B^{\rm NR}B}^{(2)}(\omega)]$$

$$[\mathbb{Z}_B^{(3)}(\omega)] = [\mathcal{A}_B^{(3)}(\omega)] - \omega^2[\mathcal{C}_{BB^{\rm NR}}^{(34)}][A_{B^{\rm NR}}^{(4)}(\omega)]^{-1}[\mathcal{C}_{B^{\rm NR}B}^{(43)}] + i\omega[\mathcal{C}_{BB^{\rm NR}}^{(32)}][\tilde{A}_{B^{\rm NR}}^{(2)}(\omega)]^{-1}[\mathcal{W}_{B^{\rm NR}B}^{(23)}(\omega)]$$

$$[\mathbb{Z}_B^{(4)}(\omega)] = [A_B^{(4)}(\omega)] - [A_{BB^{\rm NR}}^{(4)}(\omega)][A_{B^{\rm NR}}^{(4)}(\omega)]^{-1}[A_{B^{\rm NR}B}^{(4)}(\omega)] - [\mathcal{W}_{BB^{\rm NR}}^{(42)}(\omega)][\tilde{A}_{B^{\rm NR}}^{(2)}(\omega)]^{-1}[\tilde{\mathcal{W}}_{B^{\rm NR}B}^{(24)}(\omega)]$$

$$[\mathbb{W}_B^{(23)}(\omega)] = i\omega[\mathcal{C}_B^{(23)}] - i\omega[\mathcal{W}_{BB^{\rm NR}}^{(24)}(\omega)][A_{B^{\rm NR}}^{(4)}(\omega)]^{-1}[\mathcal{C}_{B^{\rm NR}B}^{(43)}] - [A_{BB^{\rm NR}}^{(2)}(\omega)][\tilde{A}_{B^{\rm NR}}^{(2)}(\omega)]^{-1}[\mathcal{W}_{B^{\rm NR}B}^{(23)}(\omega)]$$

$$[\mathbb{W}_B^{(24)}(\omega)] = [\mathcal{W}_B^{(24)}(\omega)] - [\mathcal{W}_{BB^{\rm NR}}^{(24)}(\omega)][A_{B^{\rm NR}}^{(4)}(\omega)]^{-1}[A_{B^{\rm NR}B}^{(4)}(\omega)] - [A_{BB^{\rm NR}}^{(2)}(\omega)][\tilde{A}_{B^{\rm NR}}^{(2)}(\omega)]^{-1}[\tilde{\mathcal{W}}_{B^{\rm NR}B}^{(24)}(\omega)]$$

$$[\mathbb{W}_B^{(32)}(\omega)] = -i\omega[\mathcal{C}_B^{(32)}] + i\omega[\mathcal{C}_{BB^{\rm NR}}^{(34)}][A_{B^{\rm NR}}^{(4)}(\omega)]^{-1}[\mathcal{W}_{B^{\rm NR}B}^{(42)}(\omega)] + i\omega[\mathcal{C}_{BB^{\rm NR}}^{(32)}][\tilde{A}_{B^{\rm NR}}^{(2)}(\omega)]^{-1}[\tilde{A}_{B^{\rm NR}B}^{(2)}(\omega)]$$

$$[\mathbb{W}_B^{(34)}(\omega)] = -i\omega[\mathcal{C}_B^{(34)}] + i\omega[\mathcal{C}_{BB^{\rm NR}}^{(34)}][A_{B^{\rm NR}}^{(4)}(\omega)]^{-1}[A_{B^{\rm NR}B}^{(4)}(\omega)] + i\omega[\mathcal{C}_{BB^{\rm NR}}^{(32)}][\tilde{A}_{B^{\rm NR}}^{(2)}(\omega)]^{-1}[\tilde{\mathcal{W}}_{B^{\rm NR}B}^{(24)}(\omega)]$$

$$[\mathbb{W}_B^{(42)}(\omega)] = [\mathcal{W}_B^{(42)}(\omega)] - [A_{BB^{\rm NR}}^{(4)}(\omega)][A_{B^{\rm NR}}^{(4)}(\omega)]^{-1}[\mathcal{W}_{B^{\rm NR}B}^{(42)}(\omega)] - [\mathcal{W}_{BB^{\rm NR}}^{(42)}(\omega)][\tilde{A}_{B^{\rm NR}}^{(2)}(\omega)]^{-1}[\tilde{A}_{B^{\rm NR}B}^{(2)}(\omega)]$$

$$[\mathbb{W}_B^{(43)}(\omega)] = i\omega[\mathcal{C}_B^{(43)}] - i\omega[A_{BB^{\rm NR}}^{(4)}(\omega)][A_{B^{\rm NR}}^{(4)}(\omega)]^{-1}[\mathcal{C}_{B^{\rm NR}B}^{(43)}] - [\mathcal{W}_{BB^{\rm NR}}^{(42)}(\omega)][\tilde{A}_{B^{\rm NR}}^{(2)}(\omega)]^{-1}[\mathcal{W}_{B^{\rm NR}B}^{(23)}(\omega)]$$

$$\mathbb{f}_B^{(2)}(\omega) = \mathbf{f}_B^{(2)} - [A_{BB^{\rm NR}}^{(2)}(\omega)][\tilde{A}_{B^{\rm NR}}^{(2)}(\omega)]^{-1}\mathbf{f}_{B^{\rm NR}}^{(2)}$$

$$\mathbb{f}_B^{(3)}(\omega) = +i\omega[\mathcal{C}_{BB^{\rm NR}}^{(32)}][\tilde{A}_{B^{\rm NR}}^{(2)}(\omega)]^{-1}\mathbf{f}_{B^{\rm NR}}^{(2)}$$

$$\mathbb{f}_B^{(4)}(\omega) = -[\mathcal{W}_{BB^{\rm NR}}^{(42)}(\omega)][\tilde{A}_{B^{\rm NR}}^{(2)}(\omega)]^{-1}\mathbf{f}_{B^{\rm NR}}^{(2)}$$

APPENDIX D

APPENDIX D

D.1 Analytical solution of ECPP integrals

Numerically solving the definite integrals in Eq. (VIII.24) is costly when the dimensions of the associated matrices are becoming larger and larger. A simple analytical solution is proposed in this appendix to avoid doing numerical integration. Only the analytical solution of $z^{(ij)}_{\alpha\beta,B}$ is presented below, because the solution of $x^{(ij)}_{\alpha\beta,B}$ follows the same method. Let us recall the general formulation of $z^{(ij)}_{\alpha\beta,\mathbb{B}}$, for a constructed ESOM,

$$z^{(ij)}_{\alpha\beta,B} = \frac{\int_{\mathbb{B}} i\omega \left((\omega^2[\mathbb{M}^{(ij)}_B]_{\alpha\beta} - [\mathbb{K}^{(ij)}_B]_{\alpha\beta})^2 + \omega^2[\mathbb{G}^{(ij)}_B]^2_{\alpha\beta} - \omega^2[\mathbb{D}^{(ij)}_B]^2_{\alpha\beta} - [\mathbb{R}^{(ij)}_B]^2_{\alpha\beta} \right) \left| \mathbb{h}^{(i)}_{\alpha,B} \right|^2 \mathbb{h}^{(j)}_{\beta,B} \, d\omega}{\int_{\mathbb{B}} \omega^2 [\mathbb{M}^{(i)}_B]_{\alpha\alpha} \left| \mathbb{h}^{(i)}_{\alpha,B} \right|^2 d\omega}$$
$$+ \frac{2\int_{\mathbb{B}} \omega^2 \left((\omega^2[\mathbb{M}^{(ij)}_B]_{\alpha\beta} - [\mathbb{K}^{(ij)}_B]_{\alpha\beta})[\mathbb{D}^{(ij)}_B]_{\alpha\beta} + [\mathbb{G}^{(ij)}_B]_{\alpha\beta}[\mathbb{R}^{(ij)}_B]_{\alpha\beta} \right) \left| \mathbb{h}^{(i)}_{\alpha,B} \right|^2 \mathbb{h}^{(j)}_{\beta,B} \, d\omega}{\int_{\mathbb{B}} \omega^2 [\mathbb{M}^{(i)}_B]_{\alpha\alpha} \left| \mathbb{h}^{(i)}_{\alpha,B} \right|^2 d\omega} , \qquad \text{(D.1)}$$

with $\mathbb{h}^{(i)}_{\alpha,B}$ the equivalent local FRF of generalised coordinate α for subsystem (i) that is expressed as,

$$\mathbb{h}^{(i)}_{\alpha,B} = \frac{1}{-\omega^2[\mathbb{M}^{(i)}_B]_{\alpha\alpha} + i\omega[\mathbb{D}^{(i)}_B]_{\alpha\alpha} + [\mathbb{K}^{(i)}_B]_{\alpha\alpha}} .$$

We calculate the Eq. (D.1) in 2 step: the integral in denominator and the integral in numerator. Firstly let us look at the integral in denominator, which is less complicated.

$$\int_{\mathbb{B}} \omega^2 [\mathbb{M}^{(i)}_B]_{\alpha\alpha} \left| \mathbb{h}^{(i)}_{\alpha,B}(\omega) \right|^2 d\omega = \int_{\mathbb{B}} \frac{\omega^2 [\mathbb{M}^{(i)}_B]_{\alpha\alpha}}{\left| -\omega^2[\mathbb{M}^{(i)}_B]_{\alpha\alpha} + i\omega[\mathbb{D}^{(i)}_B]_{\alpha\alpha} + [\mathbb{K}^{(i)}_B]_{\alpha\alpha} \right|^2} \, d\omega .$$

$\left|-\omega^2[\mathbb{M}_B^{(i)}]_{\alpha\alpha}+i\omega[\mathbb{D}_B^{(i)}]_{\alpha\alpha}+[\mathbb{K}_B^{(i)}]_{\alpha\alpha}\right|^2$ is an even function in the frequency band $\mathbb{B}$. The even function can then be rewritten as: $Q(\omega)=a\omega^4+b\omega^2+c$, where a,b,c are constants and all odd terms are already vanished. And it is possible to find analytically the 4 roots z_k of $Q(\omega)$ (details in Appendix. E). We can therefore decompose these integrals with any polynomial numerator $P(\omega)$, whose degree is smaller than $Q(\omega)$, into 4 integrals :

$$\int_{\mathbb{B}}\frac{P(\omega)}{Q(\omega)}d\omega=\sum_{k=1}^{4}\int_{\mathbb{B}}\frac{R_k(z_k)}{\omega-z_k}d\omega$$

with R_k the residues. However, the residues can be analytically calculated when ω is extremely close to the roots. We then have

$$R_k(z_k)=\frac{P(z_k)}{Q'(z_k)}$$

in which $Q'(\omega)=dQ(\omega)/d\omega$. So that for a frequency band $\mathbb{B}=-B\cup B=[-\omega_c\times 2^{1/6},-\omega_c\times 2^{-1/6}]\cup[\omega_c\times 2^{-1/6},\omega_c\times 2^{1/6}]$, we can therefore write,

$$\int_{\mathbb{B}}\frac{P(\omega)}{Q(\omega)}d\omega=2\times(F(\omega_c\times 2^{1/6})-F(\omega_c\times 2^{-1/6}))\,,$$

where

$$F(\omega)=\sum_{k=1}^{4}\frac{P(z_k)}{Q'(z_k)}\ln(\omega-z_k)\,.$$

Similarly, the numerator of Eq. (D.1) can also be written in fractional form,

$$\begin{aligned}
&\int_{\mathbb{B}} i\omega\left((\omega^2[\mathbb{M}_B^{(ij)}]_{\alpha\beta}-[\mathbb{K}_B^{(ij)}]_{\alpha\beta})^2+\omega^2[\mathbb{G}_B^{(ij)}]_{\alpha\beta}^2-\omega^2[\mathbb{D}_B^{(ij)}]_{\alpha\beta}^2-[\mathbb{R}_B^{(ij)}]_{\alpha\beta}^2\right)\left|\mathbb{h}_{\alpha,B}^{(i)}(\omega)\right|^2\mathbb{h}_{\beta,B}^{(j)}(\omega)d\omega\\
&+2\int_{\mathbb{B}}\omega^2\left((\omega^2[\mathbb{M}_B^{(ij)}]_{\alpha\beta}-[\mathbb{K}_B^{(ij)}]_{\alpha\beta})[\mathbb{D}_B^{(ij)}]_{\alpha\beta}+[\mathbb{G}_B^{(ij)}]_{\alpha\beta}^2[\mathbb{R}_B^{(ij)}]_{\alpha\beta}\right)\left|\mathbb{h}_{\alpha,B}^{(i)}(\omega)\right|^2\mathbb{h}_{\beta,B}^{(j)}(\omega)d\omega\\
=&\int_{\mathbb{B}}\frac{i\omega\left((\omega^2[\mathbb{M}_B^{(ij)}]_{\alpha\beta}-[\mathbb{K}_B^{(ij)}]_{\alpha\beta})^2+\omega^2[\mathbb{G}_B^{(ij)}]_{\alpha\beta}^2-\omega^2[\mathbb{D}_B^{(ij)}]_{\alpha\beta}^2-[\mathbb{R}_B^{(ij)}]_{\alpha\beta}^2\right)}{\left|-\omega^2[\mathbb{M}_B^{(i)}]_{\alpha\alpha}+i\omega[\mathbb{D}_B^{(i)}]_{\alpha\alpha}+[\mathbb{K}_B^{(i)}]_{\alpha\alpha}\right|^2\left(-\omega^2[\mathbb{M}_B^{(j)}]_{\beta\beta}+i\omega[\mathbb{D}_B^{(j)}]_{\beta\beta}+[\mathbb{K}_B^{(j)}]_{\beta\beta}\right)}d\omega\\
&+2\int_{\mathbb{B}}\frac{\omega^2\left((\omega^2[\mathbb{M}_B^{(ij)}]_{\alpha\beta}-[\mathbb{K}_B^{(ij)}]_{\alpha\beta})[\mathbb{D}_B^{(ij)}]_{\alpha\beta}+[\mathbb{G}_B^{(ij)}]_{\alpha\beta}[\mathbb{R}_B^{(ij)}]_{\alpha\beta}\right)}{\left|-\omega^2[\mathbb{M}_B^{(i)}]_{\alpha\alpha}+i\omega[\mathbb{D}_B^{(i)}]_{\alpha\alpha}+[\mathbb{K}_B^{(i)}]_{\alpha\alpha}\right|^2\left(-\omega^2[\mathbb{M}_B^{(j)}]_{\beta\beta}+i\omega[\mathbb{D}_B^{(j)}]_{\beta\beta}+[\mathbb{K}_B^{(j)}]_{\beta\beta}\right)}d\omega\,.
\end{aligned}\tag{D.2}$$

To simplify the calculation, we multiply $(-\omega^2[\mathbb{M}_B^{(j)}]_{\beta\beta}-i\omega[\mathbb{D}_B^{(j)}]_{\beta\beta}+[\mathbb{K}_B^{(j)}]_{\beta\beta})$ on both numerator and denominator, which makes the new denominator be real and even. As the denominator becomes now a even function, we keep only the even terms and eliminate all odd terms in numerator, Eq. (D.2) becomes,

$$\int_{\mathbb{B}}\frac{\omega^2[\mathbb{D}_B^{(j)}]_{\beta\beta}\left((\omega^2[\mathbb{M}_B^{(ij)}]_{\alpha\beta}-[\mathbb{K}_B^{(ij)}]_{\alpha\beta})^2+\omega^2[\mathbb{G}_B^{(ij)}]_{\alpha\beta}^2-\omega^2[\mathbb{D}_B^{(ij)}]_{\alpha\beta}^2-[\mathbb{R}_B^{(ij)}]_{\alpha\beta}^2\right)}{\left|-\omega^2[\mathbb{M}_B^{(i)}]_{\alpha\alpha}+i\omega[\mathbb{D}_B^{(i)}]_{\alpha\alpha}+[\mathbb{K}_B^{(i)}]_{\alpha\alpha}\right|^2\left|-\omega^2[\mathbb{M}_B^{(j)}]_{\beta\beta}+i\omega[\mathbb{D}_B^{(j)}]_{\beta\beta}+[\mathbb{K}_B^{(j)}]_{\beta\beta}\right|^2}d\omega$$

$$+2\int_{\mathbb{B}} \frac{\omega^2\left(-\omega^2[\mathbb{M}_B^{(j)}]_{\beta\beta}+[\mathbb{K}_B^{(j)}]_{\beta\beta}\right)\left(\omega^2[\mathbb{M}_B^{(ij)}]_{\alpha\beta}[\mathbb{D}_B^{(ij)}]_{\alpha\beta}-[\mathbb{K}_B^{(ij)}]_{\alpha\beta}[\mathbb{D}_B^{(ij)}]_{\alpha\beta}+[\mathbb{G}_B^{(ij)}]_{\alpha\beta}[\mathbb{R}_B^{(ij)}]_{\alpha\beta}\right)}{\left|-\omega^2[\mathbb{M}_B^{(i)}]_{\alpha\alpha}+i\omega[\mathbb{D}_B^{(i)}]_{\alpha\alpha}+[\mathbb{K}_B^{(i)}]_{\alpha\alpha}\right|^2\left|-\omega^2[\mathbb{M}_B^{(j)}]_{\beta\beta}+i\omega[\mathbb{D}_B^{(j)}]_{\beta\beta}+[\mathbb{K}_B^{(j)}]_{\beta\beta}\right|^2} d\omega\,.$$

As the denominator is an even function, it can be written as: $Q(\omega)=a\omega^8+b\omega^6+c\omega^4+d\omega^2+e$. This function has 8 roots, but they are not difficult to calculate. In fact we only need to calculate 4 roots of the variable ω^2, and then the calculation of 8 roots of variable ω is straightforward. Then the same method listed above can be used to calculate the solution of this integral.

APPENDIX E

E.1 Analytical solutions of a quartic polynomial

This solution of roots are based on [132]. Here we will simplify all the process and use a small number of variables to calculate the roots of a quartic polynomial.

With a given quartic equation:

$$ax^4 + bx^3 + cx^2 + dx + e = 0 \ .$$

We firstly normalize this equation into

$$x^4 + bx^3 + cx^2 + dx + e = 0 \ , \tag{E.1}$$

with $b = b/a$, $c = c/a$, $d = d/a$, $e = e/a$. Then this equation can be reduced to

$$y^4 + (c - \frac{3b^2}{8})y^2 + (d + \frac{b^3}{8} - \frac{bc}{2})y + (e - \frac{3b^4}{256} + \frac{b^2c}{16} - \frac{bd}{4}) = 0 \ , \tag{E.2}$$

with $x = y - \dfrac{b}{4}$. To make Eq. (E.2) factorizable, we need to solve firstly a cubic polynomial below:

$$z^3 + (-c)z^2 + (bd - 4e)z + (4ce - d^2 - b^2e) = 0 \ .$$

This equation has 3 roots, and it has either 1 or 3 real roots. Here we give one root that will be absolutely real.

$$z_1 = \frac{c}{3} + \sqrt[3]{-\frac{q}{2} + \sqrt{\frac{q^2}{4} + \frac{p^3}{27}}} + \sqrt[3]{-\frac{q}{2} - \sqrt{\frac{q^2}{4} + \frac{p^3}{27}}},$$

with $p = \frac{1}{3}(3(bd-4e)-c^2)$ and $q = \frac{1}{27}(-2c^3+9c(bd-4e)+27(4ce-d^2-b^2e))$. It should be noticed that here $\sqrt[3]{}$ of a negative real value gives only the negative real cubic root, not complex roots. After having the real root z_1, we can solve the original formula Eq. (**??**), but we have 2 situations:

If $\frac{b^2}{4} - c + z_1 = 0$,

$$x_1 = y_1 - \frac{b}{4} = -\frac{b}{4} + \frac{1}{2}(\sqrt{\frac{b^2}{4} - c + z_1} + \sqrt{\frac{3b^2}{4} - 2c + 2\sqrt{z_1^2 - 4e}})$$
$$x_2 = y_2 - \frac{b}{4} = -\frac{b}{4} + \frac{1}{2}(\sqrt{\frac{b^2}{4} - c + z_1} - \sqrt{\frac{3b^2}{4} - 2c + 2\sqrt{z_1^2 - 4e}})$$
$$x_1 = y_1 - \frac{b}{4} = -\frac{b}{4} - \frac{1}{2}(\sqrt{\frac{b^2}{4} - c + z_1} + \sqrt{\frac{3b^2}{4} - 2c - 2\sqrt{z_1^2 - 4e}})$$
$$x_1 = y_1 - \frac{b}{4} = -\frac{b}{4} - \frac{1}{2}(\sqrt{\frac{b^2}{4} - c + z_1} - \sqrt{\frac{3b^2}{4} - 2c - 2\sqrt{z_1^2 - 4e}})$$

If $\frac{b^2}{4} - c + z_1 \neq 0$,

$$x_1 = y_1 - \frac{b}{4} = -\frac{b}{4} + \frac{1}{2}(\sqrt{\frac{b^2}{4} - c + z_1} + \sqrt{\frac{b^2}{2} - c - z_1 + \frac{(4bc - 8d - b^3)}{4\sqrt{\frac{b^2}{4} - c + z_1}}})$$
$$x_2 = y_2 - \frac{b}{4} = -\frac{b}{4} + \frac{1}{2}(\sqrt{\frac{b^2}{4} - c + z_1} - \sqrt{\frac{b^2}{2} - c - z_1 + \frac{(4bc - 8d - b^3)}{4\sqrt{\frac{b^2}{4} - c + z_1}}})$$
$$x_1 = y_1 - \frac{b}{4} = -\frac{b}{4} + \frac{1}{2}(\sqrt{\frac{b^2}{4} - c + z_1} + \sqrt{\frac{b^2}{2} - c - z_1 - \frac{(4bc - 8d - b^3)}{4\sqrt{\frac{b^2}{4} - c + z_1}}})$$
$$x_1 = y_1 - \frac{b}{4} = -\frac{b}{4} + \frac{1}{2}(\sqrt{\frac{b^2}{4} - c + z_1} - \sqrt{\frac{b^2}{2} - c - z_1 - \frac{(4bc - 8d - b^3)}{4\sqrt{\frac{b^2}{4} - c + z_1}}})$$

BIBLIOGRAPHY

[1] T. Blinet and et al., "Acousys v3 validation booklet," tech. rep., 2016.

[2] "Accord Cadre Bois-Construction-Environment," tech. rep., 2001.

[3] Alcimed, *Marché actuel des nouveaux produits issus du bois et évolutions à échéance 2020*. Pipame, 2012.

[4] C. Guigou-Carter, M. Villot, and R. Wetta, "Prediction method adapted to wood frame lightweight constructions," *Building Acoustics*, vol. 13, p. 173–188, 2006.

[5] J. Davy, "Predicting the sound insulation of walls," *Building Acoustics*, vol. 16, pp. 1–20, 01 2009.

[6] J. Davy, "The improvement of a simple theoretical model for the prediction of the sound insulation of double leaf walls," *The Journal of the Acoustical Society of America*, vol. 127, pp. 841–9, 02 2010.

[7] J. Davy, "Sound transmission of cavity walls due to structure borne transmission via point and line connections," *The Journal of the Acoustical Society of America*, vol. 132, pp. 814–21, 08 2012.

[8] "NF EN ISO 12354-1, estimation of acoustic performance of buildings from the performance of elements," standard, Building acoustics, 2000.

[9] R. Ohayon and C. Soize, "Méthodes numériques avancées en vibroacoustique basses et moyennes fréquences," *Revue Européenne des Éléments*, vol. 8, 05 2012.

[10] H.J.-P.Morand and R.Ohayon, *Fluid-Structure Interaction: applied numerical methods*. John Wiley and Son Ltd, 1995.

[11] R.Ohayon and C.Soize, *Structural Acoustics and Vibration*. Academic Press, 1998.

[12] C. Lesueur, "Rayonnement acoustique des structures," *Eyrolles*, 1988.

[13] O.Zienckiewicz and R.Taylor, *The Finite Element Method*. McGraw-Hill, 4th edition, 1989.

[14] R. H. Lyon and G. Maidanik, "Power flow between linearly coupled oscillators," *J. Acoust. Soc. Am. 34, 623-639*, 1962.

[15] R. H. Lyon and E. Eichler, "Random vibration of connected structures," *J. Acoust. Soc. Am. 36, 1344-1354*, 1964.

[16] R. H. Lyon and T. Scharton, "Vibrational-energy transmission in a three-element structure," *J. Acoust. Soc. Am. 38, 253-261*, 1965.

[17] A. Kulowski, "Algorithmic representation of the ray tracing technique," *Applied Acoustics - APPL ACOUST*, vol. 18, pp. 449–469, 12 1985.

[18] J. J. Embrechts, "Sound field distribution using randomly traced sound ray techniques," *Acustica*, vol. 51, p. 288–295, 1982.

[19] C. Coguenanff, *Robust design of lightweight wood-based systems in linear vibroacoustics.* PhD thesis, 2015.

[20] G. Maidanik, "Some elements in statistical energy analysis," *J. Sound Vib., 52(2) :171–191*, 1977.

[21] C. H. Hodges and J. Woodhouse, "Theories of noise and vibration transmission in complex structures," *Reports in progress in physics, 49 :107–170*, 1986.

[22] R. H. Lyon, "Theory and application of Statistical Energy Analysis," *Buttersworths-Heimann, Boston, MA*, 1995.

[23] N. Totaro, C. Dodard, and J.-L. Guyader, "Sea coupling loss factors of complex vibroacoustic systems," *J. Vib. Ac., 131(041009) :1–8*, 2009.

[24] B. R. Mace, "On the statistical energy analysis hypothesis of coupling power proportionality and some implications of its failure," *J. Sound Vib., 178 :95–112*, 1994.

[25] F. J. Fahy, "Statistical energy analysis : a critical overview.," *Phil. Trans. R. Soc. Lond. A*, 1994.

[26] Y. Kishimoto and D. Berrnstein, "Thermodynamic modelling of interconnected systems, part I Conservative coupling," *J. Sound Vib. 182, 23–58*, 1995.

[27] F. J. Fahy and Y. D. Yuan, "Power flow between non-conservatively coupled oscillators," *J. Sound Vib. 114, 1–11*, 1987.

[28] J. Sun, N. Lalor, and E. Richards, "Power flow and energy balance of non-conservatively coupled structures, I: theory," *J. Sound Vib. 114, 1–11*, 1987.

[29] T. Lafont, *Vibro-acoustique statistique : Etude des hypothèses de la SEA*. PhD thesis, feb 2015.

[30] R. Ohayon and C. Soize, *Advanced Computational Vibroacoustics*. Cambridge University Press, 2014.

[31] G.Sandberg and R.Ohayon, *Computational Aspects of Structural Acoustics*. Springer-VerlagWien, 2009.

[32] D. Johnson, J. Koplik, and R. Dashen, "Theory of dynamic permeability and tortuosity in fluid-saturated porous media," *Journal of Fluid Mechanics*, vol. 176, p. 379–402, 1987.

[33] Y. Champoux and J. Allard, "Dynamic tortuosity and bulk modulus in air-saturated porous media," *Journal of Applied Physics*, vol. 70, no. 4, pp. 1975–1979, 1991.

[34] L. Maxit, "Analysis of the modal energy distribution of an excited vibrating panel coupled with a heavy fluid cavity by a dual modal formulation," *Journal of Sound and Vibration*, vol. 332, no. 25, pp. 6703–6724, 2013.

[35] L.Maxit, K. Ege, N.Totaro, and J-L.Guyader, "Non resonant transmission modelling with statistical modal energy distribution analysis," *Journal of Sound and Vibration*, vol. 333, no. 2, pp. 499–519, 2014.

[36] C. Johansson, "Field measurements of 170 nominally identical timber floors - a statistical analysis," *Proceedings Internoise*, 2000.

[37] R.Öqvist, "Variations in sound insulation in multi-storey lightweight timber constructions," *Licentiate thesis, Lulea University of Technology*, 2010.

[38] R.Öqvist, F. Ljunggren, and A. Agren, "Variations in sound insulation in nominally identical prefabricated lightweight timber constructions," *Building Acoustics, vol. 17, no. 2, pp. 91–103*, 2010.

[39] R.Öqvist, F. Ljunggren, and A. Agren, "On the uncertainty of building acoustic measurements - case study of a cross-laminated timber construction," *Applied Acoustics, vol. 73, no. 9, pp. 904–912*, 2012.

[40] R. J. Craik and J. A. Steel, "The effect of workmanship on sound transmission through buildings: Part 1—airborne sound," *Applied Acoustics, vol. 27, no. 1, pp. 57–63*, 1989.

[41] R. J. Craik and J. A. Steel, "The effect of workmanship on sound transmission through buildings: Part 2—structure-borne sound," *Applied Acoustics, vol. 27, no. 1, pp. 137–145*, 1989.

[42] K. A. Dickow, P. H. Kirkegaard, and L. V. Andersen, "An evaluation of test and physical uncertainty of measuring vibration in wooden junctions," *Proceedings of the International Conference on Uncertainty in Structural Dynamics*, 2012.

[43] A. Bolmsvik, A. Linderholt, A. Brandt, and T. Ekevid, "Fe modelling of light weight wooden assemblies – parameter study and comparison between analyses and experiments," *Engineering Structures, vol. 73, pp. 125–142*, 2014.

[44] C. Soize, "Random matrix theory for modeling uncertainties in computational mechanics," *Computer Methods in Applied Mechanics and Engineering, vol. 194, no. 12-16, pp. 1333–1366*, 2005.

[45] C. Soize, "Generalized probabilistic approach of uncertainties in computational dynamics using random matrices and polynomial chaos decompositions," *International Journal for Numerical Methods in Engineering, vol. 81, no. 8, pp. 939–970*, 2010.

[46] M. Guerich, "Optimization of noise transmission through sandwich structures," *Journal of Vibration and Acoustics*, vol. 135, pp. 051010–1, 10 2013.

[47] B. Sharp, "Prediction methods for the sound transmission of building elements," *Noise Control Engineering 11, pp 63 – 63*, 1978.

[48] L. Cremer, M. Heckl, and E. E. Ungar, *Structure-Borne Sound : Structural vibrations and sound radiation at audio frequencies*.
Springer-Verlag, New York, 1988.

[49] F. J. Fahy, *Sound and Structural Vibration*.
Academic Press, 1985.

[50] D. A. Bies and C. Hansen, *Engineering Noise Control: Theory and Practice, Fourth Edition*.
CRC Press, 2009.

[51] D.I.L.Ver and L.L.Beranek, *Noise and Vibration Control Engineering: Principles and Applications, Second Edition*.
John Wiley, 2005.

[52] O. A. B. Hassan, *Building Acoustics and Vibration: Theory and Practice*.
World Scientific Publishing, 2009.

[53] L. Landau and E. Lifchitz, *Fluid Mechanics*.
Pergamon Press, Oxford, 1992.

[54] M. R. Stinson, "The propagation of plane sound waves in narrow and wide circular tubes, and generalization to uniform tubes of arbitrary cross-sectional shape," *J. Acoust. Soc. Am. 89(2), pp. 550-558*, 1991.

[55] M. E. Delany and E. N. Bazley, "Acoustical properties of fibrous absorbent materials," *Applied Acoustics 3, pp. 105-116*, 1970.

[56] Y. Miki, "Acoustical properties of porous materials - modifications of delany-bazley models," *J. Acoust. Soc. Jpn (E). 11(1), pp. 19-24*, 1990.

[57] Y. Miki, "Acoustical properties of porous materials - generalizations of empirical models," *J. Acoust. Soc. Jpn (E). 11(1), pp. 25-28*, 1990.

[58] K. Wilson, "Relaxation-matched modeling of propagation through porous media, including fractal pore structure," *J. Acoust. Soc. Am. 94(2), pp. 1136-1145*, 1993.

[59] D. Lafarge, P. Lemarinier, J. F. Allard, and V. Tarnow, "Dynamic compressibility of air in porous structures at audible frequencies," *The Journal of the Acoustical Society of America*, vol. 102, no. 4, pp. 1995–2006, 1997.

[60] O. Doutres, N. Dauchez, J.-M. Génevaux, and O. Dazel, "Validity of the limp model for porous materials: A criterion based on the biot theory," *The Journal of the Acoustical Society of America*, vol. 122, no. 4, pp. 2038–2048, 2007.

[61] M. A. Biot, "Theory of propagation of elastic waves in a fluid-saturated porous solid. i. low-frequency range," *The Journal of the Acoustical Society of America*, vol. 28, no. 2, pp. 168–178, 1956.

[62] M. A. Biot, "Theory of propagation of elastic waves in a fluid-saturated porous solid. ii. higher frequency range," *The Journal of the Acoustical Society of America*, vol. 28, no. 2, pp. 179–191, 1956.

[63] N. Atalla, R. Panneton, and P. Debergue, "A mixed displacement-pressure formulation for poroelastic materials," *The Journal of the Acoustical Society of America*, vol. 104, no. 3, pp. 1444–1452, 1998.

[64] F.-X. Bécot and L. Jaouen, "An alternative biot's formulation for dissipative porous media with skeleton deformation," *The Journal of the Acoustical Society of America*, vol. 134, no. 6, pp. 4801–4807, 2013.

[65] B. Nennig, R. Binois, N. Dauchez, E. Perrey-Debain, and F. Foucart, "A transverse isotropic equivalent fluid model combining both limp and rigid frame behaviors for fibrous materials," *The Journal of the Acoustical Society of America*, vol. 143, pp. 2089–2098, 04 2018.

[66] C. Zwikker and C. W. Kosten, *Sound absorbing materials*.
Elsevier, 1949.

[67] L. Lei, N. Dauchez, and J. Chazot, "Prediction of the six parameters of an equivalent fluid model for thermocompressed glass wools and melamine foam," *Applied Acoustics*, vol. 139, pp. 44 – 56, 2018.

[68] J-B.Chéné and et al., "Iso 10140 series, impossible way to manage low frequency measurements and to improve overall reproducibility?," *Proceedings of Euronoise*, 2018.

[69] E. V. Haynsworth, "On the Schur complement, basel mathematical notes,(university of basel)," *BMN 20*, 1968.

[70] I. Novikov, "Low-frequency sound insulation of thin plate," *Applied Acoustics, 54 83-90*, 1998.

[71] A. Osipov, P. Mees, and G. Vermeir, "Low-frequency airborne sound transmission through single partitions in building," *Applied Acoustics, 52 273-288*, 1997.

[72] K. A. Mulholland and R. H. Lyon, "Sound insulation at low frequencies," *Journal of the Acoustical Society of America, 54 867-878*, 1973.

[73] J. Brunskog and P. Davidson, "Sound transmission of structures. a finite element approach with simplified room description," *Acta acustica united with acustica, 90 847-857*, 2004.

[74] L. Gargliardini, J. Roland, and J.-L. Guyader, "The used of functional basis to calculate acoustic transmission between two rooms," *Journal of Sound and Vibration ,145 457–478*, 1991.

[75] M. J. Crocker and A. J. Price, "Sound transmission using statistical energy analysis," *Journal of Sound and Vibration, 9 469–486*, 1969.

[76] Robert.J.M.Craik, "Non-resonant sound transmission through double walls using statistical energy analysis," *Applied Acoustics*, vol. 64, no. 3, pp. 325–341, 2003.

[77] K. Renji, P. Nair, and S. Narayanan, "Non-resonant response using statistical energy analysis," *Journal of Sound and Vibration, 241 253-270*, 2001.

[78] C.Hopkins, *Sound Insulation*.
Building and Construction, Elsevier / Butterworth-Heinemann, 2007.

[79] J. David and M. Menelle, "Validation of a medium-frequency computational method for the coupling between a plate and a water-filled cavity," *Journal of Sound and Vibration, 265 841-861*, 2003.

[80] J. David and M. Menelle, "Validation of a modal method by use of an appropriate static potential for a plate coupled to a water-filled cavity," *Journal of Sound and Vibration, 301 739-759*, 2007.

[81] R.Guyan, "Reduction of stiffness and mass matrices," *AIAA Journal*, 1965.

[82] W. Wohle, T. Beckmann, and H. Schreckenbach, "Coupling loss factors for statistical energy analysis of sound transmission at rectangular structural slab joints. I," *J. Sound Vib. 77, 323-334*, 1981.

[83] W. Wohle, T. Beckmann, and H. Schreckenbach, "Coupling loss factors for statistical energy analysis of sound transmission at rectangular structural slab joints. II," *J.Sound Vib. 77,335-344*, 1981.

[84] R. Langley and K. Heron, "Elastic wave transmission through plate/beam junctions," *J. Sound Vib. 143, 241-253*, 1990.

[85] R. H. Lyon, *Statistical Energy Analysis of dynamical systems*.
The MIT press, 1975.

[86] P. W. Smith, "Response and radiation of structural modes excited by sound," *J. Acoust. Soc. Am., 64 :640–647*, 1962.

[87] D. E. Newland, "Calculation of power flow between a class of coupled oscillators," *J. Sound Vib., 3(3) :262–276*, 1966.

[88] D. E. Newland, "Power flow between a class of coupled oscillators," *J. Acoust. Soc. Am., 43(3) :553–559*, 1968.

[89] F. J. Fahy, "Energy flow between oscillators : special case of point excitation," *J. Sound Vib., 11 :481–483*, 1970.

[90] F. J. Fahy, "L'analyse statistique énergétique," *Revue d'acoustique, 8(33) :10–25*, 1975.

[91] R. Lotz and S. H. Crandall, "Prediction and measurement of the proportionality constant in statistical energy analysis," *J. Acoust. Soc. Am., 54 :516–524*, 1973.

[92] B. R. Mace and L. Ji, "The statistical energy analysis of coupled sets of oscillators," *Proc. R. Soc. A, 463 :1359–1377*, 2007.

[93] G. Maidanik, "Response of coupled dynamic systems," *J. Sound Vib., 46(4) :561–583*, 1976.

[94] R. S. Langley, "A general derivation of the statistical energy analysis equations for coupled dynamic systems," *J. Sound Vibrat., 135 :499–508*, 1989.

[95] A. J. Keane and W. G. Price, "A note on the power flowing between two conservatively coupled multi-modal subsystems," *J. Sound Vibrat., 144 :185–196*, 1991.

[96] B. R. Mace, "The statistics of power flow between two continuous one-dimensional subsystems : a wave solution," *J. Sound Vib., 154 :289–319*, 1992.

[97] B. R. Mace, "The statistics of power flow between two continuous one-dimensional subsystems," *J. Sound Vib., 154 :321-341*, 1992.

[98] B. R. Mace, "The statistical energy analysis of two continuous one-dimensional subsystems," *J. Sound Vib., 166 :429–461*, 1993.

[99] C. B. Burroughs, R. W. Fisher, and F. R. Kem, "An introduction to statistical energy analysis," *J. Acoust. Soc. Am., 101(4) :1779–1789*, 1997.

[100] C. Soize, "Coupling between an undamped linear acoustic fluid and a damped nonlinear structure - statistical energy analysis considerations," *Acoustical Society of America*, 2019.

[101] S. Crandall and R. Lotz, "On the coupling loss factor in statistical energy analysis," *J. Acoust. Soc. Am. 49, 352-356*, 1971.

[102] A. Keane and W. Prince, "Statistical energy analysis of strongly coupled systems," *J. Sound Vib. 117, 363–386*, 1987.

[103] B. Mace, "Statistical energy analysis, energy distribution models and system modes," *J. Sound Vib. 264, 391–409*, 2003.

[104] L. Maxit and J.-L. Guyader, "Extension of SEA model to subsystems with non-uniform modal energy distribution," *J. Sound Vib. 265, 337–358*, 2003.

[105] R. Langley, "A wave intensity technique for the analysis of high frequency vibrations," *J. Sound Vib. 159, 483–502*, 1992.

[106] N. Totaro and J.-L. Guyader, "Extension of statistical modal energy distribution analysis for estimating energy density in coupled subsystem," *J. Sound Vib. 331, 3114–3129*, 2012.

[107] N. Totaro and J.-L. Guyader, "Modal energy analysis," *J. Sound Vib. 332, 3735–3749*, 2013.

[108] A. L. Bot, "A vibroacoustic model for high frequency analysis," *J. Sound Vib. 211, 537–554*, 1998.

[109] A. L. Bot, "Energy transfer for high frequencies in build-up structures," *J. Sound Vib. 250, 247–275*, 2002.

[110] A. L. Bot, *Foundations of statistical energy analysis in vibroacoustics*. Oxford University Press, 2015.

[111] I.Babuska and P.Chatzipantelidis, "On solving elliptic stochastic partial differential equations," *Computer Methods in Applied Mechanics and Engineering 191 4093-4122*, 2002.

[112] R. Ghanem, "Ingredients for a general purpose stochastic finite elements formulation," *Computer Methods in Applied Mechanics and Engineering 168 19-34*, 1999.

[113] R. Ghanem and M.Pellissetti, "Adaptive data refinement in the spectral stochastic finite element method," *Communications in Numerical Methods in Engineering 18 (2) 141-151*, 2002.

[114] R. Ghanem and A. Sarkar, "Reduced models for the medium-frequency dynamics of stochastic systems," *Journal of the Acoustical Society of America 113 (2) 834-846*, 2003.

[115] R. Ghanem and P. Spanos, *Stochastic Finite Elements: A spectral Approach*. Springer-Verlag, NewYork, 1991.

[116] M. Kleiber, D. Tran, and T. Hien, *The Stochastic Finite Element Method*. John Wiley & Sons, NewYork, 1992.

[117] M. Shinozuka and G. Deodatis, "Response variability of stochastic finite element systems," *Journal of Engineering Mechanics 114 (3) 499-519*, 1988.

[118] P. Spanos and R. Ghanem, "Stochastic finite element expansion for random media," *Journal of Engineering Mechanics, ASCE 115 (5) 1035-1053*, 1989.

[119] E. Vanmarcke and M. Grigoriu, "Stochastic finite element analysis of simple beams," *Journal of Engineering Mechanics, ASCE 109 (5) 1203-1214*, 1983.

[120] C. Soize, "A nonparametric model of random uncertainties for reduced matrix models in structural dynamics," *Probabilistic Engineering Mechanics, vol. 15, no. 3, pp. 277–294*, 2000.

[121] C. Soize, "Maximum entropy approach for modeling random uncertainties in transient elastodynamics," *Journal of Acoustic Society of America, 109(5):1979–1996*, 2001.

[122] C. Soize, "A comprehensive overview of a non-parametric probabilistic approach of model uncertainties for predictive models in structural dynamics," *Journal of Sound and Vibration, 288:623–652*, 2005.

[123] C. Soize, "Random matrix theory and nonparametric model of random uncertainties in vibration analysis," *Journal of Sound and Vibration, 263:893–916*, 2003.

[124] C. Soize, "Uncertain dynamical systems in the medium-frequency range," *Journal of Engineering Mechanics, 129(9):1017–1027*, 2003.

[125] C. Soize, "Probabilistic models for computational stochastic mechanics and applications," *In the 9th International Conference of Structural Safety and Reliability ICOSSAR'05, Rotterdam, Netherlands*, 2005.

[126] C. Soize and H. Chebli, "Random uncertainties model in dynamic substructuring using a nonparametric probabilistic model," *Journal of Engineering Mechanics, 129(4):449–457*, 2003.

[127] C. Fernandez, C. Soize, and L. Gagliardini, "Fuzzy structure theory modeling of sound-insulation layers in complex vibroacoustic uncertain sytems - theory and experimental validation," *JASA, 125(1):138–153*, 2009.

[128] J.-F. Durand, C. Soize, and L. Gagliardini, "Structural-acoustic modeling of automotive vehicles in presence of uncertainties and experimental identification and validation," *JASA, 124(3):1513–1525*, 2008.

[129] J. Duchereau and C. Soize, "Transient dynamics in structures with non-homogeneous uncertainties induced by complec joints," *Mechanical Systems and Signal Processing*, 2006.

[130] H. Chebli and C. Soize, "Experimental validation of a nonparametric probabilistic model of nonhomogeneous uncertainties for dynamical systems," *JASA, 115(2):697–705*, 2004.

[131] A. Batou and C. Soiz, "Experimental identification of turbulent fluid forces applied to fuel assemblies using an uncertain model and fretting-wear estimation," *Mechanical Systems and Signal ProcessingMechanical Systems and Signal Processing, 23(7):2141 – 2153*, 2009.

[132] Y.-B. Jia, "Roots of polynomials," *Com S, 477:577*, 2017.